

Watershed modeling to assess the sensitivity of streamflow, nutrient and sediment loads to potential climate change and urban development in 20 U.S. watersheds



EPA/600/R-12/058F
September 2013

**Watershed Modeling to Assess the Sensitivity of Streamflow, Nutrient, and
Sediment Loads to Potential Climate Change and Urban Development in
20 U.S. Watersheds**

National Center for Environmental Assessment
Office of Research and Development
U.S. Environmental Protection Agency
Washington, DC 20460

DISCLAIMER

This document has been reviewed in accordance with U.S. Environmental Protection Agency policy and approved for publication. Mention of trade names or commercial products does not constitute endorsement or recommendation for use.

ABSTRACT

Watershed modeling was conducted in 20 large, U.S. watersheds to characterize the sensitivity of streamflow, nutrient (nitrogen and phosphorus), and sediment loading to a range of plausible mid-21st century climate change and urban development scenarios. The study also provides an improved understanding of methodological challenges associated with integrating existing tools (e.g., climate models, downscaling approaches, and watershed models) and data sets to address these scientific questions. The study uses a scenario-analysis approach with a consistent set of watershed models and scenarios applied to multiple locations throughout the nation. Study areas were selected to represent a range of geographic, hydrologic, and climatic characteristics. Watershed simulations were conducted using the Soil Water Assessment Tool (SWAT) and Hydrologic Simulation Program—FORTRAN (HSPF) models. Scenarios of future climate change were developed based on statistically and dynamically downscaled climate model simulations representative of the period 2041–2070. Scenarios of urban and residential development for this same period were developed from the EPA’s Integrated Climate and Land Use Scenarios (ICLUS) project. Future changes in agriculture and human use and management of water were not evaluated.

Results provide an improved understanding of the complex and context-dependent relationships between climate change, land-use change, and water resources in different regions of the nation. As a first-order conclusion, results indicate that in many locations future conditions are likely to be different from past experience. Results also provide a plausible envelope on the range of streamflow and water quality responses to mid-21st century climate change and urban development in different regions of the nation. In addition, in many study areas the simulations suggest a likely direction of change of streamflow and water quality endpoints. Sensitivity studies evaluating the implications of different methodological choices help to improve the scientific foundation for conducting climate change impacts assessments, thus building the capacity of the water management community to understand and respond to climate change. This information is useful to inform and guide the development of response strategies for managing risk.

Preferred Citation:

U.S. EPA (Environmental Protection Agency). (2013) Watershed modeling to assess the sensitivity of streamflow, nutrient, and sediment loads to potential climate change and urban development in 20 U.S. watersheds. National Center for Environmental Assessment, Washington, DC; EPA/600/R-12/058F. Available from the National Technical Information Service, Alexandria, VA, and online at <http://www.epa.gov/ncea>.

TABLE OF CONTENTS

LIST OF APPENDICES.....	iv
LIST OF TABLES.....	vi
LIST OF FIGURES.....	ix
LIST OF ABBREVIATIONS.....	xii
PREFACE.....	xiv
AUTHORS, CONTRIBUTORS AND REVIEWERS.....	xv
ACKNOWLEDGEMENTS.....	xvi
1. EXECUTIVE SUMMARY.....	1-1
2. INTRODUCTION.....	2-1
2.1. About This Report.....	2-2
3. STUDY AREAS.....	3-1
4. MODELING APPROACH.....	4-1
4.1. MODEL BACKGROUND.....	4-2
4.1.1. HSPF.....	4-2
4.1.2. SWAT.....	4-4
4.2. MODEL SETUP.....	4-6
4.2.1. SWAT Setup Process.....	4-7
4.2.2. HSPF Setup Process.....	4-8
4.2.3. Watershed Data Sources.....	4-9
4.2.4. Baseline Meteorology Representation.....	4-14
4.3. SIMULATION OUTPUT AND ENDPOINTS.....	4-16
4.4. MODEL CALIBRATION AND VALIDATION.....	4-18
4.4.1. Hydrology.....	4-19
4.4.2. Water Quality.....	4-22
4.4.3. Accuracy of the Watershed Models.....	4-23
5. CLIMATE CHANGE AND URBAN DEVELOPMENT SCENARIOS.....	5-1
5.1. SCENARIO-BASED APPROACH.....	5-1
5.2. CLIMATE CHANGE SCENARIOS.....	5-2
5.2.1. Future Climate Models, Sources, and Downscaling.....	5-2
5.2.2. Translation of Climate Model Projections to Watershed Model Weather Inputs.....	5-4
5.3. URBAN AND RESIDENTIAL DEVELOPMENT SCENARIOS.....	5-12
5.3.1. ICLUS Urban and Residential Development Scenarios.....	5-14
5.3.2. Mapping ICLUS Housing Density Projections to NLCD Land Use Categories.....	5-14
6. STREAMFLOW AND WATER QUALITY SENSITIVITY TO DIFFERENT METHODOLOGICAL CHOICES: ANALYSIS IN THE FIVE PILOT STUDY AREAS.....	6-1
6.1. COMPARISON OF WATERSHED MODELS.....	6-1

TABLE OF CONTENTS (continued)

6.1.1.	Comparison of Model Calibration and Validation Performance	6-2
6.1.2.	Comparison of Simulated Changes Using SWAT and HSPF.....	6-7
6.1.3.	Sensitivity to Increased Atmospheric CO ₂	6-11
6.2.	SENSITIVITY TO DIFFERENT METHODS OF DOWNSCALING	
	GCM OUTPUT	6-15
6.2.1.	Climate Model Energy Inputs and PET Estimates	6-15
6.2.2.	“Degraded” NARCCAP Climate Scenarios	6-16
6.2.3.	Sensitivity of Flow and Water Quality to Approaches for Downscaling GCM Projections	6-17
7.	REGIONAL SENSITIVITY OF STREAMFLOW AND WATER QUALITY TO CLIMATE CHANGE AND LAND DEVELOPMENT: RESULTS IN ALL 20 WATERSHEDS	7-1
7.1.	SELECTION OF WATERSHED MODEL FOR USE IN ALL STUDY AREAS	7-2
7.2.	SENSITIVITY TO CLIMATE CHANGE SCENARIOS	7-3
7.3.	SENSITIVITY TO URBAN AND RESIDENTIAL DEVELOPMENT SCENARIOS	7-18
7.4.	RELATIVE EFFECTS OF CLIMATE CHANGE AND URBAN DEVELOPMENT SCENARIOS	7-20
7.5.	SENSITIVITY TO COMBINED CLIMATE CHANGE AND URBAN DEVELOPMENT SCENARIOS	7-24
7.6.	WATER BALANCE INDICATORS	7-42
7.7.	MODELING ASSUMPTIONS AND LIMITATIONS	7-60
	7.7.1. Model Calibration.....	7-62
	7.7.2. Watershed Model Selection.....	7-63
8.	SUMMARY AND CONCLUSIONS	8-1
	REFERENCES	R-1

LIST OF APPENDICES

Appendix A.	Model Setup Process	A-1
Appendix B.	Quality Assurance Project Plan (QAPP) Section 8: Model Calibration	B-1
Appendix C.	Climate Change and the Frequency and Intensity of Precipitation Events	C-1
Appendix D.	Model Configuration, Calibration and Validation for the ACF River Basin	D-1
Appendix E.	Model Configuration, Calibration and Validation for the Arizona (Salt, Verde, and San Pedro) Basins	E-1
Appendix F.	Model Configuration, Calibration and Validation for the Susquehanna River Basin	F-1

LIST OF APPENDICES (continued)

Appendix G.	Model Configuration, Calibration and Validation for the Minnesota River Basin	G-1
Appendix H.	Model Configuration, Calibration and Validation for the Willamette River Basin	H-1
Appendix I.	Model Configuration, Calibration and Validation for the Lake Pontchartrain Drainages	I-1
Appendix J.	Model Configuration, Calibration and Validation for the Tar and Neuse River Basins	J-1
Appendix K.	Model Configuration, Calibration and Validation for the Nebraska (Loup and Elkhorn River) Basins	K-1
Appendix L.	Model Configuration, Calibration and Validation for the Cook Inlet Basin	L-1
Appendix M.	Model Configuration, Calibration and Validation for the Georgia-Florida Coastal Basins	M-1
Appendix N.	Model Configuration, Calibration and Validation for the Illinois River Basin	N-1
Appendix O.	Model Configuration, Calibration and Validation for the Lake Erie Drainages	O-1
Appendix P.	Model Configuration, Calibration and Validation for the New England Coastal Basins	P-1
Appendix Q.	Model Configuration, Calibration and Validation for the Rio Grande Valley	Q-1
Appendix R.	Model Configuration, Calibration and Validation for the Sacramento River Basin	R-1
Appendix S.	Model Configuration, Calibration and Validation for the Southern California Coastal Basins	S-1
Appendix T.	Model Configuration, Calibration and Validation for the South Platte River Basin	T-1
Appendix U.	Model Configuration, Calibration and Validation for the Trinity River Basin	U-1
Appendix V.	Model Configuration, Calibration and Validation for the Upper Colorado River Basin	V-1
Appendix W.	Model Configuration, Calibration and Validation for the Powder and Tongue River Basins	W-1
Appendix X.	Scenario Results for the Five Pilot Study Areas	X-1
Appendix Y.	Scenario Results for the 15 Nonpilot Study Areas	Y-1
Appendix Z.	Overview of Climate Scenario Monthly Temperature, Precipitation, and Potential Evapotranspiration	Z-1

LIST OF TABLES

3-1.	Summary of the 20 study areas	3-4
3-2.	Current (2001) land use and land cover in the 20 study areas	3-7
4-1.	Regrouping of the NLCD 2001 land-use classes for the HSPF and SWAT models	4-11
4-2.	Calculated fraction impervious cover within each developed land class for each study area based on NLCD 2001	4-12
4-3.	Characteristics of NRCS soil hydrologic groups	4-12
4-4.	Weather station statistics for the 20 study areas (1971–2000)	4-16
4-5.	Summary of streamflow and water quality endpoints	4-18
4-6.	Performance targets for hydrologic simulation (magnitude of annual and seasonal relative mean error) from Donigian (2000)	4-20
4-7.	Key hydrology calibration parameters for HSPF.....	4-22
4-8.	Key hydrology calibration parameters for SWAT	4-22
4-9.	Summary of SWAT model fit for initial calibration site (20 study areas).....	4-27
4-10.	Summary of HSPF model fit for initial calibration sites (five pilot study areas)	4-28
5-1.	Climate models and source of model data used to develop climate change scenarios.....	5-3
5-2.	Climate change data available from each source used to develop climate scenarios	5-6
5-3.	SWAT weather generator parameters and adjustments applied for scenarios.....	5-12
5-4.	Comparison of PET estimation between different downscaling approaches.....	5-13
5-5.	ICLUS projected changes in developed land area within different imperviousness classes by 2050	5-16
6-1.	Percent error in simulated total streamflow volume for 10-year calibration and validation periods at initial and downstream calibration gages	6-3
6-2.	Nash-Sutcliffe coefficient of model fit efficiency (<i>E</i>) for daily streamflow predictions, 10-year calibration and validation periods at initial and downstream calibration gages	6-3
6-3.	Statistical comparison of HSPF and SWAT outputs at downstream station for the five pilot sites across all climate scenarios	6-8
6-4.	Effects of omitting simulated auxiliary meteorological time series on Penman-Monteith reference crop PET estimates for “degraded” climate scenarios	6-17
6-5.	Summary of SWAT-simulated total streamflow in the five pilot study areas for scenarios representing different methods of downscaling	6-18
6-6.	Summary of SWAT-simulated streamflow and water quality in the Minnesota River study area for scenarios representing different methods of downscaling	6-19
6-7.	Range of SWAT-projected changes in annual streamflow and pollutant loads for combined mid-21 st century NARCCAP climate change and ICLUS urban and residential development scenarios	6-22
7-1.	Downstream stations within each study area where simulation results are presented	7-1
7-2.	Average annual precipitation (in/yr and percent of baseline) for current conditions and mid-21 st century climate scenarios.....	7-4
7-3.	Average annual temperature (°F and change from baseline) for current conditions and mid-21 st century climate scenarios.....	7-5

LIST OF TABLES (continued)

7-4.	Average annual PET (in/yr and percent of baseline) for current conditions and mid-21 st century climate scenarios.....	7-6
7-5.	Average annual SWAT-simulated actual ET (in/yr and percent of baseline) for current conditions and mid-21 st century climate scenarios.....	7-7
7-6.	Changes in precipitation intensity for NARCCAP mid-21 st century climate scenarios.....	7-9
7-7.	Simulated total streamflow volume (climate scenarios only; percent relative to current conditions) for selected downstream stations.....	7-10
7-8.	Simulated 7-day low flow (climate scenarios only; percent relative to current conditions) for selected downstream stations.....	7-11
7-9.	Simulated 100-year peak flow (log-Pearson III; climate scenarios only; percent relative to current conditions) for selected downstream stations.....	7-12
7-10.	Simulated changes in the number of days to streamflow centroid (climate scenarios only; relative to current conditions) for selected downstream stations.....	7-13
7-11.	Simulated Richards-Baker flashiness index (climate scenarios only; percent relative to current conditions) for selected downstream stations.....	7-14
7-12.	Simulated total suspended solids load (climate scenarios only; percent relative to current conditions) for selected downstream stations.....	7-15
7-13.	Simulated total phosphorus load (climate scenarios only; percent relative to current conditions) for selected downstream stations.....	7-16
7-14.	Simulated total nitrogen load (climate scenarios only; percent relative to current conditions) for selected downstream stations.....	7-17
7-15.	Projected mid-21 st century impervious cover changes in study areas from ICLUS for A2 emissions storyline.....	7-21
7-16.	Simulated response to projected 2050 changes in urban and residential development (percent or days relative to current conditions) for selected downstream stations.....	7-22
7-17.	Simulated range of responses of mean annual streamflow to mid-21 st century climate and land-use change at the HUC-8 and larger spatial scale.....	7-25
7-18.	Simulated total streamflow volume (climate and land-use change scenarios; percent relative to current conditions) for selected downstream stations.....	7-27
7-19.	Simulated 7-day low flow (climate and land-use change scenarios; percent relative to current conditions) for selected downstream stations.....	7-30
7-20.	Simulated 100-year peak flow (log-Pearson III; climate and land-use change scenarios; percent relative to current conditions) for selected downstream stations.....	7-33
7-21.	Simulated change in the number of days to streamflow centroid (climate and land-use change scenarios; relative to current conditions) for selected downstream stations.....	7-36
7-22.	Simulated Richards-Baker flashiness index (climate and land-use change scenarios; percent relative to current conditions) for selected downstream stations.....	7-39
7-23.	Coefficient of variation of SWAT-simulated changes in streamflow by study area in response to the six NARCCAP climate change scenarios for selected downstream stations.....	7-43

LIST OF TABLES (continued)

7-24. Coefficient of variation of SWAT-simulated changes in streamflow by
NARCCAP climate scenario for selected downstream stations 7-44

7-25. Simulated total suspended solids load (climate and land-use change scenarios;
percent relative to current conditions) for selected downstream stations 7-45

7-26. Simulated total phosphorus load (climate and land-use change scenarios; percent
relative to current conditions) for selected downstream stations 7-48

7-27. Simulated total nitrogen load (climate and land-use change scenarios; percent
relative to current conditions) for selected downstream stations 7-51

7-28. Simulated percent changes in water balance statistics for study areas (NARCCAP
climate with land-use change scenarios; median percent change relative to current
conditions) 7-54

LIST OF FIGURES

3-1.	Locations of the 20 study areas with HUC 8-digit watershed boundaries.....	3-2
3-2.	Distribution of precipitation and temperature among the study areas.	3-3
3-3.	Apalachicola-Chattahoochee-Flint basins study area.	3-9
3-4.	Arizona: Salt and Verde River section of study area.	3-10
3-5.	Arizona: San Pedro River section of study area.	3-11
3-6.	Cook Inlet basin study area.	3-12
3-7.	Georgia-Florida Coastal Plain study area.	3-13
3-8.	Illinois River basin study area.	3-14
3-9.	Lake Erie drainages study area.	3-15
3-10.	Lake Pontchartrain drainage study area.	3-16
3-11.	Minnesota River basin study area.	3-17
3-12.	Nebraska: Loup and Elkhorn River basins study area.	3-18
3-13.	New England Coastal basins study area.	3-19
3-14.	Powder and Tongue River basins study area.	3-20
3-15.	Rio Grande Valley study area.	3-21
3-16.	Sacramento River basin study area.	3-22
3-17.	Southern California Coastal basins study area.	3-23
3-18.	South Platte River basin study area.	3-24
3-19.	Susquehanna River basin study area.	3-25
3-20.	Tar and Neuse River basins study area.	3-26
3-21.	Trinity River basin study area.	3-27
3-22.	Upper Colorado River basin study area.	3-28
3-23.	Willamette River basin study area.	3-29
4-1.	Example of weak correlation of rainfall and flow in the Dismal River at Thedford, NE (USGS 06775900) in the Loup River basin.	4-24
6-1.	Comparison of model calibration fit to streamflow for the calibration initial site.	6-4
6-2.	Sensitivity of model fit for total streamflow volume to temporal change.	6-5
6-3.	Sensitivity of model fit for streamflow to spatial change.	6-5
6-4.	Comparison of baseline adjusted model fit efficiency for total suspended solids monthly loads for calibration site (left) and downstream site (right).	6-6
6-5.	Comparison of baseline adjusted model fit efficiency for total phosphorus monthly loads for calibration site (left) and downstream site (right).	6-6
6-6.	Comparison of baseline adjusted model fit efficiency for total nitrogen monthly loads for calibration site (left) and downstream site (right).	6-6
6-7.	SWAT and HSPF simulated changes in total streamflow in pilot watersheds (expressed relative to current conditions).	6-7
6-8.	SWAT and HSPF simulated changes in TSS at downstream station in pilot watersheds (expressed relative to current conditions).	6-9
6-9.	SWAT and HSPF simulated changes in total phosphorus load in pilot watersheds (expressed relative to current conditions).	6-11
6-10.	SWAT and HSPF simulated changes in total nitrogen load in pilot watersheds (expressed relative to current conditions).	6-12

LIST OF FIGURES (continued)

6-11.	Differences between SWAT projections of mid-21 st century streamflow and water quality (median across six NARCCAP scenarios) with and without representation of increased atmospheric CO ₂	6-14
6-12.	Consistency in SWAT model projections of mean annual streamflow at downstream stations with downscaled (NARCCAP, BCSD) and GCM projections of the GFDL GCM.....	6-20
6-13.	Consistency in SWAT model projections of mean annual streamflow at downstream stations with downscaled (NARCCAP, BCSD) and GCM projections of the CGCM3 GCM.	6-21
7-1.	Ratio of winter (January–March) to summer (July–September) runoff volume under current and mid-21 st century NARCCAP climate scenarios.	7-19
7-2.	Box plots of the distribution of the ratio of winter (January–March) to summer (July–September) runoff volume normalized to the ratio under current conditions.	7-20
7-3.	Comparison of simulated responses of mean annual streamflow to urban development and climate change scenarios—HSPF model.....	7-24
7-4.	Simulated total future streamflow volume relative to current conditions (NARCCAP climate scenarios with urban development) for selected stations.....	7-28
7-5.	Median simulated percent changes in total future streamflow volume for six NARCCAP scenarios relative to current conditions by HUC-8 (median of NARCCAP climate scenarios with urban development).....	7-29
7-6.	Simulated 7-day low flow relative to current conditions (NARCCAP climate scenarios with urban development) for selected downstream stations.	7-31
7-7.	Median simulated percent changes in 7-day average low flow volume for six NARCCAP scenarios relative to current conditions by HUC-8 (median of NARCCAP climate scenarios with urban development).....	7-32
7-8.	Simulated 100-year peak flow relative to current conditions (NARCCAP climate scenarios with urban development) for selected downstream stations.	7-34
7-9.	Median simulated percent changes in 100-year peak flow for six NARCCAP scenarios relative to current conditions by HUC-8 (median of NARCCAP climate scenarios with urban development).	7-35
7-10.	Simulated change in days to streamflow centroid relative to current conditions (NARCCAP climate scenarios with urban development) for selected downstream stations.	7-37
7-11.	Median simulated change in the number of days to streamflow centroid for six NARCCAP scenarios relative to current conditions by HUC-8 (median of NARCCAP climate scenarios with urban development).....	7-38
7-12.	Simulated Richards-Baker flashiness index relative to current conditions (NARCCAP climate scenarios with urban development) for selected downstream stations.	7-40
7-13.	Simulated absolute changes in the Richards-Baker flashiness index for six NARCCAP scenarios relative to current conditions by HUC-8 (median of NARCCAP climate scenarios with urban development).....	7-41

LIST OF FIGURES (continued)

7-14.	Simulated total suspended solids load relative to current conditions (NARCCAP climate scenarios with urban development) for selected downstream stations.	7-46
7-15.	Median simulated percent changes in total suspended solids loads for six NARCCAP scenarios relative to current conditions by HUC-8 (median of NARCCAP climate scenarios with urban development) for selected downstream stations.	7-47
7-16.	Simulated total phosphorus load relative to current conditions (NARCCAP climate scenarios with urban development) for selected downstream stations.	7-49
7-17.	Median simulated percent changes in total phosphorus loads for six NARCCAP scenarios relative to current conditions by HUC-8 (median of NARCCAP climate scenarios with urban development).	7-50
7-18.	Simulated total nitrogen load relative to current conditions (NARCCAP climate scenarios with urban development) for selected downstream stations.	7-52
7-19.	Median simulated percent changes in total nitrogen loads for six NARCCAP scenarios relative to current conditions by HUC-8 (median of NARCCAP climate scenarios with urban development).	7-53
7-20.	Median simulated percent changes in watershed Dryness Ratio for six NARCCAP scenarios relative to current conditions (median of NARCCAP climate scenarios with urban development).	7-55
7-21.	Median simulated percent changes in watershed Low Flow Sensitivity for six NARCCAP scenarios relative to current conditions (median of NARCCAP climate scenarios with urban development).....	7-56
7-22.	Median simulated percent changes in watershed Surface Runoff Fraction for six NARCCAP scenarios relative to current conditions (median of NARCCAP climate scenarios with urban development).....	7-57
7-23.	Median simulated percent changes in watershed Snowmelt Fraction for six NARCCAP scenarios relative to current conditions (median of NARCCAP climate scenarios with urban development).....	7-58
7-24.	Median simulated percent changes in watershed Deep Recharge for six NARCCAP scenarios relative to current conditions (median of NARCCAP climate scenarios with urban development).....	7-59

LIST OF ABBREVIATIONS

ACE	air, climate, and energy
AET	actual evapotranspiration
ANOVA	analysis of variance
BASINS	Better Assessment Science Integrating Point and Nonpoint Sources
BCSD	bias-corrected and statistically downscaled
CAT	Climate Assessment Tool
CCSM	Community Climate System Model
cfs	cubic feet per second
CGCM3	Third Generation Coupled Global Climate Model
CMIP3	Coupled Model Intercomparison Project Phase 3
CN	curve number
CRCM	Canadian Regional Climate Model
CV	coefficient of variation
DEM	digital elevation model
E	Nash-Sutcliffe coefficient of model fit efficiency
E_1'	Garrick's baseline adjusted coefficient of model fit efficiency
ET	evapotranspiration
FTable	hydraulic functional table (in HSPF)
GCM	global climate model
GFDL	Geophysical Fluid Dynamics Laboratory global climate model
GFDL hi res	Geophysical Fluid Dynamics Lab. 50-km global atmospheric time slice model
GIS	geographic information system
HadCM3	Hadley Centre Coupled Model, version 3
HRM3	Hadley Region Model 3
HRU	hydrologic response unit
HRU	Hydrologic response unit
HSG	hydrologic soil group
HSPF	Hydrologic Simulation Program—FORTRAN
HUC	hydrologic unit code
HUC-2	HUC 2-digit watershed
HUC-4	HUC 4-digit watershed
HUC-8	HUC 8-digit watershed
HUC-10	HUC 10-digit watershed
ICLUS	Integrated Climate and Land Use Scenarios
IMPLND	impervious land segment (in HSPF)
INFILT	nominal infiltration rate parameter (in HSPF)
IPCC	Intergovernmental Panel on Climate Change
LZETP	lower zone evapotranspiration parameter
LZSN	lower soil zone nominal soil moisture storage
MSL	mean sea level
MUSLE	Modified Universal Soil Loss Equation
NARCCAP	North American Regional Climate Change Assessment Program
NARR	North American Regional Reanalysis
NCAR	National Center for Atmospheric Research

LIST OF ABBREVIATIONS (continued)

ND	no data
NHD	National Hydrography Dataset
NLCD	National Land Cover Dataset
NRCS	Natural Resource Conservation Service
PCS	Permit Compliance System
PERLND	pervious land segment (in HSPF)
PET	potential evapotranspiration
PRMS	Precipitation Runoff Modeling System
QAPP	Quality Assurance Project Plan
RCHRES	stream reach segment (in HSPF)
RCM	regional climate model
RCM3	Regional Climate Model, version 3
SERGoM	Spatially Explicit Regional Growth Model
SPARROW	Spatially-Referenced Regression On Watershed attributes
STATSGO	State Soil Geographic Database
SWAT	Soil Water Assessment Tool
TMDL	total maximum daily load
TN	total nitrogen
TP	total phosphorus
TSS	total suspended solids
UCI	user control input file (in HSPF)
U.S. EPA	U.S. Environmental Protection Agency
USGS	U.S. Geological Survey
USLE	Universal Soil Loss Equation
WDM	watershed data management binary file (for HSPF)
WinHSPF	Windows interface to Hydrologic Simulation Program—FORTRAN
WRFP	Weather Research and Forecasting Model
WXGEN	weather generator (in SWAT)

PREFACE

This report was prepared by U.S. Environmental Protection Agency (EPA)'s Air, Climate, and Energy (ACE) research program, located within the Office of Research and Development. The ACE research program is designed to address the increasingly complex environmental issues we face in the 21st century. The overarching vision of ACE is to provide the cutting-edge scientific information and tools to support EPA's strategic goals of protecting and improving air quality and taking action on climate change in a sustainable manner.

Climate change presents a risk to the availability and quality of water resources necessary to support people and the environment. EPA, with Contractor support from Tetra Tech, Inc., recently completed a large-scale modeling effort to assess the sensitivity of streamflow and water quality in different regions of the nation to a range of mid-21st century climate change and urban development scenarios. This report describes the methods, models, scenarios, and results of this project.

Responding to climate change is a complex issue. The information in this report is intended to inform and help build the capacity of EPA and EPA clients to understand and respond to the challenge of climate change. This final report reflects consideration of peer review and public comments received on an External Review Draft report released in March, 2013 (EPA/600/R-12/058A).

AUTHORS, CONTRIBUTORS AND REVIEWERS

The National Center for Environmental Assessment, Office of Research and Development, was responsible for preparing this final report. An earlier draft report was prepared by Tetra Tech, Inc., under EPA Contracts EP-C-05-061 and EP-C-08-004.

AUTHORS

Tetra Tech, Inc.

Jonathan Butcher

Andrew Parker

Saumya Sarkar

Scott Job

Mustafa Faizullabhoy

Peter Cada

Jeremy Wyss

Texas A&M University

Raghavan Srinivasan

Pushpa Tuppad

Deb Debjani

AQUA TERRA Consultants

Anthony Donigian

John Imhoff

Jack Kittle

Brian Bicknell

Paul Hummel

Paul Duda

U.S. Environmental Protection Agency, Office of Research and Development

Thomas Johnson

Chris Weaver

Meredith Warren (ORISE Fellow)

Daniel Nover (AAAS Fellow)

REVIEWERS

This report was much improved by many excellent and thoughtful comments provided by reviewers Dao Nguyen Khoi, Timothy Randhir, Susanna Tak Yung Tong, and Chong-Yu Xu. We are also grateful for comments on an earlier draft of this report provided by EPA staff David Bylsma, Chris Clark, and Steve Klein.

ACKNOWLEDGEMENTS

We acknowledge and thank the entire project team at Tetra Tech, Inc., Texas A&M University, AQUA TERRA, Stratus Consulting, and FTN Associates for their support contributing to the development of this report. We also thank Seth McGinnis of the National Center for Atmospheric Research (NCAR) for processing the North American Regional Climate Change Assessment Program (NARCCAP) output into change statistics for use in the watershed modeling. NCAR is supported by the National Science Foundation. We acknowledge the modeling groups, the Program for Climate Model Diagnosis and Intercomparison and the WCRP's Working Group on Coupled Modeling for their roles in making available the WCRP Coupled Model Intercomparison Project Phase 3 (CMIP3) multimodel data set. Support of this data set is provided by the Office of Science, U.S. Department of Energy.

1. EXECUTIVE SUMMARY

There is growing concern about the potential effects of climate change on water resources. The 2007 Fourth Assessment Report of the Intergovernmental Panel on Climate Change (IPCC) states that warming of the climate system is now unequivocal (IPCC, 2007). Regionally variable changes in the amount and intensity of precipitation have also been observed in much of the United States (Groisman et al., 2012). Climate modeling experiments suggest these trends will continue throughout the 21st century, with continued warming accompanied by a general intensification of the global hydrologic cycle (IPCC, 2007; Karl et al., 2009; Kharin et al., 2013). Over the same time horizon, human population is expected to continue to increase, with accompanying changes in land use and increased demand on water resources. In many areas, climate change is expected to exacerbate current stresses on water resources from population growth and economic and land-use change, including urbanization (IPCC, 2007). Responding to this challenge requires an improved understanding of how we are vulnerable and development of strategies for managing future risk.

This report describes watershed modeling in 20 large, U.S. drainage basins (6,000–27,000 mi²) to characterize the sensitivity of streamflow, nutrient (nitrogen and phosphorus), and sediment loading to a range of potential mid-21st century climate futures; to assess the potential interaction of climate change and urbanization in these basins; and to improve our understanding of methodological challenges associated with integrating existing tools (e.g., climate models, downscaling approaches, and watershed models) and data sets to address these scientific questions.

Study areas were selected to represent a range of geographic, hydroclimatic, physiographic, and land-use conditions, while also meeting practical criteria such as the availability of data to calibrate and validate watershed models. Climate change scenarios are based on mid-21st century climate model projections downscaled with regional climate models (RCMs) from the North American Regional Climate Change Assessment Program (NARCCAP; Mearns, 2009) and the bias-corrected and statistically downscaled (BCSD) data set described by Maurer et al. (2007). Urban and residential development scenarios are based on the U.S. Environmental Protection Agency (EPA)'s national-scale Integrated Climate and Land Use Scenarios (ICLUS) project (U.S. EPA, 2009c). Watershed modeling was conducted using the Hydrologic Simulation Program—FORTRAN (HSPF) and Soil and Water Assessment Tool (SWAT) watershed models.

Climate change scenarios based on global climate model (GCM) simulations in the NARCCAP and BCSD data sets project a continued general warming trend throughout the nation over the next century, although the magnitude of the warming varies from place to place. Wetter winters and earlier snowmelt are likely in many of the northern and higher elevation watersheds. Changes in other aspects of local climate, such as the timing and intensity of precipitation, show greater variability and uncertainty. ICLUS urban and residential development scenarios project continued growth in urban and developed land over the next century throughout the nation with most growth occurring in and around existing urban areas. Model simulations of watershed response to these changes provide a national-scale perspective on the range of potential changes in streamflow and water quality in different regions of the nation. Simulations evaluating the

variability in watershed response using different approaches for downscaling climate data and different watershed models provide guidance on the use of existing models and data sets for assessing climate change impacts. Key findings are summarized below.

There is a high degree of regional variability in the model simulated responses of different streamflow and water quality endpoints to a range of potential mid-21st century climatic conditions throughout the nation. Comparison of watershed simulations in all 20 study areas for the 2041–2070 time horizon suggests the following hydrologic changes may occur:

- Potential streamflow volume decreases in the Rockies and interior southwest, and increases in the east and southeast coasts.
- Higher peak streamflow will increase erosion and sediment transport; loads of nitrogen and phosphorus are also likely to increase in many watersheds.
- Many watersheds are likely to experience significant changes in the timing of streamflow and pollutant delivery. In particular, there will be a tendency to shift from snowmelt-dominated spring runoff systems to rain-dominated systems with greater winter runoff.
- Changes in nutrient and sediment loads are generally correlated with changes in hydrology.

Changes in watershed water balance and hydrologic processes are likely in many regions of the nation. Changes in streamflow are determined by the interaction of changes in precipitation and evapotranspiration (ET). Model simulations in this study suggest that in many regions of the nation, the fraction of streamflow derived from surface stormflow will increase, while groundwater-supported baseflow and recharge to deep groundwater aquifers may decrease.

The simulated responses of streamflow and water quality endpoints to climate change scenarios based on different climate models and downscaling methodologies span a wide range in many cases and sometimes do not agree in the direction of change. The ultimate significance of any given simulation of future change will depend on local context, including the historical range of variability, thresholds and management targets, management options, and interaction with other stressors. The simulation results in this study do, however, clearly illustrate that the potential streamflow and water quality response in many areas could be large. Given these uncertainties, successful climate change adaptation strategies will need to encompass practices and decisions to reduce vulnerabilities and risk across a range of potential future climatic conditions.

Simulated responses to increased urban development scenarios are small relative to those resulting from climate change at the scale of modeling in this study. This is likely due to the relatively small changes in developed lands as a percent of total watershed area at the large spatial scale of watersheds in this study. The finest spatial scale reported in this study is that of an 8-digit hydrologic unit code (HUC), and most urbanized areas are located on larger rivers

downstream of multiple 8-digit HUCs. Over the whole of individual study areas, urban and residential growth scenarios represented changes in the amount of developed land on the order of <1 to about 12% of total watershed area, and increases in impervious surfaces on the order of 0 to 5% of total watershed area. As would be expected, such small changes in development did not have a large effect on streamflow or water quality at larger spatial scales. It is well documented, however, that urban and residential development at higher levels can have significant impacts on streamflow and water quality. At smaller spatial scales where changes in developed lands represent a larger percentage of watershed area, the effects of urbanization are likely to be greater. The scale at which urbanization effects may become comparable to the effects of a changing climate is uncertain.

Simulation results are sensitive to methodological choices such as different approaches for downscaling global climate change simulations and use of different watershed models.

Watershed simulations in this study suggest that the variability in watershed response resulting from a single GCM downscaled using different RCMs can be of the same order of magnitude as the ensemble variability between the different GCMs evaluated. Watershed simulations using different models with different structures and methods for representing watershed processes (HSPF and SWAT in this study) also resulted in increased variability of outcomes. SWAT simulations accounting for the influence of increased atmospheric carbon dioxide (CO₂) on evapotranspiration significantly affected results. One notable insight from these results is that, in many watersheds, increases in precipitation amount and/or intensity, urban development, and atmospheric CO₂ can have similar or additive effects on streamflow and pollutant loading (e.g., a flashier runoff response with higher high and lower low flows).

Significance and next steps. The model simulations in this study contribute to a growing understanding of the complex and context-dependent relationships between climate change, land-use change, and water resources in different regions of the nation. As a first order conclusion, results indicate that in many locations future conditions are likely to be different from past experience. In the context of decision making, being aware and planning for this uncertainty is preferable to accepting a position that later turns out to be incorrect. Results also provide a plausible envelope on the range of streamflow and water quality responses to mid-21st century climate change and urban development in different regions of the nation. In addition, in many study areas the simulations suggest a likely direction of change of streamflow and water quality endpoints. This information can be useful in planning for anticipated but uncertain future conditions. Sensitivity studies evaluating the implications of different methodological choices help to improve the scientific foundation for conducting climate change impacts assessments, thus building the capacity of the water management community to understand and respond to climate change.

Understanding and responding to climate change is complex, and this study is only an incremental step towards fully addressing these questions. It must be stressed that results are conditional upon the methods, models, and scenarios used in this study. Scenarios represent a plausible range but are not comprehensive of all possible futures. Several of the study areas are also complex, highly managed systems; all infrastructure and operational aspects of water management are not represented in full detail. Successful climate change adaptation strategies will need to encompass practices and decisions to reduce vulnerabilities across a wide range of plausible future climatic conditions. It is the ultimate goal of this study to build awareness of the

potential range of future watershed response so that where simulations suggest large and potentially disruptive changes, the management community will respond to build climate resiliency.

2. INTRODUCTION

It is now generally accepted that human activities including the combustion of fossil fuels and land-use change have resulted, and will continue to result, in long-term changes in climate (IPCC, 2007; Karl et al., 2009). The 2007 Fourth Assessment Report of the IPCC states that “warming of the climate system is unequivocal, as is now evident from observations of increases in global average air and ocean temperatures, widespread melting of snow and ice and rising global average sea level” (IPCC, 2007). Regionally variable changes in the amount and intensity of precipitation have also been observed in much of the United States (Allan and Soden, 2008; Groisman et al., 2012). Climate modeling experiments suggest these trends will continue throughout the 21st century, with continued warming accompanied by a general intensification of the global hydrologic cycle (IPCC, 2007; Karl et al., 2009; Kharin et al., 2013; Emori and Brown, 2005). While uncertainty remains, particularly for precipitation changes at regional spatial scales, the presence of long-term trends in the record suggests many parts of the United States could experience future climatic conditions unprecedented in recent history.

Water managers are faced with important questions concerning the implications of climate change for water resources. Changes in climate will vary over space and time. The hydrologic response to climate change will be further influenced by the attributes of specific watersheds, including physiographic setting, land use, pollutant sources, and human use and management of water. Runoff is generally expected to increase at higher latitudes and in some wet tropical areas, and decrease over dry and semiarid regions at mid-latitudes due to decreases in rainfall and higher rates of evapotranspiration (IPCC, 2007; Karl et al., 2009). Northern and mountainous areas that receive snow in the winter are likely to see increased precipitation occurring as rain versus snow. In addition, most regions of the United States are anticipated to experience increasing intensity of precipitation events; that is, warming-induced intensification of the global hydrologic cycle will increase the fraction of total precipitation occurring in large magnitude events. Precipitation changes can result in hydrologic effects that include changes in the amount and seasonal timing of streamflow, changes in soil moisture and groundwater recharge, changes in land cover and watershed biogeochemical cycling, changes in nonpoint pollutant loading to water bodies, and increased demands on water infrastructure, including urban stormwater and other engineered systems. Regions exposed to increased storm intensity could experience increased coastal and inland flooding. Such changes challenge the assumption of stationarity that has been the foundation for water management for decades (e.g., Milly et al., 2008).

Changes in climate and hydrology will also affect water quality. Although less studied, potential effects include changes in stream temperature and hydrologic controls on nutrient, sediment, and dissolved constituent loads to water bodies. Hydrologic changes associated with climate change could also influence pollutant loading from urban and agricultural lands. Previous studies illustrate the sensitivity of stream nutrient loads, sediment loads, and ecologically relevant streamflow characteristics to changes in climate (e.g., see Poff et al., 1996; Williams et al., 1996; Murdoch et al., 2000; Monteith et al., 2000; Chang et al., 2001; Bouraoui et al., 2002; SWCS, 2003; Marshall and Randhir, 2008; Wilson and Weng, 2011; Tong et al., 2011). A review (Whitehead et al., 2009) details progress on these questions but emphasizes that still relatively little is known about the link between climate change and water quality.

Many watersheds are currently impacted by existing stressors, including land-use change, water withdrawals, pollutant discharges, and other factors. It is important to recognize that climate change will not act independently, but will interact in complex and poorly understood ways with existing and future changes in nonclimatic stressors. One area of concern is the interaction of climate change and urban development in different watershed settings. Throughout this century, urban and residential development is expected to increase throughout much of the nation (U.S. EPA, 2009c). Stormwater runoff from roads, rooftops, and other impervious surfaces in urban and residential environments is a well-known cause of stream impairment (Walsh et al., 2005; Paul and Meyer, 2001). Changes in rainfall associated with climate change will have a direct effect on stormwater runoff (Pyke et al., 2011). More generally, changes in climate could exacerbate or ameliorate the impacts of other nonclimatic stressors. This understanding is particularly important because in many situations, the only viable management strategies for adapting to future climatic conditions involve improved methods for managing and addressing nonclimatic stressors.

Understanding and adapting to climate change is complicated by the scale, complexity, and inherent uncertainty of the problem. We currently have a limited ability to predict long-term (multidecadal) future climate at the local and regional scales needed by decision makers (Sarewitz et al., 2000). It is therefore not possible to know with certainty the future climatic conditions to which a particular watershed will be exposed. Scenario analysis using simulation models is a useful and common approach for assessing vulnerability to plausible but uncertain future conditions (Lempert et al., 2006; Sarewitz et al., 2000; Volkery and Ribeiro, 2009). Evaluation of multiple scenarios can provide understanding of the complex interactions associated with watershed response to climate change and other watershed stressors, and identify uncertainties associated with changes in different drivers (such as climate and land-use change) and uncertainties associated with different analytical approaches and methods. This information is useful for developing an improved understanding of system behavior and sensitivity to a wide range of plausible future climatic conditions and events, identifying how we are vulnerable to these changes, and ultimately to guide the development of robust strategies for reducing risk in the face of changing climatic conditions (Sarewitz et al., 2000; Lempert et al., 2006; Johnson and Weaver, 2009).

2.1. ABOUT THIS REPORT

This report describes the structure—including methods, models, scenarios, and results—of a large-scale watershed modeling study designed to address gaps in our knowledge of the sensitivity of U.S. streamflow, nutrient (nitrogen and phosphorus), and sediment loading to potential mid-21st century climate change. Modeling also considers the potential interaction of climate change with future urban and residential development in these watersheds and provides insights concerning the effects of different methodological choices (e.g., method of downscaling climate change data, choice of watershed model, etc.) on simulation results.

Watershed modeling was conducted in 20 large U.S. watersheds using a scenario analysis approach. Study sites were selected to represent a range of geographic, hydrologic, and climatic characteristics throughout the nation.

Model projections consider the effects of climate change alone, urban and residential development alone, and the combined effects of climate change and urban development on

streamflow, total nitrogen (TN), total phosphorus (TP), and total suspended solids (TSS) loads. Climate change scenarios were based on downscaled climate model projections from two sources; the NARCCAP and the BCSD archive from the Bureau of Reclamation/Santa Clara University/Lawrence Livermore. Scenarios of urban and residential development were based on projections from EPA's ICLUS project.

All 20 watersheds were modeled with the SWAT model using a consistent set of climate and land-use change scenarios. In a subset of five study watersheds, referred to as pilot sites, additional simulations were conducted to address methodological questions related to the conduct of climate change impacts assessments. In these watersheds, a second watershed model, the HSPF, was run using the same climate and land-use scenarios used with SWAT to assess the influence of different watershed models on watershed simulations. Pilot watersheds were also evaluated for additional climate change scenarios to assess hydroclimatic sensitivity to different methods of downscaling climate data. All watershed models are constructed at a scale approximating HUC-10s, but the finest spatial resolution of model calibration and output was on the order of HUC-8 watersheds.

As with any study of this type, simulation results are conditional on the specific methods, models, and scenarios used. Given the difficulty and level of effort involved with modeling at this scale, it was necessary to standardize model development for efficiency. Several of the study areas are complex, highly managed systems. We do not attempt to represent all these operational aspects in full detail. Future changes in agriculture and human use and management of water were also not evaluated.

This report consists of a main volume and 26 appendices. The main volume describes the study methods, models, scenarios, and results. The appendices contain additional information on model setup, calibration, and additional modeling results (at HUC 8-digit spatial scale) not included in the main report. Supplementary data sets summarizing SWAT simulation results at all 20 study areas are also available at EPA's ICLUS web page <http://map3.epa.gov/ICLUSonline/>.

3. STUDY AREAS

This project evaluates watershed response to climate change and urban development scenarios in 20 large drainage basins, ranging in size from approximately 6,000 to 27,000 mi², located throughout the contiguous United States and Alaska (see Figure 3-1 below). Study areas were selected based on both geographic and practical considerations. Sites were selected to represent a broad range of geographic, physiographic, land use, and hydroclimatic settings (see Table 3-1). Site selection also considered the availability of necessary data for calibration and validation of watershed models, including a selection of U.S. Geological Survey (USGS) streamflow monitoring gages (at varying spatial scales) and an adequate set of water quality monitoring data (e.g., USGS National Water Quality Assessment study areas). Finally, study areas were selected to leverage, where possible, preexisting calibrated watershed models.

The 20 study areas selected cover a wide range of geology and climate (see Table 3-1), with elevations ranging from sea level to over 14,000 feet, average annual temperatures from 34 to 68°F, and average annual precipitation ranging from 15 to 66 inches. Figure 3-2 shows the distribution of average annual precipitation and temperature among the study sites, indicating a wide range of climatic conditions, from dry to wet and cold to warm. The ratio of winter (January–March) to summer (July–September) precipitation varies from about 0.1 to 11 while the fraction of runoff derived from snowmelt ranges from 0 to 54%. The study areas also sample all of the Level I ecoregions in the contiguous United States (CECWG, 1997), with the exception of the Tropical Wet Forests ecoregion (present within the contiguous United States only in southern Florida). Many of the study areas are in the Eastern Temperate Forests ecoregion, but this region occupies most of the eastern half of the contiguous United States.

The selected study areas also cover a range of land-use conditions, with agricultural land occupying from 0 to 78% of the land area and urbanized areas (impervious plus developed pervious land) occupying up to 38%. Overall imperviousness of the study areas (at approximately the HUC-4 scale) ranges from near zero to about 14%; however, individual subwatersheds within a study area have substantially greater imperviousness. For instance, within the Apalachicola-Chattahoochee-Flint River watersheds (ACF) study area the individual modeling subbasins (at approximately the HUC-10 scale) range from 0.15 to 27.44% impervious.

A detailed summary of current land use and land cover in the 20 study areas is shown in Table 3-2, based on 2001 data from the National Land Cover Dataset (NLCD).

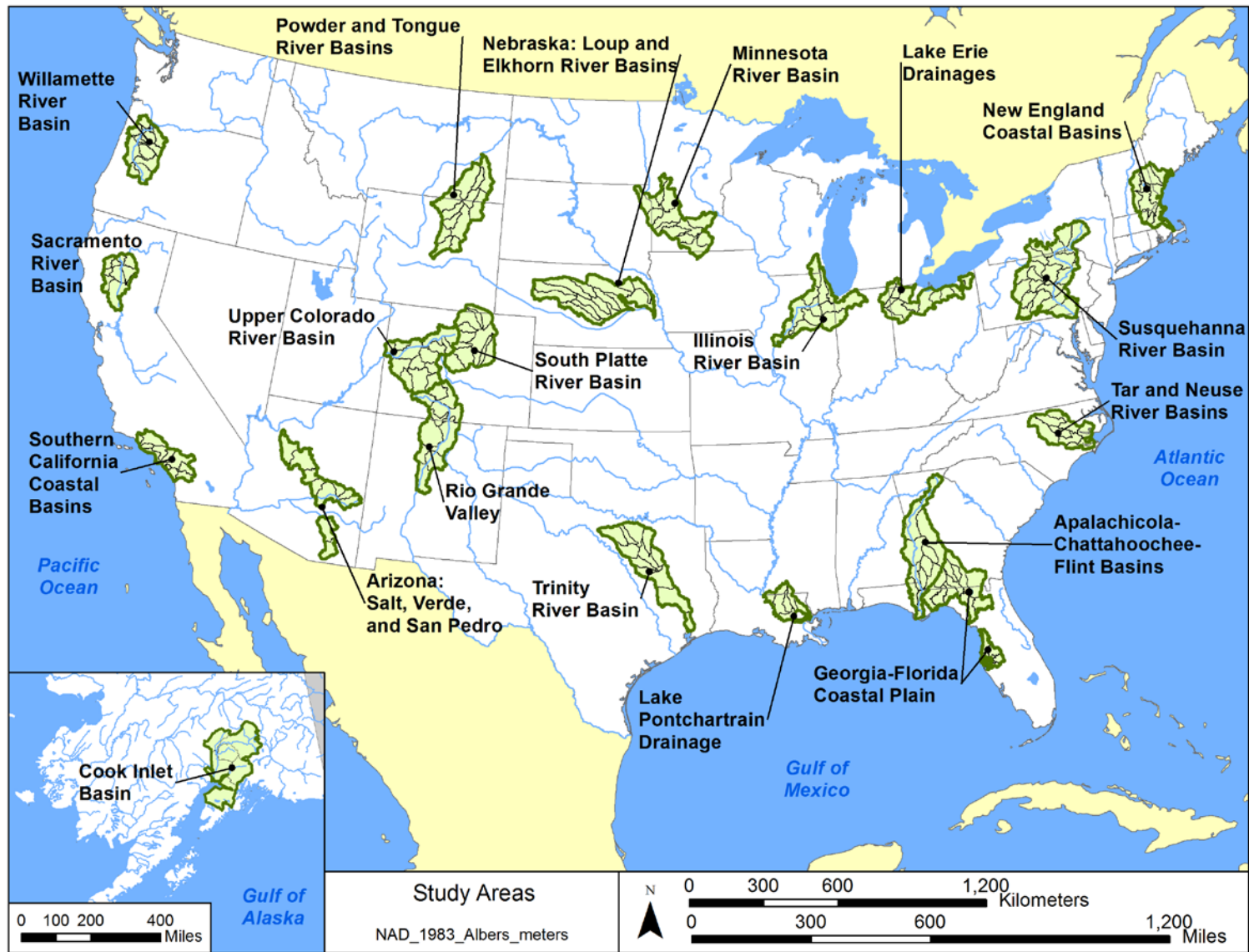


Figure 3-1. Locations of the 20 study areas with HUC 8-digit watershed boundaries.

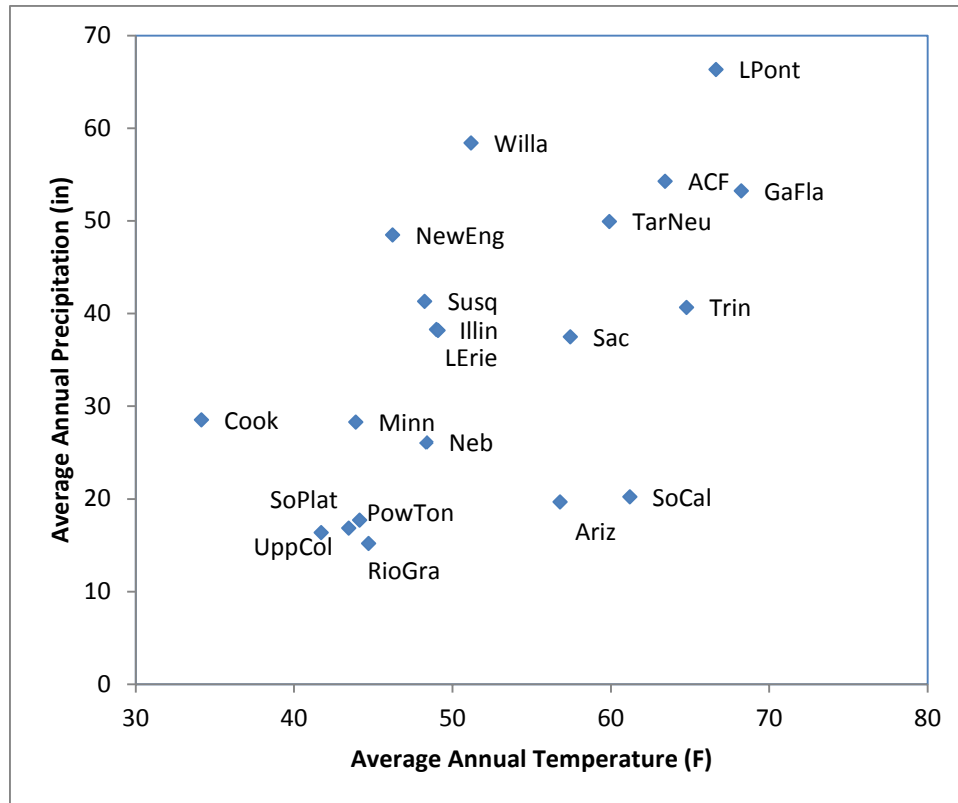


Figure 3-2. Distribution of precipitation and temperature among the study areas.

Note: Precipitation and temperature are averages over the weather stations used in simulation for the modeling period (approximately 1970–2000, depending on model area).

The USGS (Seaber et al., 1987) has classified watershed drainage areas in a hierarchical system in which each hydrologic unit is assigned a Hydrologic Unit Code (HUC). The first four levels of the hierarchy (occupying eight digits) identify the region (HUC-2), subregion (HUC-4), basin (HUC-6), and subbasin (HUC-8). The United States contains 222 HUC-4s with an average size of 16,800 mi². The 20 study areas selected for this study are of a similar scale to HUC-4 basins, ranging in size from approximately 6,000 to 27,000 mi², but do not correspond exactly with the boundaries of established HUC-4 basins. Each study area comprises from 7 to 19 HUC 8-digit watersheds. The individual HUC 8-digit watersheds in the study areas have a median size of 1,164 mi², and an interquartile range from 805 to 1,808 mi². In some cases study areas are composed of a single, contiguous watershed. In other cases, study areas include several adjacent but noncontiguous watersheds (e.g., separate rivers draining to the coast). Where possible, watersheds strongly influenced by upstream dams, diversions, or other human interventions were avoided to simplify modeling.

Maps of the individual study areas are provided in Figures 3-3 through 3-23. Detailed descriptions of each study area are presented in Appendices D through W, which describe model development and calibration for the individual study areas.

Table 3-1. Summary of the 20 study areas

Study area	Site ID	Location (states)	Total area (mi ²)	Elevation range (ft MSL)	Average precip (in/yr)	Average temp (°F)	Ratio winter to summer runoff	Fraction of runoff as snowmelt (%)	Level I ecoregions	Major cities
Apalachicola-Chattahoochee-Flint Basins (Pilot Site)	ACF	GA, AL, FL	19,283	0–4,347	54.26	63.43	2.01	0.7	Eastern Temperate Forests	Atlanta, GA
Arizona: Salt, Verde, and San Pedro (Pilot Site)	Ariz	AZ	14,910	1,918–11,407	19.67	56.81	2.06	9.3	Temperate Sierras, Southern Semi-arid Highlands, North America Deserts	Flagstaff, AZ; Sierra Vista, AZ
Cook Inlet Basin	Cook	AK	22,243	0–18,882	28.50	34.16	0.11	53.8	Marine West Coast Forests, Northwest Forested Mountains	Anchorage, AK
Georgia-Florida Coastal Plain	GaFla	GA, FL	17,541	0–485	53.21	68.24	1.29	0.1	Eastern Temperate Forests	Tallahassee, FL; Tampa, FL
Illinois River Basin	Illin	IL, IN, WI	17,004	365–1,183	38.25	49.00	1.24	13.3	Eastern Temperate Forests	Chicago, IL; Milwaukee, WI; Peoria, IL
Lake Erie Drainages	LErie	OH, IN, MI	11,682	339–1,383	38.15	49.10	2.60	13.4	Eastern Temperate Forests	Fort Wayne, IN; Cleveland, OH; Akron, OH
Lake Pontchartrain Drainage	LPont	LA, MS	5,852	0–502	66.33	66.64	1.70	0.5	Eastern Temperate Forests	New Orleans, LA; Baton Rouge, LA
Minnesota River Basin (Pilot Site)	Minn	MN, IA, SD	16,989	683–2,134	28.26	43.90	0.50	14.8	Great Plains, Eastern Temperate Forests	Mankato, MN, Minneapolis, MN

Table 3-1. Summary of the 20 study areas (continued)

Study area	Site ID	Location (states)	Total area (mi ²)	Elevation range (ft MSL)	Average precip (in/yr)	Average temp (°F)	Ratio winter to summer runoff	Fraction of runoff as snowmelt (%)	Level I ecoregions	Major cities
Nebraska: Loup and Elkhorn River Basins	Neb	NE	22,095	1,069–4,292	26.10	48.35	0.91	12.6	Great Plains	No major cities
New England Coastal Basins	NewEng	MA, NH, ME	10,359	0–5,422	48.45	46.23	1.41	21.1	Northern Forests, Eastern Temperate Forests	Portland, ME, Greater Boston, MA
Powder and Tongue River Basins	PowTon	MT, WY	18,800	2,201–13,138	17.70	44.15	1.18	30.2	Great Plains, North American Deserts, Northwestern Forested Mountains	No major cities
Rio Grande Valley	RioGra	NM, CO	18,959	4,726–14,173	15.18	44.71	0.52	23.8	Northwest Forested Mountains, North American Deserts, Temperate Sierras	Santa Fe, NM; Albuquerque, NM
Sacramento River Basin	Sac	CA	8,316	17–10,424	37.47	57.45	1.61	17.6	Mediterranean California, Northwest Forested Mountains	Chico, CA; Reading, CA
Southern California Coastal Basins	SoCal	CA	8,322	0–11,488	20.21	61.20	5.94	4.9	Mediterranean California	Greater Los Angeles, CA
South Platte River Basin	SoPlat	CO, WY	14,668	4,291–14,261	16.82	43.46	0.49	28.3	Great Plains, Northwest Forested Mountains	Fort Collins, CO; Denver, CO
Susquehanna River Basin (Pilot Site)	Susq	PA, NY, MD	27,504	0–3,141	41.30	48.26	2.06	16.6	Eastern Temperate Forests, Northern Forests	Scranton, PA; Harrisburg, PA

Table 3-1. Summary of the 20 study areas (continued)

Study area	Site ID	Location (states)	Total area (mi ²)	Elevation range (ft MSL)	Average precip (in/yr)	Average temp (°F)	Ratio winter to summer runoff	Fraction of runoff as snowmelt (%)	Level I ecoregions	Major cities
Tar and Neuse River Basins	TarNeu	NC	9,972	0–854	49.91	59.91	1.59	3.3	Eastern Temperate Forests	Raleigh, NC; Durham, NC; Greenville, NC
Trinity River Basin	Trin	TX	17,949	0–2,150	40.65	64.78	1.45	1.6	Great Plains, Eastern Temperate Forests	Dallas, TX
Upper Colorado River Basin	UppCol	CO, UT	17,865	4,323–14,303	16.36	41.73	0.31	42.4	Great Plains, Eastern Temperate Forests	Grand Junction, CO; Edwards, CO
Willamette River Basin (Pilot Site)	Willa	OR	11,209	8–10,451	58.38	51.19	10.99	4.5	Marine West Coast Forests, Northwest Forested Mountains	Portland, OR; Salem, OR; Eugene, OR

MSL = mean sea level

Notes: Precipitation and temperature are averages over the weather stations used in simulation for the modeling period (approximately 1970–2000, depending on model area). The ratio of winter (January–March) to summer (July–September) runoff and the fraction of runoff as snowmelt are derived from the calibrated SWAT model applications described in this report.

Table 3-2. Current (2001) land use and land cover in the 20 study areas

Study area	Total area (mi ²)	Water (%)	Barren (%)	Wetland (%)	Forest (%)	Shrub (%)	Pasture/hay (%)	Cultivated (%)	Developed pervious*	Impervious (%)	Snow/ice (%)
ACF	19,283	1.8	0.4	9.3	47.9	9.6	9.1	12.4	7.3	2.0	0.0
Ariz	14,910	0.2	0.3	0.3	41.9	56.0	0.1	0.1	1.0	0.2	0.0
Cook	22,243	2.55	18.97	7.59	24.10	38.11	0.05	0.11	0.58	0.24	7.70
GaFla	17,541	0.9	0.4	25.7	33.5	10.1	7.2	10.9	8.8	2.5	0.0
Illin	17,004	1.9	0.1	1.4	10.3	2.1	3.6	62.6	11.9	6.2	0.0
LErie	11,682	1.1	0.1	2.7	13.0	1.5	5.8	61.2	11.2	3.5	0.0
LPont	5,852	3.3	0.4	32.3	23.1	14.3	10.3	4.5	8.5	3.2	0.0
Minn	16,989	3.0	0.1	4.9	2.9	4.6	5.9	72.1	5.5	1.1	0.0
Neb	22,095	0.8	0.1	3.2	1.1	64.5	1.1	26.5	2.4	0.4	0.0
NewEng	10,359	4.2	0.5	7.6	63.6	2.2	4.5	1.1	10.8	5.6	0.0
PowTon	18,800	0.1	0.7	1.7	10.0	85.5	0.6	1.0	0.4	0.1	0.0
RioGra	18,959	0.3	1.0	2.1	35.3	54.2	4.1	0.7	1.7	0.5	0.0

Table 3-2. Current (2001) land use and land cover in the 20 study areas (continued)

Study area	Total area (mi ²)	Water (%)	Barren (%)	Wetland (%)	Forest (%)	Shrub (%)	Pasture/hay (%)	Cultivated (%)	Developed pervious*	Impervious (%)	Snow/ice (%)
Sac	8,316	0.5	0.5	2.0	22.4	48.3	2.3	19.7	3.6	0.7	0.0
SoCal	8,322	0.6	0.6	0.4	10.6	50.9	1.0	2.8	19.4	13.8	0.0
SoPlat	14,668	0.9	1.0	2.3	23.7	46.4	1.5	16.5	5.0	2.1	0.7
Susq	27,504	1.1	0.4	1.2	61.1	1.8	17.1	9.8	5.9	1.5	0.0
TarNeu	9,972	4.5	0.2	14.1	33.5	10.0	7.3	21.1	7.7	1.7	0.0
Trin	17,949	3.7	0.3	7.8	16.4	30.6	20.6	7.0	9.4	4.2	0.0
UppCol	17,865	0.5	3.8	1.6	53.9	33.9	3.2	1.1	1.0	0.4	0.7
Willa	11,209	0.9	0.9	1.8	56.2	12.3	12.5	8.2	4.7	2.5	0.0

*Developed pervious land includes the pervious portion of open space and low, medium, and high density land uses.

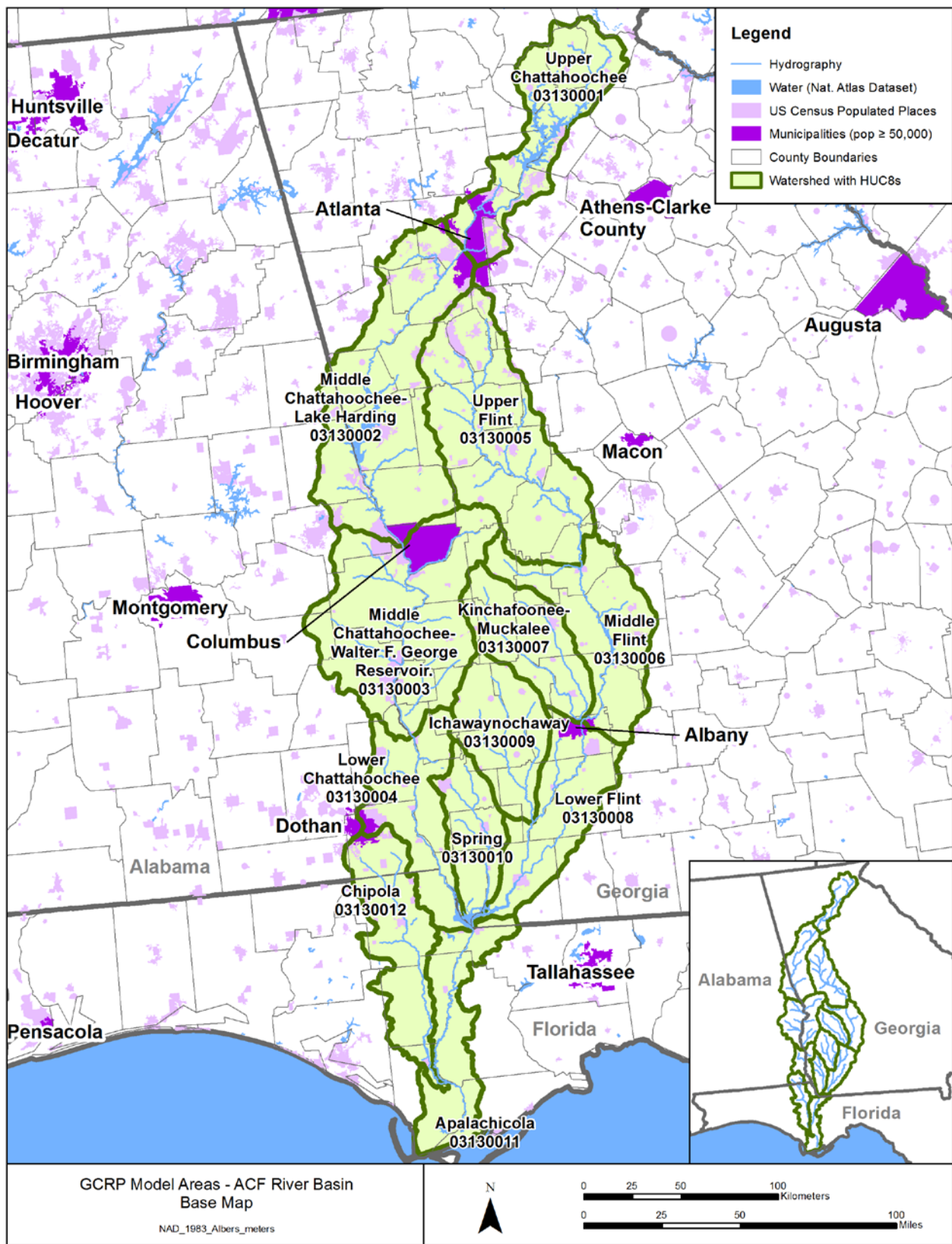


Figure 3-3. Apalachicola-Chattahoochee-Flint basins study area.

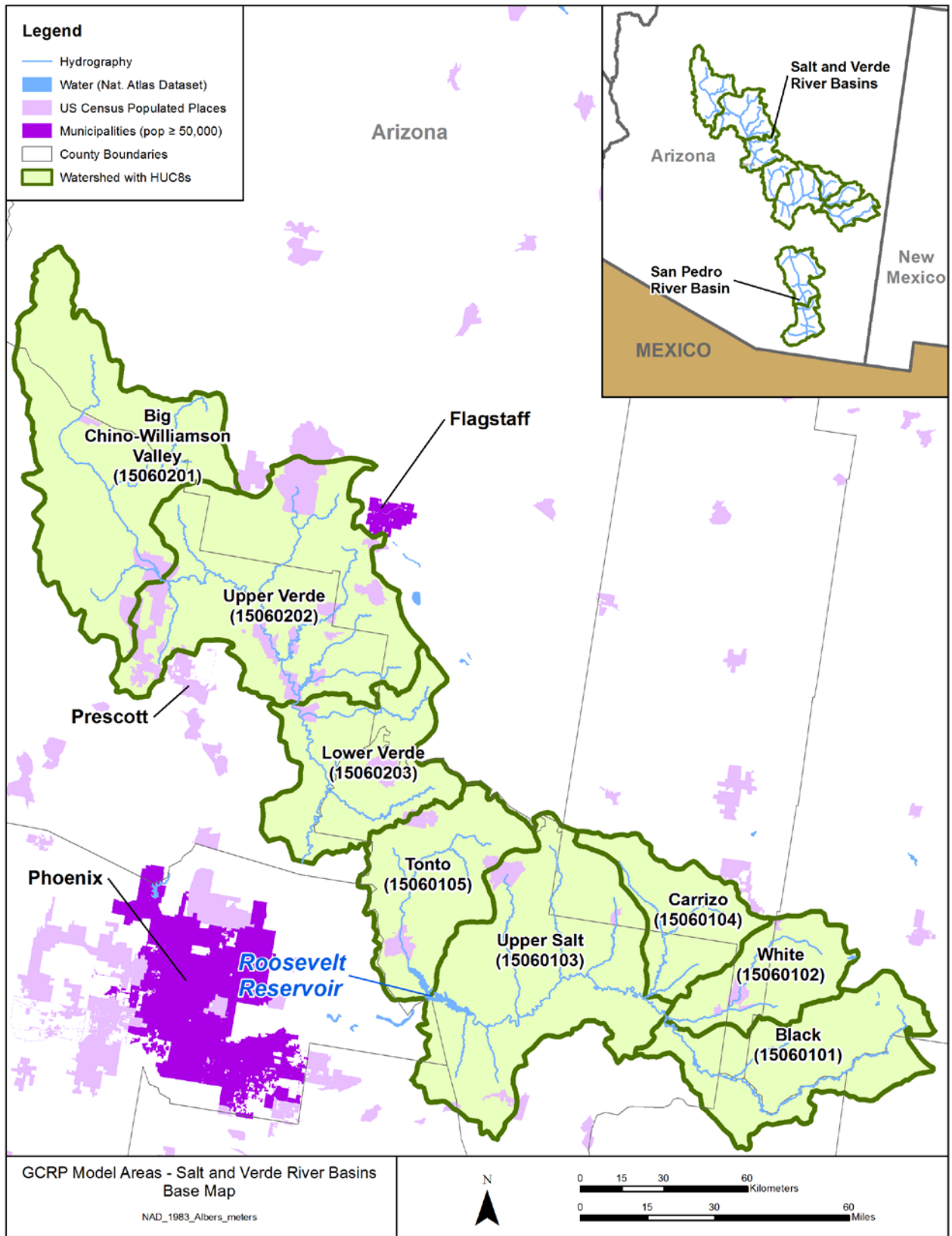


Figure 3-4. Arizona: Salt and Verde River section of study area.

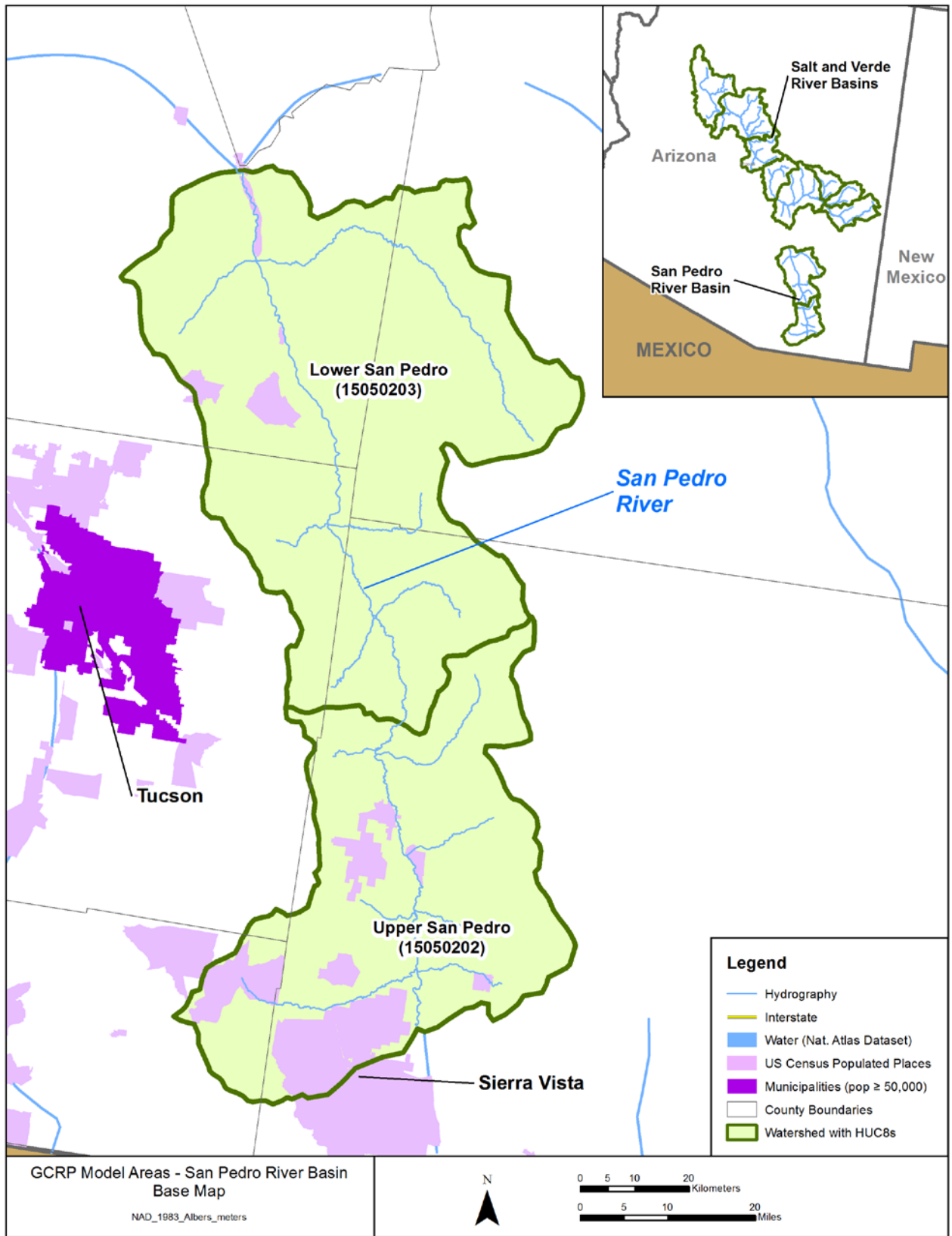


Figure 3-5. Arizona: San Pedro River section of study area.

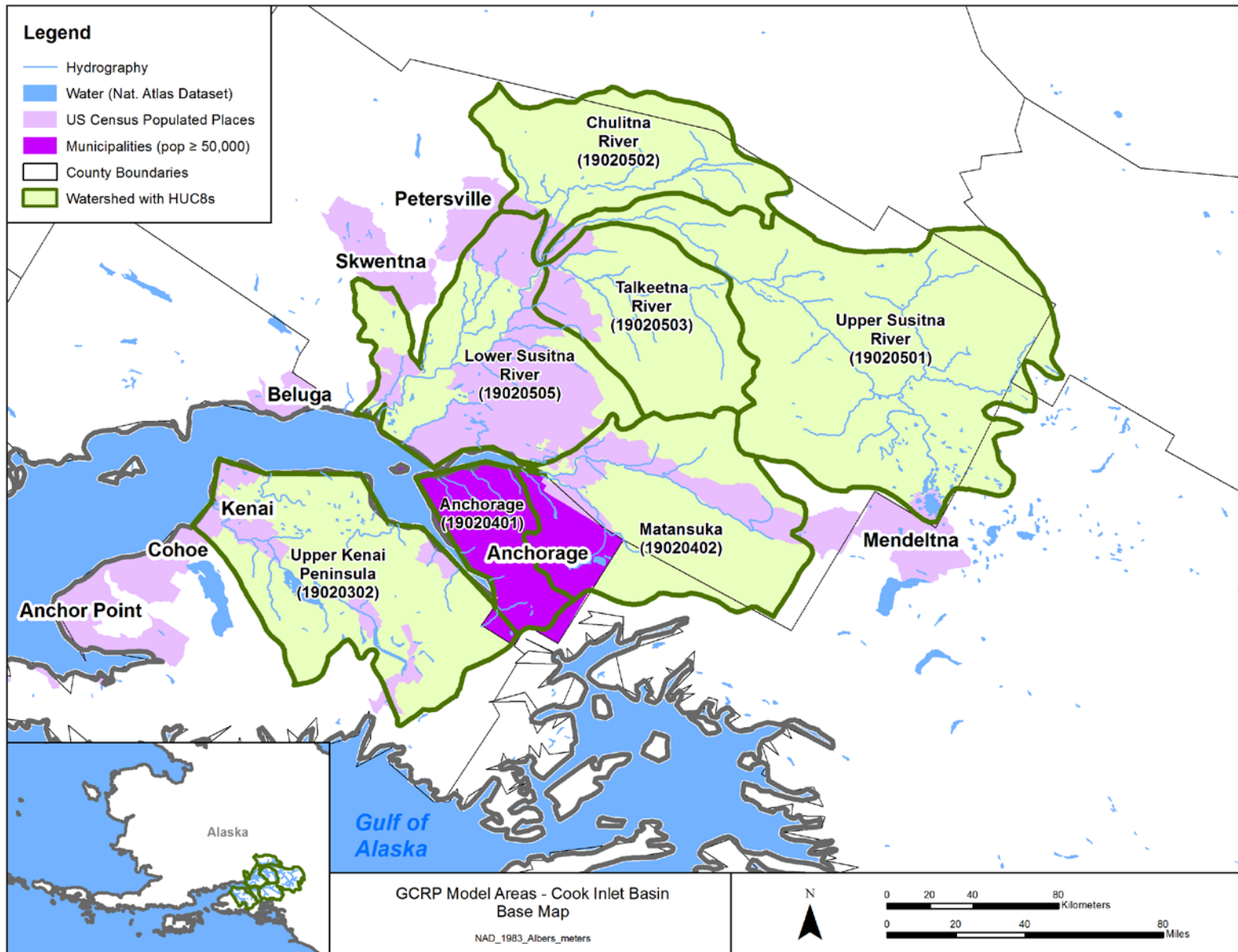


Figure 3-6. Cook Inlet basin study area.

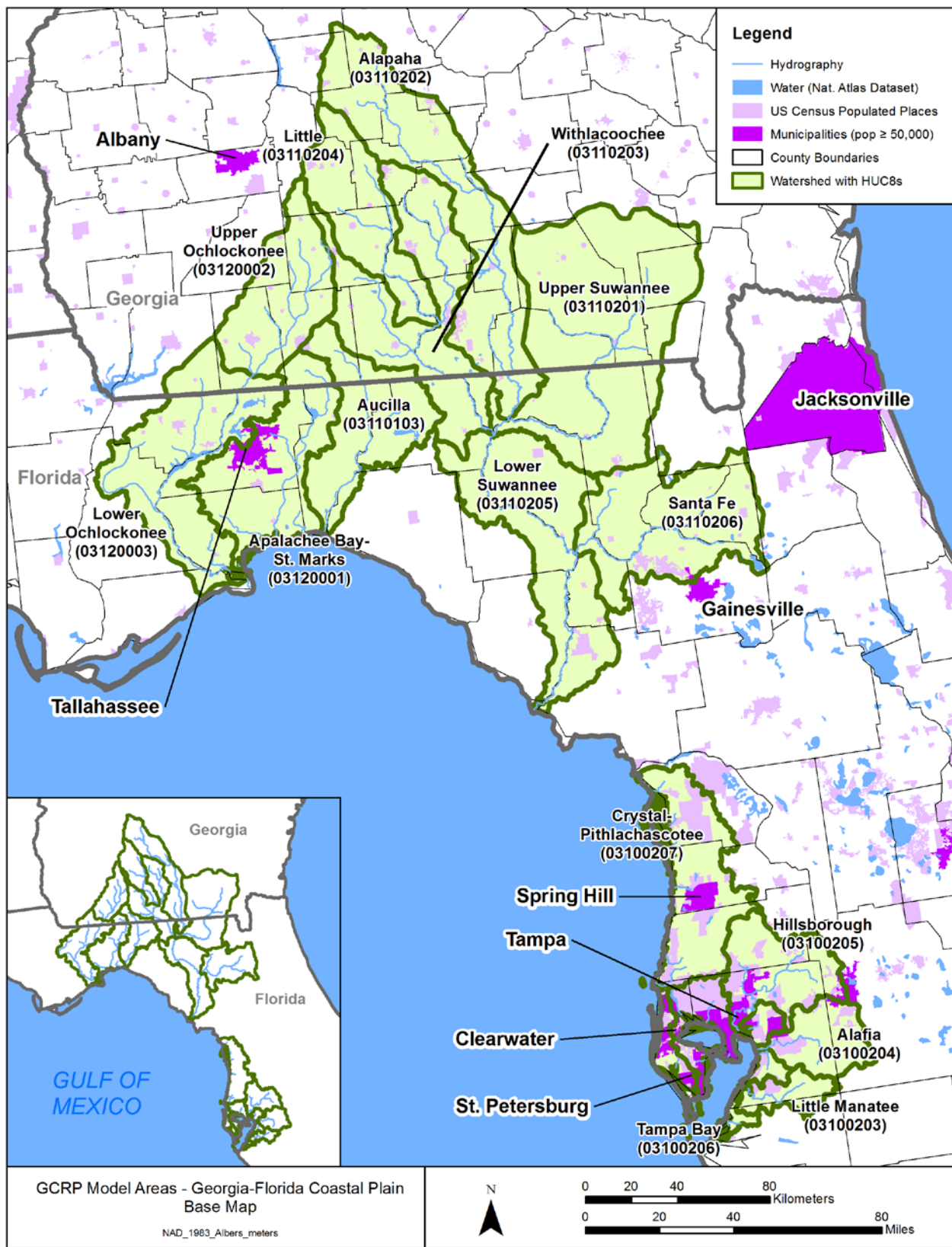


Figure 3-7. Georgia-Florida Coastal Plain study area.

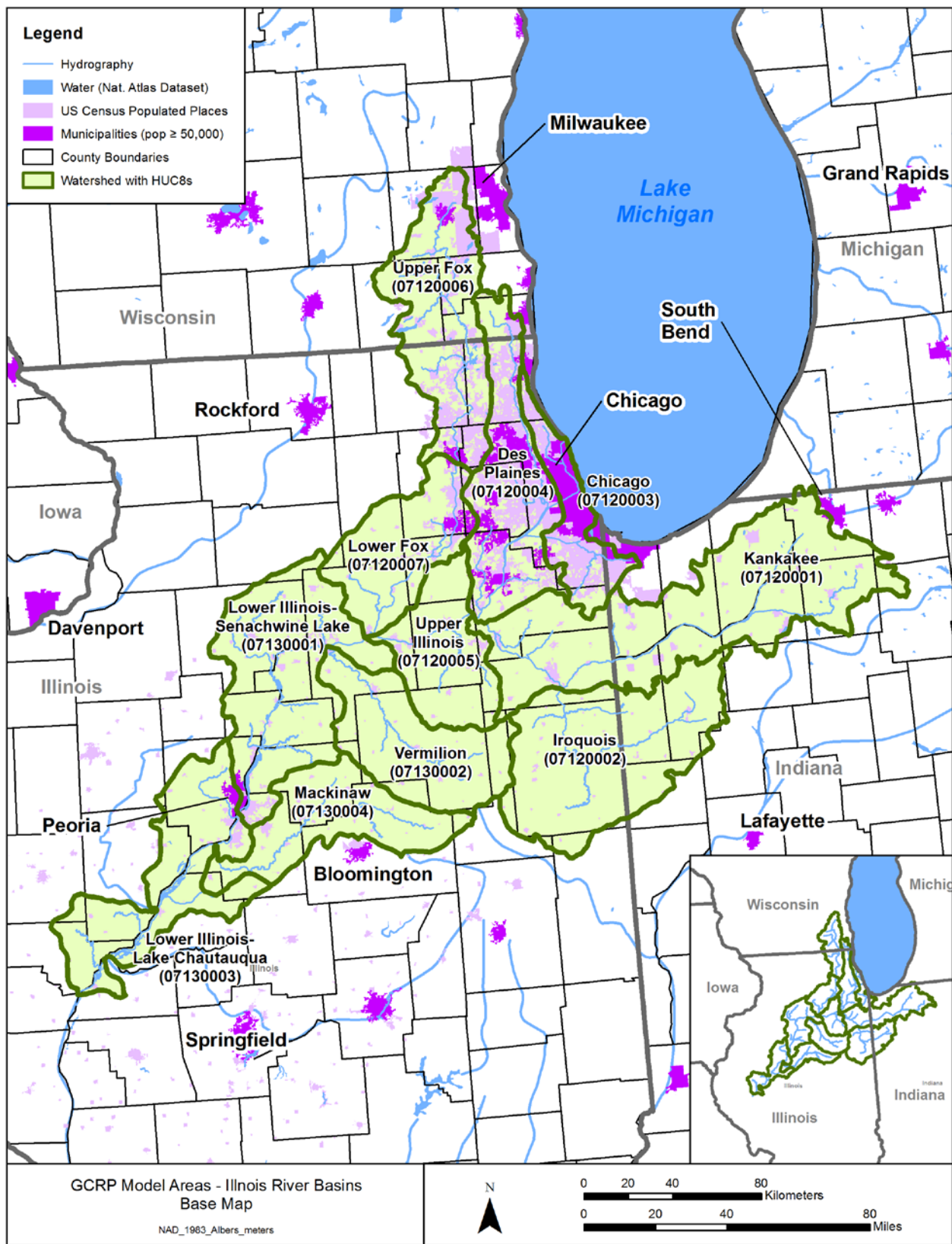


Figure 3-8. Illinois River basin study area.

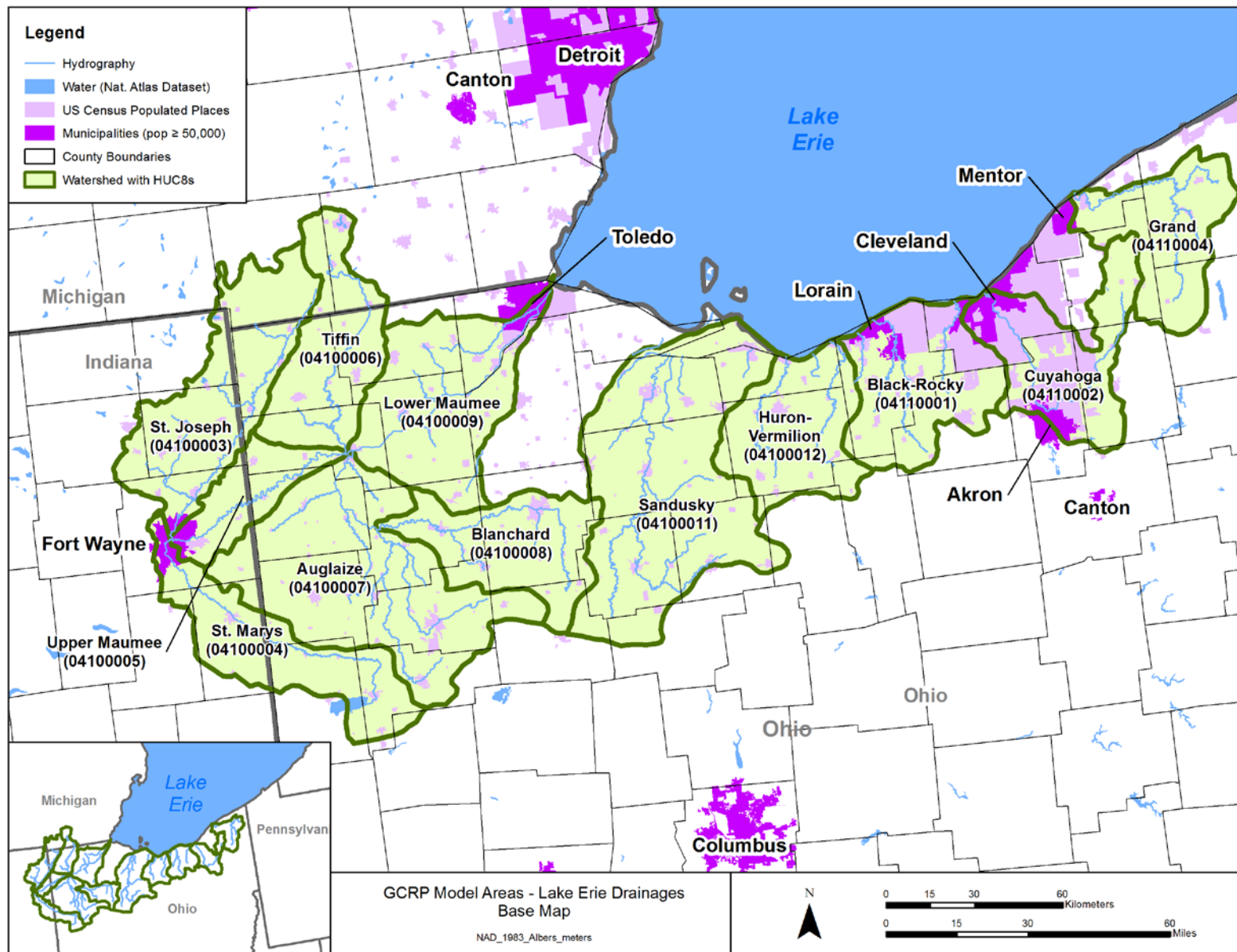


Figure 3-9. Lake Erie drainages study area.

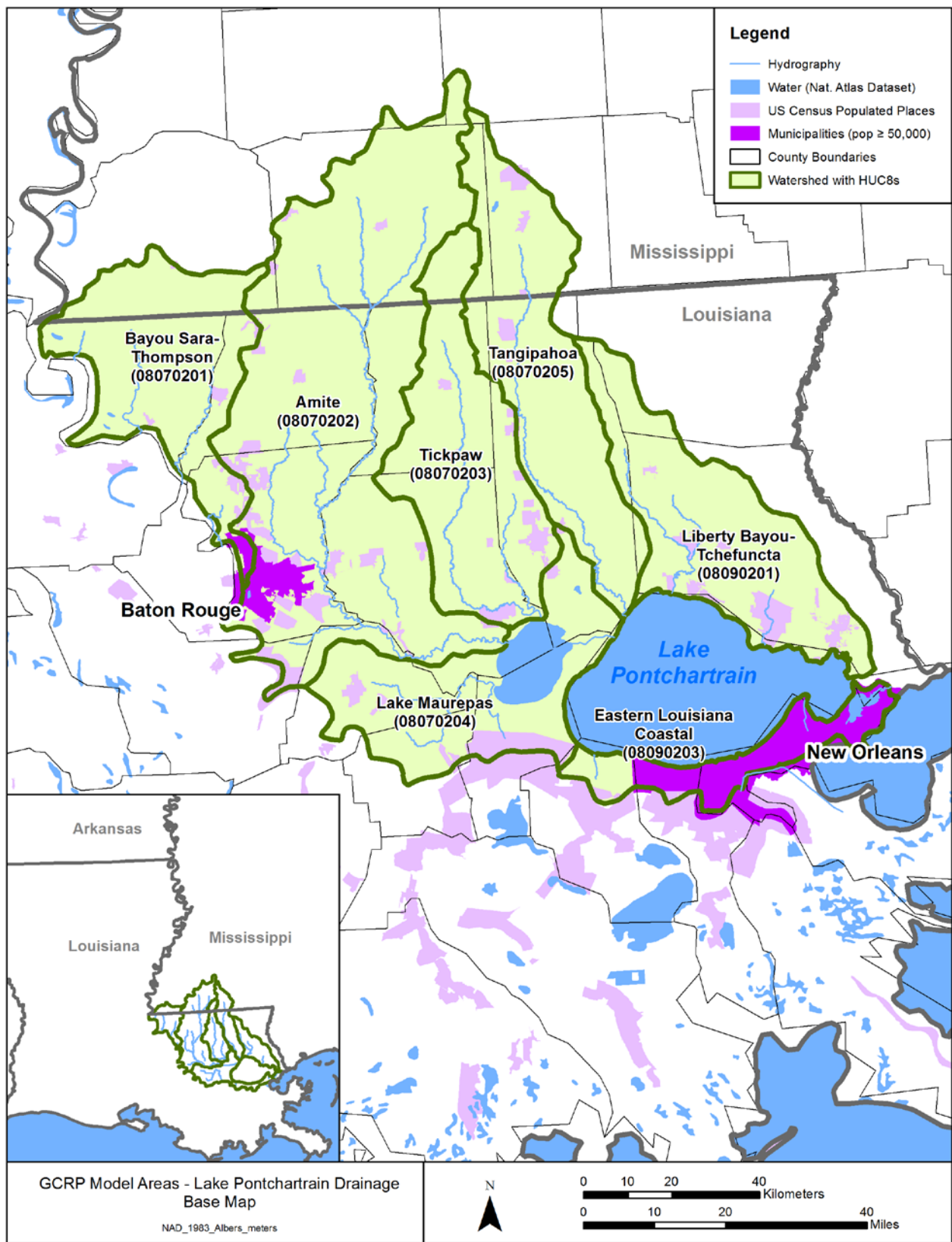


Figure 3-10. Lake Pontchartrain drainage study area.

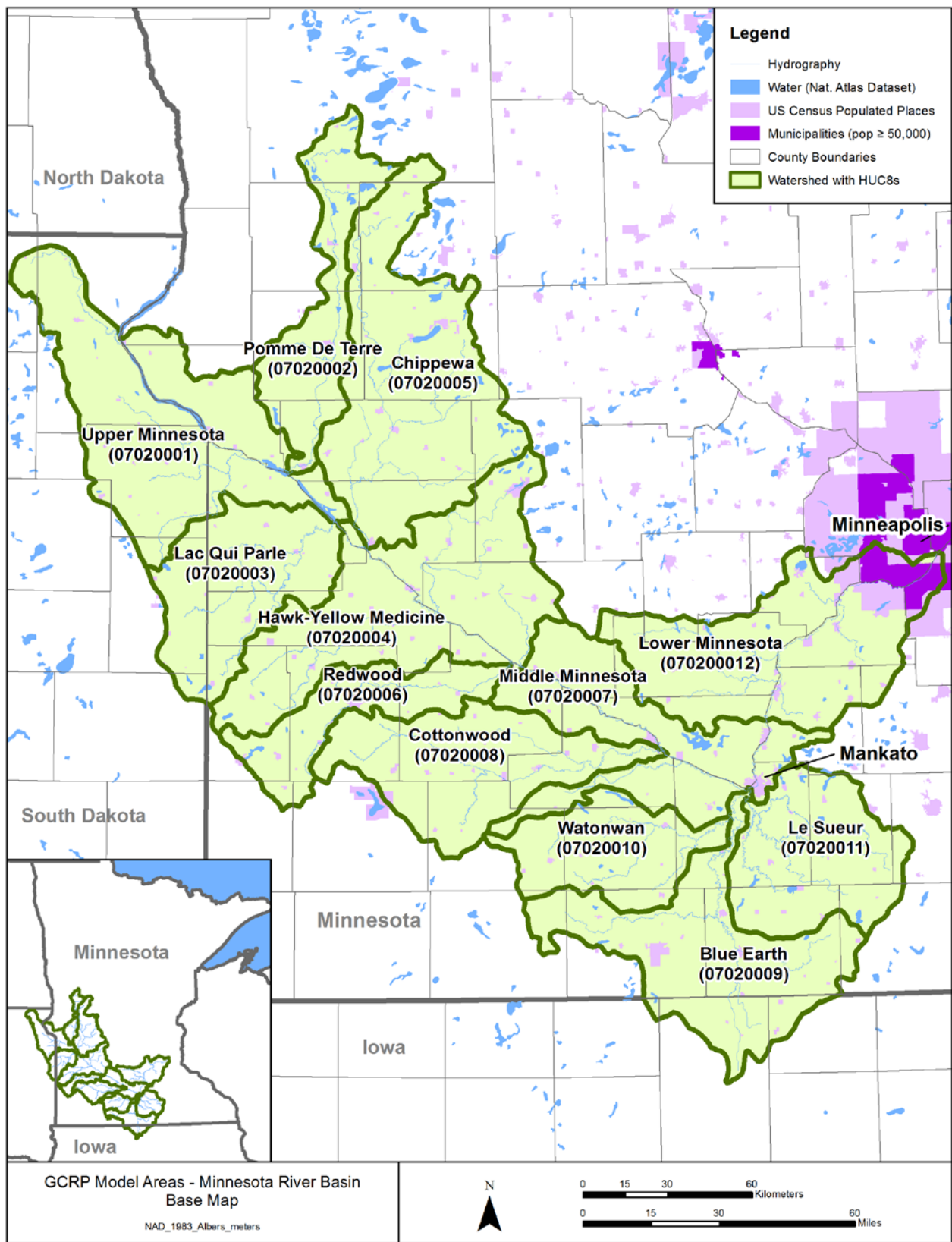


Figure 3-11. Minnesota River basin study area.

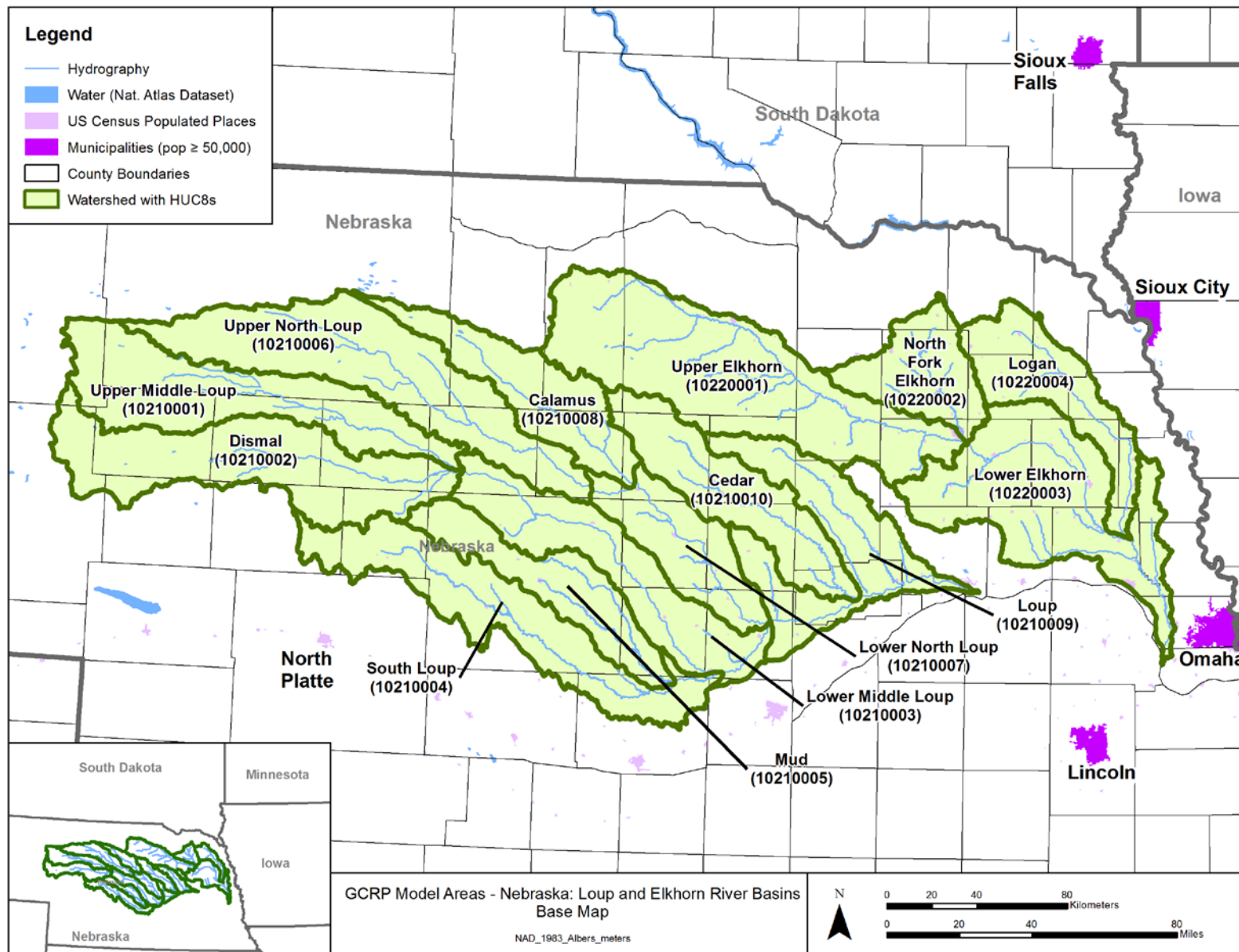


Figure 3-12. Nebraska: Loup and Elkhorn River basins study area.

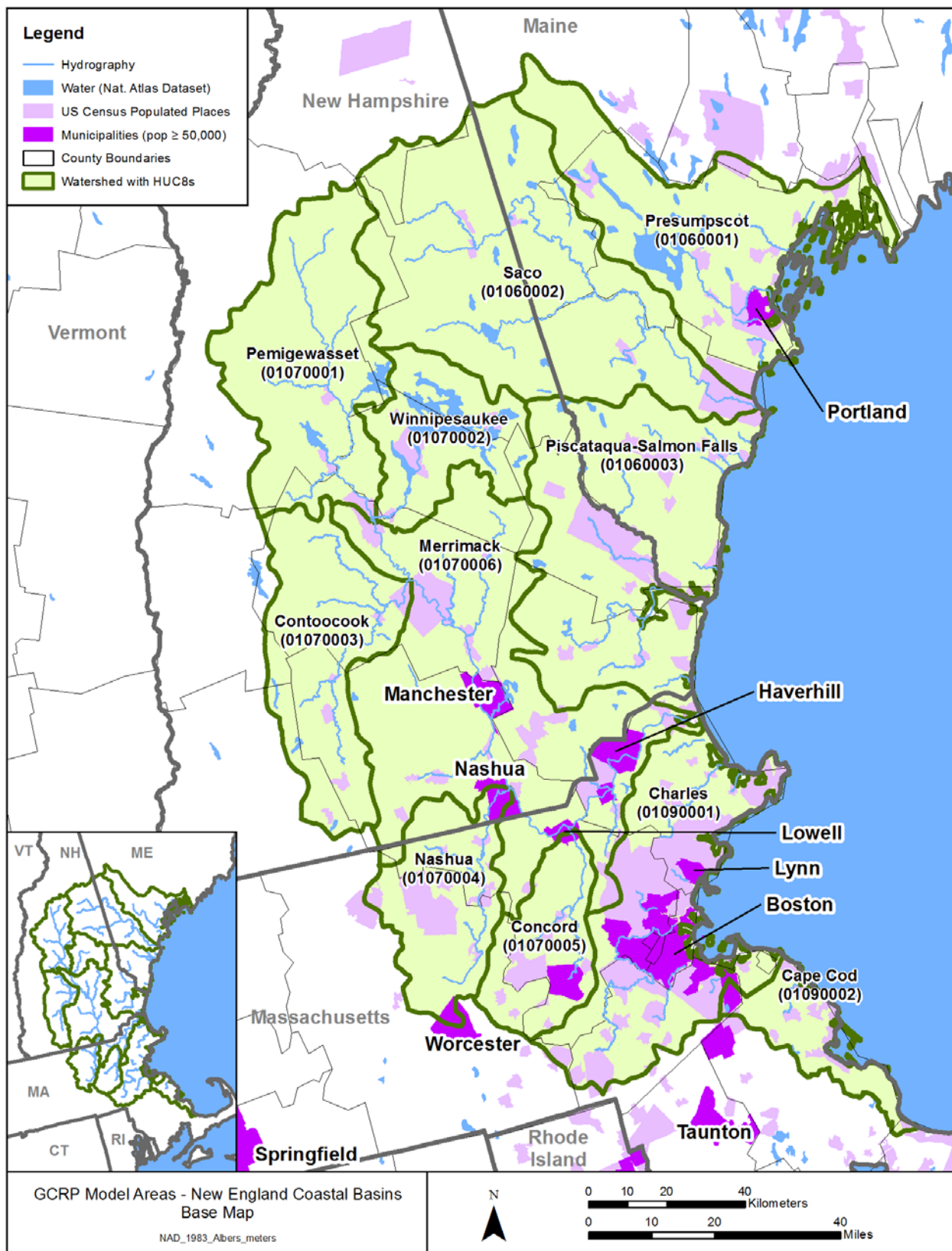


Figure 3-13. New England Coastal basins study area.

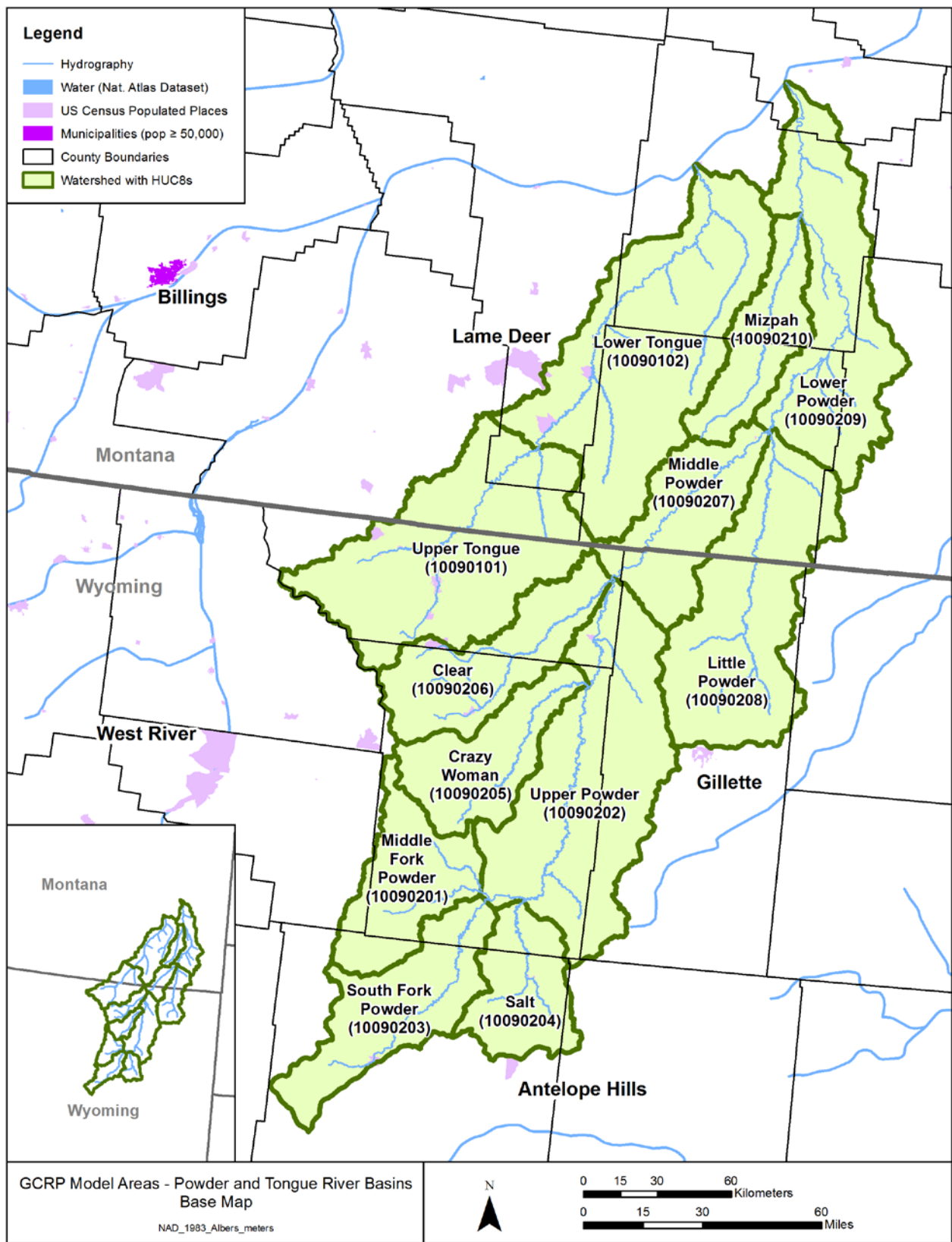


Figure 3-14. Powder and Tongue River basins study area.

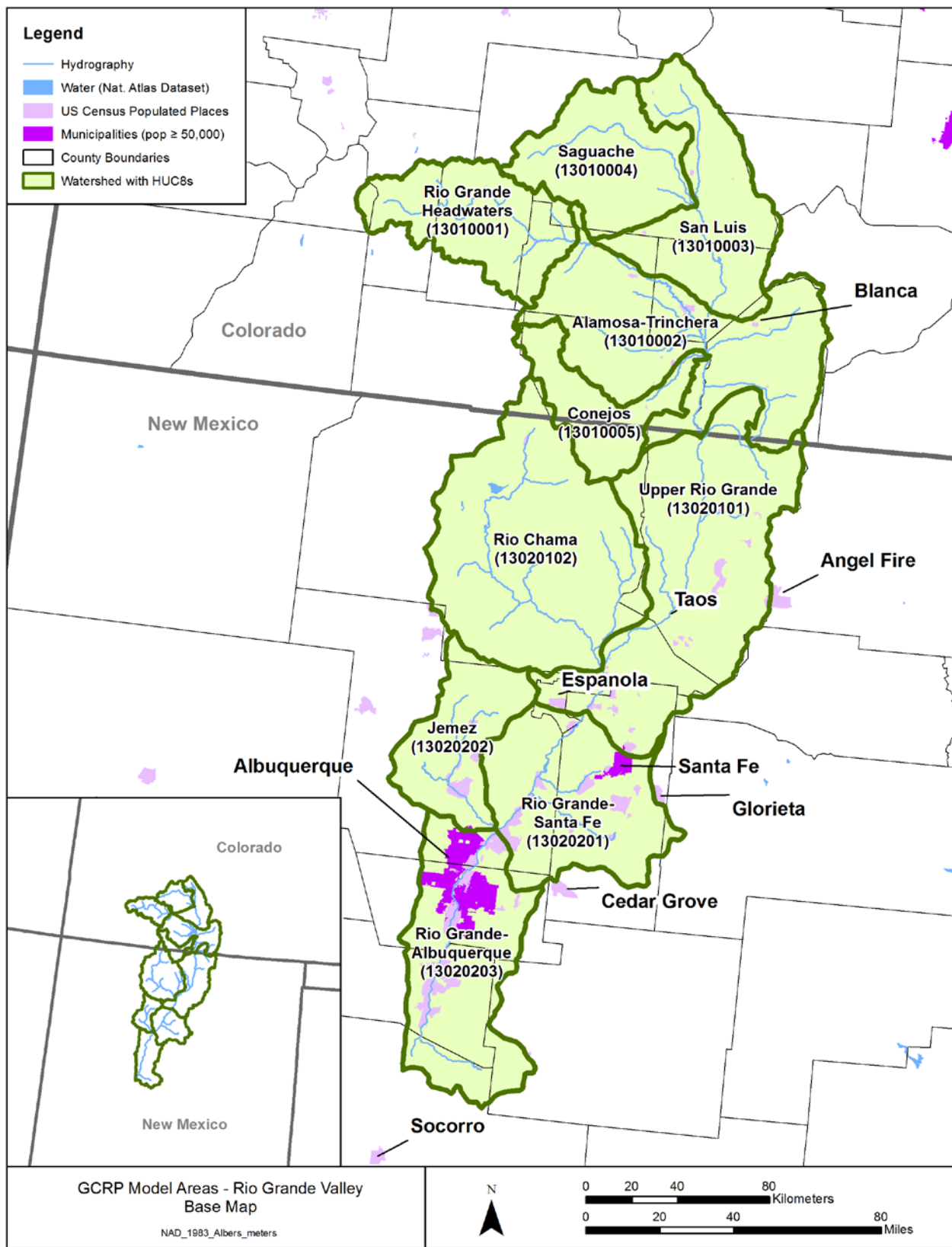


Figure 3-15. Rio Grande Valley study area.

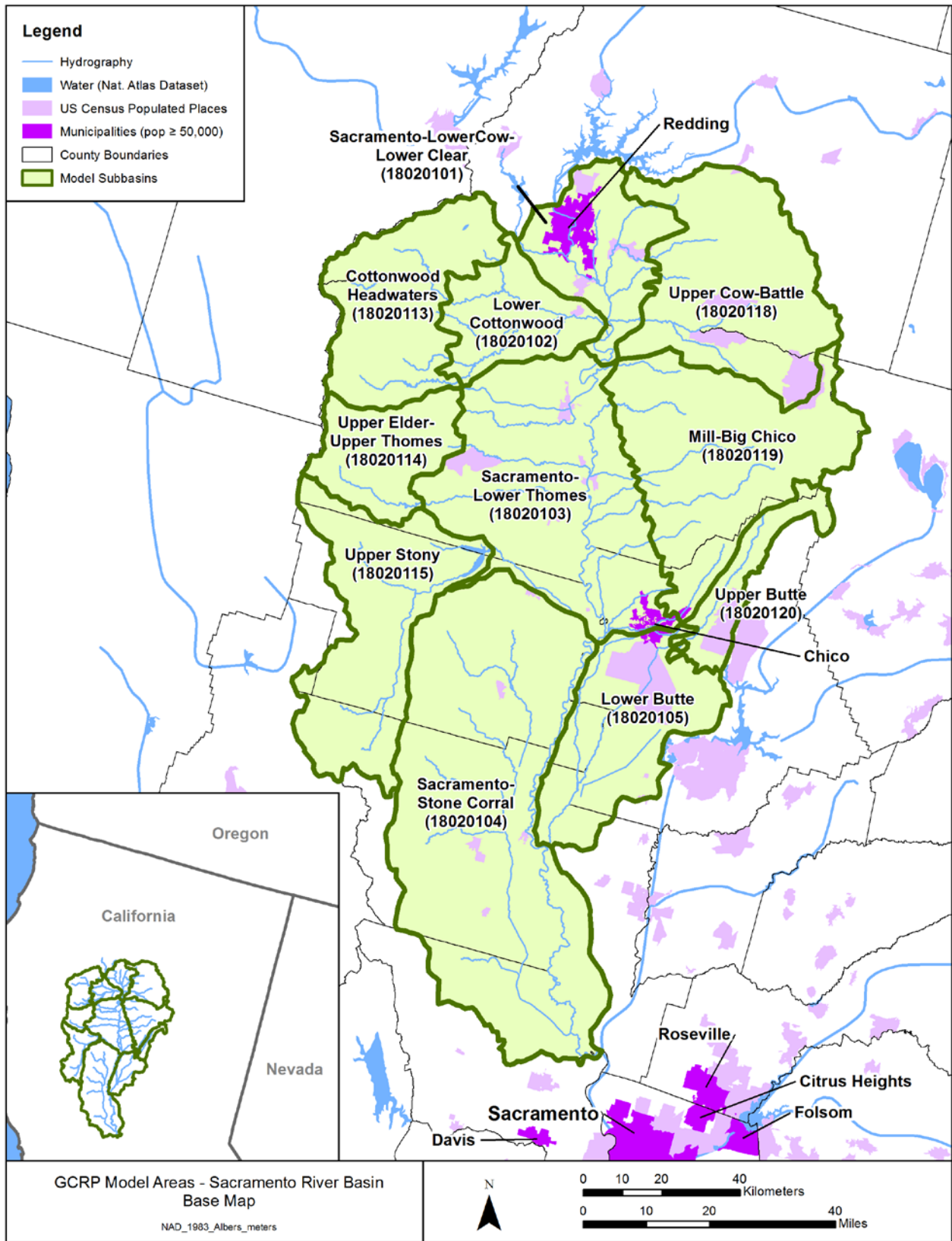


Figure 3-16. Sacramento River basin study area.

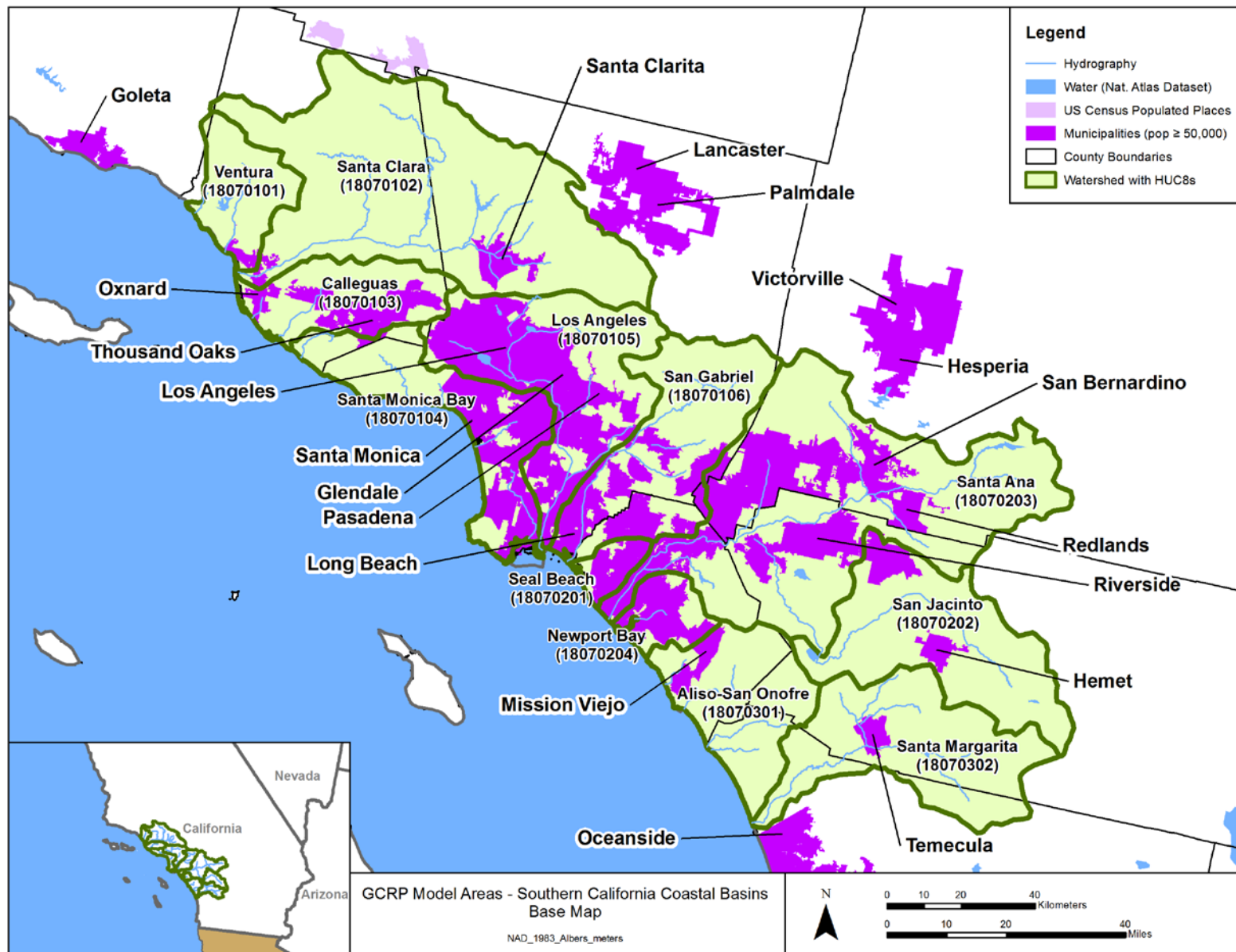


Figure 3-17. Southern California Coastal basins study area.

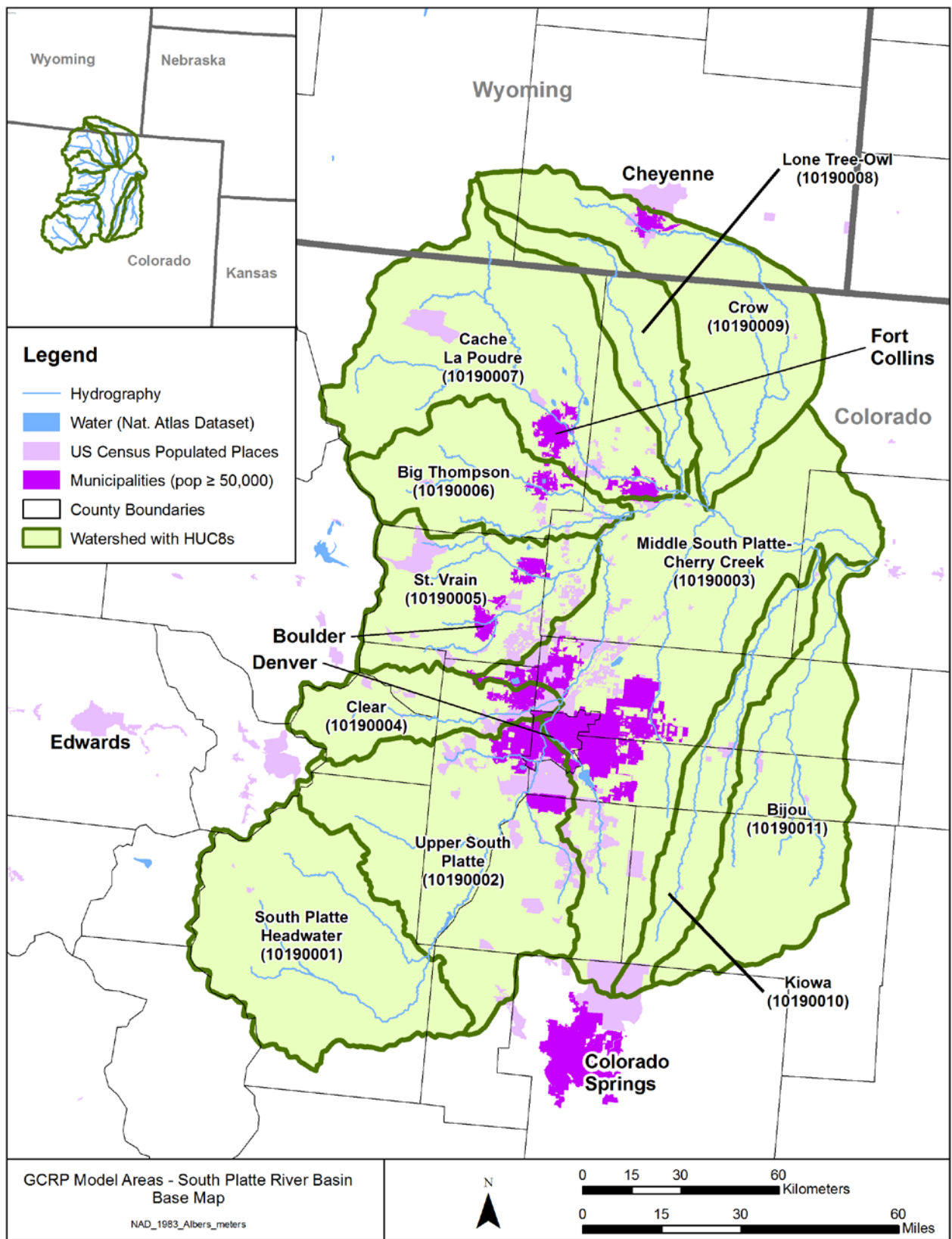


Figure 3-18. South Platte River basin study area.

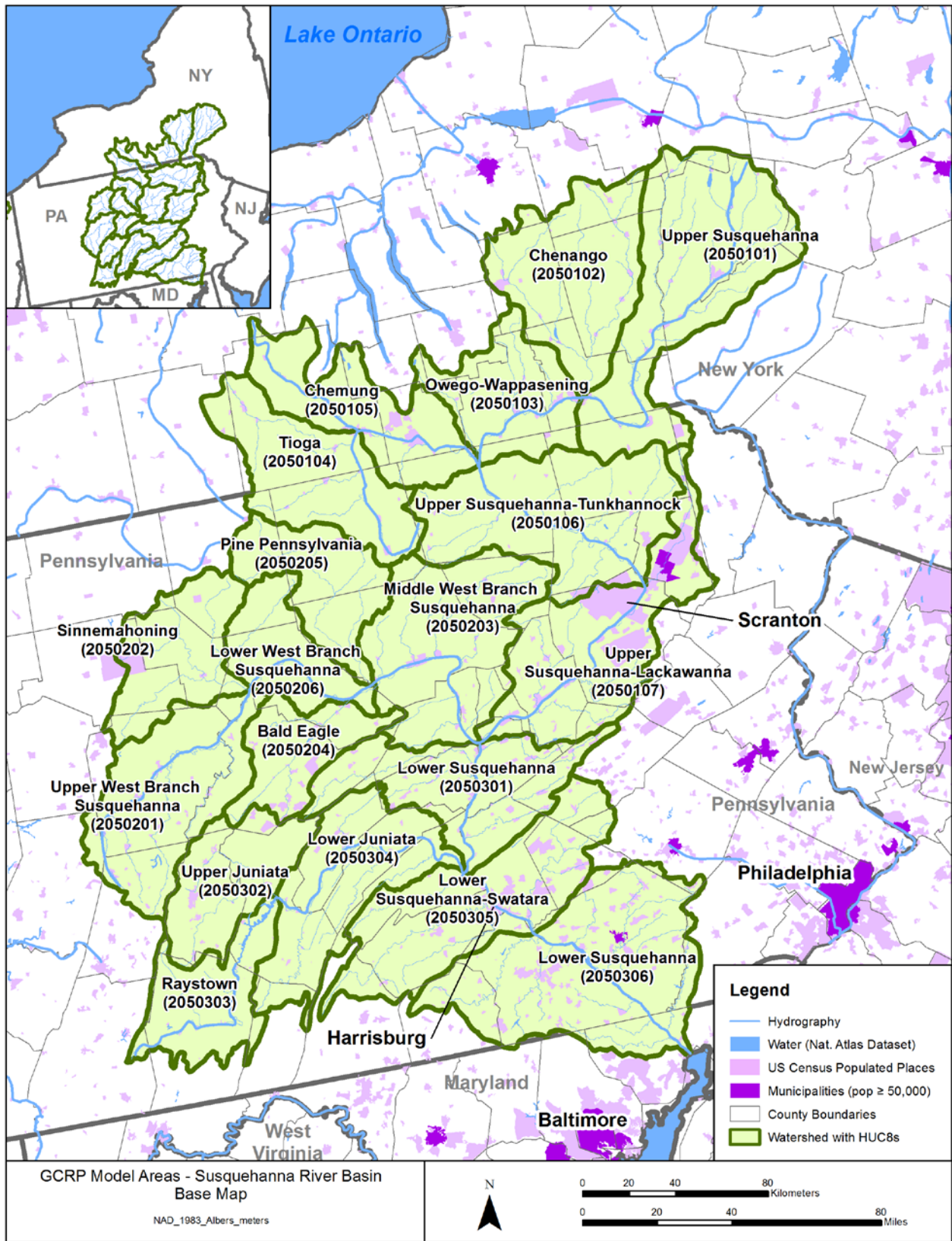


Figure 3-19. Susquehanna River basin study area.

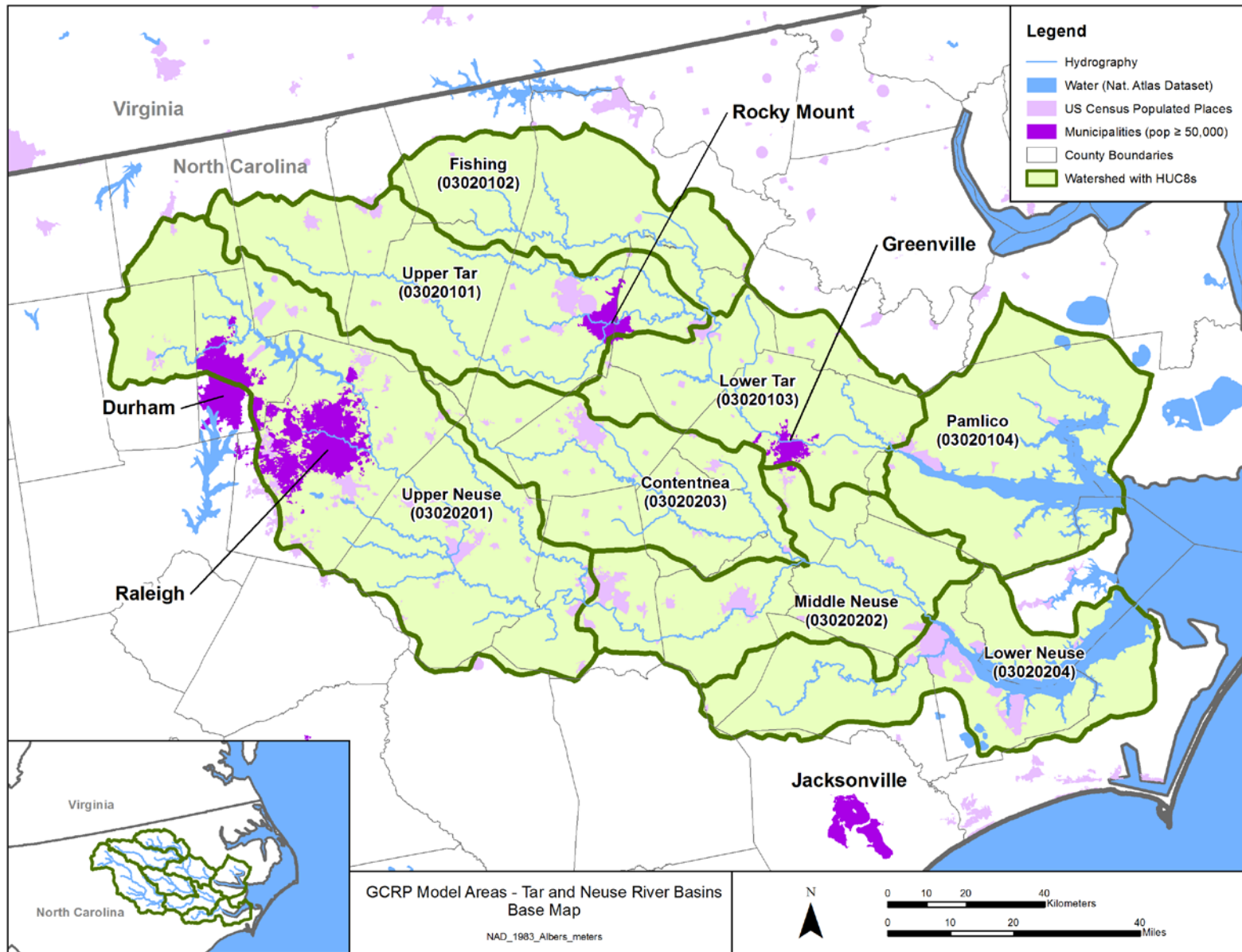


Figure 3-20. Tar and Neuse River basins study area.

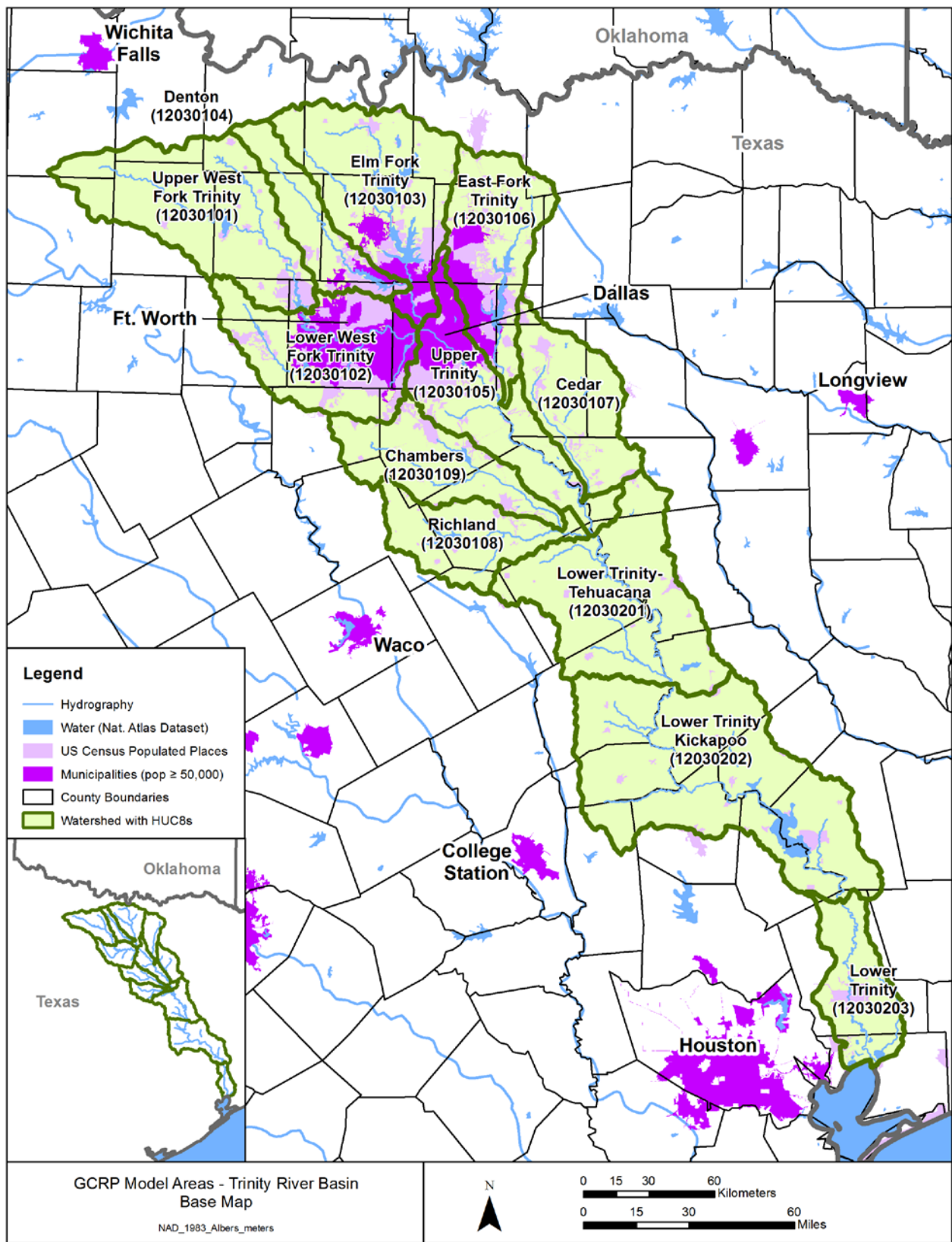


Figure 3-21. Trinity River basin study area.



Figure 3-22. Upper Colorado River basin study area.

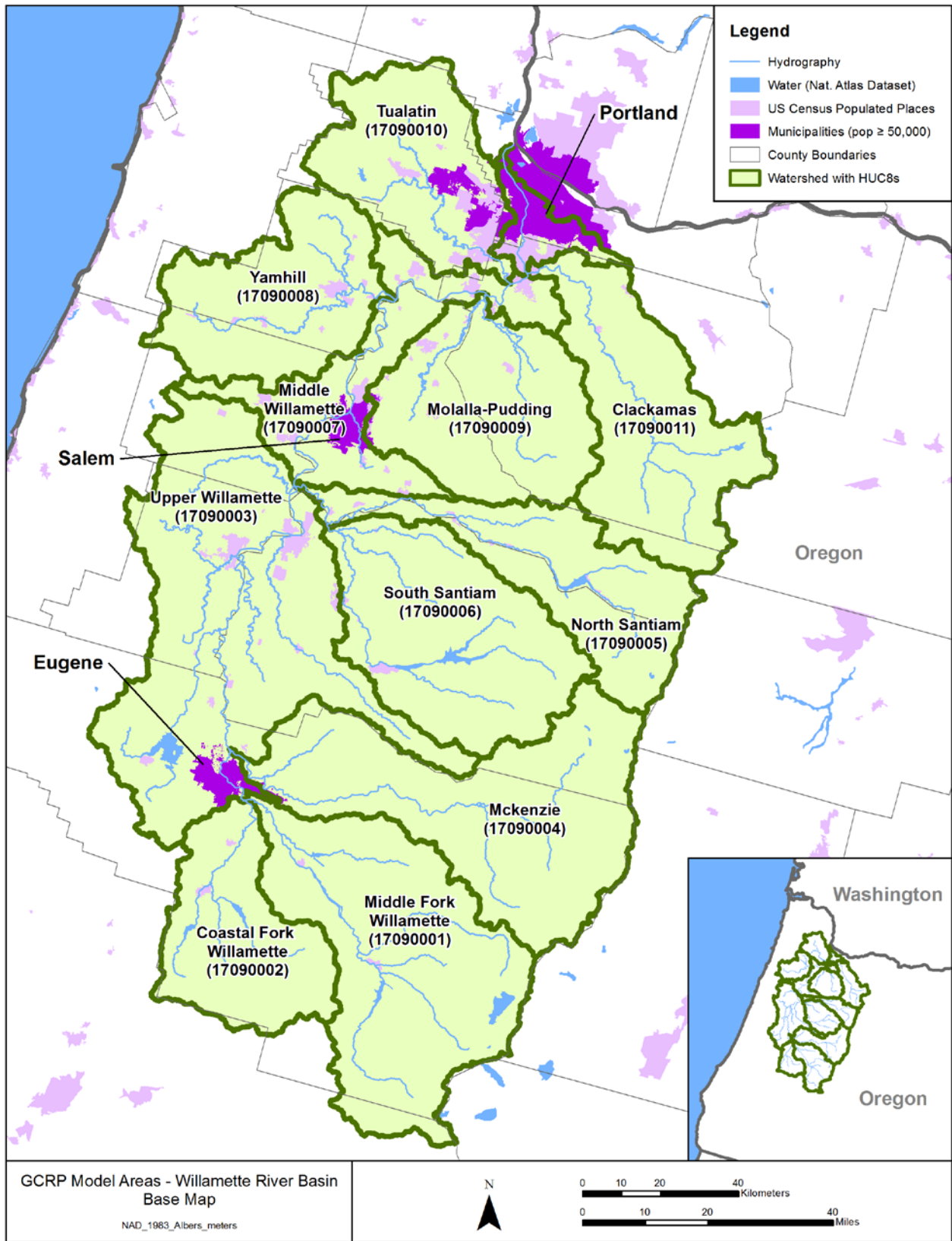


Figure 3-23. Willamette River basin study area.

4. MODELING APPROACH

This study uses dynamic watershed models to simulate the watershed response to potential mid-21st century climate change scenarios, urban and residential development scenarios, and combined climate change and urban development scenarios. Watershed models were developed for 20 large-scale study areas (approximately HUC-4 scale) located throughout the contiguous United States and Alaska. The study also evaluates the sensitivity of modeling results to different methodological choices for assessing climate change impacts, such as the use of climate change scenarios based on different methods of downscaling GCM projections and the use of different watershed models.

A watershed model is a useful tool for providing a quantitative linkage between external forcing and in-stream response. It is essentially a series of algorithms applied to watershed characteristics and meteorological data to simulate naturally occurring, land-based processes over an extended period, including hydrology and pollutant transport. Many watershed models are also capable of simulating in-stream processes. After a model has been set up and calibrated for a watershed, it can be used to quantify the existing loading of pollutants from subbasins or from different land-use categories and can also be used to assess the effects of a variety of management scenarios.

Five of the 20 sites were selected as “pilot” sites: the Minnesota River watershed (Minn), the Apalachicola-Chattahoochee-Flint River watersheds (ACF), the Willamette River watershed (Willa), the Salt/Verde/San Pedro River watershed (Ariz), and the Susquehanna River watershed (Susq). Pilot sites were selected in part due to previous experiences of the study team in applying watershed models in these areas, and in part because they provide a representative cross section of the full set of 20 study areas from a regional, meteorological, geographic, and land-use perspective. Pilot sites were used for testing and comparing model development and application methods, as well as for evaluating the sensitivity of modeling results to different types of climate change scenarios and use of different watershed models. Analysis of the pilot site results led to the selection of a reduced, more streamlined approach for the remaining 15 sites using one watershed model and a reduced set of climate change scenarios.

Two watershed models were selected for initial application to the five pilot study sites: HSPF (Bicknell et al., 2001, 2005) and SWAT (Neitsch et al., 2005). Each of these models has been widely used for hydrologic and water quality applications for regulatory purposes, such as the development of pollutant load allocations under the Total Maximum Daily Load (TMDL) provisions of the Clean Water Act. Both models are also in the public domain with open-source code, enabling ready replication of results. They both provide dynamic simulation with a subdaily or daily time step and can be built from readily available spatial coverages, but are sufficiently efficient to allow implementation of multiple runs for model calibration or scenario application purposes. Both models have also been used in previous studies of watershed responses to climate change (e.g., Taner et al., 2011; and Tong et al., 2011 for HSPF; Luo et al., 2013; Wilson and Weng, 2011; Marshall and Randhir, 2008; and Ficklin et al., 2009 for SWAT).

Application of both HSPF and SWAT to the five pilot watersheds allowed assessment of the variability associated with use of different watershed models in simulating watershed response to

climate change. The two model frameworks exhibited similar skill in reproducing observations at the large spatial scales addressed in this project (see Section 4.4.3); however, SWAT is based on a plant growth model that can explicitly represent the impacts of altered temperature, moisture, and CO₂ regimes on plants and the resulting impacts on the water balance and pollutant transport. The analysis of the pilot site results (see Section 6) emphasized the potential importance of these processes. Therefore, the SWAT model was applied in all 20 study areas. HSPF and SWAT are each described in more detail below

4.1. MODEL BACKGROUND

4.1.1. HSPF

The HSPF (Bicknell et al., 2001, 2005) is a comprehensive, dynamic watershed and receiving water quality modeling framework that was originally developed in the mid-1970s. During the past several decades, it has been used to develop hundreds of EPA-approved TMDLs, and it is generally considered among the most advanced hydrologic and watershed loading models available. The hydrologic portion of HSPF is based on the Stanford Watershed Model (Crawford and Linsley, 1966), which was one of the pioneering watershed models developed in the 1960s. The HSPF framework is developed modularly with many different components that can be assembled in different ways, depending on the objectives of a project. The model includes three major modules:

- PERLND for simulating watershed processes on pervious land areas
- IMPLND for simulating processes on impervious land areas
- RCHRES for simulating processes in streams and vertically mixed lakes

All three of these modules include many subroutines that calculate the various hydrologic and water quality processes in the watershed. Many options are available for both simplified and complex process formulations.

HSPF models hydrology as a water balance in multiple surface and subsurface layers and is typically implemented in large watersheds at an hourly time step. The water balance is simulated based on Philip's infiltration (Bicknell et al., 2001, 2005) coupled with multiple surface and subsurface stores (interception storage, surface storage, upper zone soil storage, lower zone soil storage, active groundwater, and inactive [deep] groundwater). Potential evapotranspiration (PET) is externally specified to the model.

As implemented in HSPF, the infiltration algorithms represent both the continuous variation of infiltration rate with time as a function of soil moisture and the areal variation of infiltration over the land segment. The infiltration capacity, the maximum rate at which soil will accept infiltration, is a function of both the fixed and variable characteristics of the watershed. Fixed characteristics include soil permeability and land slopes, while variables are soil surface conditions and soil moisture content. A linear probability function is used to account for spatial variation (Bicknell et al., 2005). The primary parameters controlling infiltration are *INFILT*, an index to mean soil infiltration rate (in/hr) and *LZSN*, the lower soil zone nominal soil moisture

storage. Specifically, the mean infiltration capacity over a land segment at any point in time, *IBAR*, is calculated as

$$IBAR = \left[\frac{INFILT}{\left(\frac{LZS}{LZSN} \right)^{INFEXP}} \right] \cdot INFFAC, \quad 4-1$$

where *LZS* is the current lower soil zone storage, *INFEXP* is an exponent typically set to a value of 2, and *INFFAC* is an adjustment factor to account for frozen ground effects.

Neither *INFILT* nor *LZSN* is directly observable or provided in soils databases and both must be refined in calibration. As *INFILT* is not a maximum rate nor an infiltration capacity term, its values are normally much less than published infiltration rates, soil percolation test results, or permeability rates from the literature (U.S. EPA, 2000).

Sediment erosion in HSPF uses a method that is formally similar to, but distinct from, the universal soil loss equation (USLE) sediment-detachment approach coupled with transport capacity based on overland flow. Nutrients may be simulated at varying levels of complexity, but are most typically represented by either buildup/washoff or sediment potency approaches on the land surface coupled with user-specified monthly concentrations in interflow and groundwater.

Spatially, the watershed is divided into a series of subbasins representing the drainage areas that contribute to each of the stream reaches. The stream network (RCHRES) links the surface runoff and groundwater flow contributions from each of the land segments and subbasins and routes them through water bodies. The stream model includes precipitation and evaporation from the water surfaces as well as streamflow contributions from the watershed, tributaries, and upstream stream reaches. It also simulates a full range of stream sediment and nutrient processes, including detailed representations of scour, deposition, and algal growth.

The version of HSPF used in this study is the Windows interface to Hydrologic Simulation Program—FORTRAN (WinHSPF) as distributed with BASINS version 4.0. WinHSPF is a Windows interface to HSPF and is a component of the EPA's Better Assessment Science Integrating point and Nonpoint Sources (BASINS) Version 4.0 (U.S. EPA, 2001, 2009a, 2009c). WinHSPF itself is a user interface to HSPF that assists the user in building User Control Input (UCI) files (containing model input parameters) from geographic information system (GIS) data (Duda et al., 2001). After the UCI file is built, WinHSPF is used to view, understand, and modify the model representation of a watershed. HSPF can be run from within WinHSPF. The actual model executable engine distributed with BASINS is called WinHSPFLt, which can be run in batch mode independent of the BASINS/WinHSPF interface. The model code for HSPF is stable and well documented. Detailed descriptions of the model theory and user control input are provided in Bicknell et al. (2001, 2005).

WinHSPF also provides access to the Climate Assessment Tool (CAT), which is a component of BASINS 4.0. BASINS CAT facilitates watershed-based assessments of the potential effects of

climate variability and change on water and watershed systems (namely streamflow and pollutant loads) using the HSPF model (U.S. EPA, 2009a, 2009b). BASINS CAT is capable of creating climate change scenarios that allow users to assess a wide range of *what if* questions related to climate change.

4.1.2. SWAT

The SWAT model was developed by the U.S. Department of Agriculture to simulate the effect of land management practices on water, sediment, and agricultural chemical yields in large, complex watersheds with varying soils, land use, and management conditions over long periods of time (Neitsch et al., 2005). SWAT requires data inputs for weather, soils, topography, vegetation, and land use to model water and sediment movement, nutrient cycling, and numerous other watershed processes. SWAT is a continuous model appropriate for long-term simulations.

SWAT, as implemented in this study, employs a curve number approach (SCS, 1972) to estimate surface runoff and then completes the water balance through simulation of subsurface flows, evapotranspiration, soil storages, and deep seepage losses. The curve number approach requires a daily time step. PET is typically calculated internally by SWAT based on other weather inputs.

SWAT provides an option for subdaily Green-Ampt infiltration, but this is infrequently used. The curve number approach is popular because parameters are simple and readily available. The curve number approach estimates the depth of daily runoff (Q) from rainfall depth (P), initial abstractions (Ia , depth), a storage parameter (S , depth), and a curve number (CN), as (SCS, 1972):

$$Q = \frac{(P - Ia)^2}{P - Ia + S} \quad 4-2$$

Ia is typically assumed to be 20% of S (indeed, this is a hard-coded default in SWAT). In units of millimeters for S , this yields:

$$Q = \frac{(P - 0.2S)^2}{(P + 0.8S)}, \quad S = \frac{25,400}{CN} - 254 \quad 4-3$$

The curve number is estimated as a function of land use, cover, condition, hydrologic soil group (HSG), and antecedent soil moisture. SWAT provides capabilities to automatically adjust the CN based on soil moisture, plant evapotranspiration, slope, and the presence of frozen ground. The conceptual simplicity of the curve number approach also introduces some potential problems. Specifically, the curve number was developed as a design methodology to estimate average runoff volume of a specific return period, given average total event rainfall of the same return period. It was not designed to predict runoff from specific individual events or runoff from more frequent smaller events, and applicability to continuous simulation is inexact,

especially at small spatial scales. For a summary of these issues and their potential implications in continuous simulation modeling, see Garen and Moore (2005).

Sediment yield and erosion are calculated by SWAT using the Modified Universal Soil Loss Equation (MUSLE; Williams, 1975). The MUSLE is based on several factors, including surface runoff volume, peak runoff rate, area of hydrologic response unit (HRU), soil erodibility, land cover and management, support practice, topography, and a coarse fragment factor. MUSLE implicitly combines the processes of sediment detachment and delivery. Nutrient load generation and movement are simulated using overland runoff and subsurface flow.

A key feature of SWAT is the incorporation of an explicit plant growth model, including plant interactions with water and nutrient stores. The transformation of various nitrogen and phosphorus species is simulated in detail in the soil; however, concentrations of nutrients in groundwater discharges are user specified, as in HSPF.

In-stream simulation of sediment in SWAT 2005 includes a highly simplified representation of scour and deposition processes. Nutrient kinetics in receiving waters are based on the numeric representation used in the QUAL2E model but implemented only at a daily time step.

SWAT is generally considered to be an effective tool for watershed simulation that is especially appropriate for estimating streamflow and cumulative pollutant loads in agricultural and rural watersheds (see review by Gassman et al., 2007). Bosch et al. (2011) found that SWAT was an effective tool for estimating hydrology, sediment, and nutrient loads in Lake Erie watersheds, but performed less well in urbanized settings. SWAT has some potential weaknesses relative to HSPF for the simulation of urban lands because it is typically run using a curve number approach at a daily time step while HSPF is typically run at an hourly time step using Philip infiltration. The daily time step is insufficient to resolve details of urban runoff hydrographs that have important implications for stability of small stream channels, while the curve number approach can result in poor resolution of surface versus subsurface flow pathways (Garen and Moore, 2005). The impacts of these differences are, however, believed to be minor at the larger spatial scales addressed in this study.

An important component of the SWAT model is the weather generator (WXGEN). SWAT requires daily values of precipitation, maximum and minimum temperature, solar radiation, relative humidity, and wind speed. The user may read these inputs from a file or generate the values using SWAT's weather generator model based on monthly average data summarized over a number of years (Neitsch et al., 2005). The weather generator model (Sharpley and Williams, 1990) can be used to generate climatic data or to fill in gaps in weather data. The weather generator first independently generates precipitation for the day. Maximum temperature, minimum temperature, solar radiation, and relative humidity are then generated based on the presence or absence of rain for the day. Finally, wind speed is generated independently.

The version of SWAT used in this study is SWAT 2005 as distributed with ArcSWAT 2.1, which was the most recent stable version of SWAT available at the start of this study. ArcSWAT 2.1 is an ArcGIS-ArcView extension and a graphical user input interface for the SWAT watershed model (TAMU, 2010). As with HSPF, the underlying executable code can be run in batch mode independent of the user interface. Unlike HSPF, the SWAT code is

continuously evolving, with frequent enhancements and bug fixes. For a detailed description of the version of SWAT used here, see Neitsch et al. (2005).

4.2. MODEL SETUP

Watershed models were configured to simulate each study area as a series of hydrologically connected subbasins. Each study area was subdivided into subbasin-scale modeling units. Continuous simulations of streamflow, total nitrogen, total phosphorus, and total suspended solids were then made for each unit using meteorological, land use, soil, and stream data.

Many study areas are highly managed systems influenced by humans, including dams, water transfers and withdrawals, point source discharges and other factors. Given the difficulty of modeling at the large spatial scale in this study, detailed representation of all management was not possible. The following assumptions were made to simplify modeling among all 20 study areas:

- External boundary conditions (where needed), such as upstream inflows and pollutant loads, are assumed constant.
- Interactions with deep groundwater systems are assumed constant.
- Large-scale shifts in natural cover type in response to climate change are not simulated.
- Point source discharges and water withdrawals are assumed constant at current levels.
- Only large dams that have a significant impact on hydrology at the HUC-8 (subbasin) scale are included in the models. Where these dams are simulated, an approximation of current operating rules (using a target storage approach) is assumed to apply in all future scenarios.
- Human adaptation response to climate change, such as shifts in water use or cropping practices, are not simulated.

The project team consisted of multiple modelers working in different locations. To ensure consistency of results, a common set of procedures and assumptions was established (e.g., see Appendix A). Both HSPF and SWAT were implemented using a HRU approach to upland simulation. An HRU consists of a unique combination of land use/land cover, soil, and land management practice characteristics, and thus represents areas of similar hydrologic response. Individual land parcels included within an HRU are expected to possess similar hydrologic and load generating characteristics and can thus be simulated as a unit. The HRU approach is the default for SWAT but is also good practice with HSPF. Consistent with the broad spatial scale of the models, the land cover component is aggregated into a relatively small number of categories (e.g., forest, wetland, range, grass/pastureland, crop, developed pervious, low-density impervious, and high-density impervious).

Initial preparation of spatial data was done primarily in ArcGIS for the entire study area. Processed GIS inputs were then used in ArcSWAT (which runs as an extension in ArcGIS), and imported into BASINS4 (which uses MapWindow GIS) to complete the setup of SWAT and HSPF, respectively. Spatial data sources are discussed in more detail in Section 4.2.3. Additional initial setup tasks included identification of weather stations, streamflow gaging and water quality monitoring locations, and major watershed features that significantly affect the water balance, such as presence of major lakes, reservoirs, and diversions.

4.2.1. SWAT Setup Process

SWAT model setup used the ArcSWAT extension in ArcGIS. The general procedure for SWAT setup is described below; a more detailed modeling protocol used for this project is included in Appendix A.

Subbasin boundaries and reach hydrography for each study area were generally defined from NHDPlus catchments (U.S. EPA, 2010) aggregated to approximately the HUC-10 spatial scale. The subbasin and reach shapefiles were imported into the SWAT interface and subbasin parameters were calculated automatically.

Study area boundaries were configured to minimize the presence of large reservoirs due to the difficulty of representing operational rules. Models included only major reservoirs that have a significant effect on streamflow at the scale of HUC-8s or greater. Inclusion of reservoirs was left to the discretion of individual modelers; however, the reservoirs included are generally those that drain an area greater than a single HUC-8 and provide a retention time of half a year or greater. If a reservoir was located at the terminus of the model area, it was generally ignored so that the model represented input to, rather than output from, the terminal reservoir. Models include point source discharges from major permitted facilities (greater than 1 million gallons per day [MGD] discharge). It was also necessary to define an upstream boundary condition “point source” for study areas where the model did not extend to the headwaters (e.g., Sacramento River basin).

HRUs were developed from an intersection of land use, slope, and major soils, using the geospatial data sources described in Section 4.2.3. In the HRU analysis, SWAT was used to classify the slopes into two categories: above and below 10%. A single breakpoint was chosen to represent major differences in runoff and erosive energy without creating an unmanageable number of individual HRUs. The State Soil Geographic Database (STATSGO) soils coverage was assigned using the dominant component method in which each soil polygon is represented by the properties of the dominant constituent soil. The NLCD 2001 land use coverage was loaded directly into ArcSWAT without modification. The default NLCD class to SWAT class mapping was appropriate for most areas. Impervious percentage was assigned to developed land-use classes in the SWAT urban database using values calculated from the NLCD impervious coverage. The same assumptions were applied for the future developed land-use classes (i.e., the future classes have the same total and connected impervious fractions as the corresponding existing urban land uses). HRUs were created by overlaying land use, soil, and slope at appropriate cutoff tolerance levels to prevent the creation of large numbers of insignificant HRUs. Land-use classes were retained if they occupied at least 5% of the area of a subbasin (with the exception of developed land uses, which were retained regardless of area). Soils were retained if they occupied at least 10% of the area within a given land use in a

subbasin. Slope classes were retained if they occupied at least 5% of the area within a given soil polygon. Land uses, soils, and slope classes that fall below the cutoff value are reapportioned to the dominant classes so that 100% of the watershed area is modeled (Winchell et al., 2008).

The SWAT models were linked to meteorological stations contained in EPA's BASINS 4 meteorological data set (U.S. EPA, 2008). The models used observed time series for precipitation and temperature; other weather data were simulated with the SWAT weather generator, as discussed in Section 4.2.4. Elevation bands were turned on if necessary to account for orographic effects in areas with a sparse precipitation network and significant elevation changes. This was generally appropriate where elevations within subbasins spanned a range of 250 m or more. Daily curve number hydrology with observed precipitation and air temperature was used.

Land management operations were assigned, primarily to account for agricultural practices. For urban lands, the USGS regression method for pollutant load estimation was specified. In-stream water quality options started with program defaults.

The target time period for simulation was 31 water years, with the first year dropped from analysis to account for model spinup (initialization). Some weather stations may have been absent for the spinup year, but SWAT fills in the missing records using the weather generator. The remaining 30 years span a period for which the supplied weather data were complete and included the year 2000 (with the exception of the Loup/Elkhorn basins in Nebraska, for which the simulation period ended in 1999 due to the termination of a number of precipitation gauges before the end of 2000).

4.2.2. HSPF Setup Process

HSPF models were developed on a common basis with the SWAT models using the same geospatial data, but only for the five pilot watersheds. Subbasin boundaries and reach hydrography were defined using the same NHDPlus catchments as the SWAT models. The HRUs for HSPF were calculated from the SWAT HRUs, but differ in that soils were aggregated into hydrologic soil group. Pervious (PERLND) and impervious (IMPLND) land areas are specified and simulated separately in HSPF, whereas SWAT specifies an impervious fraction for different land-use categories.

The WinHSPF interface distributed with BASINS (U.S. EPA, 2001) was used to create the user control input (UCI) and watershed data management (WDM) files. A starter UCI file was prepared that assigned default values for HRUs. Initial parameter values were based on previous modeling where available. For areas without previous modeling, hydrologic parameters were based on recommended ranges in BASINS Technical Note 6 (U.S. EPA, 2000) and related to soil and meteorological characteristics where appropriate. Snowmelt simulation used the simplified degree-day method.

The stage-storage-discharge hydraulic functional tables (FTables) for stream reaches were generated automatically during model creation. The WinHSPF FTable tool calculates the tables using relationships to drainage area. FTables were adjusted in WinHSPF if specific information was available to the modeler. Hydraulic characteristics for major reservoirs and flow/load characteristics for major point sources were defined manually based on available information.

Nutrients on the land surface were modeled as inorganic nitrogen, inorganic phosphorus, and total organic matter. The latter was transformed to appropriate fractions of organic nitrogen and organic phosphorus in the linkage to the stream. The in-stream simulation represented total nitrogen and total phosphorus as general quality constituents subject to removal approximated as an exponential decay process. Initial values for decay rates were taken from studies supporting the USGS SPARROW model (e.g., Alexander et al., 2008).

4.2.3. Watershed Data Sources

The HSPF and SWAT models each use identical geospatial and other input data sources as described below.

4.2.3.1. Watershed Boundaries and Reach Hydrography

Subbasin boundaries and reach hydrography (with connectivity) for both SWAT and HSPF were defined using NHDPlus data (U.S. EPA, 2010), which is a comprehensive set of digital spatial data representing the surface water of the United States including lakes, ponds, streams, rivers, canals, and oceans. NHDPlus provided catchment/reach flow connectivity, allowing for creation of large model subbasins with automation. NHDPlus incorporates the National Hydrography Dataset (NHD), the National Elevation Dataset, the NLCD, and the Watershed Boundary Dataset. A MapWindow script was developed to automate (with supervision) the aggregation of NHDPlus catchments/reaches into model subbasins and reaches. The general approach was to first run the aggregation script with a smaller target subbasin size (i.e., create several hundred to a thousand subbasins), then run the script again to create watersheds of the target model size (comparable to the HUC-10 spatial scale). The two-tiered approach has several benefits; it was found to be more time efficient, it allowed for greater control over the final basin size, and it provided a midpoint that could be used to redefine subbasin boundaries to match specified locations, such as gaging stations and dams/diversions.

Each delineated subbasin was conceptually represented with a single stream assumed to be a completely mixed, one-dimensional segment with a constant cross section. For the HSPF model, reach slopes were calculated based on Digital Elevation Model (DEM) data, and stream lengths were measured from the original NHD stream coverage. Assuming representative trapezoidal geometry for all streams, mean stream depth and channel width were estimated using regression curves that relate upstream drainage area to stream dimensions developed for three regions in the Eastern United States. Existing and more detailed models provided additional site-specific information on channel characteristics for some watersheds (e.g., Minnesota River; Tetra Tech, 2008b).

The SWAT model also automatically calculates the initial stream geometric values based on subbasin drainage areas, standard channel forms, and elevation, using relationships developed for numerous areas of the United States. Channel slope is automatically calculated from the DEM.

4.2.3.2. Elevation

Topography was represented by digital elevation models (DEMs) with a resolution of 30 meters obtained from USGS' National Elevation Dataset (Gesch et al., 2002). Multiple DEM coverages were grouped and clipped to the extent of the model watershed area (with a 10-mile buffer to allow for unforeseen changes to watershed boundaries).

4.2.3.3. Land Use and Land Cover

The SWAT and HSPF models use a common land use platform representing current (calibration) conditions and derived from the 2001 NLCD (Homer et al., 2004, 2007). The 2001 NLCD land cover was used to ensure consistency between all models for the project. The 2001 land use was chosen rather than the 2006 coverage because it is closer in time to the calibration period of the models, which typically runs through 2002/3. The 2001 land use is assumed to apply throughout the baseline model application period.

Some additional processing of the NLCD data was necessary. Several of the land use classes were aggregated into more general categories to provide a more manageable set of HRUs. The developed land classes were kept separate for SWAT but aggregated for HSPF. This is because SWAT assigns percent imperviousness to total developed area, whereas HSPF explicitly separates developed pervious and impervious areas. The regrouping of the NLCD classes for SWAT and HSPF is shown in Table 4-1.

The percent impervious area was specified for each developed land class from the NLCD Urban Impervious data coverage. The NLCD 2001 Urban Imperviousness coverage was clipped to the extent of the model watershed area (with 10-mile buffer) to calculate the impervious area. The percent impervious area was then specified by combining data from the 2001 NLCD Land Cover and Urban Impervious data products. Specifically, average percent impervious area was calculated over the whole basin for each of the four developed land use classes. These percentages were then used to separate out impervious land. The analysis was performed separately for each of the 20 study areas, since regional differences occur. Table 4-2 presents the calculated 2001 impervious areas for each study area.

4.2.3.4. Soils

Soils data were implemented using SWAT's built-in STATSGO (USDA, 1991) national soils database. The SWAT model uses the full set of characteristics of dominant soil groups directly, including information on infiltration, water holding capacity, erodibility, and soil chemistry. A key input is infiltration capacity, which is used, among other things, to estimate the runoff curve number. Curve numbers are a function of hydrologic soil group, vegetation, land use, cultivation practice, and antecedent moisture conditions. The Natural Resource Conservation Service (NRCS; SCS, 1972) has classified more than 4,000 soils into four hydrologic soil groups (HSGs) according to their minimum infiltration rate for bare soil after prolonged wetting. The characteristics associated with each HSG are provided in Table 4-3.

In the HSPF setup the HRUs are not based directly on dominant soils; instead, these were aggregated to represent HSGs. The HSGs include special agricultural classes (A/D, B/D, and C/D) in which the first letter represents conditions with artificial drainage and the second letter represents conditions without drainage. The first designator was assumed to apply to all crop land, while the second designator was assumed for all other land uses.

Table 4-1. Regrouping of the NLCD 2001 land-use classes for the HSPF and SWAT models

NLCD class	SWAT class	HSPF class
11 Water ^a	WATR (water)	WATER
12 Perennial ice/snow	WATR (water)	BARREN
21 Developed open space	URLD (Urban Residential—Low Density)	DEVPERV (Developed Pervious) IMPERV (Impervious)
22 Dev. Low Intensity	URMD (Urban Residential—Medium Density)	
23 Dev. Med. Intensity	URHD (Urban Residential—High Density)	
24 Dev. High Intensity	UIDU (Urban Industrial and High Intensity)	
31 Barren Land	SWRN (Range-Southwestern U.S.)	BARREN
41 Forest—Deciduous	FRSD (Forest—Deciduous)	FOREST
42 Forest—Evergreen	FRSE (Forest—Evergreen)	
43 Forest—Mixed	FRST (Forest—Mixed)	
51–52 Shrubland	RNGB (Range—Brush)	SHRUB
71–74 Herbaceous Upland	RNGE (Range—grasses)	GRASS BARREN
81 Pasture/Hay	HAY	GRASS
82 Cultivated	AGR (Agricultural Land-Row Crops)	AGRI (Agriculture)
91–97 Wetland (emergent)	WETF (Wetlands—Forested), WETL (Wetlands), WETN (Wetlands—Nonforested)	WETL (Wetlands)
98–99 Wetland (nonemergent)	WATR (water)	WATER

^aWater surface area is usually accounted for as reach area.

Table 4-2. Calculated fraction impervious cover within each developed land class for each study area based on NLCD 2001

Site ID	Open space (%)	Low intensity (%)	Medium intensity (%)	High intensity (%)
ACF	8.04	30.16	60.71	89.90
Ariz	7.37	29.66	53.71	73.85
Cook	10.11	29.79	61.48	87.17
GaFla	7.20	31.87	60.14	87.47
Illin	8.83	32.36	61.24	88.70
LErie	7.30	32.53	60.72	86.75
LPont	7.53	32.91	60.11	88.08
Minn	6.59	29.20	55.01	83.31
Neb	8.34	29.68	60.14	86.59
NewEng	8.22	32.81	60.90	87.25
PowTon	7.42	31.64	59.16	85.99
RioGra	8.76	32.36	60.49	84.32
Sac	5.95	30.02	55.41	81.20
SoCal	7.75	35.39	61.31	88.83
SoPlat	6.41	33.46	60.79	86.76
Susq	6.90	31.26	60.90	85.41
TarNeu	7.17	30.90	61.05	87.31
Trin	7.74	31.65	60.78	89.15
UppCol	9.78	31.89	60.48	87.41
Willa	9.56	32.31	61.49	88.94

Table 4-3. Characteristics of NRCS soil hydrologic groups

Soil group	Characteristics	Minimum infiltration capacity (in/hr)
A	Sandy, deep, well drained soils; deep loess; aggregated silty soils	0.30–0.45
B	Sandy loams, shallow loess, moderately deep and moderately well drained soils	0.15–0.30
C	Clay loam soils, shallow sandy loams with a low permeability horizon impeding drainage (soils with a high clay content), soils low in organic content	0.05–0.15
D	Heavy clay soils with swelling potential (heavy plastic clays), water-logged soils, certain saline soils, or shallow soils over an impermeable layer	0.00–0.05

4.2.3.5. Point Source Discharges

The primary objective of this study is to examine relative changes that are potentially associated with changes in climate and land use. From that perspective, point source discharges can be

characterized as a nuisance parameter. However, point sources that are large enough relative to receiving waters to affect the observed streamflow and nutrient loads in river systems need to be included to calibrate the models. This is done in a simplified way, and the point sources were then held constant for future conditions, allowing analysis of relative change. Only the major dischargers, typically those with a discharge rate greater than 1 MGD were included in the models. The major dischargers account for the majority of the total flow from all permitted discharges in most watersheds, so the effect on the calibration of omitting smaller sources is relatively small, except perhaps during extreme low streamflow conditions. Data were sought from the EPA's Permit Compliance System database for the major dischargers in the watersheds. Facilities that were missing TN, TP, or total suspended solids (TSS) concentrations were filled with a typical pollutant concentration value from the literature based on Standard Industrial Classification (SIC) code. The major dischargers were represented at long-term average flows, without accounting for changes over time or seasonal variations.

4.2.3.6. Atmospheric Deposition

Atmospheric deposition can be a significant source of inorganic nitrogen to watersheds and water bodies. SWAT2005 allows the user to specify wet atmospheric deposition of nitrate nitrogen. This is specified as a constant concentration across the entire watershed. Wet deposition of ammonia and dry deposition of nitrogen is not addressed in the SWAT2005 model.

HSPF allows the specification of both wet and dry deposition of both nitrate nitrogen (NO_3) and ammonium nitrogen (NH_4), and both were included in the model. Dry deposition is specified as a loading series, rather than concentration series. Because wet deposition is specified as a concentration, it will vary in accordance with precipitation changes in future climate scenarios, whereas the dry deposition series (HSPF only) is assumed constant for future scenarios.

Total oxidized nitrogen (NO_x) emissions in the United States remained relatively constant to a first approximation across the model period considered in this study from the early 1970s up through 2002 (U.S. EPA, 2002). There is strong geographic variability in atmospheric deposition, but much smaller year-to-year variability at the national scale over this period (Suddick and Davidson, 2012). The National Acid Deposition Program (NADP; <http://nadp.sws.uiuc.edu/>) monitors wet deposition across the country and produces yearly gridded maps of NO_3 and NH_4 wet deposition concentrations. Dry deposition rates are monitored (and interpreted with models) by the EPA Clean Air Status and Trends Network (<http://epa.gov/castnet/javaweb/index.html>). Results for year 2000 were selected as generally representative and each study watershed was characterized by a spatial average wet deposition concentration (and dry deposition loading rate for HSPF). Atmospheric deposition of phosphorus and sediment was not considered a significant potential source and is not addressed in the models.

4.2.3.7. Impoundments, Diversions, and Withdrawals

The hydrology of many large watersheds in the United States is strongly impacted by anthropogenic modifications, including large impoundments and withdrawals for consumptive use. It is necessary to take these factors into account to develop a calibrated model. At the same time, these anthropogenic factors constitute a problem for evaluating responses to future changes, as there is no clear basis for evaluating future changes in reservoir operations or water

withdrawals. In addition, information on impoundments, withdrawals, and trans-basin water imports is often difficult to obtain. The approach taken in this project is to minimize the importance of impoundments and withdrawals by focusing on relative changes between present and future conditions with these factors held constant. In this way, the results that are presented are estimates of the change that may be anticipated based on changes to meteorological and land use forcing within the subject study area, with other factors held constant. Simulation results do not account for potential future changes in water management.

The general approach adopted for this project was to select study areas by avoiding major human interventions (e.g., reservoirs) in the flow system where possible, to ignore relatively minor interventions, and where necessary to represent significant interventions in a simplified manner. In the first instance, study watersheds were delineated to avoid major reservoirs where possible. For example, the model of the Verde River watershed (Arizona) is terminated at the inflow to Horseshoe Reservoir. In some cases, as in the Sacramento River watershed, an upstream reservoir is treated as a constant boundary condition because information on future reservoir management responses to climate change was not available.

Impoundments, withdrawals, and water imports that do not have a major impact on downstream streamflow were generally omitted from the large scale models. Inclusion or omission of such features was a subjective choice of individual modelers; however, it was generally necessary to include such features if they resulted in a modification of flow at downstream gages on the order of 10% or more. Where these features were included they were represented in a simplified manner: (1) impoundments were represented by simplified (two-season) stage-discharge operating rules, developed either from documented operational procedures or from analysis of monitored discharge; (2) large withdrawals were represented as either annual or monthly constant average rates; and (3) major trans-basin water imports were also represented as either annual or monthly constant average rates depending on availability of data. Use of surface water for irrigation was simulated only in those basins where it was determined during calibration that it was a significant factor in the overall water balance. These simplifying assumptions decrease the quality of model fit during calibration and validation, but provide a stable basis for the analysis of relative response to climate and land-use change within the basin.

More detailed information about the representation of impoundments and other anthropogenic influences on hydrology in each study area are presented in Appendices D through W.

4.2.4. Baseline Meteorology Representation

Time series of observed meteorological data (for both SWAT and HSPF) were obtained from the 2006 BASINS 4 Meteorological Database (U.S. EPA, 2008). The database contains records for 16,000 stations from 1970–2006, set up on an hourly basis, and has the advantage of providing a consistent set of parameters with missing records filled and daily records disaggregated to an hourly time step. The disaggregation was performed using automated scripts that distribute the daily data using one of several nearby hourly stations, using the one whose daily total is closest to the daily value being disaggregated. If the daily total for the hourly stations being used were not within a specified tolerance of the daily value, the daily value was distributed using a triangular distribution centered at the middle of the day. The process involved extensive quality control review; however, the true temporal distribution of precipitation at daily stations is unknown and the automated approach can occasionally result in anomalously high hourly

estimates. Both factors introduce some irreducible uncertainty into hydrologic simulations using disaggregated daily precipitation stations.

A typical site-specific watershed project would assemble additional weather data sources to address under-represented areas, but this requires significant amounts of additional quality control and data processing to fill gaps and address accumulated records. It was assumed that the use of the BASINS 2006 data was sufficient to produce reasonable results at the broad spatial scale that is the focus of this project, particularly for evaluating the relative magnitude of change. Significant orographic variability was accounted for through the use of lapse rates because the available stations typically under-represent high mountain areas.

The required meteorological time series for both SWAT and HSPF (as implemented for this project) included precipitation, air temperature, and either calculated PET or time series required to generate PET. SWAT uses daily meteorological data, while HSPF requires hourly data. Stations were selected to provide a common 30-year or more period of record (or one that could be filled from an approximately co-located station).

Table 4-4 presents a summary of annual precipitation and temperature observations for each of the study areas from 1971–2000. For more specific details on the meteorological data used in each of the study areas, refer to the model calibration reports provided in Appendices D through W.

PET is the third major weather time series input to the watershed models. As evapotranspiration is typically the largest outgoing term in the water balance, watershed models are highly sensitive to the specification of PET, particularly for simulating low streamflow conditions and events. Many watershed modeling efforts perform well with simplified approaches to estimating PET, such as the Hamon method (included as an option in the BASINS data set), which depend primarily on air temperature. However, the robustness of watershed model calibrations conducted with simplified PET is suspect under conditions of climate change, since a variety of other factors that influence PET, such as wind speed and cloud cover, are also likely to change. Therefore, we implemented Penman-Monteith PET, which employs a full energy balance (Monteith, 1965; Jensen et al., 1990). The implementation varies slightly between SWAT and HSPF. In SWAT, the full Penman-Monteith method (Allen et al., 2005) is implemented as an internal option in the model and includes feedback from crop height simulated by the plant growth model. For HSPF, Penman-Monteith reference evapotranspiration at each weather station was calculated externally using the SWAT2005 model subroutines with observed precipitation and temperature. In both cases, the additional inputs to the energy balance (solar radiation, wind movement, cloud cover, and relative humidity) were provided by the SWAT weather generator, which relies on monthly conditional probability statistics for each of these inputs. An evaluation of the BASINS meteorological data set indicated substantial amounts of missing data for these inputs (especially for solar radiation and cloud cover); hence, the SWAT weather generator was preferred to enable consistent 30-year simulations. HSPF does not simulate crop growth, so monthly coefficients are incorporated in the model to convert reference crop PET to values appropriate to different crop stages using the Food and Agriculture Organization (FAO) method (Allen et al., 1998).

Table 4-4. Weather station statistics for the 20 study areas (1971–2000)

Model area	Number of precipitation stations	Average annual precipitation total (inches)	Number of temperature stations	Average annual temperature (°F)
Apalachicola-Chattahoochee-Flint Basins	37	54.26	22	63.43
Arizona: Salt, Verde, and San Pedro	29	19.67	25	56.81
Cook Inlet Basin	14	28.50	14	34.16
Georgia-Florida Coastal Plain	51	53.21	37	68.24
Illinois River Basin	72	38.25	47	49.00
Lake Erie Drainages	57	38.15	41	49.10
Lake Pontchartrain Drainage	26	66.33	15	66.64
Minnesota River Basin	39	28.26	32	43.90
Nebraska: Loup and Elkhorn River Basins	81	26.10	31	48.35
New England Coastal Basins	52	48.45	36	46.23
Powder and Tongue River Basins	37	17.70	30	44.15
Rio Grande Valley	53	15.18	41	44.71
Sacramento River Basin	28	37.47	18	57.45
Southern California Coastal Basins	85	20.21	33	61.20
South Platte River Basin	50	16.82	23	43.46
Susquehanna River Basin	60	41.30	27	48.26
Tar and Neuse River Basins	40	49.91	28	59.91
Trinity River Basin	64	40.65	32	64.78
Upper Colorado River Basin	47	16.36	39	41.73
Willamette River Basin	37	58.38	29	51.19

4.3. SIMULATION OUTPUT AND ENDPOINTS

Simulations focused on streamflow, total nitrogen, total phosphorus, and total suspended solids loads. Output from both models was analyzed as daily time series over the 30-year analysis period. Several summary metrics or endpoints were also calculated based on the daily time series. Because of calibration uncertainty inherent in modeling at this scale, estimates of relative change between historical and future simulations are most relevant. In addition to basic streamflow statistics, comparisons are made for 100-year flood peak (fit with Log Pearson type III distribution; USGS, 1982), average annual 7-day low flow, Richards-Baker flashiness index (a measure of the frequency and rapidity of short-term changes in streamflow; Baker et al., 2004), and days to the centroid of mass for the annual streamflow on a water-year basis (i.e.,

days from previous October 1 at which half of the streamflow for the water year is achieved, an important indicator of changes in the snow accumulation and melt cycle). For the Log Pearson III estimator, use of a regionalized skew coefficient is not appropriate to climate change scenario applications as the regional map represents existing climate. Therefore, the K factor is estimated using the skew coefficient from the model output only, without any weighting with the regional estimate.

Each of the streamflow endpoints discussed in the preceding section has been calculated for each scenario at the output of each HUC-8 contained within a study area. Several other summary measures of the water balance, largely drawn from the work of Hurd et al. (1999), are summarized as averages at the whole-watershed scale. These are the Dryness Ratio (fraction of precipitation that is lost to ET as reported by the SWAT model), Low Flow Sensitivity (expressed as the rate of baseflow generation by shallow groundwater, tile drainage, and lateral subsurface flow pathways in units of cfs/mi²), Surface Runoff Fraction (the fraction of total streamflow from the uplands that occurs through overland flow pathways), Snowmelt Fraction (the fraction of total streamflow from the uplands that is generated by melting snow), and Deep Recharge Rate (the annual average depth of water simulated as recharging deep aquifers that do not interact with local streams). Table 4-5 provides a summary of streamflow and water quality endpoints evaluated in this study.

The mobilization and transport of pollutants will also be affected by climate and land-use change, both as a direct result of hydrologic changes and through changes in land cover and plant growth. Monthly and annual loads of sediment, phosphorus, and nitrogen are likely the most useful and reliable measures of water quality produced by the analysis. Accordingly, the focus of comparison among scenarios is on monthly and average annual loads for total suspended solids, total nitrogen, and total phosphorus. As with the streamflow simulation, it is more robust to examine relative rather than absolute changes in simulated pollutant loads when comparing scenarios to current conditions. Thus, we also calculate and express results as percent changes. All models are calibrated and validated, but in many cases current loads are imprecisely known due to limited monitoring data.

Because the sediment load in rivers/streams is often dominated by channel adjustment processes, which are highly site specific and occur at a fine spatial scale, it is anticipated that precision in the simulation of sediment and sediment-associated pollutant loads will be relatively low. Nutrient balances can also be strongly affected by biological processes in the channels, which can only be roughly approximated at the scale of modeling undertaken. It should also be noted that the modeling makes the following assumptions that limit uses for absolute (as opposed to relative) simulations of future pollutant loads: (1) external boundary conditions (if needed), such as upstream inflows and pollutant loads, are constant; (2) point source discharges and water withdrawals are assumed constant at current rates; (3) no provision is made for human adaptation in rural land management, such as shifts in crop type in response to climate change; and (4) plant growth responses to climate change are simulated to the extent they are represented in the SWAT plant growth model; however, large-scale shifts in natural cover type in response to climate change are not simulated.

Table 4-5. Summary of streamflow and water quality endpoints

Endpoint	Dimension	Description	Calculation
Future Flow Volume	L^3/t	Average of simulated streamflow volume per unit time	Sum of annual streamflow volume simulated by the watershed model
Average Seven Day Low Flow	L^3/t	Average annual 7-day low streamflow event volume	Lowest 7-day-average streamflow simulated for each year
100 Year Peak Flow	L^3/t	Estimated peak streamflow rate based on annual flow maxima series, Log Pearson III method	Log Pearson III extreme value estimate following USGS (1982), based on simulated annual maxima series
Days to Flow Centroid	t (days)	Number of days from the previous October 1 (start of water year) at which half of the streamflow volume for that water year is achieved	Count of days to 50% of simulated total annual streamflow volume for each water year.
Richards-Baker Flashiness Index	dimensionless	Indicator of the frequency and rapidity of short term changes in daily streamflow rates	Analyzed by method given in Baker et al. (2004), applied to daily streamflow series for each year
Dryness Ratio	dimensionless	Fraction of input precipitation lost to ET	Calculated as (precipitation – outflow)/precipitation for consistency with Hurd et al. (1999)
Low Flow Sensitivity	L/t	Rate of baseflow contributions from shallow groundwater, tile drainage, and lateral subsurface flow pathways, depth per unit time	Sum of simulated streamflow from shallow groundwater, tile drainage, and lateral subsurface flow pathways divided by area.
Surface Runoff Fraction	dimensionless	Fraction of streamflow contributed by overland flow pathways	Surface runoff divided by total outflow.
Snowmelt Fraction	dimensionless	Fraction of streamflow contributed by snowmelt	Estimated as water equivalent of simulated snowfall divided by total precipitation
Deep Recharge	L/t	Depth of water recharging deep aquifers per unit time	Total water volume simulated as lost to deep recharge divided by area
AET	L/t	Actual depth of evapotranspiration lost to the atmosphere per unit time	Evapotranspiration simulated by the watershed model
PET	L/t	Theoretical potential evapotranspiration as depth per unit time, assuming moisture not limiting	Potential evapotranspiration simulated by the Penman-Monteith method (Jensen et al., 1990)
Total Suspended Solids (TSS)	$mass/t$	Mass load of suspended sediment exiting stream reach per unit time	Sum of simulated mass exiting a stream reach
Total Phosphorus (TP)	$mass/t$	Mass load of total phosphorus exiting reach per unit time	Sum of simulated mass exiting a stream reach
Total Nitrogen (TN)	$mass/t$	Mass load of total nitrogen exiting stream reach per unit time	Sum of simulated mass exiting a stream reach

4.4. MODEL CALIBRATION AND VALIDATION

The watershed models were calibrated and validated in each of the study areas in accordance with the project Quality Assurance Project Plan (QAPP; see Appendix B). The following section

provides a brief summary of calibration and validation methods and results. Detailed description of calibration and validation methods and results for the individual study areas are presented in Appendices D through W.

Calibration refers to the adjustment of model parameters to reproduce or fit simulation results to observed data. Calibration is required for parameters that cannot be deterministically and uniquely evaluated from topographic, climatic, physical, and chemical characteristics of the watershed and compounds of interest. Validation is performed by application of the calibrated model to a different period of observed data to test the robustness of the calibrated parameter set. If the model exhibited a significant degradation in performance in the validation period, the calibration process is repeated until results are considered acceptable.

The calibration and validation approach for the study areas was to first focus on a single HUC-8 within the larger study area (preferably one for which some modeling was already available along with a good record of flow gaging and water quality monitoring data), and then extend the calibration to adjacent areas with modifications as needed to achieve a reasonable fit at multiple spatial scales. Each HUC-8 watershed was generally subdivided into approximately 8 subbasins, approximating the HUC-10 watershed scale.

The base period of observed data used for calibration and validation was approximately 1970 to 2000, with some variation depending on availability of meteorological data, while the base land use was from 2001 NLCD. In watersheds with significant land-use change, moving back too far from 2001 may not provide a firm basis for calibration. Therefore, calibration generally focused on approximately the 1991–2001 time period, although the full 1971–2000 period was used for comparison to future changes. Validation was typically performed on the period before 1991 and/or data from post-1991 at different locations.

4.4.1. Hydrology

The goal of hydrologic calibration for both HSPF and SWAT was to achieve error statistics for total streamflow volume, seasonal streamflow volume, and high and low streamflow within the range recommended by Lumb et al. (1994) and Donigian (2000) while also maximizing the Nash-Sutcliffe coefficient of model fit efficiency (E). Standardized spreadsheet tools were developed to help ensure consistency in the calibration and validation process across watersheds, and to provide a standardized set of statistics and graphical comparisons to data. These statistics were used to adjust appropriate model parameters until a good statistical match was shown between the model output and observed data.

Lumb et al. (1994) and Donigian (2000) recommend performance targets for HSPF based on relative mean errors calculated from simulated and observed daily average streamflow. Donigian classified these into qualitative ranges, which were modified slightly in this project for application to both HSPF and SWAT (see Table 4-6). In general, hydrologic calibration endeavored to achieve a “good” level of model fit where possible. It is important to note that the tolerance ranges are intended to be applied to mean values and that individual events or observations may show larger differences and still be acceptable (Donigian, 2000).

Table 4-6. Performance targets for hydrologic simulation (magnitude of annual and seasonal relative mean error) from Donigian (2000)

Model component	Very good (%)	Good (%)	Fair (%)	Poor (%)
1. Error in total volume	≤5	5–10	10–15	>15
2. Error in 50% lowest streamflow volumes	≤5	5–10	10–25	>25
3. Error in 10% highest streamflow volumes	≤10	10–15	15–25	>25
4. Error in storm volume	≤10	10–20	20–30	>30
5. Winter volume error	≤15	15–30	30–50	>50
6. Spring volume error	≤15	15–30	30–50	>50
7. Summer volume error	≤15	15–30	30–50	>50
8. Fall volume error	≤15	15–30	30–50	>50
9. Error in summer storm volumes	≤25	25–50	50–75	>75

The Nash-Sutcliffe coefficient of model fit efficiency (E) is also widely used to evaluate the performance of models that predict time series. Nash and Sutcliffe (1970) define E as:

$$E = 1 - \frac{\sum_{i=1}^n (O_i - P_i)^2}{\sum_{i=1}^n (O_i - \bar{O})^2}, \quad 4-4$$

where O_i and P_i represent members of a set of n paired time series observations and predictions, respectively, and \bar{O} is the mean of the observed values. E ranges from minus infinity to 1.0, with higher values indicating better agreement. The coefficient represents the ratio of the mean square error to the variance in the observed data, subtracted from unity (Wilcox et al., 1990). A value of zero for E indicates that the observed mean is as good a predictor of time series values as the model, while negative values indicate that the observed mean is a better predictor than the model. A value of E greater than 0.7 is often taken as an indicator of a good model fit (Donigian, 2000). Note, however, that the value depends on the time basis on which the coefficient is evaluated. That is, values of E for monthly average streamflow are typically noticeably greater than values of E for daily streamflow, as watershed models, in the face of uncertainty in the representativeness of precipitation records, are often better predictors of interseasonal trends than of intraseasonal variability. Moriasi et al., (2007) recommend a Nash-Sutcliffe E of 0.50 or better (applied to monthly sums) as an indicator of adequate hydrologic calibration when accompanied by a relative error of 25% or less.

A potential problem with the use of E is that it depends on squared differences, making it overly sensitive to extreme values (Legates and McCabe, 1999). This is particularly problematic for sparse time series, such as water quality observations, in which poor estimation of one or a few high outliers may strongly influence the resulting statistic. It is an even greater problem for the

comparison of model output to load estimates based on sparse concentration data, as these estimates are themselves highly uncertain (using point-in-time grab samples to represent daily averages and interpolating to unobserved days), further increasing the leverage associated with high outliers.

To address these issues and lessen the effect of outliers, Garrick et al. (1978) proposed use of a baseline adjusted coefficient of model fit efficiency, E_1' , which depends on absolute differences rather than squared differences:

$$E_1' = 1 - \frac{\sum_{i=1}^n |O_i - P|}{\sum_{i=1}^n |O_i - \bar{O}'|} \quad 4-5$$

Garrick's proposed statistic is actually more general, allowing \bar{O}' to be a baseline value that may be a function of time or of other variables, rather than simply the mean. E_1' may be similar to or greater or less than E for a given set of predictions and measurements depending on the type of outliers that are present.

For most watershed models, E is an appropriate measure for the fit of streamflow time series in which complete series of observations are known with reasonable precision. E_1' is a more appropriate and stable measure for the comparison of simulated pollutant loads to estimates based on sparse observed data.

4.4.1.1. Flow Calibration Adjustments

HSPF and SWAT hydrology calibration adjustments were made for a range of sensitive model parameters selected to represent key watershed processes affecting runoff (U.S. EPA, 2000; Neitsch et al., 2005; see Tables 4-7 and 4-8, respectively, for selected key parameters most frequently adjusted). The adjustment of other parameters and the degree of adjustment to each parameter vary by watershed. Details are provided in the individual calibration reports for each of the watersheds in Appendices D through W.

Table 4-7. Key hydrology calibration parameters for HSPF

Parameter name	Definition
INFILT	Nominal infiltration rate parameter
AGWRC	Groundwater recession rate
LZSN	Lower zone nominal soil moisture storage
BASETP	ET by riparian vegetation
KMELT	Degree-day melt factor
PET factor	Potential evapotranspiration
DEEPPFR	Fraction of groundwater inflow that will enter deep groundwater
LZETP	Lower zone E-T parameter

Table 4-8. Key hydrology calibration parameters for SWAT

Parameter name	Definition
CN	Curve numbers—varied systematically by land use
ESCO	Soil evaporation compensation factor
SURLAG	Surface runoff lag coefficient
ALPHA_BF	Baseflow alpha factor
GW_DELAY	Groundwater delay time
CANMAX	Maximum canopy storage
OV_N, CH_N2, CH_N1	Manning’s “n” values for overland flow, main channels, and tributary channels
SoI_AWC	Available water capacity of the soil layer, mm water/mm of soil
Bank storage and recession rates	Bank storage and recession rates
Snow parameters SFTMP, SMTMP, SMFMX and SMFMN	Snowfall temperature, snowmelt base temperature, maximum melt rate for snow during year, and minimum melt rate for snow during year
TIMP	Snow pack temperature lag factor
CH_K1	Effective hydraulic conductivity in tributary channel alluvium

4.4.2. Water Quality

The models in this study are designed to simulate total nitrogen, total phosphorus, and total suspended solids. The first objective of calibration was to reduce the relative absolute deviation between simulated and estimated loads to below 25% if possible. The water quality calibration focuses on the replication of monthly loads, as specified in the project QAPP (see Appendix B). While a close match to individual, instantaneous concentration observations cannot be expected given the approach taken in the model simulations of water quality, the calibration also examined the general relationship of observed and predicted concentrations with the intent of minimizing bias relative to streamflow regime or time of year. Comparison to monthly loads presents challenges, as monthly loads are not observed. Instead, monthly loads must be estimated from

scattered concentration grab samples and continuous streamflow records. As a result, the monthly load calibration is inevitably based on the comparison of two uncertain numbers. Nonetheless, calibration is able to achieve a reasonable agreement. The direct comparison of estimated and simulated monthly loads was supplemented by detailed examinations of the relationships of streamflow to loads and concentrations, and the distribution of concentration prediction errors versus streamflow, time, and season to help minimize bias in the calibration.

For application on a nationwide basis, it was assumed that total suspended solids and total phosphorus loads will likely exhibit a strong positive correlation to streamflow (and associated erosive processes), while total nitrogen loads, which often have a dominant subsurface loading component, will not (Allan, 1986; Burwell et al., 1975; Follett, 1995). Accordingly, total suspended solids and total phosphorus loads were estimated from observations using a flow-stratified log-log regression approach, while total nitrogen loads were estimated using a flow-stratified averaging estimator, consistent with the findings of Preston et al. (1989).

4.4.2.1. *Water Quality Calibration Adjustments*

Water quality calibration began with sediment transport processes. Observed suspended solids concentrations are the result of multiple processes, including sediment detachment, sediment transport in overland flow, and channel scour and deposition processes. The sediment detachment routines for both SWAT and HSPF were related to USLE parameters available in the soils database. For most basins, calibration focuses on sediment transport in overland flow, using the peak rate or transport rate factors available in both models. Channel scour and deposition processes were modified where needed to achieve a fit to observations or where detailed work with prior models provided a basis for modifying the default parameters.

In HSPF, nitrogen loading from the land surface was simulated as a buildup/washoff process, while phosphorus was simulated as sediment-associated. Both nitrogen and phosphorus also were simulated with dissolved-phase loads from interflow and groundwater discharge. Calibration for nutrients in HSPF primarily addressed adjustments of the buildup/washoff coefficients or sediment potency (concentration relative to sediment load) factors and monthly subsurface discharge concentrations. In SWAT, the nutrient simulation is intimately linked to the plant growth model, but is sensitive to initial nutrient concentrations and the ability of plants to withdraw nutrients from various soil layers. In watersheds where significant channel scour was simulated, the nutrient content of scoured sediment was also an important calibration parameter.

4.4.3. Accuracy of the Watershed Models

The quality of model fit varies with the study area and parameter considered. In general, the full suite of SWAT models for the 20 watersheds—after calibration—provide a good to excellent representation of the water balance at the monthly scale and a fair to good representation of hydrology at the daily scale (see Table 4-9 for the initial calibration site results). The quality of model fit to hydrology as measured at multiple stations (HUC-8 spatial scale and larger) throughout the watershed was, not surprisingly, better when a spatial calibration approach was used. At all calibration and validation sites, the median monthly Nash-Sutcliffe *E* coefficient from the SWAT models was 0.74 for both the pilot and nonpilot study areas. More detailed calibration and validation results for each study area are provided in Appendices D through W.

Less precise model fit to observations resulted in several study areas for various reasons. In addition to differences in individual modeler preferences and skill, Low E coefficients in the Rio Grande Valley likely reflect insufficient knowledge of operations of the many reservoirs in the basin. Calibrating watershed hydrology was problematic in systems dominated by large-scale interactions with regional groundwater systems—notably, Verde River in Arizona and the Loup/Elkhorn River system in the Nebraska sandhills. Both HSPF and SWAT use simplistic storage reservoir representations of groundwater in which water can percolate from the soil profile into local shallow groundwater storage, from which it is gradually released following an exponential decay pattern characterized by a recession coefficient. Perennial streamflow in the Verde River is sustained by groundwater discharges of nonlocal origin that derive from the upstream Chino basin. The Loup and Elkhorn Rivers drain highly porous sands where surface runoff is minimal and streamflow in some tributary rivers is nearly constant and only weakly correlated to rainfall patterns (e.g., see Figure 4-1), a situation that is difficult to address in a rainfall-runoff model without linking to a true groundwater simulation model.

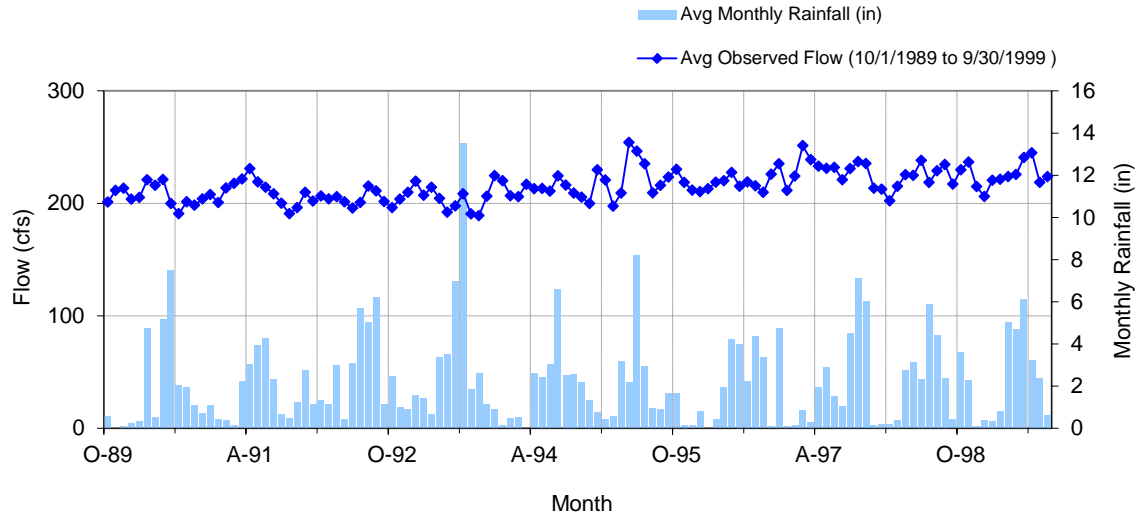


Figure 4-1. Example of weak correlation of rainfall and flow in the Dismal River at Thedford, NE (USGS 06775900) in the Loup River basin.

Different modelers handled the situation in these two regions in different ways. For the Verde River (where both HSPF and SWAT were applied) the regional groundwater inflow was specified as an external forcing time series. This has the advantage of allowing the model calibration to focus on rainfall-runoff events that are responsible for most year-to-year variability in streamflow and most pollutant transport. The major disadvantage is that there is not a clear means to specify how this groundwater forcing might respond to changes in climate. Instead, results for the Verde River show relative changes that would be expected under the assumption that the regional groundwater discharge does not change.

For the Loup and Elkhorn River basins, a reasonable fit to both calibration and validation periods was obtained by specifying extremely slow groundwater recession rates in conjunction with use

of the soil crack flow option (which allows a fraction of rainfall to flow directly to groundwater) in the sandhill region. This approach can replicate the major observed features of the water balance, although it does not achieve a high degree of precision in explaining day-to-day variability in observed streamflow. Further, the simulated groundwater discharges are responsive to changes in climate forcing. However, use of this approach comes at a cost due to the way that groundwater is simulated in the SWAT model. Specifically, SWAT simulates baseflow discharge on a given day as a function of discharge on the previous day, modified by the recession coefficient, plus the effects of new recharge to groundwater. Groundwater discharge at the start of the simulation is constrained to be zero. Use of a very slow recession rate gives a reasonable fit to the calibration and validation periods in this study area; however, it also results in very slow convergence of estimated groundwater discharge from the initial zero. This resulted in a situation in which it took approximately 10 years for streamflow to reach levels in line with observations. Thus, simulated streamflow for the early years are often zero. Adding a longer spinup period does not resolve the problem as the low recession rate results in a nonstationary solution in which baseflow continues to gradually increase over time and the simulated streamflow eventually overshoots observations during the calibration period if the spinup period is extended. Due to this issue, change scenario results are presented only for the 20-year calibration and validation periods in the Loup and Elkhorn River study area.

Calibration and validation for water quality is subject to higher uncertainty than streamflow calibration due to limited amounts of monitoring data and a simplified representation of the multiple complex processes that determine in-stream pollutant concentrations. The primary objective of water quality simulation in this project is to assess relative changes in pollutant loads, but loads are not directly observed. Inferring loads from point-in-time concentration data and streamflow introduces another layer of uncertainty into the calibration process. Calibration also examined observed versus predicted concentrations; however, SWAT, as a daily curve number model, does not have a high level of skill in simulating instantaneous concentrations, particularly during high flow events, and is better suited to the simulation of loads at the weekly to monthly scale.

As with the hydrology calibration, the reliability of the models for simulating changes in water quality appears to increase with calibration at multiple locations. In general, it is more difficult to obtain a high level of precision for simulated water quality than for hydrology in a watershed model, as the processes are complex, the data typically sparse, and any errors in hydrology tend to be amplified in the water quality simulation. The water quality calibration is based on loads, but loads are not directly observed. Instead, loads are inferred from sparse concentration monitoring data and streamflow gaging. Thus, both the simulated and “observed” loads are subject to considerable uncertainty. Comparison based on concentrations can also be problematic, as most water quality samples are grab samples that represent points in time and space, whereas model output is integrated over a stream segment and may produce large apparent errors due to small shifts in timing. Finally, most stations at the HUC-8 scale include upstream point sources, which often have a strong influence on low-flow concentrations and load estimates. Limited knowledge about point source loads thus also creates a challenge for the water quality calibration. In most cases, the pollutant load simulations from the SWAT model appear to be in the fair to good range (see Table 4-9)—except in a few cases where parameters were extended from one station to another watershed without adjustment, giving poor results. This suggests limits to the reliability of simulation results in the portions of watersheds for which

calibration was not pursued. Nonetheless, simulations of the relative response to climate change and land development scenarios are more reliable than for the actual observed future values—as long as the significant processes that determine pollutant load and transport within a watershed are represented.

HSPF model calibration for the five pilot sites provided a somewhat stronger fit to daily streamflow in four of the five watersheds (see Table 4-10), presumably at least in part due to HSPF's use of subdaily precipitation. In two models, the fit to total suspended solids load was notably worse for HSPF, apparently due to the difficulties in adjusting the more complex channel scour and deposition routines of this model with limited data and on a compressed schedule.

Table 4-9. Summary of SWAT model fit for initial calibration site (20 study areas)

Study area	Initial calibration/validation watershed	Initial calibration/validation USGS gage	Hydrology cal./val. yr	Total volume cal./val. (daily and monthly <i>E</i>)	Total volume cal./val. (% error)	Water quality cal./val yr	TSS monthly load cal./val. (% error)	TP monthly load cal./val. (% error)	TN monthly load cal./val. (% error)
ACF	Upper Flint River	02349605	1993–2002/ 1983–1992	0.62/0.56 0.88/0.83	7.28/3.33	1999–2002/ 1991–1998	–9/17	–50/–30	–18/9
Ariz	Verde River	09504000	1992–2002/ 1982–1992	0.03/–1.0 0.88/0.32	–2.46/5.68	1993–2002/ 1986–1992	16.9/–42.6	83.5/31.4	–14.4/–15.9
Cook	Kenai River	15266300	1992–2001/ 1982–1991	0.68/0.55 0.80/0.75	–18.96/19.49	1985–2001/ 1972–1984	66.4/64.1	83.2/82.18	57.3/50.4
GaFla	Ochlockonee River	02329000	1992–2002/ 1982–1992	0.71/0.80 0.79/0.90	4.25/–5.54	1992–2002/ 1982–1992	9.5/–6.6	–7.4/–5.8	–8/–5
Illin	Iroquois River	05526000	1992–2001/ 1982–1992	0.70/0.67 0.77/0.71	–16.99/–2.98	1985–2001/ 1978–1984	38/39	5/–1	56/60
LErie	Cuyahoga River	04208000	1990–2000/ 1980–1990	0.61/0.62 0.70/0.73	–3.32/–13.38	1990–2000/ 1980–1990	67.9/69.8	23.9/–12.5	35.8/13.7
LPont	Amite River	07378500	1995–2004/ 1985–1994	0.79/0.69 0.95/0.90	–1.61/–0.93	1984–1994/ ND	9.2/NA	2.4/NA	–8.9/NA
Minn	Cottonwood River	05317000	1992–2002/ 1982–1992	0.79/0.74 0.91/0.83	–5.41/–0.84	1993–2000/ 1986–1992	9.2/9	9.3/–21.6	–8.9/–1.3
Neb	Elkhorn River	06800500	1989–1999/ 1978–1988	0.42/0.52 0.70/0.66	–2.59/–8.81	1990–1995/ 1979–1989	59.6/66.8	24.2/34.9	28.1/18.1
NewEng	Saco River	01066000	1993–2003/ 1983–1993	0.61/0.76 0.71/0.84	1.08/0.67	1993–2003/ 1983–1993	–9/3.2	9.6/–11.5	27.5/26.3
PowTon	Tongue River	06306300	1993–2003/ 1983–1993	0.72/0.7 0.83/0.82	9.26/–9.95	1993–2003/ 1982–2002	–21.8/–3.4	8.8/35.1	3.9/31.5
RioGra	Saguache Creek	08227000	1993–2003/ 1983–1993	0.47/0.07 0.53/0.31	–4.92/32.99	1985–2003/ 1973–1984	57.3/41	–46.9/–653.98	–28.3/–909.1
Sac	Sacramento River	11377100	1992–2001/ 1983–1992	0.75/0.57 0.94/0.92	10.23/10.06	1997–2001/ 1973–1996	–2/–55	–8/–33	–135/–156
SoCal	Santa Ana River	11066460	1991–2001/ 1981–1991	0.63/0.59 0.75/0.68	3.71/1.61	1998–2000/ ND	19/NA	–14.7/NA	–5.5/NA
SoPlat	South Platte River	06714000	1991–2000/ 1981–1990	0.74/0.52 0.86/0.63	9.82/–16.28	1993–2000/ ND	86.6/NA	–14/NA	6.1/NA

Table 4-9. Summary of SWAT model fit for initial calibration site (20 study areas) (continued)

Study area	Initial calibration/validation watershed	Initial calibration/validation USGS gage	Hydrology cal./val. yr	Total volume cal./val. (daily and monthly <i>E</i>)	Total volume cal./val. (% error)	Water quality cal./val yr	TSS monthly load cal./val. (% error)	TP monthly load cal./val. (% error)	TN monthly load cal./val. (% error)
Susq	Raystown Branch of the Juniata River	02050303	1995–2005/ 1985–1995	0.29/0.42 0.67/0.66	–5.41/16.3	1991–2000/ 1990	–10.1/–33.6	–0.5/–9.2	28.6/43.9
TarNeu	Contentnea Creek	02091500	1993–2003/ 1983–1993	0.68/0.64 0.86/0.74	–3.98/–1.18	1993–2003/ 1983–1993	–19.9/9.9	15.9/5.3	–5.6/5.3
Trin	Trinity River	08066500	1992–2001/ 1982–1991	0.62/0.47 0.74/0.76	–6.88/0.70	1985–2001/ 1972–1984	9.2/–17.4	3/–21.58	–3.8/–31.9
UppCol	Colorado River	09070500	1992–2002/ 1982–1992	0.83/0.78 0.86/0.82	8.18/0.93	1992–2002/ — ND	0.4/NA	47.4/NA	15.1/NA
Willa	Tualatin River	14207500	1995–2005/ 1985–1995	0.49/0.39 0.88/0.81	–4.76/–12.1	1991–1995/ 1986–1990	–12/–7	–114/–105	–72/–66

Table 4-10. Summary of HSPF model fit for initial calibration sites (five pilot study areas)

Study area	Initial calibration/validation watershed	Initial calibration/validation USGS gage	Hydrology cal./val. yr	Total volume cal./val. (daily and monthly <i>E</i>)	Total volume cal./val. (% error)	Water quality cal./val yr	TSS monthly load cal./val. (% error)	TP monthly load cal./val. (% error)	TN monthly load cal./val. (% error)
ACF	Upper Flint River	02349605	1993–2002/ 1983–1992	0.71/0.65 0.93/0.90	5.50/5.79	1999–2002/ 1991–1998	–117/–78	–59/–23	–30/–22
Ariz	Verde River	09504000	1992–2002/ 1982–1992	0.48/0.45 0.85/0.66	2.43/6.31	1993–2002/ 1986–1992	31/–41	87/66	1.6/–2.7
Minn	Cottonwood River	05317000	1992–2002/ 1982–1992	0.75/0.78 0.69/0.86	1.61/14.78	1993–2002/ 1986–1992	7.5/13.1	23/15.8	15.4/16.2
Susq	Raystown Branch of the Juniata River	02050303	1995–2005/ 1985–1995	0.70/0.55 0.90/0.87	–0.16/–8.0	1991–2000/ 1990	–78.2/–89.7	26.0/21.5	7.0/17.2
Willa	Tualatin River	14207500	1995–2005/ 1985–1995	0.73/0.81 0.96/0.92	–3.92/–9.80	1991–1995/ 1986–1990	3.0/4.8	–1.2/–9.3	2.2/–6.3

5. CLIMATE CHANGE AND URBAN DEVELOPMENT SCENARIOS

Watershed simulations were conducted using SWAT and HSPF in each study area to assess the sensitivity of streamflow, total nitrogen, total phosphorus, and total suspended solids loads to a range of plausible mid-21st century climate change and urban development scenarios. Climate change scenarios are based on downscaled climate model projections for mid-21st century from the NARCCAP and BCSD (Maurer et al., 2007) data sets. Fourteen climate scenarios were applied to the five pilot sites, and a subset of 6 climate scenarios from the NARCCAP archive were applied to the nonpilot sites. Scenarios of urban and residential development were based on projections from EPA's ICLUS project (U.S. EPA, 2009c).

Simulations were conducted to assess the response to climate change scenarios alone, urban and residential development scenarios alone, and combined climate change and urban development scenarios. The following sections discuss the use and implementation of climate change and urban development scenarios in this study.

5.1. SCENARIO-BASED APPROACH

The scientific uncertainties related to our understanding of the physical climate system are large, and they will continue to be large for the foreseeable future. It is beyond our current capabilities to predict with accuracy decadal (and longer) climate changes at the regional spatial scales of relevance for watershed processes (e.g., see Cox and Stephenson, 2007; Stainforth et al., 2007; Raisanen, 2007; Hawkins and Sutton, 2009; among many others). The uncertainties associated with socioeconomic trajectories, technological advances, and regulatory changes that will drive greenhouse gas emissions changes (and land-use changes) are even larger and less potentially tractable.

Faced with this uncertainty, an appropriate strategy is to take a scenario-based approach to the problem of understanding climate change impacts on water quality. A scenario is a plausible description of how the future may develop, based on a coherent and internally consistent set of assumptions about driving forces and key relationships (IPCC, 2007). Scenarios are used in assessments to provide alternative views of future conditions considered likely to influence a given system or activity. By systematically exploring the implications of a wide range of plausible alternative futures, or scenarios, we can reveal where the greatest vulnerabilities lie. This information can be used by decision makers to help understand and guide the development of response strategies for managing climate risk. A critical step in this approach is to create a number of plausible future states that span the key uncertainties in the problem. The goal is not to estimate a single, "most likely" future trajectory for each study watershed, but instead to understand, to the extent feasible, how big an envelope of potential future impacts we are unable to discount and must therefore incorporate into future planning.

Note that for climate change studies, the word "scenario" is often used in the context of the IPCC greenhouse gas storylines. The IPCC emissions scenarios describe alternative development pathways, covering a range of demographic, economic, and technological driving forces that affect greenhouse gas emissions. This can produce some confusion when phrases like "climate change scenarios" are used to refer to the future climates simulated using these greenhouse gas

storylines. For the purposes of this study, “scenario” is a generic term that can be applied to any defined future, including a climate future or a land-use future, among others.

5.2. CLIMATE CHANGE SCENARIOS

It is standard practice when assessing climate change impacts to consider an ensemble of climate change scenarios based on different climate models and emissions pathways. Use of a single model run is not considered scientifically rigorous because different GCMs often produce very different results, and there is no consensus in the climate modeling community that any model is comprehensively better or more accurate than the others (e.g., see Gleckler et al., 2008). Different methods of “downscaling” GCM model output to finer spatial scales can also influence the variability among models.

5.2.1. Future Climate Models, Sources, and Downscaling

To sample across this model-based uncertainty, this project focused on six climate change scenarios derived from four GCMs covered by the regional downscaling efforts of the NARCCAP (<http://www.narccap.ucar.edu>). NARCCAP uses higher-resolution RCMs to dynamically downscale output from four of the GCMs used in the IPCC 4th Assessment Report (IPCC, 2007) to a $50 \times 50 \text{ km}^2$ grid over North America. This downscaled output is archived for the two 30-year periods (1971–2000 and 2041–2070) at a temporal resolution of 3 hours. NARCCAP uses the IPCC’s A2 greenhouse gas storyline (which at the time of development was a relatively “pessimistic” future greenhouse gas trajectory, but is now more middle-of-the-road compared to current trends and the most recently developed scenarios). We note that, by mid-21st Century, the different IPCC greenhouse gas storylines have not yet diverged much, so impact of the choice of any one particular storyline is diminished compared to later in the century.

At the time we initiated the watershed modeling, six downscaled scenarios were available from NARCCAP, and we are using these six as our common set of climate scenarios across all the 20 watersheds, as listed in Table 5-1.

One of the objectives of this work was to investigate the influence of downscaling approaches on watershed model simulations. To evaluate the sensitivity of our results to downscaling methodology, we ran the watershed models in the five pilot sites with eight additional scenarios (also listed in Table 5-1) derived from the same four GCMs used in NARCCAP: four scenarios interpolated to station locations directly from the GCM output (without downscaling), and four scenarios based on the BCSD statistically downscaled climate projections described by Maurer et al. (2007), and served at: http://gdo-dcp.ucllnl.org/downscaled_cmip3_projections/. The BCSD data provides monthly mean surface air temperature and precipitation rates for the contiguous United States (along with portions of Canada and Northern Mexico) at a horizontal grid spacing of 1/8 degree (roughly $12 \times 12 \text{ km}^2$) for the period 1950–2099.

The BCSD climate projections use statistical downscaling to interpret GCMs to a finer resolution based on current observations. The principal potential weakness of this approach is an assumption of stationarity. That is, the assumption is made that the relationship between large-scale precipitation and temperature and local precipitation and temperature in the future will be the same as in the past. Thus, the method can successfully account for orographic effects that are

observed in current data, but not for impacts that might result from the interaction of changed wind direction and orographic effects. A second assumption included in the bias-correction step of the BCSD method is that any biases exhibited by a GCM for the historical period will also be exhibited in simulations of future periods.

Table 5-1. Climate models and source of model data used to develop climate change scenarios

Scenario #	Climate model(s) (GCM/RCM)
NARCCAP (dynamically downscaled)	
1	CGCM3/CRCM
2	HadCM3/HRM3
3	GFDL/RCM3
4	GFDL/GFDL hi res
5	CGCM3/RCM3
6	CCSM/WRFP
GCM (without downscaling)	
7	CGCM3
8	HadCM3
9	GFDL
10	CCSM
BCSD (statistically downscaled)	
11	CGCM3
12	HadCM3
13	GFDL
14	CCSM

Model Abbreviations:

- CGCM3: Third Generation Coupled Global Climate Model
<http://www.ec.gc.ca/ccmac-cccma/default.asp?lang=En&n=4A642EDE-1>
- HadCM3: Hadley Centre Coupled Model, version 3
http://www-pcmdi.llnl.gov/ipcc/model_documentation/HadCM3.htm
- GFDL: Geophysical Fluid Dynamics Laboratory GCM
http://www-pcmdi.llnl.gov/ipcc/model_documentation/GFDL-cm2.htm
- CCSM: Community Climate System Model
http://www-pcmdi.llnl.gov/ipcc/model_documentation/CCSM3.htm
- CRCM: Canadian Regional Climate Model
<http://www.ec.gc.ca/ccmac-cccma/default.asp?lang=En&n=4A642EDE-1>
- RCM3: Regional Climate Model, version 3
<http://users.ictp.it/~pubregcm/RegCM3/>
- HRM3: Hadley Region Model 3
<http://precis.metoffice.com/>
- WRFP: Weather Research and Forecasting Model
<http://www.wrf-model.org/index.php>
- GFDL hi res: Geophysical Fluid Dynamics Laboratory 50-km global atmospheric time slice
http://www-pcmdi.llnl.gov/ipcc/model_documentation/GFDL-cm2.htm

The BCSD scenarios, while all derived from the A2 climate storyline, do not in all cases use the output of the exact same GCM run that was used to construct the NARCCAP archive. Specifically, the BCSD results for the Geophysical Fluid Dynamics Laboratory global climate model (GFDL) and Third Generation Coupled Global Climate Model (CGCM3) GCMs use exactly the same GCM output as NARCCAP, but BCSD results for Hadley Centre Coupled Model, version 3 (HadCM3) and Community Climate System Model (CCSM) use different runs of the A2 scenario than used by NARCCAP. The HadCM3 run used in NARCCAP was a custom run generated specifically for NARCCAP and has not been downscaled for the BCSD archive. The CCSM run used in NARCCAP is run number 5, which is not available in the CMIP3 archive used by BCSD. Instead, BCSD uses the HadCM3 run 1 and CCSM run 4 from the CMIP3 archive for the A2 scenario. As a result, the most direct comparisons between the NARCCAP and BCSD data sets are for the GFDL and CGCM3 GCM models. However, we still expect comparisons between NARCCAP and BCSD for the HadCM3 and CCSM to provide useful insights when considered along with the GFDL and CGCM3 comparisons. These scenarios were evaluated only at the five pilot study areas.

Scenarios for the five pilot sites also examined use of the direct output from the GCM runs used to drive the NARCCAP downscaling (i.e., no downscaling). Comparison of results from these scenarios to full dynamical downscaling is expected to inform the accuracy with which simpler methods can be used to address watershed response. These scenarios were evaluated only at the five pilot study areas.

Table 5-1 summarizes the climate change scenarios used in this study and also contains a numbering key for shorthand reference to climate scenarios. For example, climate scenario 2 refers to the HadCM3 GCM, downscaled with the Hadley Region Model 3 (HRM3) RCM. All 14 scenarios are applied in the five pilot sites. Only scenarios 1 through 6 are applied for the nonpilot sites.

5.2.2. Translation of Climate Model Projections to Watershed Model Weather Inputs

Even the 50-km NARCCAP scale is relatively coarse for watershed modeling. In this study, meteorological time series for input to the watershed models were created using a “change factor” or “delta change” method (Anandhi et al., 2011). Using this approach, a period of baseline observed weather data was selected for each study area (to which the watershed models have been calibrated), and the data series adjusted or perturbed to represent a specific type of climate change projected by a climate model (i.e., a climate change scenario). The benefits of the change factor approach include its simplicity, elimination of the need for bias correction, and ability to create spatially variable climate change scenarios that maintain the observed historical spatial correlation structure among different watershed locations. Specifically, there is a tendency for GCMs to generate too many low-intensity events and to under-simulate the intensity of heavy events (Sun et al., 2006; Dai, 2006). The frequency and duration of large events can have significant effects on hydrology, pollutant loading, and other watershed processes. Applying the model-derived change factors to the observed precipitation time series mitigates this problem. Limitations of this approach include the inability to adjust the number and timing of precipitation events (e.g., to add precipitation events on dry days), and potential bias introduced through the selection of an arbitrary historical base period as the template for

future climate time series. In addition, climate models do not necessarily archive all the meteorological forcing variables required to run watershed models.

Monthly change factors derived from climate models for each climate change scenario were calculated by comparing simulated monthly average values for baseline (1971–2000) and future (2041–2070) climate conditions. It should be noted that the intention is not to simulate the impacts of change in land use and climate that occurred over the decades from 1971 to 2000. Rather, the 1971–2000 meteorological data is assumed to provide a static estimate of natural climate variability under “current” land-use conditions, which are defined by the selection of the 2001 NLCD baseline land cover.

Change statistics from the climate models were interpolated to locations corresponding to each of the BASINS meteorological stations and SWAT weather generator stations used in the watershed models. Change factors were used to perturb existing records of hourly observed precipitation and temperature using the CAT (U.S. EPA, 2009b). CAT permits the sequential modification of weather records to introduce a number of alterations, each reflecting various assumptions concerning the regional manifestations of climate change. Precipitation records can be modified by (1) multiplying all records by an empirical constant reflecting projected climate change to simulate a shift in total precipitation, applied uniformly to all periods and intensity classes, (2) selective application of such a multiplier to specific seasons or months, (3) selective application of the multiplier to a range of months or years within the record, and (4) selective application of the multiplier to storm events of a specific size or intensity class. Modification can be iteratively applied to more than one event size class, allowing changes in frequency and intensity as well as changes in overall volume of precipitation to be represented. Temperature records can be modified by adding or subtracting a constant to all values in the record, or selective application to certain months or years within the record.

The third meteorological time series required by the watershed models is PET, which is calculated based on other meteorological time series as described in Section 5.2.2.3.

The full suite of statistics available to calculate PET using the Penman-Monteith energy balance method is not available for the statistically downscaled model runs or the nondownscaled GCM archives. Data availability is summarized in Table 5-2 and assumptions for creating PET time series in the absence of specific data sets is discussed in Section 5.2.2.3.

It is important to note that using this approach, multiyear climate change scenarios created by perturbing multiple years of historical weather data are representative of a single, future time period and do not represent continuous climatic change during this period (i.e., they are not transient simulations). Instead, the variability in multiyear scenarios created in this way provides a snapshot of the natural variability in climate based on historical conditions.

5.2.2.1. Temperature Changes

Monthly variations (deltas) to the temperature time series throughout the entire time period were applied using the BASINS CAT. Monthly adjustments based on each scenario were used and a modified HSPF binary data (WDM) file was created. The temperature time series were adjusted based on an additive change using the monthly deltas (temperature difference in Kelvin [K]) calculated from the 2041–2070 to 1971–2000 climate simulation comparison. Beginning with

the HSPF WDM, an automated script then creates the SWAT observed temperature files (daily maximum and daily minimum).

Table 5-2. Climate change data available from each source used to develop climate scenarios

Scenario #	RCM	GCM	Temp.	Prec.	Dew point temp	Solar radiation	Wind speed	Min temp.	Max temp.	Prec. bin data
<i>NARCCAP RCM-downscaled scenarios</i>										
1	CRCM	CGCM3	X	X	X	X	X	X	X	X
2	HRM3	HadCM3	X	X	X	X	X	X	X	X
3	RCM3	GFDL	X	X	X	X	X	X	X	X
4	GFDL hi res	GFDL	X	X	X	X	X	X	X	X
5	RCM3	CGCM3	X	X	X	n/a	X	X	X	X
6	WRF	CCSM	X	X	X	X	X	X	X	X
<i>Driving GCMs of the NARCCAP and BCSD scenarios (i.e., no downscaling)</i>										
7		CGCM3	X	X	X	X	X	n/a	n/a	n/a
8		HadCM3	X	X	n/a	n/a	n/a	n/a	n/a	n/a
9		GFDL	X	X	n/a	X	X	n/a	n/a	n/a
10		CCSM	X	X	X	X	n/a	n/a	n/a	n/a
<i>BCSD statistically downscaled scenarios</i>										
11		CGCM3	X	X	n/a	n/a	n/a	n/a	n/a	n/a
12		HadCM3	X	X	n/a	n/a	n/a	n/a	n/a	n/a
13		GFDL	X	X	n/a	n/a	n/a	n/a	n/a	n/a
14		CCSM	X	X	n/a	n/a	n/a	n/a	n/a	n/a

Note: X indicates data are available; n/a indicates not available.

5.2.2.2. Precipitation Changes

Relative changes in the *frequency* and *intensity* of precipitation events associated with climate change may prove to be more influential in determining future patterns of discharge than changes in overall (annual, seasonal) precipitation. Appendix C provides a summary review of recent literature on potential changes in the precipitation regime, including volume and intensity, and the ability of climate models to simulate these changes.

As a general pattern, warming of the lower atmosphere is projected to lead to a more vigorous hydrologic cycle, characterized by increases in global precipitation, and proportionally larger increases in high-intensity precipitation events (Trenberth et al., 2007). Much of the United States is anticipated to experience an increasing proportion of annual precipitation as larger, more intense events (Kundzewicz et al., 2007; Groisman et al., 2012). Increasing intensity of precipitation could increase direct runoff during events and increase nonpoint source loading of sediment, nutrients, and other pollutants to streams (Gutowski et al., 2008). To ensure that model simulations embody the most important dimensions of climate change affecting watershed

response, it is important that climate change scenarios represent potential changes in precipitation intensity-frequency-duration relationships.

The most rigorous approach to applying the downscaled climate scenario results to modification of the existing precipitation series would be to undertake a detailed analysis (by month) of the distribution of precipitation *event* volumes and intensities. Working on an event basis is important because many of the existing precipitation time series in the BASINS meteorological data set are disaggregated from daily totals. However, analyzing volume-event data for each of the climate scenarios for all the precipitation stations was not feasible and the ability of the climate models to correctly simulate event durations is suspect.

Using the change factor method, future climate time series are constructed by applying changes to observed precipitation time series that represent the ratio between historical simulations and future climate simulations in a given climate model. No modifications were made to the number of rainfall events in the observed record. The following approach was developed to apply changes in intensity in the baseline precipitation time series.

Total accumulated precipitation data for different percentile bins (for each station location by month) were provided by NARCCAP for the dynamically downscaled climate change scenarios. The data consisted of total simulated precipitation volume (over 30 years) and the 0–25, 25–50, 50–70, and 70–90, and >90 percentile bins of the 3-hour intensity distribution (relative to the existing intensity distribution). These intensity percentiles yield information on where precipitation intensification occurs, but represent fixed 3-hour windows, not discrete event volumes, as required for the CAT program. Most of the climate scenarios showed increases in precipitation volume in the larger events, while volume in the smaller events remained constant or decreased. The net effect of this was an increase in the proportion of annual precipitation occurring in larger events. Analysis of the comprehensive (percentile, total volume) climate scenario data showed that, for most weather stations, the change in the lower percentiles of the intensity distribution appeared to be relatively small compared to the changes above the 70th percentile. However, in some cases (e.g., in Arizona), there is greater change in the 25–50th percentile bin.

Analyses of observed changes in precipitation during the 20th and early 21st century indicate that more than half of the precipitation increase has occurred in the top 10 or 5% of events (Karl and Knight, 1998; Alexander et al., 2006). However, GCMs have been shown to systematically underestimate the frequency of heavy events in the top few percentages (Trenberth et al., 2003; Sun et al., 2006; Dai, 2006). Therefore, the top 30% range is selected as a compromise that accounts for intensification but remains within the general skill of the climate models.

To account for changes in intensity, climate change scenarios were thus created using the delta method by applying climate change adjustments separately to precipitation events $\geq 70^{\text{th}}$ percentile and events $< 70^{\text{th}}$ percentile, while maintaining the appropriate mass balance as described below.

Percentile bin-intensity data were available only for climate scenarios 1 through 6 (RCM-downscaled scenarios). Bin data were not available for climate scenarios 7 through 14 (GCM and statistically downscaled scenarios). Two approaches were developed to account for

intensification of precipitation, depending on whether precipitation bin data were available. Each approach is discussed in detail below.

Approach 1: Precipitation Bin Data Are Available

For scenarios where bin data was available (the six NARCCAP scenarios) the following approach was used. For these data, the change in the volume above the 70th percentile intensity can be taken as an *index* of the change in the top 30% of *events*. At the same time, it is necessary to maintain mass balance by honoring the predicted relative change in total volume. This can be accomplished mathematically as follows:

Let the ratio of total volume in a climate scenario (V_2) relative to the baseline scenario volume (V_1) be given by $r = (V_2/V_1)$. Further assume that the total event volume (V) can be decomposed into the top 30% (V_H) and bottom 70% (V_L). These may be related by a ratio $s = V_H/V_L$. To conserve the total volume we must have:

$$V_2 = rV_1 \tag{5-1}$$

Equation 5-1 can be rewritten to account for intensification of the top 30% of events (V_H) by introducing an intensification parameter, q :

$$V_2 = rV_{L,1} + rV_{H,1} + (rqV_{H,1} - rqV_{H,1}) = [rV_{L,1} - rqV_{H,1}] + [r(1+q)V_{H,1}], \tag{5-2}$$

Substituting for the first instance of $V_{H,1} = s V_{L,1}$ in eq 5-2 yields:

$$V_2 = (r - rqs)V_{L,1} + (r + qr)V_{H,1} \tag{5-3}$$

In eq 5-3 the first term represents the change in the volume of the lower 70% of events and the second term the change in the top 30%. This provides multiplicative factors that can be applied to event ranges using the BASINS CAT program on a month-by-month basis.

The intensification parameter, q , can be calculated by defining it relative to the lower 70% of values (i.e., from 0 to 70th percentile). Specifically $(r - rqs)$, which represents the events below the 70th percentile, can be written as the ratio of the sum of the volumes below the 70th percentile in a climate scenario relative to the sum of the volumes below the 70th percentile for the current condition:

$$(r - rqs) = \frac{(V_{70})_2}{(V_{70})_1} \approx \frac{(Q_{70})_2}{(Q_{70})_1} \tag{5-4}$$

where $(Q_{70})_1$ and $(Q_{70})_2$ are the sum of the volumes reported up to the 70th percentile for a month for the current condition and future condition respectively.

Solving eq 5-4 for q yields:

$$q = (1 - A/r) / s \tag{5-5}$$

where A is defined as $A = \frac{(Q_{70})_2}{(Q_{70})_1}$

In sum, for each month at each station the following were calculated:

$r = \frac{V_2}{V_1}$ from the summary of the climate scenario output,

$s = \frac{V_H}{(V - V_H)}$ from the existing observed precipitation data for the station, sorted into events and postprocessed to evaluate the top 30% (V_H) and bottom 70% (V_L) event volumes. The numerator is calculated as the difference between total volume and the top 30% volume, rather than directly from V_L to correct for analyses in which some scattered precipitation is not included within defined “events.” The s value was calculated by month and percentile (for every station, every month) using the observed precipitation time-series data that forms the template for the delta method representation of future climate time series.

$q = (1 - A/r) / s$ where A is obtained from the percentile bin climate scenario output summary

The multiplicative adjustment factors for use in the CAT tool can then be assembled as:

$r(1 - qs)$, for the events below the 70th percentile, and
 $r(1 + q)$, for the events above the 70th percentile.

In addition to the typical pattern of increasing rainfall occurring in large events, this approach is applicable for the cases in which there is a relative increase in the low-percentile intensities. In those cases, the change in the 70th percentile intensity is relatively small and tends to be less than current conditions under the future scenario, resulting in q being a small negative number. In such cases, application of the method results in a decrease in the fraction of the total volume

belonging to the larger events, with a shift to the smaller events—thus approximating observed increases in intensity for smaller events.

In general, it is necessary to have $-1 < q < 1/s$ to prevent negative solutions to the multipliers. The condition that $q < 1/s$ is guaranteed to be met by the definition of q (because A/r is always positive); however, the lower bound condition is not guaranteed to be met. Further, the calculation of q from the percentile bin data is at best an approximation of the actual intensification pattern. To address this problem, a further constraint is placed on q requiring that some precipitation must remain in both the high and low ranges after adjustment by requiring $-0.8 < q < 0.8/s$. It should be noted that the cases in which negative solutions arose were rare and mainly occurred for stations located in Arizona in the summer months.

Approach 2: Precipitation Bin Data not Available

For scenarios where bin data were not available (scenarios 7 through 14 based on BCSD and nondownscaled GCM output) the following approach was used. For all these climate scenarios the distribution of volume changes in events of different sizes was not known. However, because the majority of stations in the NARCCAP dynamically downscaled scenarios that had precipitation volume increases also showed strong intensification, it was assumed that any increases in precipitation would occur in the top 30% of events. In the cases where there was a decline in precipitation for a given month, the decreases were applied across all events.

For the case when $r = V_2/V_1 > 1$ (increasing precipitation), the future volume representing the climate scenario (V_2) can be defined as:

$$V_2 = V_{1L} + r^* \cdot V_{1H} \tag{5-6}$$

where r^* is the change applied to the upper range (>30%), V_H is the volume in the top 30%, and V_L is the volume in the bottom 70% of events.

Rearranging eq 5-6 and expressing $r^* = r + (r - 1) \cdot \frac{V_{1L}}{V_{1H}}$, the overall change is satisfied, as:

$$V_2 = V_{1L} + r^* \cdot V_{1H} = V_{1L} + r \cdot V_{1H} - V_{1L} + r \cdot V_{1L} = r(V_{1H} + V_{1L}) = r \cdot V_1 \tag{5-7}$$

Further, as $r > 1$, r^* is always positive.

For the case of $r \leq 1$ (decreasing precipitation), an across-the-board decrease in precipitation was applied as follows:

$$V_2 = r \cdot V_{1L} + r \cdot V_{1H} \tag{5-8}$$

The adjustment factors can then be assembled as follows:

For the events above the 70th percentile, if
 $r > 1$, then use r^*
 $r \leq 1$, then use r .

For the events below the 70th percentile, if
 $r > 1$, then use 1 (no change)
 $r \leq 1$, then use r .

5.2.2.3. *Potential Evapotranspiration Changes*

Potential evapotranspiration is an important parameter that is sensitive to climate change and urban development. In this study, PET is simulated with the Penman-Monteith energy balance method. In addition to temperature and precipitation, the Penman-Monteith method requires dew point (or relative humidity), solar radiation, and wind as inputs. Because only a few stations have time series for all four additional variables that are complete over the entire 1971–2000 period, these variables are derived from the SWAT 2005 statistical weather generator (Neitsch et al., 2005). This is done internally by SWAT. For HSPF implementation a stand-alone version of the weather generator code was created and used to create time series for each of the needed variables at each BASINS meteorological station based on the nearest SWAT weather generator station after applying an elevation correction.

The SWAT weather generator database (.wgn) contains the statistical data needed to generate representative daily climate data for the different stations. Adjustments to the wgn file parameters were made using monthly change statistics for the NARCCAP dynamically downscaled scenarios. Specifically solar radiation, dew point temperature, and wind speed were adjusted for each scenario (see Table 5-3).

The probability of a wet day following a dry day in the month and the probability of a wet day following a wet day in the month were kept the same as in the original SWAT climate generator file for the station. Climate models showed a systematic bias, likely introduced by the scale mismatch (between a 50-km grid and a station observation) for weather generator parameters like wet day/dry day timing, resulting in too many trace precipitation events relative to observed. Thus it was not possible to use climate models to determine changes in these parameters. Also, an analysis of the dynamically downscaled 3-hourly time series for the Canadian Regional Climate Model (CRCM) downscaling of the CGCM3 GCM at five randomly selected locations in the southeast, southwest, mid-Atlantic, upper Midwest, and Pacific Northwest demonstrated that the probability that a rainy day is followed by a rainy day (transition probability) in the model output did not change significantly at any of the sample locations.

For the BCSD climate scenarios, information on these additional meteorological variables is not available. Many of these outputs are also unavailable from the archived nondownscaled GCM output. For these scenarios it was assumed that the statistical parameters remained unchanged at current conditions. While the lack of change is not physically realistic (e.g., changes in rainfall will be associated with changes in cloud cover and thus with changes in direct solar radiation

reaching the land surface), this reflects the way in which output from these models is typically used.

Table 5-3. SWAT weather generator parameters and adjustments applied for scenarios

SWAT wgn file parameter	Description	Adjustment applied
SOLARAV1	Average daily solar radiation for month (MJ/m ² /day)	Adjusted based on Surface Downwelling Shortwave Radiation change (%)
DEWPT1	Average daily dew point temperature in month (°C)	Additive Delta value provided for climate scenario for each month
WNDV1	Average daily wind speed in month (m/s)	Adjusted based on 10-meter Wind Speed change (%)

Inconsistencies in the available data among different scenarios required special treatment. One of the NARCCAP scenario archives (Scenario 5: CGCM3 downscaled with regional climate model, version 3 [RCM3]) does not include solar radiation, which may be affected by changes in cloud cover. Current condition statistics for solar radiation contained in the weather generator were used for this scenario. This does not appear to introduce a significant bias as the resulting changes in PET fall within the range of those derived from the other NARCCAP scenarios.

Table 5-4 compares the reference crop estimates of Penman-Monteith PET for the five pilot watersheds. This is the PET used directly by the HSPF model, while the SWAT model performs an identical calculation internally, and then adjusts actual evapotranspiration (AET) for crop height and leaf area development. Because PET is most strongly a function of temperature, a fairly consistent increase in PET is simulated for most basins. It can be seen from the figures in Appendix Z, however, that the statistically downscaled and nondownscaled GCM scenarios (scenarios 7–14) that do not include solar radiation, dew point, and wind time series consistent with the simulated precipitation and temperature, generally provide higher estimates of PET than do the dynamically downscaled models. This issue is explored in more detail in Section 6.2.

5.3. URBAN AND RESIDENTIAL DEVELOPMENT SCENARIOS

Watershed simulations were also conducted to assess the sensitivity of study areas to potential mid-21st century changes in urban and residential development.

Table 5-4. Comparison of PET estimation between different downscaling approaches

Scenario type		NARCCAP dynamically downscaled		Nondownscaled GCM	BCSD statistically downscaled	NARCCAP dynamically downscaled		Nondownscaled GCM	BCSD statistically downscaled
Climate scenario		1. CRCM-CGCM3	5.RCM3-CGCM3	7. CGCM3	11. CGCM3	3. RCM3-GFDL	4. GFDL (high res)	9. GFDL	13. GFDL
ACF (GA, AL, FL)	annual average PET (in)	60.32	58.59	59.85	64.75	60.46	57.16	67.88	65.97
	difference from NARCCAP mean	1.46%	-1.46%	0.67%	8.90%	2.81%	-2.81%	15.42%	12.17%
Minnesota River (MN, SD)	annual average PET (in)	58.57	55.24	56.22	63.90	54.92	60.02	64.99	63.65
	difference from NARCCAP mean	2.92%	-2.92%	-1.21%	12.29%	-4.44%	4.44%	13.08%	10.75%
Salt/Verde/San Pedro (AZ)	annual average PET (in)	83.67	82.89	84.19	85.01	81.32	82.93	86.73	84.74
	difference from NARCCAP mean	0.47%	-0.47%	1.09%	2.07%	-0.98%	0.98%	5.60%	3.18%
Susquehanna (PA, NY, MD)	annual average PET (in)	43.78	42.24	42.91	51.15	43.06	42.69	50.18	50.17
	difference from NARCCAP mean	1.79%	-1.79%	-0.23%	18.94%	0.43%	-0.43%	17.05%	17.02%
Willamette (OR)	annual average PET (in)	44.18	44.51	45.24	50.73	45.44	43.91	49.16	49.17
	difference from NARCCAP mean	-0.37%	0.37%	2.01%	14.41%	1.70%	-1.70%	10.04%	10.06%

5.3.1. ICLUS Urban and Residential Development Scenarios

Projected changes in urban and residential development were acquired from EPA’s ICLUS project (U.S. EPA, 2009c). ICLUS has produced seamless, national-scale change scenarios for developed land that are compatible with the assumptions about population growth, migration, and economic development that underlie the IPCC greenhouse gas emissions storylines. ICLUS projections were developed using a demographic model coupled with a spatial allocation model that distributes the population as housing units across the landscape. Specifically, population is allocated to 1-hectare (ha) pixels, by county, using the Spatially Explicit Regional Growth Model (SERGoM). The model is run for the conterminous United States and output is available for each emissions storyline by decade to 2100. The final spatial data sets provide decadal projections of housing density and impervious surface cover as a function of population for the period 2000 through 2100 (U.S. EPA, 2009c).

Data from the ICLUS project are composed of grid-based housing density estimates with 100-m cells, whose values are set equal to $units/ha \times 1,000$. Existing housing densities were estimated using a variety of sources and models, and future housing densities developed under various scenarios for each decade through 2100. For the existing housing density grid, two types of “undevelopable” area where residential development was precluded were masked out during the production—a comprehensive spatial data set of protected lands (including land placed in conservation easements), and land assumed to be commercial/industrial under current conditions. Undevelopable commercial/industrial land use was masked out according to the SERGoM method (U.S. EPA, 2009c) that eliminated commercial, industrial, and transportation areas that preclude residential development, identified as “locations (1-ha cells) that had >25% urban/built-up land cover with lower than suburban levels of housing density.”

The ICLUS projections used in this study thus do not account for potential growth in commercial/industrial land use. It is also important to note that the ICLUS projections do not explicitly account for changes in rural or agricultural land uses. These categories change in the analysis based on ICLUS only when they convert to developed land.

5.3.2. Mapping ICLUS Housing Density Projections to NLCD Land Use Categories

The ICLUS projections used in this study are for changes in housing density and impervious cover. This data cannot be used directly with the SWAT and HSPF watershed models, which require land use data consistent with the NLCD. It was therefore necessary to translate between ICLUS projections and NLCD land-use classes.

In addition, ICLUS housing density class estimates and the NLCD developed classes do not have a one-to-one spatial relationship because they are constructed on different underlying scales. ICLUS represents housing density based largely on the scale of census block groups. As a result, it represents the overall density within a relatively large geographic area when compared to the 30 × 30 meter resolution of NLCD 2001 land cover and can represent a mix of different NLCD classes. Therefore, land-use changes must be evaluated on a spatially aggregated basis at the scale of model subbasins.

Baseline land use, derived from the 2001 NLCD, contains four developed land classifications (NLCD classes 21 through 24), nominally representing “developed, open space” (less than 20%

impervious), developed, low intensity (20–49% impervious), developed, medium intensity (50–79% impervious), and developed, high intensity (greater than 80% impervious). Impervious fractions within each developed NLCD land-use class were estimated separately for each study area, using the 2001 NLCD Land Cover and Urban Impervious data products. ICLUS land-use change scenarios were implemented by modifying the existing land-use distribution in the watershed models.

ICLUS estimates housing density on a continuous scale. To process the data more efficiently, the data were reclassified into 10 housing density ranges. In each study area, the ICLUS housing density ranges were cross-tabulated with NLCD 2001 classes based on percent imperviousness. It was assumed that the number of housing units changes, but that the characteristic percent impervious values for each NLCD developed class remains constant. The change in land area needed to account for the change in impervious area was then back calculated.

To represent the net change in future land cover, the change in developed land use was added (or subtracted) from the existing totals in each subbasin. Land area was then removed from each undeveloped NLCD class (excluding water and wetlands) according to their relative ratios in each subbasin to account for increases in developed area. If the undeveloped land area was not sufficient to accommodate the projected growth, development on wetlands was allowed. The reductions in undeveloped land were distributed proportionately among modeled soils (in SWAT) or hydrologic soil groups (in HSPF). The new developed lands were then assumed to have the parameters of the most dominant soil and lowest HRU slope in the subbasin. For HSPF, the changed area was implemented directly in the area table of the user control input (.uci) file. For SWAT, the land-use change was implemented by custom code that directly modified the SWAT geodatabase that creates the model input files.

The gains (and losses) in NLCD class interpreted from ICLUS were tabulated separately for each subbasin. In almost every case, the gains far exceeded the losses and a net increase was projected in all four NLCD developed classes. However, in a few cases there was an overall loss of the lowest density NLCD class. This tended to occur when a subbasin was already built out, and ICLUS projected redevelopment at a higher density.

The projected overall changes in developed land for 2050 as interpreted to the NLCD land-cover classes and used for modeling are presented in Table 5-5. Note that even in areas of expected high growth (e.g., the area around Atlanta in the ACF basin), new development by 2050 is expected to constitute only a small fraction of the total watershed area at the scale of the study areas in this project. The highest rate of land-use change in the studied watersheds is Coastal Southern California, at 11.7%. (Note that the ICLUS project does not cover the Cook Inlet watershed in Alaska. Urban and residential development scenarios were thus not evaluated at this study area.)

Table 5-5. ICLUS projected changes in developed land area within different imperviousness classes by 2050

Study area	Change, <20% impervious class (km ²)	Change, 20–49% impervious class (km ²)	Change, 50–79% impervious class (km ²)	Change, >80% impervious class (km ²)	Total change in developed land (km ²)	Increase as percent of study area (%)
ACF	+665.2	+809.7	+212.3	+90.8	+1,778.0	+3.56
Ariz	+92.1	+87.0	+16.0	+1.3	+196.4	+0.51
Cook	ND	ND	ND	ND	ND	ND
GaFla	+873.9	+776.1	+361.5	+102.2	+2,113.8	+4.65
Illin	+353.5	+1,506.6	+447.5	+116.2	+2,424.0	+5.50
LErie	+152.1	+204.8	+51.0	+15.6	+423.4	+1.40
LPont	+307.2	+308.3	+91.4	+23.4	+730.1	+4.82
Minn	+71.3	+142.9	+60.9	+18.5	+293.5	+0.67
Neb	+8.9	+18.7	+4.1	+1.6	+33.2	+0.06
NewEng	+238.6	+327.2	+215.5	+59.2	+840.4	+3.13
PowTon	+1.3	+0.5	+0.1	0.0	+1.9	+0.00
RioGra	+139.0	+228.8	+57.1	+7.4	+432.4	+0.88
Sac	+103.6	+58.1	+29.5	+8.2	+199.3	+0.93
SoCal	+162.0	+1,001.0	+1,089.1	+114.1	+2,466.2	+11.72
SoPlat	+329.4	+1,364.6	+473.5	+83.6	+2,251.1	+5.93
Susq	+211.1	196.2	+69.6	+25.6	+502.5	+0.71
TarNeu	+492.4	+306.6	+107.4	+29.2	+935.6	+3.66
Trin	+978.9	+1,896.7	+891.1	+304.3	+4,071.0	+8.76
UppCol	+56.9	+168.1	+66.3	+8.3	+299.6	+0.65
Willa	+75.8	+193.4	+95.0	+33.3	+397.6	+1.37

Note: The ICLUS project does not cover the Cook Inlet watershed. Results shown are total new developed area, including pervious and impervious fractions.

6. STREAMFLOW AND WATER QUALITY SENSITIVITY TO DIFFERENT METHODOLOGICAL CHOICES: ANALYSIS IN THE FIVE PILOT STUDY AREAS

One goal of this study was to assess the implications of different methodological choices for conducting climate change impacts assessments on the variability of simulation results. Sensitivity studies in the five pilot study areas allow assessment of the variability resulting from the use of different watershed models, and variability resulting from use of climate change scenarios developed using different methods of downscaling GCM output. The five pilot study areas are the Minnesota River, ACF, Susquehanna, Willamette, and Salt/Verde/San Pedro Rivers. In each of these sites, independent simulations were conducted using the SWAT and HSPF watershed models, and in addition to the six dynamically downscaled NARCCAP scenarios, an additional set of climate change scenarios was evaluated, four based on the BCSD statistically downscaled data set, and four based directly on GCMs with no downscaling. This section presents a summary of these results.

6.1. COMPARISON OF WATERSHED MODELS

The magnitude of the additional variability introduced by choice of a hydrologic model is of interest when simulating hydrologic responses to climate change and urban development. Two different watershed models, SWAT and HSPF, were calibrated and applied to the five pilot study areas. Evaluation of different watershed models can be considered an extension of the scenario-based, ensemble approach commonly used in climate change studies. Detailed examination of the calibration of each model in the five pilot study areas and the results of change scenarios conducted with each model are presented in separate sections and the appendices to this report.

HSPF and SWAT take different approaches to watershed simulation and have different structures and algorithms, resulting in different strengths and weaknesses. Most notably, the two models differ in the way that they represent infiltration and plant-climate interactions. SWAT (in standard application mode) simulates rainfall-runoff processes using a curve number approach, operating at a daily time step. The curve number approach first partitions incoming moisture into direct runoff and a remainder that is available for infiltration. In contrast, HSPF simulates rainfall-runoff processes using Green-Ampt infiltration, in which infiltration into the soil is simulated first, with the remainder available for direct runoff or surface storage.

HSPF is typically run at a subdaily time step, usually hourly for large watersheds, and has a more sophisticated representation of runoff, infiltration, and channel transport processes than does SWAT. SWAT's advantage is that it incorporates a plant growth model (including representation of changes in atmospheric CO₂ concentration) and can therefore simulate some of the important feedbacks between plant growth and hydrologic response. Both models simulate evapotranspiration of soil water stores, but HSPF does this using empirical monthly coefficients relative to potential evapotranspiration, while SWAT incorporates a plant growth model that can, in theory, dynamically represent plant transpiration of soil moisture.

6.1.1. Comparison of Model Calibration and Validation Performance

Models were calibrated and validated using multiple measures as summarized previously in this report and described in detail in Appendices D–W. Calibration of both models was conducted in accordance with the modeling QAPP (see Appendix B; Tetra Tech, 2008a) for each of the five pilot study areas. Development and setup of the two watershed models proceeded from a common basis, with both models using the same subbasin delineations, land use coverage (2001 NLCD), soils coverage (STATSGO), hydrography, digital elevation model, impervious area fractions for developed land classes, and point source and dam representations. Other aspects of model setup were designed to be similar, although it was not possible to be identical because of differences in the way the two models conceptualize discretization of the land surface. For instance, hydrologic response units (the fundamental building blocks of the upland simulation) were created as an overlay of land use and HSG for HSPF, while SWAT uses an overlay of land use and STATSGO dominant soil, associating various other properties from the soil database in addition to HSG with the model hydrologic response units. In addition, HSPF simulates impervious surfaces as a separate land use, while SWAT assigns an impervious fraction to an underlying land use.

Calibration/validation locations and observed data series were the same for both models. Further, the calibration of both models was guided by prespecified statistical analyses that were performed using identical spreadsheet setups obtained from a common template. Despite these commonalities, the scope of the modeling effort in this study required that models be developed by different modeling teams, with inevitable differences in results. To reduce the likelihood of bias, model calibration assignments were structured so that the same team did not apply both HSPF and SWAT to a single study area, and each watershed model was implemented by at least three different modeling teams for the pilot studies.

6.1.1.1. Streamflow Results

This section examines hydrologic simulations as compared to observed streamflow records based on total volume error and the daily Nash-Sutcliffe coefficient of model fit efficiency. Model performance is first examined in terms of the quality of fit for the initial calibration watershed, followed by similar analyses for the largest-scale downstream watershed. Intercomparisons then provide some insight into model performance relative to temporal change (calibration vs. validation period) and relative to spatial change within each study area (calibration watershed vs. downstream watershed).

Summary results for percent error in total volume and the Nash-Sutcliffe E coefficient for daily streamflow are shown in Tables 6-1 and 6-2, respectively, for the initial calibration site along with the calibration fit for the most downstream gage in the watershed. In general, the quality of model fit is good for both models. In most, but not all cases, the quality of model fit is slightly better (smaller magnitude of percent error, larger E coefficient) for the HSPF simulations (e.g., see Figure 6-1 for the calibration period). This is likely due in large part to the use of daily precipitation in SWAT versus hourly precipitation in HSPF, although the advantage accruing to HSPF is muted by the fact that many of the “hourly” precipitation input series used are actually disaggregated from daily totals. Monthly values of Nash-Sutcliffe E are higher for both models, but attention is called to the daily scale because it better reflects the models’ ability to separate surface and subsurface flow pathways. Note that E is low for the Arizona initial site on the

Verde River because streamflow is dominated by relatively constant deep groundwater discharges.

Table 6-1. Percent error in simulated total streamflow volume for 10-year calibration and validation periods at initial and downstream calibration gages

Study area	Model	Initial site calibration	Initial site validation	Downstream calibration
Apalachicola-Chattahoochee-Flint (ACF)	HSPF	5.50	5.79	16.79
	SWAT	7.28	3.33	16.53
Salt/Verde/San Pedro (Ariz)	HSPF	2.43	6.31	4.48
	SWAT	-2.46	5.68	9.43
Minnesota River (Minn)	HSPF	1.61	14.78	-4.25
	SWAT	-5.41	-0.84	7.89
Susquehanna (Susq)	HSPF	-0.16	-8.00	1.79
	SWAT	-5.41	-16.30	-9.74
Willamette (Willa)	HSPF	-3.92	-9.80	2.58
	SWAT	-4.76	12.10	-4.96

Table 6-2. Nash-Sutcliffe coefficient of model fit efficiency (*E*) for daily streamflow predictions, 10-year calibration and validation periods at initial and downstream calibration gages

Study area	Model	Initial site calibration	Initial site validation	Downstream calibration
Apalachicola-Chattahoochee-Flint (ACF)	HSPF	0.71	0.65	0.72
	SWAT	0.62	0.56	0.64
Salt/Verde/San Pedro (Ariz)	HSPF	0.48	0.45	0.53
	SWAT	0.03	-1.00	0.22
Minnesota River (Minn)	HSPF	0.75	0.78	0.92
	SWAT	0.79	0.74	0.63
Susquehanna (Susq)	HSPF	0.70	0.55	0.77
	SWAT	0.29	0.42	0.45
Willamette (Willa)	HSPF	0.80	0.81	0.88
	SWAT	0.49	0.39	0.67

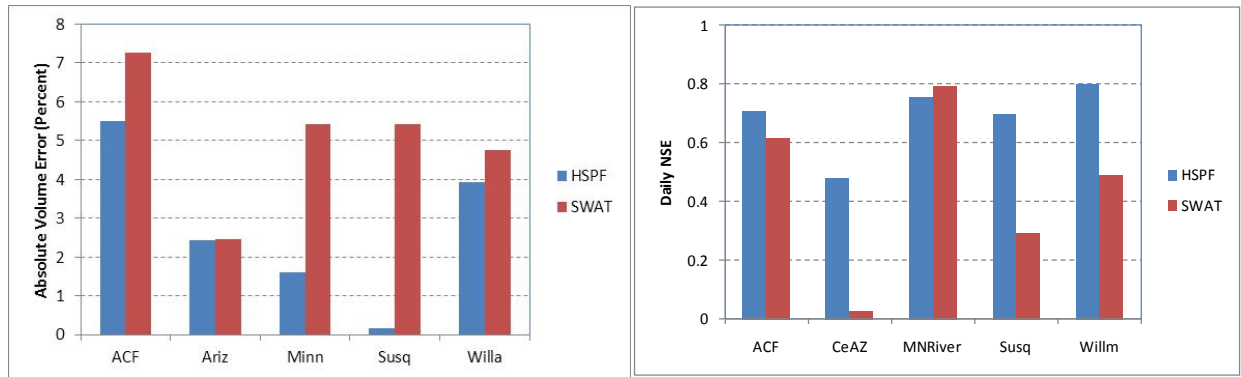


Figure 6-1. Comparison of model calibration fit to streamflow for the calibration initial site.

Note: Figures compare calibration results for HSPF and SWAT. Total volume error is converted to its absolute value.

The ability of the model to assess relative changes in response to altered climate forcing is of paramount importance in this project. Some insight on this topic can be gained by looking at the sensitivity of model fit to temporal and spatial changes in application. Figure 6-2 summarizes the sensitivity to temporal changes by examining the percent error in the calibration period and the validation test. It is interesting to observe that for both the ACF and the Minnesota River, the SWAT model achieved an improvement in total volume error during the validation period. These are the two study areas with the greatest amount of row crop agriculture, and the results may reflect SWAT’s ability to reflect changing responses of crops to changes in climate over the last 20 years.

Figure 6-3 examines model sensitivity to spatial scale, comparing performance during the calibration period for the initial calibration target gage (HUC-8 spatial scale) and the most downstream gage in the model (approximately HUC-4 spatial scale). The left panel shows the change in the absolute magnitude of percent error, while the right panel shows the change in E . A smaller magnitude of change in total volume error or a larger increase in E represents better performance. The changes in total volume errors are generally small, regardless of whether detailed spatial calibration was pursued. In most cases, the models achieved an improvement in E in going from the smaller to the larger scale.

6.1.1.2. Water Quality Results

The water quality calibration compared simulated monthly loads to monthly load estimates obtained from a stratified regression on (typically sparse) observed data. To compare these results between models, the baseline adjusted E_1 ’ coefficient of model fit efficiency is most appropriate. Results are summarized graphically for the calibration period at the calibration initial site and downstream site in Figures 6-4 through 6-6. For suspended solids and total phosphorus, the performances of the two models are similar, while HSPF appears to provide a somewhat better fit for total nitrogen.



Figure 6-2. Sensitivity of model fit for total streamflow volume to temporal change.

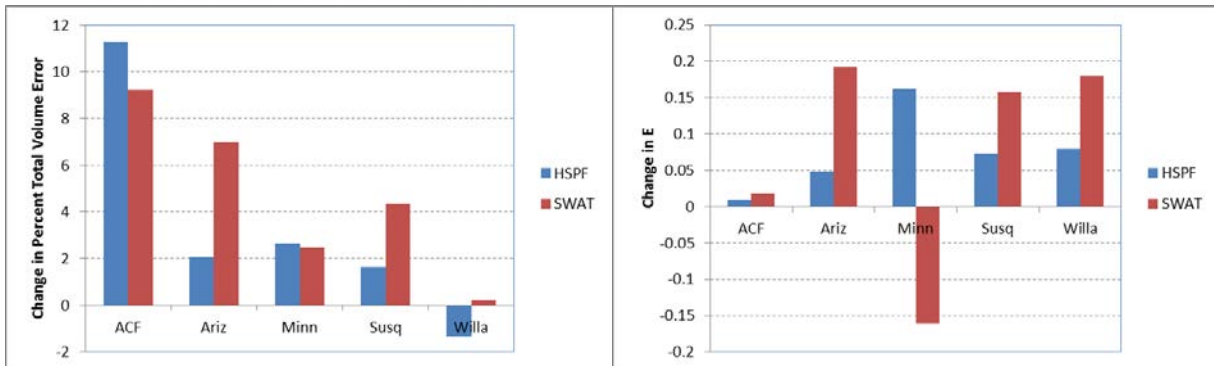


Figure 6-3. Sensitivity of model fit for streamflow to spatial change.

Note: Change in percent total volume error represents the difference in the absolute value of percent error in going from the initial calibration site to a larger scale, typically the furthest downstream site. Change in E represents the difference in the Nash-Sutcliffe E coefficient in going from the calibration site to the larger-scale site.

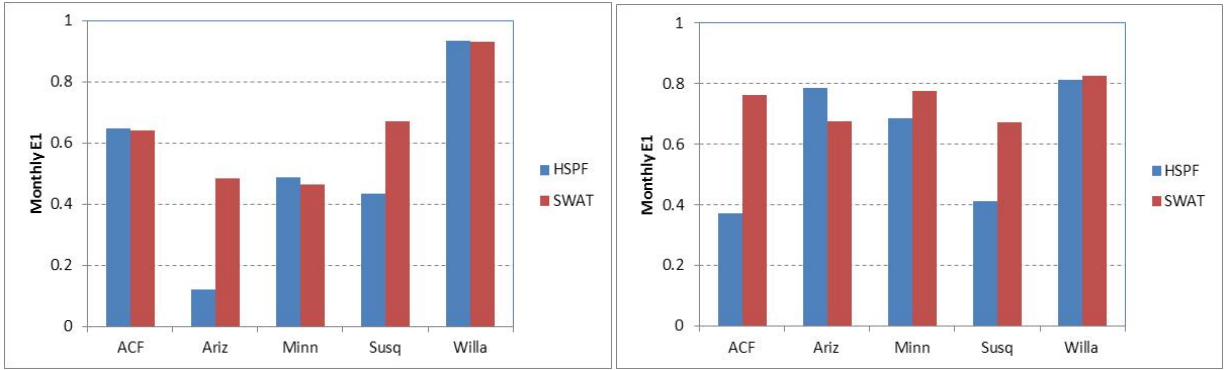


Figure 6-4. Comparison of baseline adjusted model fit efficiency for total suspended solids monthly loads for calibration site (left) and downstream site (right).

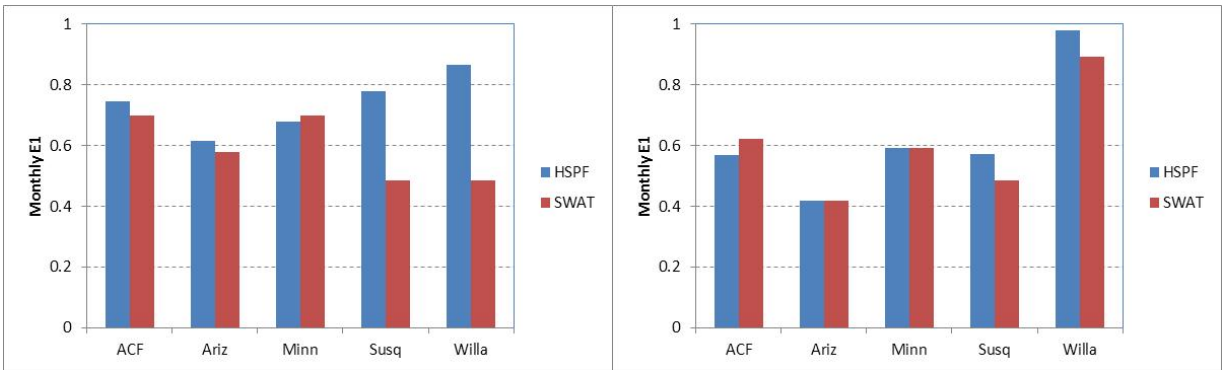


Figure 6-5. Comparison of baseline adjusted model fit efficiency for total phosphorus monthly loads for calibration site (left) and downstream site (right).

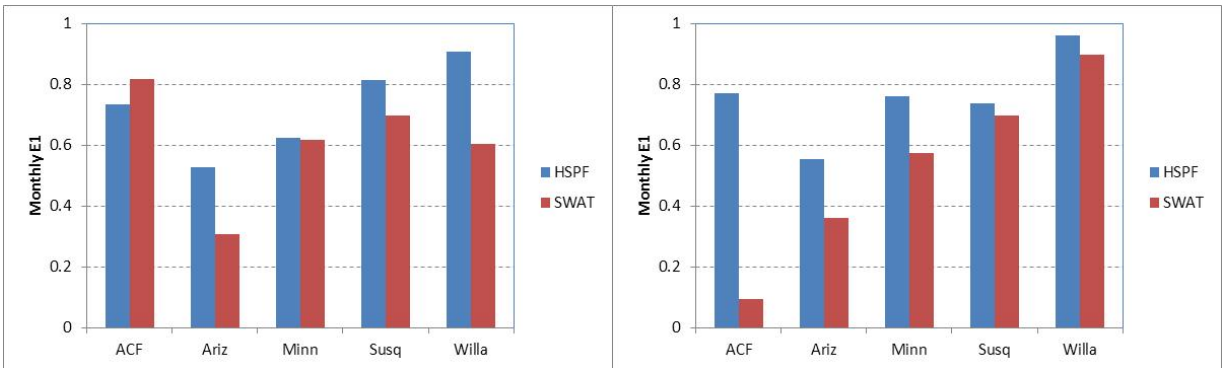


Figure 6-6. Comparison of baseline adjusted model fit efficiency for total nitrogen monthly loads for calibration site (left) and downstream site (right).

6.1.1.3. Summary of Relative Model Performance

In general, the HSPF model provides a somewhat better fit to observed streamflow and water quality data for the calibration periods. The effect is most noticeable in the coefficient of model fit efficiency (E) for daily streamflow, where the HSPF approach of applying Philip infiltration using hourly precipitation appears to yield an advantage over the SWAT daily curve number method. However, relative performance of the two models is more similar as the analysis moves to the validation period or to other sites for which detailed calibration has not been undertaken. Most importantly, both models appear to be capable of performing adequately.

6.1.2. Comparison of Simulated Changes Using SWAT and HSPF

Figure 6-7 compares HSPF and SWAT simulated changes in mean annual streamflow at the downstream station of each of the five pilot watersheds for all 28 combinations of climate and land-use change scenarios (expressed as a percent of the baseline conditions, representing approximately 1970–2000). In general, the mean annual streamflow results provided by the two models are similar, as is shown quantitatively below. One notable difference is for the Minnesota River where SWAT projects higher flows relative to HSPF under future climate conditions—an issue that is explored further in Section 6.1.3. Note that points plotting close to or on top of each other for a given study site in Figure 6-7 are scenarios representing the same climate change scenario with and without changes in urban development.

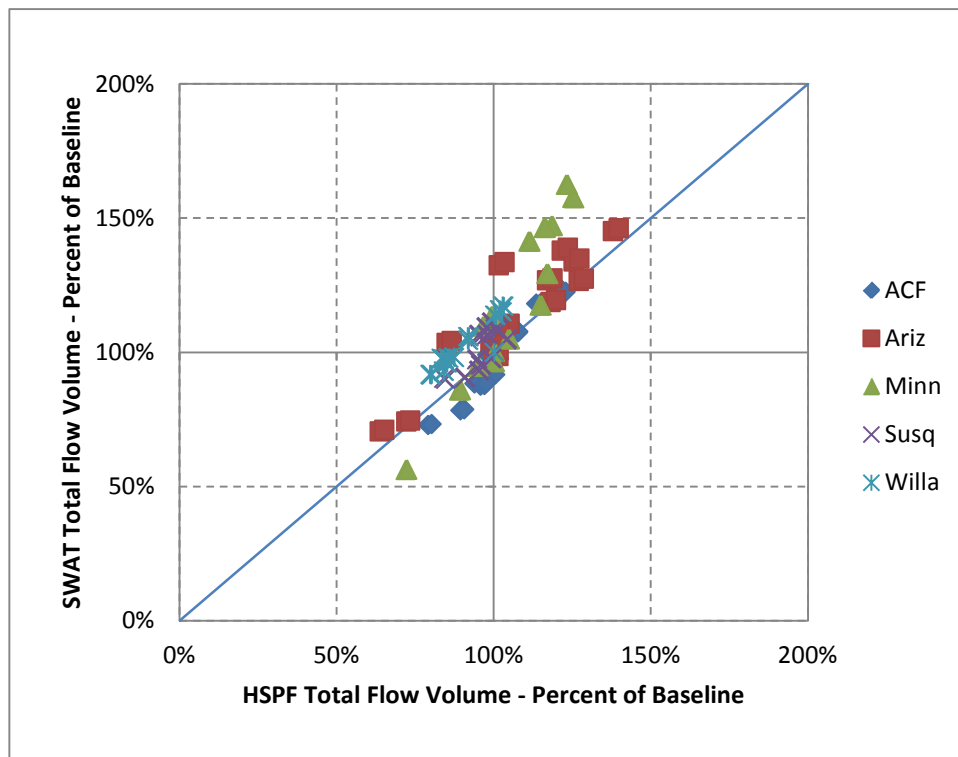


Figure 6-7. SWAT and HSPF simulated changes in total streamflow in pilot watersheds (expressed relative to current conditions).

Table 6-3 provides a statistical comparison of the HSPF and SWAT results at the downstream station. Three types of tests are summarized. The first is a *t*-test on the series of paired means (HSPF and SWAT for each climate and land use scenario), which has a null hypothesis that the mean of the differences between the series is not significantly different from zero. The second test is a two-way analysis of variance (ANOVA) that looks at choice of watershed model (HSPF or SWAT) as blocks and climate scenario as treatment. The null hypotheses for this test are that the difference between series for a given source of variance is zero. The third test is a linear regression on SWAT results as a function of HSPF results. Where the models are in full agreement, the intercept of such a regression should not be significantly different from zero and the slope should not be significantly different from unity.

For mean annual streamflow, both models produce similar results with a high Pearson correlation coefficient. The null hypothesis from the *t*-test that the mean difference is zero cannot be rejected. However, the two-way ANOVA shows that both the choice of watershed model and the climate scenario are significant sources of variability in streamflow, with probability values (*p*-value) well less than 0.1. Together these results suggest that the SWAT and HSPF results are similar in the aggregate, but may contain an underlying systematic shift. A regression analysis shows that the slope coefficient for SWAT and HSPF is 0.93, with a 95% confidence interval that does not overlap 1.0, and an intercept of 1,262 that also does not overlap zero. Thus, SWAT projects a somewhat smaller response to increased rainfall, but results in higher baseflow estimates (likely due to the effects of increased CO₂ on evapotranspiration, as explained further below).

Table 6-3. Statistical comparison of HSPF and SWAT outputs at downstream station for the five pilot sites across all climate scenarios

Measure	Mean annual flow (cfs)	TSS load (t/yr)	TP load (t/yr)	TN load (t/yr)
Paired <i>t</i>-test on sample means				
HSPF Mean	20,546	2,398,714	2,748	35,346
SWAT Mean	20.435	2,865,178	3,344	43,275
Pearson Correlation	0.989	0.733	0.644	0.948
<i>t</i> -statistic	0.616	-3.123	-4.783	-7.385
<i>p</i> (two-tail)	0.539	0.002	<0.001	<0.001
Two-way ANOVA on watershed model and climate scenario				
<i>p</i> value—Model	<0.001	0.071	0.006	0.044
<i>p</i> value—Climate	<0.001	0.960	0.999	1.000
Linear regression; SWAT result as a function of HSPF result				
Intercept	1,261.7	141,717	954.0	-1,173.1
Intercept, 95% confidence	695-1,828	-363,064-646,498	431-1,477	-4,194-1,848
Coefficient (slope)	0.933	1.136	0.870	1.257
Coefficient (slope) 95% confidence	0.911-0.956	0.964-1.307	0.702-1.038	1.189-1.326

The comparison for total suspended solids is obscured by the extremely large projected increases under certain scenarios for the Arizona basins (Verde River, in this case). Those increases are mostly due to simulated channel erosion, for which both models are likely to be highly uncertain because future simulated peak flows are outside the range of calibration data. Figure 6-8 shows the simulated total suspended solids results but with the *x*-axis truncated to exclude these extreme results for the Verde River. Results for the other four pilot sites appear generally consistent between models, although simulated increases from SWAT are generally less than those from HSPF for the ACF, Susquehanna, and Willamette. In part this is due to differences in the baseline simulation. For example, HSPF simulations show less channel transport and much smaller total suspended solids loads at the mouth of the Susquehanna than does SWAT for the baseline scenario, resulting in a larger relative change with increased future streamflow. The difference between results for SWAT and HSPF may also reflect the effects of increased atmospheric CO₂ concentration and longer growing periods simulated by SWAT, leading to more litter cover and reduced soil erosion.

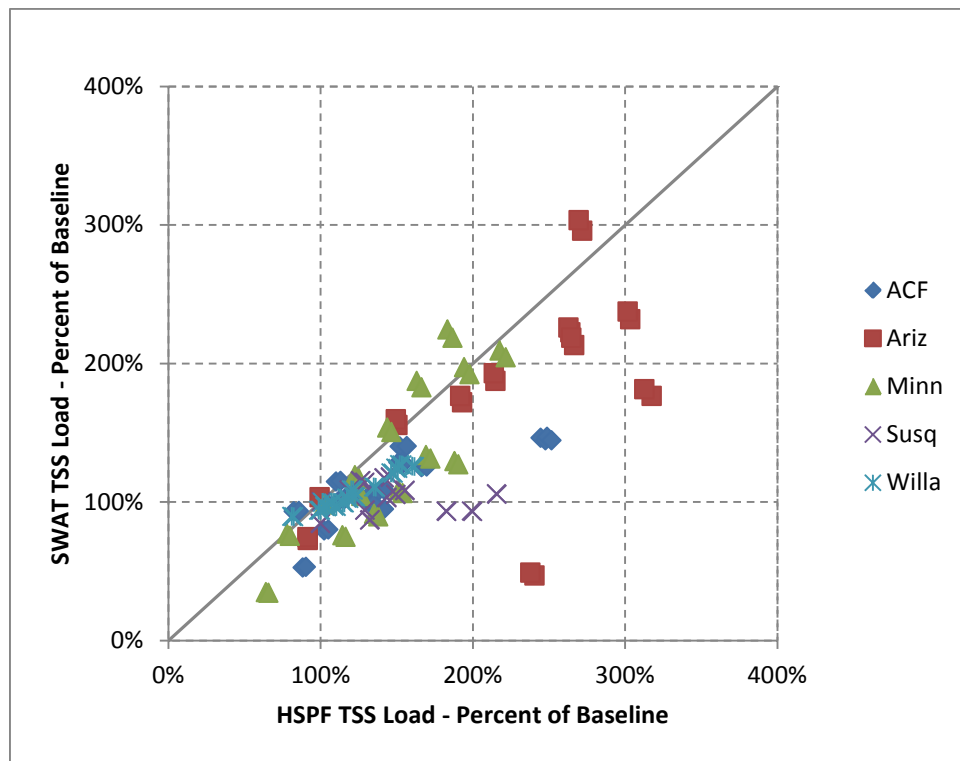


Figure 6-8. SWAT and HSPF simulated changes in TSS at downstream station in pilot watersheds (expressed relative to current conditions).

Note: HSPF simulation for climate scenarios 9 (GFDL, nondownscaled GCM), 10 (CCSM, nondownscaled GCM), 12 (HadCM3, BCSD), and 13 (CCSM, BCSD) yield increases in simulated total suspended solids load of greater than 400% and are omitted from this plot.

For total suspended solids, the baseline load is higher in SWAT than in HSPF for three of the five watersheds; thus the statistical comparison (see Table 6-3) shows a higher mean load from

SWAT, even though the percentage increases are often smaller. The *t*-test on means shows that this difference is highly significant. However, the ANOVA show that neither the model choice nor the climate scenario is a significant explanatory variable for the variance at the 95% confidence level. The regression analysis shows that the intercept is large, but not significantly different from zero, while the slope is not significantly different from 1. Together these statistics indicate that the total suspended solids simulation is subject to considerable uncertainty and that differences between sites are more important than other factors.

Results for total phosphorus are generally similar to those seen for total suspended solids, with much more extreme increases projected by both models for the Verde River (Ariz; see Figure 6-9). HSPF simulations are especially high due to an assumption of phosphorus concentrations in scoured channel sediment. SWAT tends to simulate higher rates of increases for total nitrogen (see Figure 6-10) than does HSPF (likely due to more rapid cycling of organic matter), with the notable exception of the ACF study area. However, it appears that projections of total nitrogen at the downstream end of the ACF may be significantly underestimated in the calibrated SWAT model. Total nitrogen varies little in the Susquehanna model due to small changes in streamflow and significant point source contributions.

For both total nitrogen and total phosphorus the choice of model is a significant factor in the ANOVA and higher mean loads are produced by SWAT. The slope of a regression of SWAT on HSPF is not significantly different from 1 for total phosphorus, consistent with the solids simulation, but the intercept is significantly different from zero, indicating differences in the baseflow simulation of total nitrogen. For total nitrogen, the intercept is not significantly different from zero, but the slope is significantly greater than 1, suggesting that SWAT projects a greater increase in total nitrogen loads under future climate conditions.

In sum, the comparison of relative response to change scenarios indicates that the two models provide generally consistent results for hydrology, with differences that may be in part due to the inclusion of explicit representation of several processes in SWAT (increased atmospheric CO₂, changes in planting time, changes in crop growth and litter production, and changes in nutrient recycling rates) that are not automatically included in HSPF. Water quality results exhibit greater variability between the models, due in large part to the uncertainty inherent in model calibration.

An additional contributing cause to differences in results from the two models is the extent to which spatial calibration of the model was pursued, which was left to modeler judgment. In all study areas, initial calibration and validation was pursued at an “initial calibration” gage and monitoring station at an HUC-8 spatial scale. The calibration results were then carried to the larger study area. At this point, individual modeler preferences introduced some variability into results. Some modelers undertook detailed spatial adjustments to parameters; others extended the initial parameter set with only minor modifications. With more spatial adjustments a higher degree of fit is generally to be expected for model calibration—although this does not necessarily result in better performance in model validation. In general, only limited spatial calibration adjustments beyond the initial parameter set was carried out for the Minnesota River, Susquehanna, and Willamette SWAT models and also for the Susquehanna HSPF model.

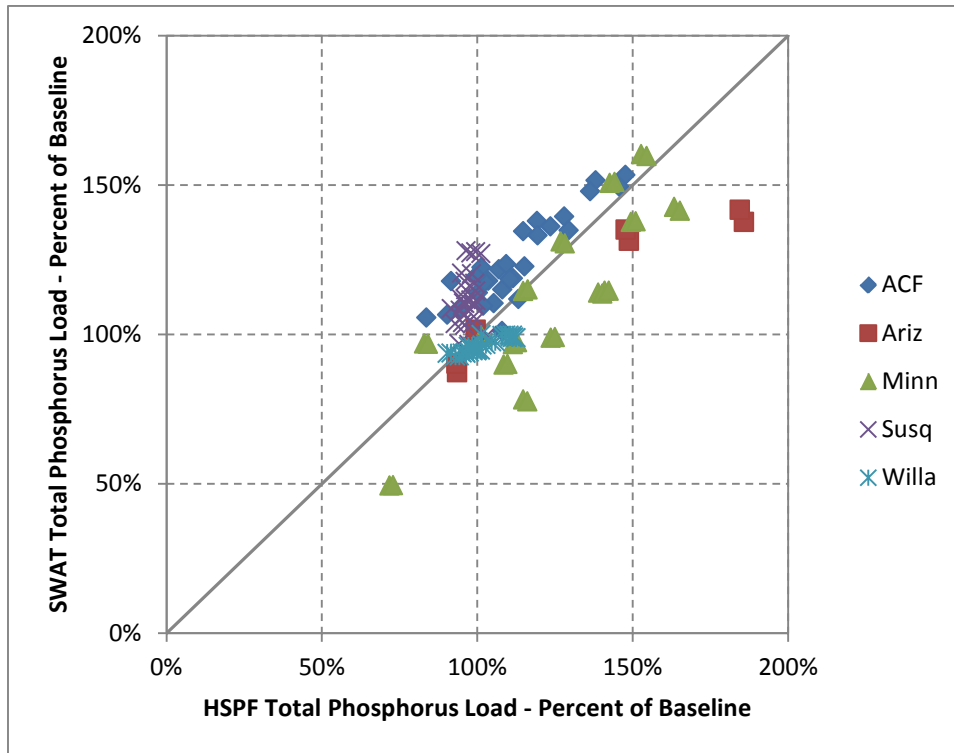


Figure 6-9. SWAT and HSPF simulated changes in total phosphorus load in pilot watersheds (expressed relative to current conditions).

Note: 22 HSPF simulations for Ariz ranging from 200 to 875% are omitted.

Due to the potential influence of modeler choice and skill, it is cautioned that the results should not be interpreted as a true head-to-head comparison of the two models, as the results for any given watershed may be skewed by exogenous factors such as modeler calibration strategy. Instead, it is most relevant to examine relative performance and potential inconsistencies between simulations using the two models.

6.1.3. Sensitivity to Increased Atmospheric CO₂

A key difference between HSPF and SWAT is that SWAT has a dynamic plant growth module with ability to represent changes in atmospheric CO₂ on plant growth and water loss to ET. We performed paired sets of SWAT simulations with and without increased CO₂ for all five pilot sites to assess the sensitivity of streamflow and water quality endpoints to the effects of increased atmospheric CO₂ concentrations.

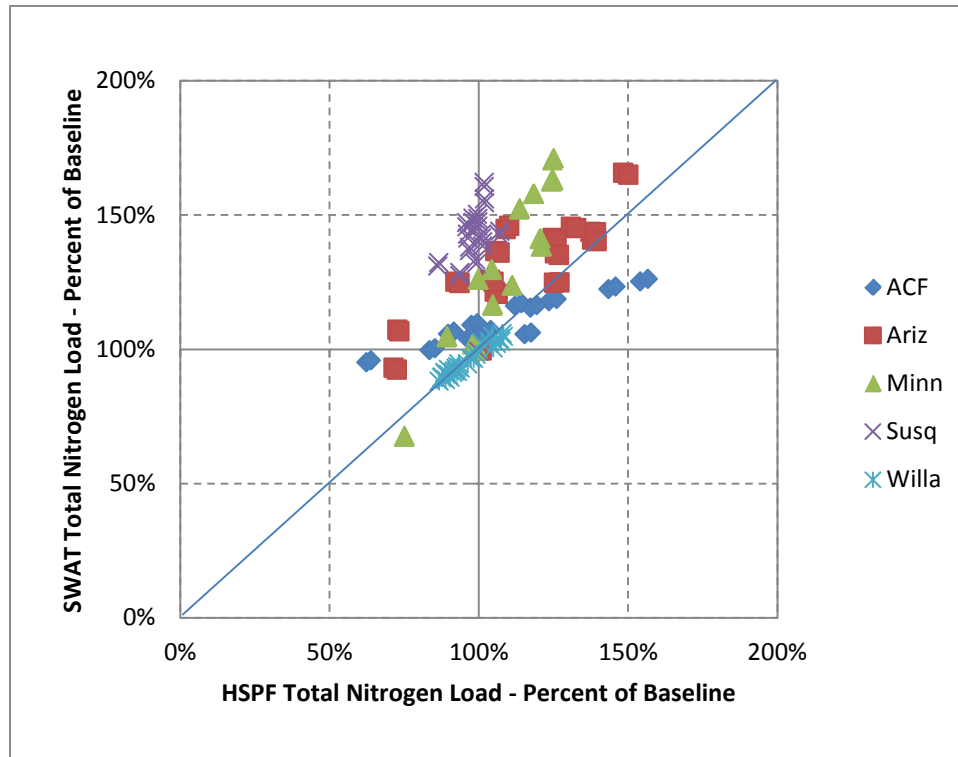


Figure 6-10. SWAT and HSPF simulated changes in total nitrogen load in pilot watersheds (expressed relative to current conditions).

IPCC estimates of future atmospheric CO₂ concentrations under the assumptions of the A2 emissions scenario (the basis of climate and land-use change scenarios in this study) call for an increase from 369 ppmv CO₂ in 2000 to about 532 ppmv (using the ISAM model reference run) or 522 ppmv (using the Bern-CC model reference run) in 2050 (Appendix II in IPCC, 2001). Plants require CO₂ from the atmosphere for photosynthesis. An important effect of increased atmospheric CO₂ is a reduction in the time plant leaf stomata must be open to obtain the CO₂ needed for growth, resulting in reduced water loss as transpiration (Leakey et al., 2009; Cao et al., 2010; Ainsworth and Rogers, 2007). This effect can potentially counterbalance projected increases in transpiration associated with increased air temperatures. It may also reduce water stress on plants, resulting in greater biomass and litter production, which in turn will influence pollutant loads.

In the past it has been argued that these effects, long documented at the leaf and organism level, might not translate to true ecosystem effects. However, recent research, particularly results from the Free-Air CO₂ Enrichment (FACE) experiments (Leakey et al., 2009) suggests that significant reductions in evapotranspiration do occur at the ecosystem level with increased atmospheric CO₂ concentrations. Although there are differences in responses among plant species, with lesser effects with C₄ photosynthesis, the magnitude of the response to CO₂ levels projected by the mid-21st century appears to be on the order of a 10% reduction in evapotranspiration response (e.g., Bernacchi et al., 2007). Further, a recent study by Cao et al. (2010) suggests that up to

25% of the temperature increase projected for North America could result directly from decreased plant evapotranspiration under increased CO₂ concentrations.

SWAT includes a plant growth module that accounts for the effects of changes in atmospheric CO₂ concentration on stomatal conductance using the equation developed by Easterling et al. (1992). Using this approach, increased CO₂ leads to decreased leaf conductance, which in turn results in an increase in the canopy resistance term in the PET calculation. The model also simulates the change in radiation use efficiency of plants as a function of CO₂ concentration using the method developed by Stockle et al. (1992). Figure 6-11 shows the differences between projected mid-21st century streamflow and water quality endpoints in the five pilot sites simulated using SWAT with and without representation of the effects of increased atmospheric CO₂ concentrations (SWAT projections for the six NARCCAP climate scenarios incorporating the ICLUS future land use for each watershed). These simulations suggest increases in mean annual streamflow from 3 to 38% due to increased CO₂, with a median of 11%, in the same range as the results summarized by Leakey et al. (2009). Simulations also suggest increased atmospheric CO₂ results in increased pollutant loads. Total suspended solids loads show increases from 3 to 57%, with a median of 15%. Total phosphorus loads increase from 0 to 29%, with a median of 6%. Total nitrogen loads increase from zero to 34%, with a median of 6%. The large increases in total suspended solids loads indicate that the effects of higher runoff under increased atmospheric CO₂ (largely due to greater soil moisture prior to rainfall events) may outweigh benefits associated with greater ground cover—a finding that could have important land management implications in the midwestern watersheds, including many of the Great Lakes drainages. For the nutrients, the simulated load increases are less than for streamflow and total suspended solids increases. This presumably is due to the fact that increased atmospheric CO₂ concentrations allow greater plant growth per unit of water, resulting in greater uptake and sequestration of nutrients, and thus smaller increases in nutrient loads relative to streamflow and total suspended solids.

The response to increased atmospheric CO₂ concentration varies greatly by study area, with the greatest effect simulated by SWAT for the Minnesota River basin and the smallest effect for the Willamette basin. The large effect in the Minnesota River basin apparently occurs because the land in this basin is predominantly in high-biomass corn-soybean rotation agricultural cropland with precipitation and evapotranspiration in approximate balance. In contrast, the Willamette basin is dominated by evergreen forest and has a moisture surplus for much of the year.

Ficklin et al. (2009), working with the SWAT model in the San Joaquin watershed in California, also showed that increased atmospheric CO₂ could cause a significant relative decrease in simulated evapotranspiration and a corresponding increase in water yield relative to simulations that did not account for increased CO₂. However, Luo et al. (2013) recently suggested that the approach used in SWAT to estimate the effects of CO₂ on evapotranspiration is appropriate only for arable land and may overestimate CO₂-associated reductions from forest, pasture, and range land. This remains an important topic for further investigation.

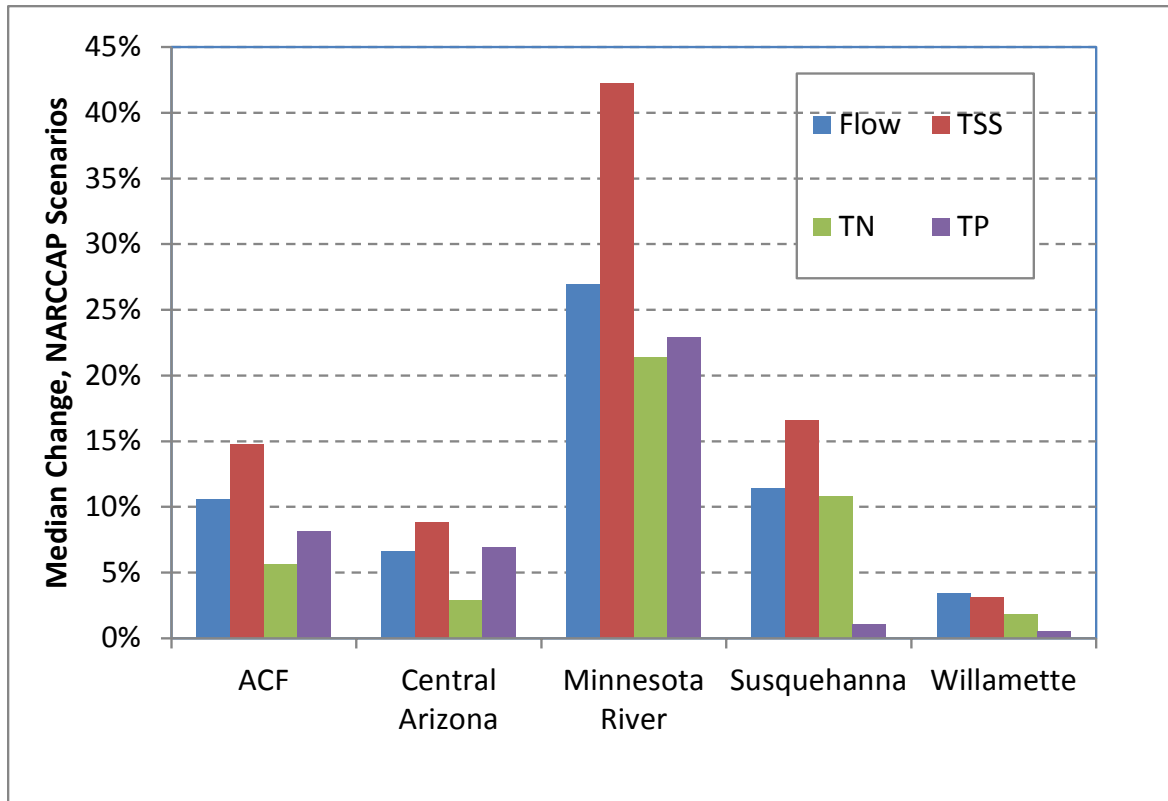


Figure 6-11. Differences between SWAT projections of mid-21st century streamflow and water quality (median across six NARCCAP scenarios) with and without representation of increased atmospheric CO₂.

Note: Figure shows model simulation with increased CO₂ minus projection with CO₂ assumed constant at current levels.

Several important feedback loops other than the CO₂ effect on stomatal conductance are also included in the SWAT plant growth model. First, planting, tillage, fertilization, and harvest timing for crops (and start and end of growth for native plants) is represented by heat unit scheduling relative to existing climate normals, allowing automatic adjustment in timing under a changed temperature regime. Evapotranspiration is also simulated with the full Penman-Monteith method, allowing dynamic simulation of leaf area development and crop height, both of which impact ET. Finally, organic matter residue accumulation and degradation on the land surface are dynamically simulated as a function of plant growth, and the effects of altered cover on land surface erosion are represented.

All these factors are of potential importance in examining response to climate change. In contrast to SWAT, HSPF does not automatically compute these adjustments. Instead, the user would need to estimate changes in monthly parameters such as the lower zone evapotranspiration coefficient (LZETP) and erosion cover externally and bring them into the model. While not well understood, use of calibrated parameters in HSPF without these modifications could introduce error to simulations under climatic conditions different from those during the calibration period.

6.2. SENSITIVITY TO DIFFERENT METHODS OF DOWNSCALING GCM OUTPUT

A variety of methods for downscaling large-scale GCM output to local scale projections are available. Both the selection of an underlying GCM and the choice of downscaling method have a significant influence on the streamflow and water quality simulations. Indeed, in some basins (e.g., Minnesota River, ACF) the difference among watershed model simulations as driven by the six NARCCAP dynamically downscaled scenarios appears to be noticeably greater than the range of model simulations driven by BCSD statistically downscaled or nondownscaled GCM scenarios. The results of the larger ensemble leads to the observation that incorporating additional information, either from dynamic RCMs or via statistical methods, can increase the range of variability of simulated changes.

6.2.1. Climate Model Energy Inputs and PET Estimates

PET is calculated using the Penman-Monteith PET energy balance approach. The BCSD and nondownscaled GCM scenarios do not provide all the required meteorological time series (see Table 5-2 in Section 5.2.1.). As a result, PET for these scenarios was estimated using current climate statistics for solar radiation, dew point, and wind time series. Comparisons presented in Appendix Z suggest that PET estimates for the and GCM scenarios (scenarios 7–14) that do not include solar radiation, dew point, and wind time series that are consistent with the simulated precipitation and temperature are noticeably higher than estimates of PET derived from the dynamically downscaled models that do provide these time series.

A comparison of the effects of data availability on PET calculations can be done through comparison of scenarios that are based on the identical underlying GCM runs for CGCM3 and GFDL that were each dynamically downscaled with two different RCMs (as discussed in Section 5.2.2.). Annual average PET estimates from these pairs are generally close to one another, but may differ by up to 4.5% from their mean (see Table 5-4). For the CGCM3 model, PET generated from the nondownscaled GCM is similar to that from the dynamically downscaled scenarios, but PET calculated from the statistically downscaled scenario is from 2 to 19% higher. This appears to be due to the fact that dew point temperature, which has an important impact on PET, is provided with the CGCM3 GCM but is not available from the BCSD scenarios (see Table 5-2 above). The difference is smallest for the Salt/Verde/San Pedro River basins in Arizona, where dew point temperature is very low and not expected to change much under future climates. In contrast, the GFDL model does not provide dew point temperature from the nondownscaled GCM. For that model, both the nondownscaled and statistically downscaled climate change scenarios produce higher PET estimates than the NARCCAP dynamically downscaled scenarios. As with CGCM3, the smallest effect is seen in the Salt/Verde/San Pedro River basins in Arizona, and the largest effect in the Susquehanna basin, where a greater change in dew point temperature and relative humidity is projected. The observed sensitivity of PET estimates to climate variables other than air temperature and precipitation suggests that simulation of future climates that does not account for changes in the full suite of variables that influence PET could thus introduce significant biases into the simulated water balance. Further investigation of this phenomenon was pursued through use of “degraded” NARCCAP climate scenarios, as described below.

6.2.2. “Degraded” NARCCAP Climate Scenarios

To provide a consistent basis for comparison, all scenarios were created with a common minimum set of variables. Specifically, NARCCAP provided data on changes in precipitation intensity (bin data), solar radiation, wind, and humidity that were not available in the GCM and BCSD based scenarios. The following steps were taken to develop a consistent set of climate scenario input series that differ only in the underlying climate model and downscaling technique:

- Representation of intensification in each of the NARCCAP dynamically downscaled scenarios was based on Approach 2 in Section 5.2.2., which assumes that all increases in precipitation occur in the top 30% of events, rather than using the direct analysis of intensity changes provided by NARCCAP.
- Complete information on changes in weather generator statistics for dew point temperature, solar radiation, and wind speed was removed for the NARCCAP dynamically downscaled scenarios, consistent with the information available for the BCSD scenarios. Incomplete information on these variables provided by the nondownscaled GCMs was also removed. (For the nondownscaled GCMs this affects weather scenarios 7, 9, and 10—see Table 5-2 above).
- Penman-Monteith PET was recalculated with the revised set of climate variables.
- Simulations use current land use to remove land-use change effects.

Note that these simplified or “degraded” NARCCAP scenarios are used only for the comparisons presented in this section. Results presented in subsequent sections of this report use the scenarios that contain all available meteorological information.

Comparison of the PET series generated with full climatological data to the degraded series in which only precipitation and temperature are updated illustrates the effect of including these additional variables (see Table 6-4). Further, the effect of individual meteorological time series is discernible because the original set lacked solar radiation for Scenario 5, dewpoint temperature for Scenario 9, and wind speed for Scenario 10 (see Table 5-2). Dewpoint temperature (which tends to increase in future, warmer climates) has the biggest impact. Including a climate model-simulated dewpoint that is consistent with the scenario temperature and precipitation regime results in a reduction in estimated annual PET of about 11% across all the meteorological stations used for the five pilot watersheds. The effect appears to be greater at higher latitudes. The reduction in PET from including simulated dewpoint is around 10–20% for the Minnesota, New York, Oregon, and Pennsylvania stations, but only 3–10% for the Alabama, Arizona, Florida, and Georgia stations. In contrast, for Scenario 9 (for which dewpoint temperature was not available), the original PET series were on average 1.9% higher than the degraded series. Omission of solar radiation or wind speed results from the climate scenario appears to have at most a minor impact on the estimated PET.

In retrospect, these results suggest that a better approach to simulation of PET in cases where the climate models do not provide dewpoint would be to assume that relative humidity remains

constant and recalculate a new dewpoint based on the relative humidity and climate-modified air temperature, thus providing a more physically realistic estimate of vapor pressure deficit.

Table 6-4. Effects of omitting simulated auxiliary meteorological time series on Penman-Monteith reference crop PET estimates for “degraded” climate scenarios

State	Climate Scenario (GCM/RCM)								
	1 CGCM3/ CRCM	2 HadCM3/ HRM3	3 GFDL/ RCM3	4 GFDL/ GFDL hi res	5 CGCM3/ RCM3	6 CCSM/ WRF	7 CGCM3 (not down- scaled)	9 GFDL (not down- scaled)	10 CCSM (not down- scaled)
AL	-4.87%	-4.44%	-5.21%	-10.90%	-5.76%	-4.47%	-4.89%	2.66%	-7.11%
AZ	-2.38%	-3.01%	-4.12%	-3.59%	-2.97%	-3.08%	-0.99%	2.69%	-3.02%
FL	-7.14%	-8.48%	-7.45%	-16.69%	-9.04%	-9.02%	-7.35%	2.92%	-10.91%
GA	-9.30%	-7.21%	-7.79%	-18.01%	-10.15%	-7.27%	-8.71%	1.79%	-14.04%
MN	-14.68%	-10.30%	-13.73%	-10.30%	-16.46%	-21.16%	-13.83%	1.68%	-16.46%
NY	-23.27%	-16.99%	-17.68%	-20.62%	-22.95%	-18.30%	-23.01%	-1.29%	-20.48%
OR	-15.82%	-14.28%	-7.75%	-12.90%	-13.67%	-13.29%	-12.73%	0.11%	-10.17%
PA	-17.62%	-12.54%	-14.77%	-18.93%	-18.59%	-13.40%	-17.96%	0.28%	-17.28%
All (%)	-12.53%	-9.93%	-9.97%	-12.62%	-12.86%	-12.48%	-11.37%	1.19%	-12.39%
All (in/yr)	-6.36	-5.27	-5.16	-6.48	-6.42	-6.31	-5.63	0.90	-6.55

Note: Auxiliary time series are solar radiation, dewpoint temperature, and wind. Scenario 5 did not have a solar radiation time series; Scenario 9 did not have a dewpoint temperature time series; Scenario 10 did not have a wind time series. Results are averages across entire study area. See Table 5-1 for details of the climate scenarios.

These results suggest that downscaling approaches that omit dewpoint temperature can introduce significant biases. Specifically, simulation without adjusting for future changes in dewpoint temperature is likely to overestimate PET, leading to an underestimation of soil moisture and streamflow.

6.2.3. Sensitivity of Flow and Water Quality to Approaches for Downscaling GCM Projections

The effect of downscaling approach on the variability of watershed model simulations can be investigated quantitatively by comparing the results from simulations based on degraded NARCCAP, GCM, and BCSD scenarios. Table 6-5 presents results obtained with current land use and the SWAT watershed model (with increased atmospheric CO₂) at the most downstream gage in each study area. Table 6-6 presents detailed results for multiple streamflow and water quality parameters in the Minnesota River study area. Differences among results with different downscaling methods are qualitatively similar for HSPF output (not shown).

Table 6-5. Summary of SWAT-simulated total streamflow in the five pilot study areas for scenarios representing different methods of downscaling

Study area	Downscaling method	Number of scenarios	Median (cms)	Maximum (cms)	Minimum (cms)	CV
Apalachicola-Chattahoochee-Flint (ACF)	NARCCAP	6	710.4	818.8	478.6	0.208
	BCSD	4	675.5	722.0	655.3	0.042
	GCM	4	655.0	750.7	581.3	0.105
Salt/Verde/San Pedro (Ariz)	NARCCAP	6	19.4	24.5	12.9	0.233
	BCSD	4	24.0	28.4	21.3	0.122
	GCM	4	26.0	27.0	19.9	0.131
Minnesota River (Minn)	NARCCAP	6	229.5	274.3	149.4	0.230
	BCSD	4	236.8	286.3	209.7	0.153
	GCM	4	238.3	277.0	124.4	0.301
Susquehanna (Susq)	NARCCAP	6	834.8	855.5	705.6	0.068
	BCSD	4	935.7	948.4	879.2	0.035
	GCM	4	868.7	1,017.1	807.0	0.106
Willamette (Willa)	NARCCAP	6	878.8	951.8	763.6	0.086
	BCSD	4	833.0	1,003.7	800.3	0.108
	GCM	4	843.3	970.7	810.6	0.082

Notes: Results shown are for most downstream station in each study area; coefficient of variation (CV) = standard deviation divided by the mean. Climate scenarios are degraded to a common basis of scenario precipitation and air temperature information only.

Results show considerable variability among climate models and downscaling techniques in different basins and for different streamflow and water quality endpoints. No consistent pattern attributable to downscaling method is evident for the case in which all climate model outputs are evaluated using a common basis of precipitation and air temperature only. As was discussed in Section 6.1.3., the additional information on other meteorological variables can have a profound effect on PET and watershed responses.

It is noteworthy that the dynamically downscaled results may differ significantly from the statistically downscaled results from the same GCM, and that the results may also be quite different when the same GCM is downscaled with a different RCM (e.g., refer to Table 5-1 and compare climate scenarios 1 and 5 for CGCM3, also 3 and 4 for the GFDL). As noted in Section 5.2., direct comparison between NARCCAP and BCSD downscaling of a single GCM can only be reliably undertaken for the GFDL and CGCM3 models, because slightly different GCM runs were used to produce NARCCAP and BCSD results for other GCMs.

Table 6-6. Summary of SWAT-simulated streamflow and water quality in the Minnesota River study area for scenarios representing different methods of downscaling

Endpoint	Downscaling method	Number of scenarios	Median	Maximum	Minimum	CV
Total Streamflow (cms)	NARCCAP	6	229.5	274.3	149.4	0.230
	BCSD	4	236.8	286.3	209.7	0.153
	GCM	4	238.3	277.0	124.4	0.301
100-Yr High Flow (cms)	NARCCAP	6	3,415.4	3,700.2	3,155.7	0.058
	BCSD	4	3,960.2	5,055.0	3,617.6	0.153
	GCM	4	3,565.7	4,432.3	2,508.7	0.227
7 Day Average Low Flow (cms)	NARCCAP	6	27.7	38.5	14.3	0.353
	BCSD	4	25.8	37.9	22.3	0.247
	GCM	4	28.2	37.0	12.9	0.395
Total Suspended Solids (MT/yr)	NARCCAP	6	1,926,166	2,520,444	896,806	0.385
	BCSD	4	2,002,421	2,428,565	1,376,608	0.265
	GCM	4	1,914,800	2,557,634	633,793	0.460
Total Phosphorus (MT/yr)	NARCCAP	6	36,304	42,119	25,843	0.191
	BCSD	4	40,579	44,936	32,451	0.150
	GCM	4	38,747	42,087	21,538	0.264
Total Nitrogen (MT/yr)	NARCCAP	6	2,700	3,283	2,007	0.194
	BCSD	4	3,073	3,453	2,356	0.183
	GCM	4	2,889	3,162	1,489	0.292

MT = metric ton

Notes: Results shown are for most downstream station in each study area; coefficient of variation (CV) = standard deviation divided by the mean. Climate scenarios are degraded to a common basis of scenario precipitation and air temperature information only.

Both the GFDL and CGCM3 A2 scenario runs for 2041–2070 were downscaled with two different NARCCAP RCMs—with one RCM (RCM3) in common between the two. A comparison in terms of the ratio of simulated future mean annual streamflow to simulated current mean annual streamflow, using SWAT, is made in Figure 6-12 for the GFDL and in Figure 6-13 for the CGCM3 model. For both GCMs, the NARCCAP downscaling, BCSD downscaling, and nondownscaled GCM output produce relatively consistent results for the Willamette and Susquehanna basins, but diverge for the Minnesota River. For the Arizona basin, the two different downscaling approaches diverge for the GFDL but not the CGCM3 GCM. Elevated coefficients of variation (CVs) on mean annual streamflow in both the Minnesota River and Arizona basins appear to be largely due to the difference in downscaling results obtained with

the GFDL high-resolution regional model, which suggests lower flow than other dynamically downscaled interpretations of the GFDL GCM.

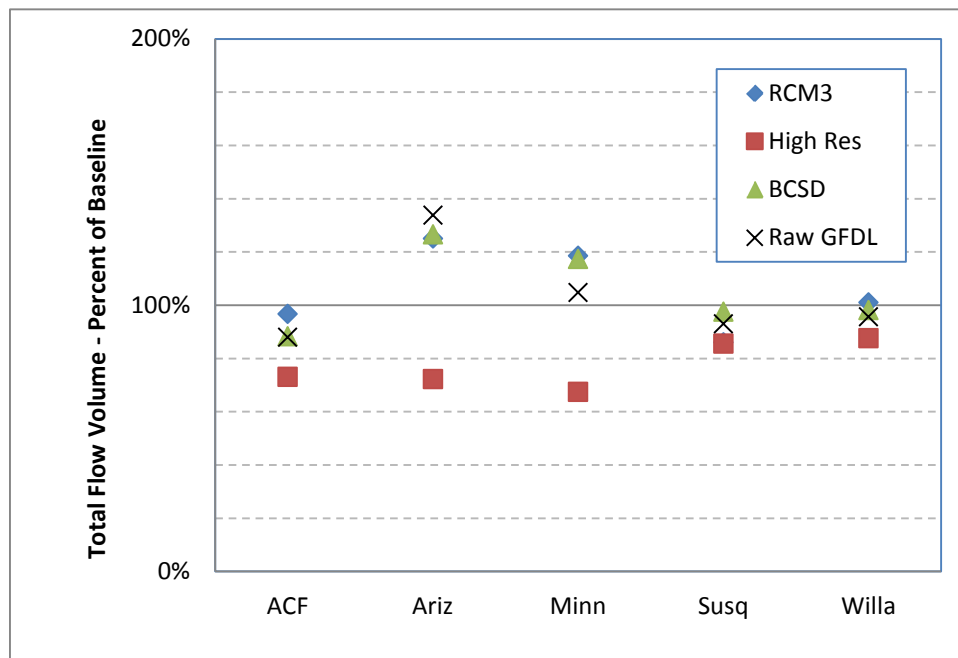


Figure 6-12. Consistency in SWAT model projections of mean annual streamflow at downstream stations with downscaled (NARCCAP, BCSD) and nondownscaled GCM projections of the GFDL GCM.

Note: The climate change scenarios used in this analysis are simplified to include changes only in air temperature and precipitation (variables common to the NARCCAP, BCSD, and GCM data sets) to provide a common basis for comparison.

Figures 6-12 and 6-13 demonstrate that a single GCM may yield rather different results depending on the RCM used for dynamical downscaling. In the current state of the science it does not appear that the use of dynamical downscaling reduces uncertainty; however, use of multiple downscaling approaches helps to inform the potential range of climate futures.

To date, relatively few comparisons of RCM model performance in the NARCCAP data sets have been undertaken. An exception is the study of Wang et al. (2009) for the Intermountain Region of the Western United States. Significant orographic effects in this area lead to a complex combination of precipitation annual and semiannual cycles that form four major climate regimes in this area. Wang et al. compared results from six RCMs over this region to the North American Regional Reanalysis (NARR) precipitation study (Mesinger et al., 2006) and found that each model produces its own systematic bias in the central Intermountain Region where the four different climate regimes meet. All six of the RCMs appeared to produce simulated annual cycles that are too strong and winter precipitation that is too high under current conditions. The BCSD statistical approach can correct this for current conditions; however, the statistical approach would not account for any future large-scale changes in the interaction of the major climate regimes.

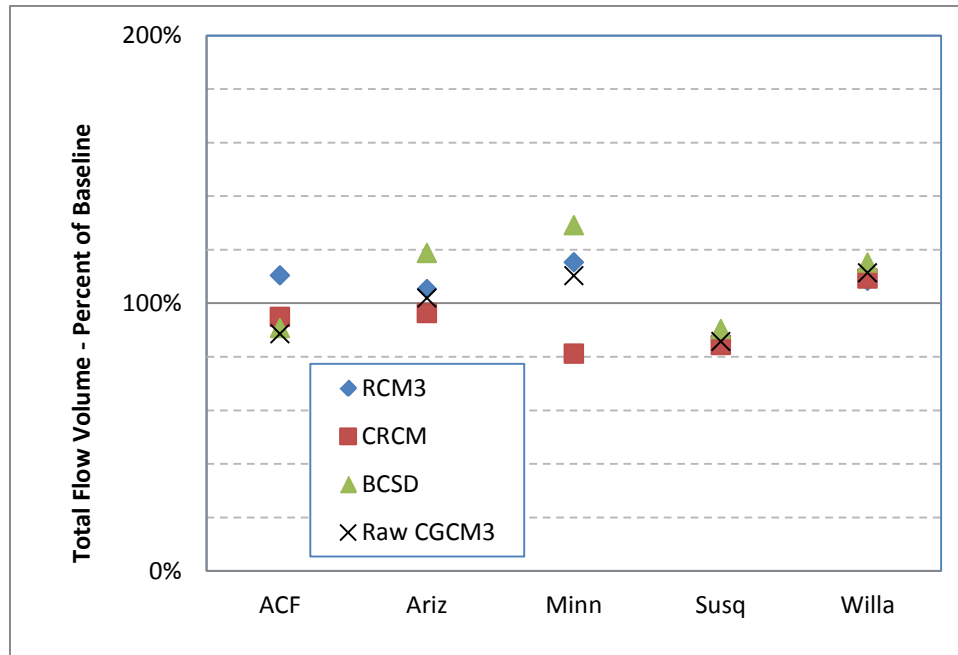


Figure 6-13. Consistency in SWAT model projections of mean annual streamflow at downstream stations with downscaled (NARCCAP, BCSD) and nondownscaled GCM projections of the CGCM3 GCM.

Note: The climate change scenarios used in this analysis are simplified to include changes only in air temperature and precipitation (variables common to the NARCCAP, BCSD, and GCM data sets) to provide a common basis for comparison.

Wang et al. (2009) also demonstrate that the different RCMs are largely consistent in the Cascade Range (OR, WA), where the dominant upper level flow first encounters land, which fits with the reduced level of variability between downscaling methods noted for the Willamette study area. The differences among RCMs reported by Wang et al., and the difference from NARR, are greatest on the windward side of the Rocky Mountains in Colorado and remain large into Arizona. Interestingly, the apparent wet bias of the CRCM and dry bias of most other RCMs relative to NARR in Arizona reported by Wang et al. does not appear to carry through into the future scenarios reported here, suggesting that the RCMs may be providing different simulated solutions to the future interaction of large-scale climate regimes in this area.

In addition to uncertainties in representing climate forcing at the watershed level, as discussed in this section, previous sections have shown that the results are sensitive to the selection of a watershed model, and to modeler skill in calibrating the model. Furthermore, the results are undoubtedly also sensitive to feedback loops that are not incorporated into the models. Results produced in this study thus likely do not span the full range of potential future impacts (even conditional on the A2 storyline) for the reasons given above, among others. Nonetheless, the range of uncertainty is considerable, and generally covers the zero point, as is summarized at selected downstream analysis points shown in Table 6-7.

Table 6-7. Range of SWAT-projected changes in annual streamflow and pollutant loads for combined mid-21st century NARCCAP climate change and ICLUS urban and residential development scenarios

Downstream location	Change in flow (%)	Change in total solids load (%)	Change in total nitrogen load (%)	Change in total phosphorus load (%)
ACF: Apalachicola River Outlet	-26.9 to +23.6	-47.2 to +6.1	-4.6 to +25.6	-6.6 to +73.1
Ariz: Verde River ab Tangle Creek	-29.4 to +26.7	-52.6 to +118.4	-7.2 to +46.6	-32.8 to +63.4
Susq: Susquehanna River Outlet	-10.0 to +11.0	-15.6 to +17.8	+32.1 to +61.9	+6.3 to +28.1
Minn: Minnesota River Outlet	-14.3 to +62.1	-22.9 to +122.9	+4.9 to +71.0	-6.3 to +59.5
Will: Willamette River Outlet	-8.4 to +15.9	-10.3 to +24.5	-10.9 to +3.3	-13.3 to +4.2

The ranges shown in Table 6-7 suggest that for 2041–2070 conditions it is not possible in most cases to even state the sign of change in watershed response with a high degree of assurance unless one is willing to assert that one of the RCMs is more reliable than another. Rather, the results tell us that the range of potential responses is large.

Based on the analysis presented here, however, the differences in simulation results in our study are largely a result of combined differences in the underlying GCM and the downscaling approach used, and more specifically, largely a result of heterogeneity in simulated precipitation amounts and patterns. For the 2041–2070 timeframe, these warming-induced increases in simulated PET are generally insufficient to overcome this range of variability in projected precipitation. This may not be the case, however, for more distant future simulation periods—given continually increasing temperature and PET, evapotranspiration increases are likely to ultimately exceed the range of variability in projected precipitation in many basins, resulting in more uniform decreases in runoff.

7. REGIONAL SENSITIVITY OF STREAMFLOW AND WATER QUALITY TO CLIMATE CHANGE AND LAND DEVELOPMENT: RESULTS IN ALL 20 WATERSHEDS

This section presents simulation results in all 20 study areas using SWAT. Model simulations evaluate the effects of mid-21st century climate change alone (see Section 7.1.), urban and residential development alone (see Section 7.2.), and the combined effects of climate change and urban development (see Section 7.4) on streamflow, TN, TP, and TSS. Scenarios also assume future increases in atmospheric CO₂. Results are presented for a single representative analysis point in each study area (see Table 7-1). For study areas composed of a single watershed, this is the outlet (pour point) of the entire study area. For study areas composed of multiple, adjacent watersheds draining to the coast, the analysis point reported here is at or near the outlet of the largest river within the study area. Results for additional locations within each study area are presented in Appendix X for the five pilot study areas and in Appendix Y for the other 15 study areas.

Table 7-1. Downstream stations within each study area where simulation results are presented

Study area	Location presenting results
Apalachicola-Chattahoochee-Flint Basins (ACF)	Apalachicola R at outlet
Southern California Coastal (SoCal)	Los Angeles R at outlet
Cook Inlet Basin (Cook)	Kenai R at Soldotna
Georgia-Florida Coastal Plain (GaFla)	Suwanee R at outlet
Illinois River Basin (Illin)	Illinois R at Marseilles, IL
Lake Erie Drainages (LErie)	Maumee R at outlet
Lake Pontchartrain Drainage (LPont)	Amite R at outlet
Nebraska: Loup and Elkhorn River Basin (Neb)	Elkhorn R at outlet
Minnesota River Basin (Minn)	Minnesota R at outlet
Tar and Neuse River Basins (TarNeu)	Neuse R at outlet
New England Coastal Basins (NewEng)	Merrimack R at outlet
Powder and Tongue River Basin (PowTon)	Tongue R at outlet
Rio Grande Valley (RioGra)	Rio Grande R below Albuquerque
Sacramento River Basin (Sac)	Sacramento R at outlet
Arizona: Salt, Verde, and San Pedro (Ariz)	Salt River near Roosevelt
South Platte River Basin (SoPlat)	S. Platte R at outlet
Susquehanna River Basin (Susq)	Susquehanna R at outlet
Trinity River Basin (Trin)	Trinity R at outlet
Upper Colorado River Basin (UppCol)	Colorado R near State Line
Willamette River Basin (Willa)	Willamette R at outlet

7.1. SELECTION OF WATERSHED MODEL FOR USE IN ALL STUDY AREAS

Resource limitations for this study precluded the application of SWAT and HSPF in all 20 study areas. Analyses at Pilot sites were used to select a single model for application in all 20 study areas. Analyses in the Pilot sites show HSPF and SWAT are each capable of providing a good fit to streamflow and pollutant loads for existing conditions. The quality of fit depends in part on the strategy and skill of the individual modeler. In this study, the quality of fit was also influenced by the availability in certain areas of preexisting, calibrated models which were adapted for use as compared to locations where new models were developed and calibration subject to resource limitations.

For the purposes of this study, the SWAT model was considered to have a technical advantage because it can account for the influence of changes in atmospheric CO₂ concentration and other feedback responses of plant growth to climate change. HSPF does not automatically account for these effects. While it is uncertain how well SWAT is able to represent the complex processes affecting plant growth, nutrient dynamics, and water budgets under changing climate (see Luo et al., 2013), it was considered important to include some representation of these processes to better understand potential watershed sensitivity to a wide range of conditions. In addition, there are also practical advantages to the choice of SWAT, as the model is somewhat easier to set up and calibrate than is HSPF.

Conversely, the HSPF model proved generally better able to replicate observations during calibration, as shown in Section 6.1.1., although the difference between HSPF and SWAT model performance was small for the selected response variables. HSPF is often able to provide a better fit to streamflow after calibration due to the use of hourly precipitation and a more sophisticated algorithm compared to SWAT's daily curve number approach—although this advantage is diminished by the need to use disaggregated daily total rainfall to drive the models in many areas. Increased accuracy in hydrology—especially the accurate partitioning between surface and subsurface runoff—should also provide increased accuracy in the simulation of sediment yield and the transport of sediment-associated nutrients. However, at the larger watershed scales studied here (HUC-8 and greater), such advantages will tend to diminish as observations reflect the integration of flows and loads from multiple subwatersheds driven by multiple weather stations. Further, SWAT is generally considered to perform better under limited calibration and thus may have an advantage for extension to changed conditions of land use and climate (Gassman et al., 2007).

The file structure of the HSPF model is also considerably more efficient for implementing and running multiple scenarios. SWAT's use of the curve number approach to hydrology and a daily time step can also cause difficulties in representing the full hydrograph and introduces uncertainties into the simulation of erosion and pollutant loading as a function of surface flow (Garen and Moore, 2005). This is a concern in particular for the simulation of urban hydrology at small spatial scales; however, these concerns are of lesser importance at the larger spatial scales that are the focus of this study.

Given that both models were capable of performing adequately, the SWAT model was selected for use in the 15 nonpilot watersheds due to its integrated plant growth model and practical advantages of ease of calibration.

It should be recognized that there are other feedback cycles that are not incorporated in either model, such as the potential for any increased rate of catastrophic forest fires (Westerling et al., 2006), changes to vegetative communities as a result of pests and disease (Berg et al., 2006), and human adaptations such as shifts to different crops and agricultural management strategies (Polsky and Easterling, 2001).

7.2. SENSITIVITY TO CLIMATE CHANGE SCENARIOS

This section presents the results of SWAT simulations in all 20 study areas for climate change scenarios alone (that is, with land use held constant at existing conditions). In general, the different climate scenarios provide a consistent picture of temperature increases by mid-century (on the order of 2 to 3°C or 3 to 6°F), although there do appear to be systematic differences between the scenarios (for example, the NARCCAP scenario using the GFDL model downscaled with RCM3 typically is the coolest scenario for the watersheds studied here). In contrast, changes in precipitation between the historical and future periods differ widely across climate change scenarios, with some producing increases and some decreases in total precipitation.

Projected mid-21st century precipitation, air temperature, PET, and simulated AET (from SWAT) for each of the six NARCCAP climate change scenarios in each study area are shown in Tables 7-2 through 7-5. For Cook Inlet (Alaska) results are shown only for the three NARCCAP scenarios that provide climate projections for this portion of Alaska. The projected future climate annual average as a percent of baseline resulting from each of the six NARCCAP scenarios is shown for precipitation, PET, and AET; absolute change is shown for the annual average temperature. It should be noted that while the projected future average annual temperature increases in all cases, PET does not always increase. This is particularly noticeable in some of the southwestern study areas (e.g., Rio Grande Valley) where at least some future climate scenarios project increases in humidity and cloudiness that offset the temperature impact on PET. While shown here for comparison to PET, AET is a model input, not a model output. AET is driven by PET, but can also be limited by lack of soil moisture and is affected by changes in the seasonal timing of both precipitation and plant growth.

Table 7-2. Average annual precipitation (in/yr and percent of baseline) for current conditions and mid-21st century climate scenarios

Study area	Current conditions	CRCM_cgcm3 (%)	HRM3_hadcm3 (%)	RCM3_gfdl (%)	GFDL_slice (%)	RCM3_cgcm3 (%)	WRFP_ccsm (%)	Median ratio (%)
ACF—Apalachicola-Chattahoochee-Flint Basins	52.14	105.1	114.3	106.2	97.2	111.2	90.4	105.6
Ariz—Arizona: Salt, Verde, and San Pedro	19.38	87.4	94.3	110.4	85.9	98.5	87.9	91.1
Cook—Cook Inlet Basin	24.22	ND	118.3	ND	113.9	ND	122.6	118.3
GaFla—Georgia-Florida Coastal Plain	52.98	101.3	117.3	106.5	95.3	112.0	85.1	103.9
Illin—Illinois River Basin	37.63	101.5	114.2	103.9	104.1	105.3	93.3	104.0
LErie—Lake Erie Drainages	36.88	102.4	114.2	104.9	109.0	104.0	91.7	104.5
LPont—Lake Pontchartrain Drainage	64.76	96.0	109.2	106.4	92.5	100.9	87.8	98.5
Minn—Minnesota River Basin	27.61	102.3	106.7	110.3	97.8	110.7	112.1	108.5
Neb—Nebraska: Loup and Elkhorn River Basins	24.43	99.5	103.4	103.4	86.2	106.3	104.8	103.4
NewEng—New England Coastal Basins	46.42	106.1	113.2	107.7	107.4	104.7	98.1	106.7
PowTon—Powder and Tongue River Basins	13.85	99.1	100.2	104.8	86.5	105.6	120.0	102.5
RioGra—Rio Grande Valley	12.20	89.1	91.1	106.5	90.6	88.3	99.4	90.8
Sac—Sacramento River Basin	35.81	102.3	88.6	95.8	99.6	99.1	96.3	97.7
SoCal—Southern California Coastal Basins	19.62	96.2	117.1	97.0	95.5	99.4	87.6	96.6
SoPlat—South Platte River Basin	15.93	95.4	92.2	97.5	87.1	98.9	101.2	96.5
Susq—Susquehanna River Basin	39.73	106.6	109.2	103.6	105.4	105.7	97.9	105.6
TarNeu—Tar and Neuse River Basins	48.90	99.5	122.3	112.6	103.2	108.0	92.4	105.6
Trin—Trinity River Basin	42.83	94.8	110.4	98.6	83.4	101.8	105.9	100.2
UppCol—Upper Colorado River Basin	15.88	90.3	97.3	108.3	95.7	94.8	95.2	95.4
Willa—Willamette River Basin	55.43	106.5	101.1	97.6	88.4	105.1	94.5	99.4

Table 7-3. Average annual temperature (°F and change from baseline) for current conditions and mid-21st century climate scenarios

Study area	Current conditions	CRCM_cgcm3	HRM3_hadcm3	RCM3_gfdl	GFDL_slice	RCM3_cgcm3	WRFPP_ccsm	Median change
ACF—Apalachicola-Chattahoochee-Flint Basins	64.33	+3.81	+4.16	+3.62	+4.49	+3.45	+4.35	+3.98
Ariz—Arizona: Salt, Verde, and San Pedro	56.41	+4.93	+5.19	+4.35	+4.96	+4.75	+4.62	+4.84
Cook—Cook Inlet Basin	33.13	ND	+5.20	ND	+3.99	ND	+5.30	+5.20
GaFla—Georgia-Florida Coastal Plain	68.29	+3.56	+3.99	+3.45	+4.36	+3.32	+3.68	+3.62
Illin—Illinois River Basin	49.57	+5.36	+4.66	+4.38	+4.84	+4.75	+5.36	+4.80
LErie—Lake Erie Drainages	49.13	+5.19	+4.65	+4.29	+4.75	+4.67	+5.11	+4.71
LPont—Lake Pontchartrain Drainage	66.48	+3.77	+4.53	+3.61	+4.13	+3.41	+3.79	+3.78
Minn—Minnesota River Basin	44.18	+5.61	+5.29	+4.01	+5.02	+4.60	+4.90	+4.96
Neb—Nebraska: Loup and Elkhorn River Basins	47.94	+5.20	+5.10	+3.88	+5.09	+4.53	+4.65	+4.87
NewEng—New England Coastal Basins	46.32	+4.97	+4.81	+4.07	+4.12	+4.67	+4.50	+4.58
PowTon—Powder and Tongue River Basins	44.84	+4.77	+4.97	+3.81	+4.71	+4.50	+4.27	+4.61
RioGra—Rio Grande Valley	44.72	+5.13	+5.37	+4.20	+5.84	+5.02	+4.74	+5.08
Sac—Sacramento River Basin	58.23	+4.16	+4.76	+3.75	+3.47	+3.94	+4.06	+4.00
SoCal—Southern California Coastal Basins	61.38	+3.58	+3.97	+3.72	+3.27	+3.98	+3.57	+3.65
SoPlat—South Platte River Basin	45.06	+4.98	+5.20	+4.14	+5.51	+4.93	+4.77	+4.96
Susq—Susquehanna River Basin	48.18	+4.98	+4.98	+4.16	+4.72	+4.59	+4.60	+4.66
TarNeu—Tar and Neuse River Basins	59.93	+4.28	+4.51	+3.83	+4.18	+3.70	+4.14	+4.16
Trin—Trinity River Basin	64.91	+4.35	+4.66	+3.97	+4.45	+3.79	+4.38	+4.36
UppCol—Upper Colorado River Basin	40.80	+5.20	+5.14	+4.13	+5.53	+4.90	+5.04	+5.09
Willa—Willamette River Basin	51.48	+3.79	+4.37	+2.80	+3.03	+3.59	+3.57	+3.58

Table 7-4. Average annual PET (in/yr and percent of baseline) for current conditions and mid-21st century climate scenarios

Study area	Current conditions	CRCM_cgcm3 (%)	HRM3_hadcm3 (%)	RCM3_gfdl (%)	GFDL_slice (%)	RCM3_cgcm3 (%)	WRFPP_ccsm (%)	Median ratio (%)
ACF—Apalachicola-Chattahoochee-Flint Basins	62.04	101.2	103.8	101.6	97.5	98.3	105.2	101.4
Ariz—Arizona: Salt, Verde, and San Pedro	81.27	103.6	103.8	100.3	103.0	102.6	106.4	103.3
Cook—Cook Inlet Basin	16.56	ND	106.2	ND	99.7	ND	104.1	104.1
GaFla—Georgia-Florida Coastal Plain	65.82	99.9	101.1	99.6	100.3	98.6	100.6	100.1
Illin—Illinois River Basin	42.91	112.3	110.5	109.3	111.2	110.0	111.2	110.9
LErie—Lake Erie Drainages	45.27	102.0	100.7	99.6	101.1	100.2	101.3	100.9
LPont—Lake Pontchartrain Drainage	59.19	101.4	106.9	103.0	103.9	99.3	101.2	102.2
Minn—Minnesota River Basin	49.36	106.3	110.4	98.6	110.5	99.7	94.2	103.0
Neb—Nebraska: Loup and Elkhorn River Basins	61.94	100.4	100.5	97.0	101.4	98.1	97.9	99.2
NewEng—New England Coastal Basins	43.22	103.3	105.9	100.3	100.6	100.6	101.3	100.9
PowTon—Powder and Tongue River Basins	55.39	101.3	102.7	99.0	102.3	100.3	99.0	100.8
RioGra—Rio Grande Valley	54.48	94.4	100.1	90.4	99.9	95.9	92.6	95.1
Sac—Sacramento River Basin	66.77	99.2	103.0	102.5	98.8	98.8	101.6	100.4
SoCal—Southern California Coastal Basins	64.41	99.2	100.2	99.9	99.0	100.0	99.2	99.6
SoPlat—South Platte River Basin	53.25	102.0	103.4	100.3	104.1	101.9	101.4	102.0
Susq—Susquehanna River Basin	43.81	102.9	107.6	101.2	101.4	99.5	104.9	102.1
TarNeu—Tar and Neuse River Basins	56.38	100.5	100.9	99.2	100.1	99.0	100.1	100.1
Trin—Trinity River Basin	77.27	99.5	100.1	99.0	99.8	98.1	98.7	99.3
UppCol—Upper Colorado River Basin	38.14	106.8	107.7	103.9	108.8	105.8	106.2	106.5
Willa—Willamette River Basin	43.64	97.4	102.0	100.5	98.9	98.6	98.7	98.8

Table 7-5. Average annual SWAT-simulated actual ET (in/yr and percent of baseline) for current conditions and mid-21st century climate scenarios

Study area	Current conditions	CRCM_cgcm3 (%)	HRM3_hadcm3 (%)	RCM3_gfdl (%)	GFDL_slice (%)	RCM3_cgcm3 (%)	WRFPP_ccsm (%)	Median ratio (%)
ACF—Apalachicola-Chattahoochee-Flint Basins	32.22	106.1	110.6	106.6	106.2	104.9	102.8	106.2
Ariz—Arizona: Salt, Verde, and San Pedro	14.47	86.8	94.8	102.8	86.3	97.3	89.8	92.3
Cook—Cook Inlet Basin	7.95	ND	109.1	ND	103.6	ND	108.6	108.6
GaFla—Georgia-Florida Coastal Plain	30.86	98.5	101.1	99.7	98.9	99.1	95.0	99.0
Illin—Illinois River Basin	22.90	101.5	103.4	101.3	101.0	101.7	98.9	101.4
LErie—Lake Erie Drainages	22.75	94.4	95.3	96.0	97.2	93.3	90.8	94.9
LPont—Lake Pontchartrain Drainage	29.83	100.1	107.0	101.3	103.4	99.0	98.2	100.7
Minn—Minnesota River Basin	21.64	96.1	99.9	94.9	97.2	95.7	92.7	95.9
Neb—Nebraska: Loup and Elkhorn River Basins	18.00	97.8	101.8	100.6	94.3	98.9	97.9	98.4
NewEng—New England Coastal Basins	23.31	103.3	110.4	103.5	102.5	104.3	104.8	103.9
PowTon—Powder and Tongue River Basins	16.83	93.3	94.9	96.7	83.7	97.2	105.4	95.8
RioGra—Rio Grande Valley	10.32	84.2	87.9	98.0	88.7	85.2	94.7	88.3
Sac—Sacramento River Basin	15.26	99.2	97.6	94.7	97.0	95.9	94.9	96.5
SoCal—Southern California Coastal Basins	8.75	97.2	102.7	92.9	93.7	96.8	94.1	95.5
SoPlat—South Platte River Basin	13.06	96.1	94.0	96.0	90.4	97.1	98.5	96.0
Susq—Susquehanna River Basin	23.73	104.8	108.4	102.6	103.7	102.0	104.8	104.2
TarNeu—Tar and Neuse River Basins	29.48	97.2	99.9	98.0	97.8	97.4	95.6	97.6
Trin—Trinity River Basin	27.58	95.0	99.9	97.0	90.1	96.4	97.8	96.7
UppCol—Upper Colorado River Basin	13.13	91.7	98.0	101.2	98.6	94.0	95.5	96.7
Willa—Willamette River Basin	19.84	87.9	92.9	85.4	82.9	88.7	88.3	88.1

In addition to changes in precipitation amount, this study considers the impacts of changes in precipitation intensity, which may have significant effects on the partitioning between surface and subsurface flows and associated generation of pollutant loads. As described in Section 5.2., a change factor approach was used to modify historical meteorological time series to represent mid-21st century climate futures projected by a variety of downscaled (and nondownscaled) GCM projections. Potential intensification of precipitation is represented by reapportioning the net change in precipitation volume according to GCM forecasts of the distribution of event intensities above and below the 70th percentile of the distribution of current (1971–2000) rainfall events. Under current conditions, the fraction of rainfall volume occurring in events above the 70th percentile ranges from a low of 61% (Cook Inlet and Willamette) to a high of 93% (Southern California Coastal). Projected mid-21st century changes in precipitation intensity from the six NARCCAP scenarios, shown in Table 7-6, are mixed. Across all study areas there is an average increase in the fraction of total volume above the 70th percentile of the current distribution of 1.19 percentage points. However, for most study areas the six NARCCAP scenarios are not in full agreement as to whether intensification of precipitation (as defined relative to the 70th percentile event) will increase. An increase in the volume in high-intensity events is consistently projected across all six of the NARCCAP mid-21st century projections in only six of the 20 study areas (Susq, Minn, Cook, LErie, Illin, and NewEng). Two RCM/GCM combinations (HRM3_hadcm3 = Scenario 2) and (RCM3_cgcm3 = Scenario 5) project increases in intensity in all study areas. No study area is expected to have a decrease in precipitation volume in high intensity events across all NARCCAP scenarios, while six study areas (Cook, Illin, LErie, Minn, NewEng, and Susq) are projected to have an increase in high-intensity events across all six NARCCAP scenarios. By far the largest increases in high-intensity events are projected for the Cook Inlet watershed in Alaska, followed by the Upper Colorado basin.

The simulated watershed responses to mid-21st century climate change scenarios are shown in Tables 7-7 through 7-14. For endpoints other than days to streamflow centroid, the results are displayed as a percentage relative to the current baseline (generally, 1972–2003), allowing comparison across multiple basins with different magnitudes of streamflow and pollutant loads. For Cook Inlet (Alaska), the results are shown only for the three NARCCAP scenarios that provide climate projections for this portion of Alaska.

Table 7-7 summarizes results for total average annual streamflow volume, with results ranging from 62% to 240% of current average flows. Results for 7-day low streamflow and 100-year peak flows (estimated with log-Pearson III fit) are shown in Tables 7-8 and 7-9, respectively. The Kenai River has by far the greatest increase in 7-day low flows because warmer temperatures alter the snow/ice melt regime, while the largest increases in 100-year peak flows are for the Neuse River on the east coast.

Table 7-10 summarizes the estimated change in days to streamflow centroid relative to the start of the water year. Many stations show negative shifts, indicating earlier snowmelt resulting in an earlier center of streamflow mass. In contrast, several stations show positive shifts due to increased summer precipitation.

Results for the Richards-Baker flashiness index (see Table 7-11) show generally small percentage changes, with a few exceptions. Baker et al. (2004) suggest that changes on the order

of 10% or more may be statistically significant. It is likely, however, that the focus on larger watersheds reduces the observed flashiness response.

Table 7-6. Changes in precipitation intensity for NARCCAP mid-21st century climate scenarios

	CRCM_cgcm3 (%)	HRM3_hadcm3 (%)	RCM3_gfdl (%)	GFDL_slice (%)	RCM3_cgcm3 (%)	WRFG_ccsm (%)
ACF	3.28	1.35	1.87	-0.68	2.43	-0.12
Ariz	-0.19	0.53	0.03	0.36	0.79	-0.43
Cook	ND	7.51	ND	3.71	ND	4.62
GaFla	2.74	1.60	2.33	-1.23	2.99	-0.89
Illin	1.95	1.56	1.09	0.87	1.25	0.20
LErie	2.25	2.01	1.64	1.81	1.12	0.27
LPont	2.49	0.71	2.50	-0.48	1.61	-0.87
Minn	1.92	1.22	1.94	0.09	1.38	0.43
Neb	1.08	1.56	1.61	-0.12	0.99	0.14
NewEng	2.55	1.51	1.74	0.36	1.21	0.15
PowTon	1.67	1.54	1.66	-1.09	1.59	0.97
RioGra	-0.04	0.96	1.64	0.37	0.91	0.52
Sac	1.87	0.47	0.00	-1.06	2.28	1.42
SoCal	0.24	1.83	-0.76	-0.28	0.29	-0.15
SoPlat	-0.20	0.85	1.13	-0.15	1.27	0.51
Susq	3.28	1.58	2.08	0.41	1.77	0.41
TarNeu	2.59	1.38	1.55	-0.42	1.21	-0.02
Trin	1.32	1.24	0.61	-0.66	0.14	0.46
UppCol	-0.10	1.95	2.36	0.79	2.06	0.71
Willa	2.50	2.59	0.46	-2.63	2.71	0.97

Note: Potential change in precipitation intensity is shown as the change total volume of precipitation event above the 70th percentile of the current (1971–2000) distribution of rainfall event volumes.

Simulated changes in pollutant loads (TN, TP, TSS) are summarized in Tables 7-12 through 7-14. The patterns are generally similar to changes in streamflow. Increases in pollutant loads are suggested for many watersheds, but there are also basins where loads decline, mostly due to reduced flows.

Table 7-7. Simulated total streamflow volume (climate scenarios only; percent relative to current conditions) for selected downstream stations

Station	Study area	CRCM_cgcm3 (%)	HRM3_hadem3 (%)	RCM3_gfdl (%)	GFDL_slice (%)	RCM3_cgcm3 (%)	WRFPP_ccsm (%)	Median (%)
Apalachicola R at outlet	ACF	107	122	108	88	124	73	107
Salt River near Roosevelt	Ariz	80	80	149	75	94	73	80
Kenai R at Soldotna	Cook	ND	154	ND	132	ND	167	154
Suwanee R at outlet	GaFla	114	153	128	92	156	75	121
Illinois R at Marseilles, IL	Illin	94	125	101	102	105	78	101
Maumee R at outlet	LErie	116	150	120	136	122	88	121
Amite R at outlet	LPont	96	110	115	84	106	77	101
Minnesota R at outlet	Minn	109	113	147	86	146	162	130
Elkhorn R at outlet	Neb	117	125	137	68	138	143	131
Merrimack R at outlet	NewEng	108	115	111	111	106	94	109
Tongue R at outlet	PowTon	101	85	140	70	130	240	115
Rio Grande R below Albuquerque	RioGra	72	69	112	66	69	84	71
Sacramento R at outlet	Sac	104	89	98	98	100	99	99
Los Angeles R at outlet	SoCal	92	138	102	103	106	84	103
S. Platte R at outlet	SoPlat	90	74	90	65	107	119	90
Susquehanna R at outlet	Susq	109	106	106	108	111	90	107
Neuse R at outlet	TarNeu	103	158	137	110	125	86	118
Trinity R at outlet	Trin	98	146	106	62	118	134	112
Colorado R near State Line	UppCol	86	95	116	89	92	91	91
Willamette R at outlet	Willa	116	106	105	92	114	98	105

Table 7-8. Simulated 7-day low flow (climate scenarios only; percent relative to current conditions) for selected downstream stations

Station	Study area	CRCM_ cgem3 (%)	HRM3_ hadem3 (%)	RCM3_ gfdl (%)	GFDL_ slice (%)	RCM3_ cgem3 (%)	WRF_ ccsn (%)	Median (%)
Apalachicola R at outlet	ACF	97	120	105	85	113	64	101
Salt River near Roosevelt	Ariz	58	77	130	87	79	90	83
Kenai R at Soldotna	Cook	ND	267	ND	280	ND	401	280
Suwanee R at outlet	GaFla	104	141	121	95	136	78	113
Illinois R at Marseilles, IL	Illin	85	123	97	91	100	70	94
Maumee R at outlet	LErie	104	184	126	132	128	58	127
Amite R at outlet	LPont	73	106	88	74	89	62	81
Minnesota R at outlet	Minn	115	136	201	81	182	228	159
Elkhorn R at outlet	Neb	119	133	151	48	148	154	140
Merrimack R at outlet	NewEng	110	140	130	118	124	120	122
Tongue R at outlet	PowTon	102	92	145	67	127	235	115
Rio Grande R below Albuquerque	RioGra	81	64	120	62	74	86	77
Sacramento R at outlet	Sac	101	91	95	96	99	93	95
Los Angeles R at outlet	SoCal	96	114	98	98	100	92	98
S. Platte R at outlet	SoPlat	93	87	97	74	102	113	95
Susquehanna R at outlet	Susq	91	120	104	89	107	86	98
Neuse R at outlet	TarNeu	94	170	135	113	125	70	119
Trinity R at outlet	Trin	26	167	64	23	70	85	67
Colorado R near State Line	UppCol	85	94	121	85	91	90	91
Willamette R at outlet	Willa	131	113	108	83	127	102	111

Table 7-9. Simulated 100-year peak flow (log-Pearson III; climate scenarios only; percent relative to current conditions) for selected downstream stations

Station	Study area	CRCM_ cgem3 (%)	HRM3_ hadcm3 (%)	RCM3_ gfdl (%)	GFDL_ slice (%)	RCM3_ cgcm3 (%)	WRFPP_ ccsn (%)	Median (%)
Apalachicola R at outlet	ACF	119	144	110	90	128	94	114
Salt River near Roosevelt	Ariz	119	101	104	68	120	66	102
Kenai R at Soldotna	Cook	ND	132	ND	125	ND	132	132
Suwanee R at outlet	GaFla	130	145	129	94	157	107	130
Illinois R at Marseilles, IL	Illin	120	153	107	99	128	97	114
Maumee R at outlet	LErie	96	106	87	93	93	92	93
Amite R at outlet	LPont	105	150	108	99	105	65	105
Minnesota R at outlet	Minn	84	83	96	88	90	96	89
Elkhorn R at outlet	Neb	126	117	109	92	139	103	113
Merrimack R at outlet	NewEng	114	130	111	138	89	80	112
Tongue R at outlet	PowTon	118	113	133	82	121	146	119
Rio Grande R below Albuquerque	RioGra	90	77	108	66	72	92	83
Sacramento R at outlet	Sac	105	98	125	117	102	131	111
Los Angeles R at outlet	SoCal	83	89	161	95	127	77	92
S. Platte R at outlet	SoPlat	132	127	98	126	151	150	129
Susquehanna R at outlet	Susq	107	130	106	128	172	100	118
Neuse R at outlet	TarNeu	71	292	161	111	224	63	136
Trinity R at outlet	Trin	97	106	107	60	86	106	102
Colorado R near State Line	UppCol	78	84	97	91	94	84	87
Willamette R at outlet	Willa	116	130	114	79	116	95	115

Table 7-10. Simulated changes in the number of days to streamflow centroid (climate scenarios only; relative to current conditions) for selected downstream stations

Station	Study area	CRCM_cgcm3	HRM3_hadcm3	RCM3_gfdl	GFDL_slice	RCM3_cgcm3	WRFPP_ccsm	Median
Apalachicola R at outlet	ACF	-2	-2	1	8	-6	1	-1
Salt River near Roosevelt	Ariz	-18	41	28	17	-6	53	22
Kenai R at Soldotna	Cook	ND	-3	ND	-5	ND	-1	-3
Suwanee R at outlet	GaFla	-3	17	25	-8	-5	11	4
Illinois R at Marseilles, IL	Illin	-12	6	-3	-12	-2	-15	-7
Maumee R at outlet	LErie	-2	-4	1	0	10	-8	-1
Amite R at outlet	LPont	-14	13	-24	-7	-6	-11	-9
Minnesota R at outlet	Minn	-13	-19	-6	-15	-3	2	-10
Elkhorn R at outlet	Neb	-12	6	1	-15	-6	2	-2
Merrimack R at outlet	NewEng	-17	-14	-19	-13	-9	-18	-16
Tongue R at outlet	PowTon	-6	-3	1	-16	-4	7	-3
Rio Grande R below Albuquerque	RioGra	25	6	3	11	14	17	13
Sacramento R at outlet	Sac	-4	-7	-4	-1	-3	-8	-4
Los Angeles R at outlet	SoCal	5	48	-3	10	-3	1	3
S. Platte R at outlet	SoPlat	-12	-20	-14	-19	-3	-12	-13
Susquehanna R at outlet	Susq	-18	16	-6	-12	-6	0	-6
Neuse R at outlet	TarNeu	-14	23	30	-12	10	-5	2
Trinity R at outlet	Trin	16	21	30	3	6	37	18
Colorado R near State Line	UppCol	-11	-14	-7	-10	-8	-10	-10
Willamette R at outlet	Willa	3	-8	-1	3	1	8	2

Table 7-11. Simulated Richards-Baker flashiness index (climate scenarios only; percent relative to current conditions) for selected downstream stations

Station	Study area	CRCM_ cpcm3 (%)	HRM3_ hadcm3 (%)	RCM3_ gfdl (%)	GFDL_ slice (%)	RCM3_ cpcm3 (%)	WRF_ ccsn (%)	Median (%)
Apalachicola R at outlet	ACF	106	125	109	94	125	90	108
Salt River near Roosevelt	Ariz	81	102	121	98	103	119	102
Kenai R at Soldotna	Cook	ND	94	ND	102	ND	96	96
Suwanee R at outlet	GaFla	93	62	76	117	59	187	84
Illinois R at Marseilles, IL	Illin	106	104	103	106	105	104	105
Maumee R at outlet	LErie	99	101	99	100	100	96	100
Amite R at outlet	LPont	105	105	106	104	104	102	104
Minnesota R at outlet	Minn	104	112	107	100	109	108	108
Elkhorn R at outlet	Neb	95	98	94	95	96	94	95
Merrimack R at outlet	NewEng	101	103	99	101	98	93	100
Tongue R at outlet	PowTon	102	108	104	100	103	109	104
Rio Grande R below Albuquerque	RioGra	109	117	95	119	103	106	108
Sacramento R at outlet	Sac	124	103	112	109	116	123	114
Los Angeles R at outlet	SoCal	103	119	100	105	105	99	104
S. Platte R at outlet	SoPlat	99	91	101	87	108	106	100
Susquehanna R at outlet	Susq	107	111	107	110	112	103	109
Neuse R at outlet	TarNeu	96	113	115	98	103	91	101
Trinity R at outlet	Trin	71	68	72	73	69	68	70
Colorado R near State Line	UppCol	101	107	111	105	104	101	105
Willamette R at outlet	Willa	101	105	100	97	101	102	101

Table 7-12. Simulated total suspended solids load (climate scenarios only; percent relative to current conditions) for selected downstream stations

Station	Study area	CRCM_ cgcm3 (%)	HRM3_ hadcm3 (%)	RCM3_ gfdl (%)	GFDL_ slice (%)	RCM3_ cgcm3 (%)	WRFp_ ccsm (%)	Median (%)
Apalachicola R at outlet	ACF	125	146	129	93	144	53	127
Salt River near Roosevelt	Ariz	89	79	184	66	106	74	84
Kenai R at Soldotna	Cook	ND	234	ND	196	ND	244	234
Suwanee R at outlet	GaFla	121	176	138	90	181	74	130
Illinois R at Marseilles, IL	Illin	116	142	115	128	120	90	118
Maumee R at outlet	LErie	123	169	126	153	129	86	128
Amite R at outlet	LPont	100	115	128	83	111	71	106
Minnesota R at outlet	Minn	107	119	187	77	197	225	153
Elkhorn R at outlet	Neb	122	131	147	60	162	162	139
Merrimack R at outlet	NewEng	118	128	117	122	111	85	118
Tongue R at outlet	PowTon	108	84	169	66	153	351	131
Rio Grande R below Albuquerque	RioGra	60	53	114	49	59	71	59
Sacramento R at outlet	Sac	139	94	122	118	99	108	113
Los Angeles R at outlet	SoCal	71	111	81	81	84	65	81
S. Platte R at outlet	SoPlat	91	87	94	80	100	104	93
Susquehanna R at outlet	Susq	117	108	108	115	118	84	112
Neuse R at outlet	TarNeu	106	199	162	115	143	82	129
Trinity R at outlet	Trin	63	124	62	27	83	113	73
Colorado R near State Line	UppCol	80	90	124	82	89	85	87
Willamette R at outlet	Willa	124	111	109	90	121	97	110

Table 7-13. Simulated total phosphorus load (climate scenarios only; percent relative to current conditions) for selected downstream stations

Station	Study area	CRCM_cgcm3 (%)	HRM3_hadcm3 (%)	RCM3_gfdl (%)	GFDL_slice (%)	RCM3_cgcm3 (%)	WRFP_ccsm (%)	Median (%)
Apalachicola R at outlet	ACF	138	152	134	118	148	106	136
Salt River near Roosevelt	Ariz	82	83	155	70	106	88	86
Kenai R at Soldotna	Cook	ND	89	ND	90	ND	113	90
Suwanee R at outlet	GaFla	115	171	135	89	173	76	125
Illinois R at Marseilles, IL	Illin	107	112	107	113	108	99	108
Maumee R at outlet	LErie	118	150	132	148	117	88	125
Amite R at outlet	LPont	113	131	135	94	115	83	114
Minnesota R at outlet	Minn	97	115	151	97	138	160	126
Elkhorn R at outlet	Neb	118	124	138	65	145	147	131
Merrimack R at outlet	NewEng	111	118	111	115	106	94	111
Tongue R at outlet	PowTon	107	86	163	67	148	324	127
Rio Grande R below Albuquerque	RioGra	54	43	127	51	41	67	53
Sacramento R at outlet	Sac	100	86	104	115	95	108	102
Los Angeles R at outlet	SoCal	53	88	71	60	62	54	61
S. Platte R at outlet	SoPlat	90	78	99	72	108	111	95
Susquehanna R at outlet	Susq	128	106	111	127	115	109	113
Neuse R at outlet	TarNeu	112	230	169	120	166	94	143
Trinity R at outlet	Trin	124	163	130	83	135	160	132
Colorado R near State Line	UppCol	79	88	119	81	84	83	84
Willamette R at outlet	Willa	100	98	96	94	100	96	97

Table 7-14. Simulated total nitrogen load (climate scenarios only; percent relative to current conditions) for selected downstream stations

Station	Study area	CRCM_cgcm3 (%)	HRM3_hadcm3 (%)	RCM3_gfdl (%)	GFDL_slice (%)	RCM3_cgcm3 (%)	WRFPP_ccsm (%)	Median (%)
Apalachicola R at outlet	ACF	116	125	115	106	122	95	116
Salt River near Roosevelt	Ariz	90	91	142	86	105	84	90
Kenai R at Soldotna	Cook	ND	200	ND	175	ND	223	200
Suwanee R at outlet	GaFla	127	160	135	112	166	85	131
Illinois R at Marseilles, IL	Illin	103	118	106	110	108	93	107
Maumee R at outlet	LErie	128	158	162	191	125	94	143
Amite R at outlet	LPont	123	141	143	106	120	91	121
Minnesota R at outlet	Minn	126	130	163	105	158	171	144
Elkhorn R at outlet	Neb	93	97	145	88	104	107	101
Merrimack R at outlet	NewEng	119	128	117	121	114	101	118
Tongue R at outlet	PowTon	109	91	165	71	148	320	128
Rio Grande R below Albuquerque	RioGra	49	38	125	47	37	64	48
Sacramento R at outlet	Sac	99	89	100	110	98	107	100
Los Angeles R at outlet	SoCal	93	140	131	98	90	101	100
S. Platte R at outlet	SoPlat	86	70	91	63	109	116	89
Susquehanna R at outlet	Susq	162	147	147	156	150	132	149
Neuse R at outlet	TarNeu	111	189	154	118	144	99	131
Trinity R at outlet	Trin	121	165	125	80	136	164	130
Colorado R near State Line	UppCol	73	82	110	76	80	79	80
Willamette R at outlet	Willa	104	97	95	89	103	93	96

For most measures in most watersheds, there is a substantial amount of variability between scenario projections based on different methods of downscaling GCM outputs. This reflects our uncertainty in predicting future climate, especially the future joint distribution of precipitation and potential evapotranspiration that is fundamental to watershed response, and reinforces the need for an ensemble approach for evaluating the range of potential responses.

Climate change could also alter the seasonal dynamics of streamflow and nutrient loading. Seasonal effects are investigated here in summary form through calculation of the ratio of winter (January–March) to summer (July–September) runoff volume averaged over all HUC-8s in a study area. More detailed results showing simulated changes in streamflow by month are presented in Appendices X and Y. The different study areas have very different seasonal runoff volume ratios under current conditions, ranging from a winter:summer low of 0.11 in the Cook Inlet basin to a high of 11 in the Willamette River basin. The average ratios under the mid-21st century NARCCAP climate change scenarios are shown relative to the current ratio in Figure 7-1. In most cases, the future climate scenarios span the current ratio; however, in the case of the South Platte and Upper Colorado study areas, currently dominated by snowmelt runoff from the Rocky Mountains, all future climate scenarios project an increase in the ratio. In some basins the range of future projected seasonal runoff ratios is quite large. For the Salt, Verde, and San Pedro River basins (Ariz) the average future ratios by climate scenario range from 0.8 to 5.4, depending on whether the climate scenario projects greater increases in the summer monsoon or winter rainy period, while in the Lake Erie drainages (LErie) the range is from 1.5 to 7.8. The distribution for each of the six NARCCAP climate scenarios is summarized in Figure 7-2. There are clear differences between the different scenarios, with some projecting a much greater increase in the winter:summer runoff ratio than others.

7.3. SENSITIVITY TO URBAN AND RESIDENTIAL DEVELOPMENT SCENARIOS

This section presents the results of SWAT simulations in all 20 study areas for mid-21st century urban and residential development alone (that is, with climate held constant at existing conditions). Results in the pilot study areas (see Section 6.) suggested that effects of urban and residential development by 2050 on streamflow and pollutant loads is likely to be comparatively small relative to the potential range of impacts associated with climate change. This is largely a reflection of the scale of the analysis: at the scale of large (HUC-4 to HUC-8) watersheds, developed land is rarely a large portion of the total land area. Significant effects may occur in smaller subbasins where extensive new land development occurs.

Over the full extent of individual study areas, current impervious surface area ranges from near zero to 13.8% of the total area, while projected changes (increases) in impervious cover area range from 0 to 5.3% of the total area (see Table 7-15). While several fast-growing metropolitan areas are included within the study areas, the impact of these areas is diminished at larger spatial scales. At the HUC-8 and larger scale, it is not surprising that projected changes in urban and residential development have only a relatively small effect compared to climate change, which affects all portions of a watershed. The largest response of total streamflow volume to land-use change at the full-basin scale is simulated for the Trinity River in Texas, where total flow increased by 6%, while the estimated 100-year peak flow decreased and days to streamflow centroid increased (i.e., later runoff). This reflects increases in development upstream in the Dallas-Fort Worth metropolitan area. A stronger response to land development is seen at smaller

spatial scales where development can account for a larger fraction of watershed area. Development effects are also more likely be reflected in high or low streamflow statistics. For example, in the Los Angeles River projected changes in urban and residential development result in little change in model-simulated total streamflow volume, but the 100-year peak flow increases by nearly 25%.

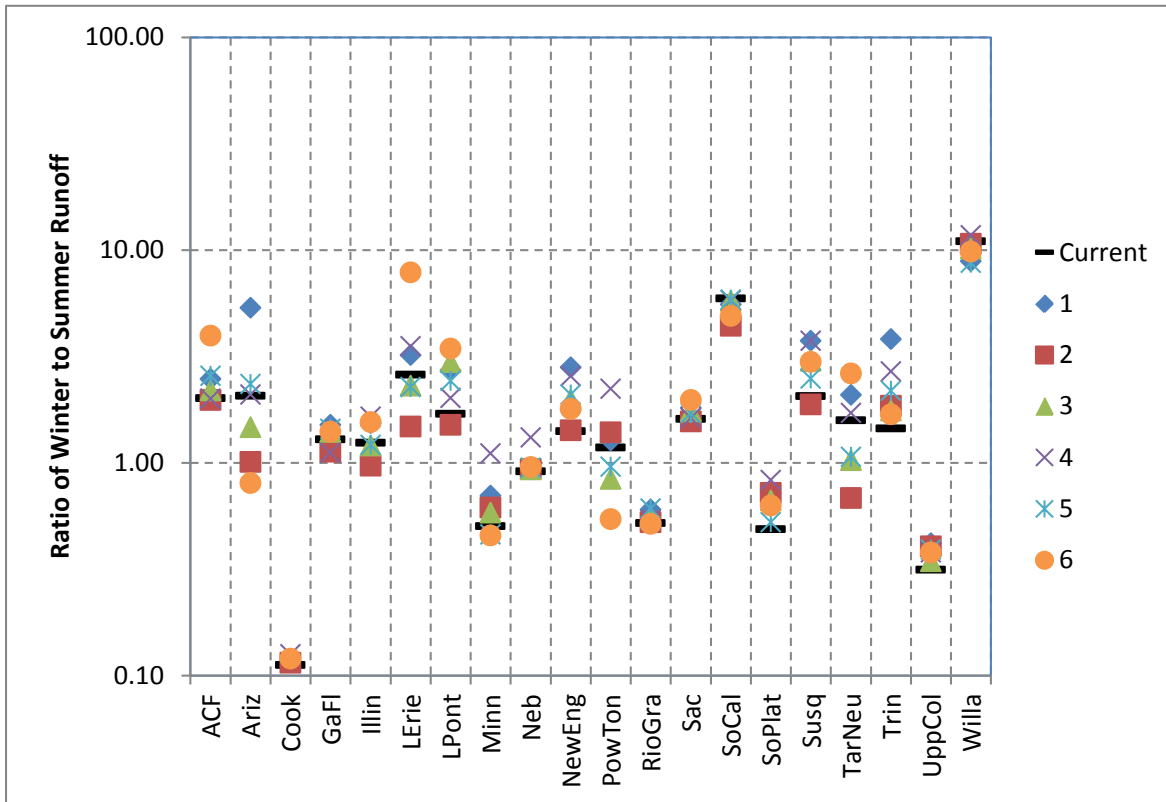


Figure 7-1. Ratio of winter (January–March) to summer (July–September) runoff volume under current and mid-21st century NARCCAP climate scenarios.

Notes: Results are averages over all HUC-8s simulated within a study area. Climate scenarios are (RCM and GCM): (1) CRCM_cgcm3, (2) HRM3_hadcm3, (3) RCM3_gfdl, (4) GFDL High Res_gfdl, (5) RCM3_cgcm3, and (6) WRFP_ccsm.

The simulated watershed responses to projected mid-21st century urban and residential development are shown in (see Table 7-16). Results across all 20 watersheds are small, as would be expected given the small changes in developed lands, when expressed as a fraction of total watershed area, at the scale of modeling in this study. Larger effects are likely in smaller subbasins within the study areas where urban and residential development is concentrated. Note that results are not available for the Kenai River (Cook Inlet, AK study area) because ICLUS projections do not include Alaska.

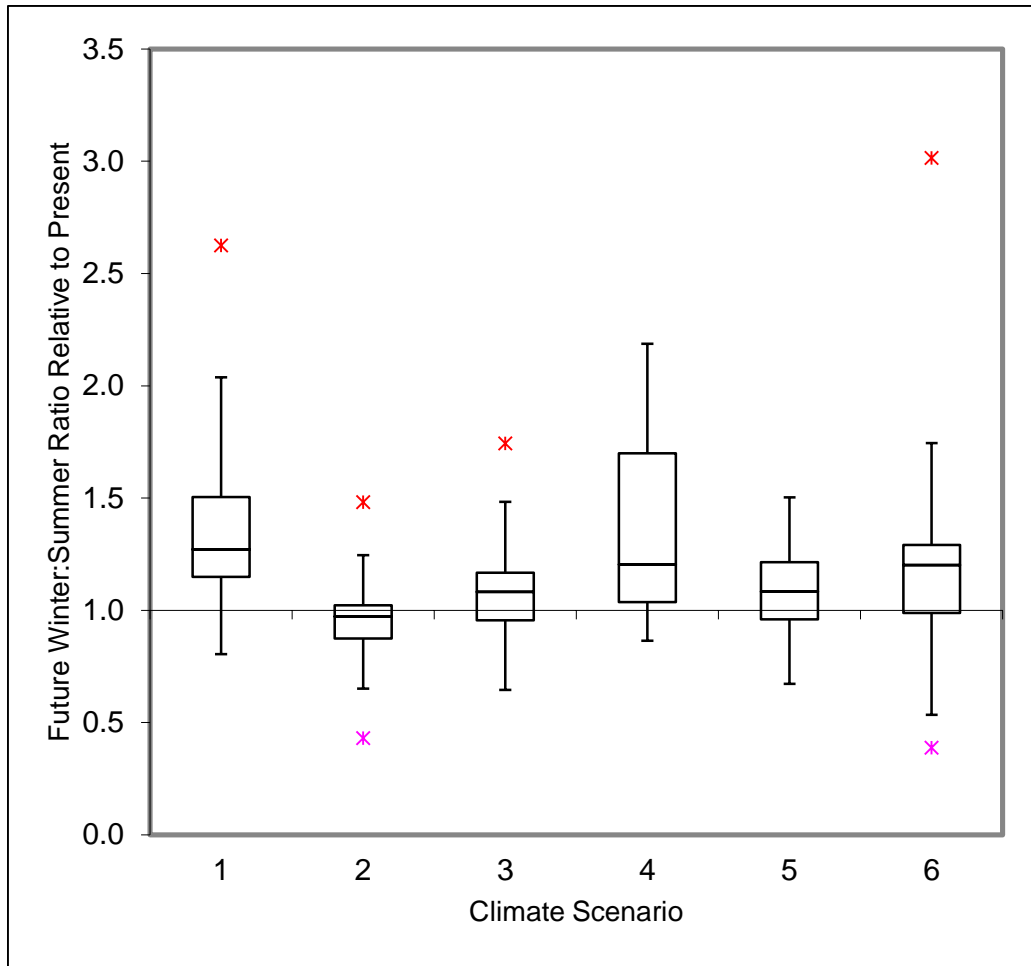


Figure 7-2. Box plots of the distribution of the ratio of winter (January–March) to summer (July–September) runoff volume normalized to the ratio under current conditions.

Notes: The box shows the interquartile range, with median indicated by a horizontal line, and the whiskers extend 1.5 times the interquartile range. Outliers beyond the whiskers are shown by individual points. The data are averages over all HUC-8s simulated within a study area. Climate scenarios are (RCM and GCM): (1) CRCM_cgcm3, (2) HRM3_hadcm3, (3) RCM3_gfdl, (4) GFDL High Res_gfdl, (5) RCM3_cgcm3, and (6) WRFPP_ccsm.

7.4. RELATIVE EFFECTS OF CLIMATE CHANGE AND URBAN DEVELOPMENT SCENARIOS

The changes in urban and residential development projected by ICLUS for 2050 suggest changes may be large locally but are small relative to the area of basins modeled in this study (see Table 5-5). Urban and residential development has long been recognized as a source of hydrologic changes and water quality degradation at local scales in developing areas (e.g., U.S. EPA, 1984). The cumulative impacts of development, however, tend to be relatively small at the larger basin scale evaluated in this study simply because only a small fraction of most HUC-4 scale watersheds is developed or projected to be developed by 2050.

Table 7-15. Projected mid-21st century impervious cover changes in study areas from ICLUS for A2 emissions storyline

Study area	Current (2001) impervious cover (%)	Projected mid-21 st century impervious cover (%)	Change in impervious cover (%)
ACF	2.04	3.06	1.02
Ariz	0.19	0.30	0.11
Cook	0.24	ND	ND
GaFla	2.50	3.86	1.36
Illin	6.19	8.22	2.03
LErie	3.48	3.88	0.40
LPont	3.24	4.56	1.32
Minn	1.06	1.28	0.22
Neb	0.38	0.39	0.01
NewEng	5.59	6.74	1.15
PowTon	0.08	0.08	0.00
RioGra	0.55	0.81	0.26
Sac	0.73	0.95	0.22
SoCal	13.80	19.11	5.31
SoPlat	2.06	4.27	2.21
Susq	1.50	1.69	0.19
TarNeu	1.70	2.55	0.85
Trin	4.17	7.37	3.20
UppCol	0.37	0.61	0.24
Willa	2.51	3.06	0.55

The relative magnitude of effects from urban development versus climate change in our simulations can be examined by looking at changes in mean annual streamflow. Figure 7-3 compares the HSPF simulated change in mean annual streamflow in the pilot study areas for mid-21st century urban and residential development compared to the six NARCCAP climate change scenarios. The results summarize the range of responses across selected HUC-8 subbasins and calibration locations contained within each study area. Table 7-17 compares the range of SWAT simulated changes in mean annual streamflow in all study locations for mid-21st century urban and residential development and the six NARCCAP climate change scenarios. Results summarize the ranges at the HUC-8 and larger scale within the study areas.

Table 7-16. Simulated response to projected 2050 changes in urban and residential development (percent or days relative to current conditions) for selected downstream stations

Station	Study area	Total flow (%)	7-day low flow (%)	100-yr peak flow (%)	Days to flow centroid	Richards-Baker flashiness (%)	TSS load (%)	TP load (%)	TN load (%)
Apalachicola R at outlet	ACF	100.3	100.4	100.3	-0.1	100.0	100.6	101.1	100.5
Salt River near Roosevelt	Ariz	100.1	100.0	100.2	0.1	100.3	100.2	100.4	100.2
Kenai R at Soldotna	Cook	ND	ND	ND	ND	ND	ND	ND	ND
Suwanee R at outlet	GaFla	100.3	99.9	100.6	0.3	99.5	100.4	108.9	102.5
Illinois R at Marseilles, IL	Illin	102.4	104.0	102.1	1.0	98.4	100.5	100.2	99.2
Maumee R at outlet	LErie	100.5	100.8	101.4	0.2	100.9	100.6	101.3	99.6
Amite R at outlet	LPont	100.8	102.6	101.6	0.2	100.4	98.7	106.8	103.9
Minnesota R at outlet	Minn	100.2	100.3	99.9	0.3	100.1	98.0	99.3	99.5
Elkhorn R at outlet	Neb	100.3	100.3	101.5	0.0	102.8	100.1	100.1	99.8
Merrimack R at outlet	NewEng	100.4	100.5	101.4	0.0	101.3	101.2	103.8	102.0
Tongue R at outlet	PowTon	100.0	100.0	100.0	0.0	100.0	100.0	100.0	100.0
Rio Grande R below Albuquerque	RioGra	100.1	100.1	100.4	0.0	100.2	101.1	95.4	99.6
Sacramento R at outlet	Sac	100.1	100.1	99.9	-0.1	100.4	99.7	102.1	104.7
Los Angeles R at outlet	SoCal	101.4	101.3	114.4	0.0	103.9	106.6	138.2	111.1
S. Platte R at outlet	SoPlat	102.8	100.7	101.1	0.9	103.9	103.9	104.0	103.4
Susquehanna R at outlet	Susq	100.2	100.7	99.7	0.1	100.1	100.2	99.7	99.2
Neuse R at outlet	TarNeu	101.7	105.2	102.1	0.7	99.1	102.3	106.7	103.3
Trinity R at outlet	Trin	106.4	188.1	74.2	3.7	68.8	61.9	110.0	106.2
Colorado R near State Line	UppCol	100.1	100.6	100.3	-0.1	99.8	100.0	100.8	100.2
Willamette R at outlet	Willa	99.9	100.0	100.1	0.0	100.7	99.7	99.9	102.5

Simulations using both HSPF and SWAT show a smaller range of response to projected future changes in urban development than to projected climate change. As discussed previously, at the spatial scale of these simulations projected future changes in developed land were a relatively small fraction of total watershed area. At smaller spatial scales, however, the effects of urban and residential development could be greater. Results for pollutant loads are similar to those for streamflow.

The simulated response to land-use change is also sensitive to model choice—or, more precisely, an interaction between the model and the way in which the ICLUS is interpreted. In the SWAT setup, there are representations of both directly connected (effective) and disconnected impervious area. New developed land use implied by ICLUS is identified to the model as a total area in a given development density class, then subdivided by the model into pervious and impervious fractions using basin-specific estimates of total and effective impervious area. The effective impervious fraction for a given development category is calculated from the 2000 NLCD and assumed invariant. The model then assumes that the effective impervious area has a curve number of 98, while the remaining disconnected impervious area provides a small modification to the curve number assigned to the pervious fraction of the HRU.

In contrast, HSPF has pervious (PERLND) and impervious (IMPLND) land uses, but does not distinguish a separate disconnected impervious class. For HSPF, the new developed area in ICLUS is assigned to the relevant pervious and impervious land-use fractions based on the basin-specific percent imperviousness for the land-use class. In essence, this means that somewhat greater future connected imperviousness is being specified to the HSPF model than is specified to the SWAT model. While the two approaches are rather different, they are consistent with typical modeling practice for the two models.

Several other details of the SWAT modeling process adopted in this study affect results. The approach to implementing changes in urban development in SWAT was to remove land from existing undeveloped and nonexempt land uses and reassign it to new developed classes that have the parameters of the most dominant soil and lowest HRU slope in the subbasin. In some cases (particularly when a subbasin is already largely developed) the dominant soil in the watershed may have characteristics different from the soils and slopes of the remaining undeveloped land. For HSPF, the urban land uses are not associated with a specific soil or HSG.

In addition, a special circumstance occurs in the Willamette SWAT model. In that model, new developed land primarily comes from dense forest cover. The model tends to simulate greater evapotranspiration for urban grass than for intact evergreen forest, which appears to offset increases in total streamflow volume due to increased impervious area.

The effects of land-use change on simulated streamflow extremes can be more dramatic in basins where strong growth is expected, but also tend to be smaller than the range of simulated climate responses. For example, in the ACF basin, land-use change alone can increase the simulated 100-year flood peak by up to 27%, but the range of responses to the six NARCCAP climate scenarios is from 17 to 66%.

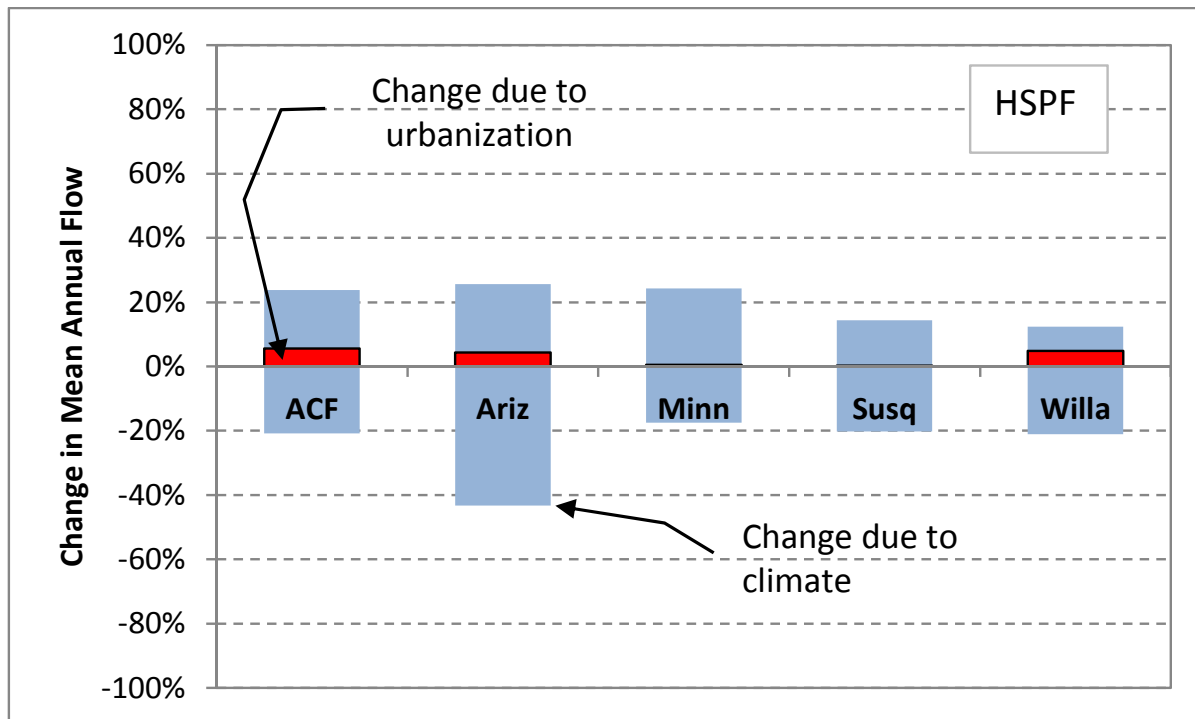


Figure 7-3. Comparison of simulated responses of mean annual streamflow to urban development and climate change scenarios—HSPF model.

Note: The blue area represents the range of responses to the six NARCCAP RCM-downscaled 2050 climate scenarios across the different HUC-8 scale reporting sites (with no change in land use). The red bars represent the maximum response to land-use change among the reporting sites (with no change in climate). Results are shown for Apalachicola River at outlet (ACF), Sat River near Roosevelt (Ariz), Minnesota River at outlet (Minn), Susquehanna River at outlet (Susq), and Willamette River at outlet (Willa).

7.5. SENSITIVITY TO COMBINED CLIMATE CHANGE AND URBAN DEVELOPMENT SCENARIOS

This section presents the results of SWAT simulations in all 20 study areas for the combined effects of mid-21st century climate change and urban and residential development scenarios. Simulation results are generally consistent with results for climate scenarios alone (presented in Section 7.2.) given the relatively small response to projected urban and residential development at the spatial scale of modeling in this study. Results are presented for selected locations in each study area in Tables 7-18 through 7-27. For study sites comprised of a single watershed, results are shown for a downstream outlet. For study sites comprised of multiple adjacent basins results are shown for a single representative basin, typically the largest. These same results for each study area are also shown as scatterplots in Figures 7-4 through 7-24, followed by maps showing the simulated median values for the six NARCCAP scenarios at the HUC-8 scale within study areas. It should be noted that use of the median values alone without taking into account the full range of simulated responses to all scenarios is potentially misleading. Median values are presented here only as an indicator of variability between study areas and should not alone be considered indicative of broad regional trends. It should also be noted that simulation results for

Kenai River in the Cook Inlet basin do not include urban and residential development scenarios. ICLUS projections are not available for the Alaska study area, but are anticipated to be small.

Table 7-17. Simulated range of responses of mean annual streamflow to mid-21st century climate and land-use change at the HUC-8 and larger spatial scale

	Climate Change Response		Land-Use Change Response	
	Minimum (%)	Maximum (%)	Minimum (%)	Maximum (%)
ACF	-45.73	24.84	0.00	0.68
Ariz	-35.29	152.52	0.00	1.48
GaFla	-39.73	69.85	0.01	7.36
Illin	-22.20	34.00	0.00	11.90
LErie	-22.89	72.13	0.00	1.84
LPont	-24.75	21.82	0.00	1.24
Minn	-23.39	85.38	0.00	0.19
Neb	-79.14	72.64	0.00	0.27
NewEng	-12.55	19.80	0.02	0.76
PowTon	-42.49	206.01	0.00	0.00
RioGra	-45.38	19.86	-0.07	0.13
Sac	-20.79	10.29	-0.03	0.47
SoCal	-26.91	62.19	-3.60	6.36
SoPlat	-53.04	59.23	-1.00	2.82
Susq	-23.80	25.79	0.00	0.23
TarNeu	-13.65	61.60	0.28	4.31
Trin	-60.57	125.65	7.09	34.91
UppCol	-20.21	22.93	-0.38	0.47
Willa	-17.51	23.21	-1.18	0.00

Note: Cook Inlet basin is not shown because ICLUS land-use change information is not available. Results based on SWAT simulations for the six NARCCAP climate change scenarios and ICLUS 2050 projected changes in developed land.

The simulated ranges of total streamflow volume changes shown in Figure 7-4 suggest several observations. The first is that increases in streamflow volume for the Kenai River (Cook Inlet basin) are on average larger than for other basins. Perhaps more importantly, for a majority of the basins the different downscaled models do not provide a consistent sign for changes in streamflow for the 2041–2070 period, with some simulating increases and some decreases. The models are in complete agreement as to the sign of change only for Kenai River (increase). It is

also worth noting that the Weather Research and Forecasting Model (WRF) downscaling of the CCSM GCM often seems to be an outlier relative to the other models.

Figure 7-5 shows the median simulated annual streamflow volume (as the median over the six NARCCAP scenarios; expressed as percent of baseline conditions) at the HUC-8 spatial scale for each study area. On this map, a neutral gray tone represents no change from current conditions (100% of current conditions). Browns indicate streamflow volumes less than current, with greater color intensity reflecting lower streamflow; blues represent flow volumes greater than current, with greater intensity reflecting higher flows. Simulated median values suggest a general trend of decreasing streamflow volume in the central Rockies, accompanied by increases in streamflow in the northern plains. Only moderate changes are seen for the west coast and Mississippi Valley, while streamflow volume generally increases on the east coast.

In addition to streamflow volume, changes in the timing and rate of streamflow can also be affected by climate change. At a national scale, the number of days to the streamflow centroid—the point at which half the streamflow volume of an average year is achieved (calculated from the October 1 start of the water year)—is a useful measure of changes in the seasonal distribution of streamflow. Figure 7-11 shows that the centroid of streamflow comes earlier in the year in model-simulated response to warmer temperatures for many of the snow-melt dominated basins, particularly Cook Inlet in Alaska and higher elevations in the Rockies, but also for many basins in the southeast. The latter result reflects changes in precipitation timing, with increased winter precipitation and decreased summer precipitation. Several of the western basins have later dates for the streamflow centroid due to a substantial increase in model-simulated spring or summer precipitation relative to winter snowpack that counteracts the effects of earlier snowmelt. Appendices X and Y provide more detailed information about seasonal shifts in streamflow timing in the study areas.

The geographic distribution of 100-year peak flows (Log-Pearson III) fit is displayed in Figure 7-9 and shows considerably more heterogeneity. Simulated peak flows increase in many basins, but show less of a clear pattern (see Figure 7-8). Peak flows tend to decline in the area of the Southwest where total streamflow volumes decline, while the greatest increases are seen in Alaska and the populated areas of the east and west coast. The increase in 100-year peak flows is generally greater (or, in some instances, the reduction less) than the change in total streamflow volume, consistent with the findings of Taner et al. (2011) for Lake Onondaga.

Results also suggest a large (factor of 5) increase in low flows for the Kenai River (see Figure 7-6). This reflects greater dry season melt rates of ice under a warmer climate in Alaska. The models also consistently show large declines in low flows for the Rio Grande Valley.

Table 7-18. Simulated total streamflow volume (climate and land-use change scenarios; percent relative to current conditions) for selected downstream stations

Station	Study area	CRCM_ cgcm3 (%)	HRM3_ hadcm3 (%)	RCM3_ gfdl (%)	GFDL_ slice (%)	RCM3_ cgcm3 (%)	WRFP_ ccsm (%)	Median (%)
Apalachicola R at outlet	ACF	107	122	108	89	124	73	108
Salt River near Roosevelt	Ariz	80	80	149	75	94	73	80
Kenai R at Soldotna	Cook	ND	154	ND	132	ND	167	154
Suwanee R at outlet	GaFla	115	154	128	93	157	75	122
Illinois R at Marseilles, IL	Illin	96	126	103	104	106	79	103
Maumee R at outlet	LErie	117	151	120	136	123	89	122
Amite R at outlet	LPont	96	111	116	85	107	78	102
Minnesota R at outlet	Minn	110	113	147	86	146	162	130
Elkhorn R at outlet	Neb	117	126	137	68	138	143	131
Merrimack R at outlet	NewEng	108	116	111	112	106	94	110
Tongue R at outlet	PowTon	101	85	140	70	130	240	115
Rio Grande R below Albuquerque	RioGra	73	69	112	66	69	84	71
Sacramento R at outlet	Sac	104	89	98	98	100	99	99
Los Angeles R at outlet	SoCal	92	140	104	103	107	85	103
S. Platte R at outlet	SoPlat	92	76	92	67	110	121	92.27
Susquehanna R at outlet	Susq	109	107	106	108	111	90	108
Neuse R at outlet	TarNeu	104	160	138	111	127	88	119
Trinity R at outlet	Trin	102	150	110	66	122	138	116
Colorado R near State Line	UppCol	86	95	116	89	92	91	91
Willamette R at outlet	Willa	116	106	104	92	114	98	105

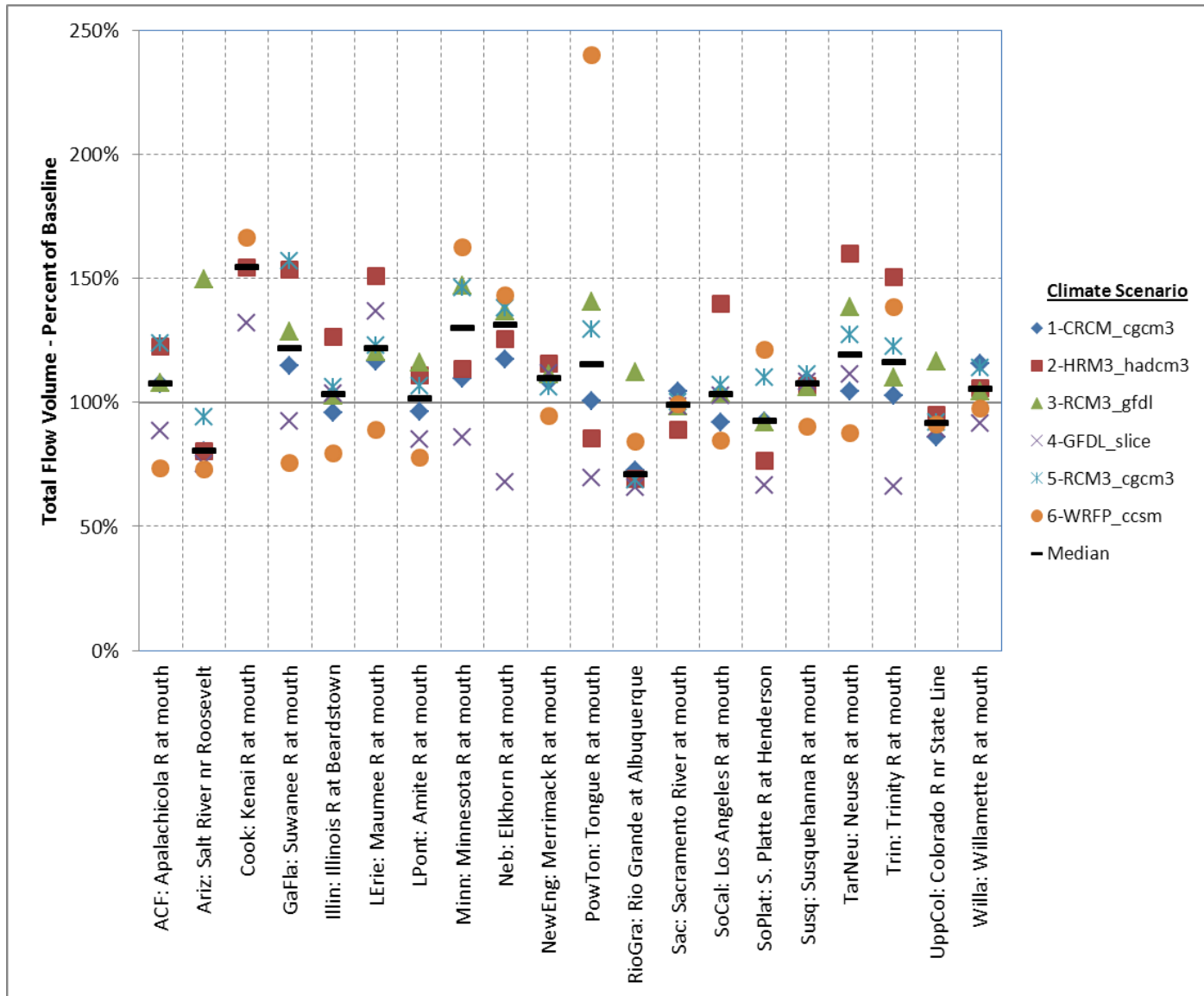


Figure 7-4. Simulated total future streamflow volume relative to current conditions (NARCCAP climate scenarios with urban development) for selected stations.

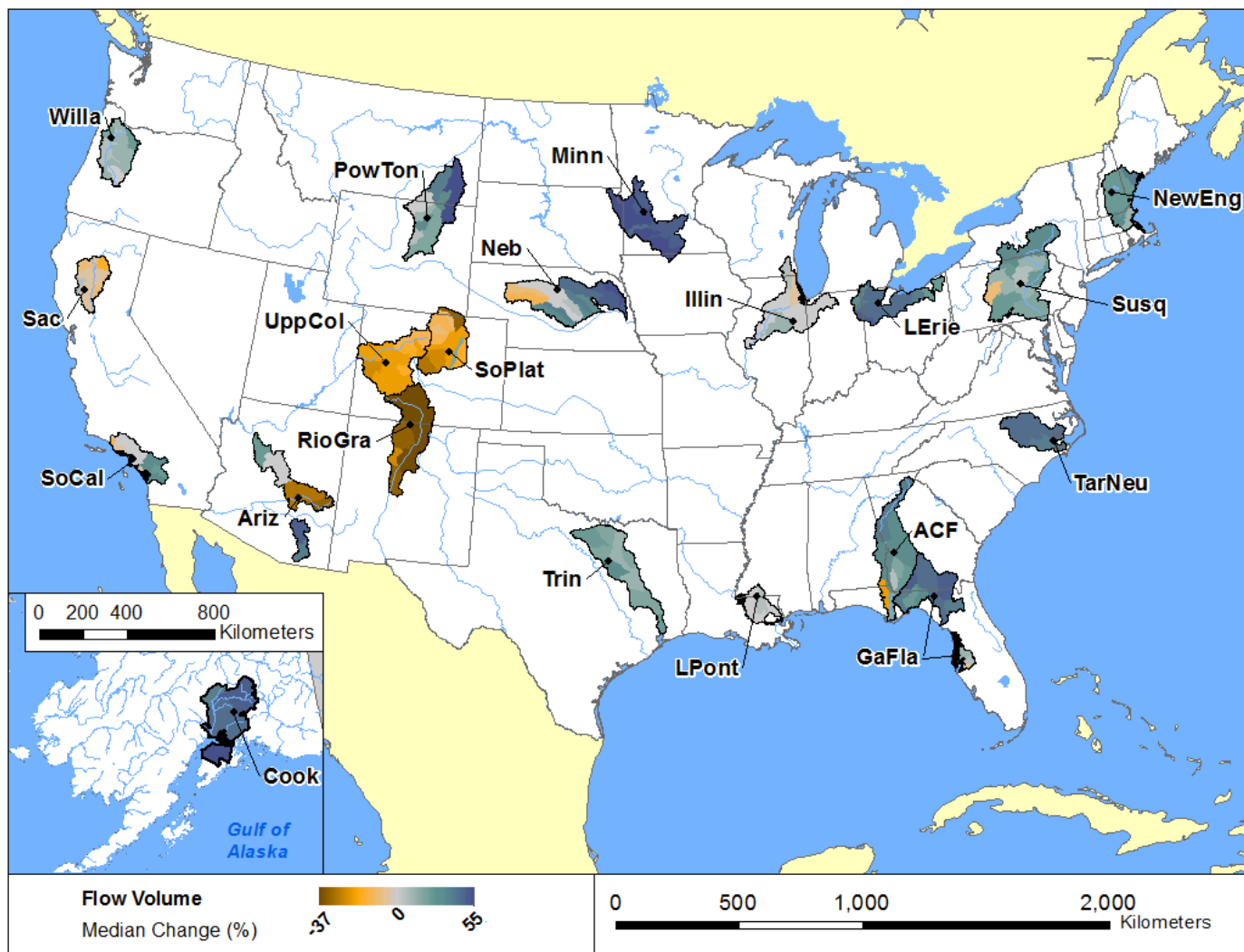


Figure 7-5. Median simulated percent changes in total future streamflow volume for six NARCCAP scenarios relative to current conditions by HUC-8 (median of NARCCAP climate scenarios with urban development).

Note: Cook Inlet results do not include land-use change.

Table 7-19. Simulated 7-day low flow (climate and land-use change scenarios; percent relative to current conditions) for selected downstream stations

Station	Study area	CRCM_ cgcm3 (%)	HRM3_ hadcm3 (%)	RCM3_ gfdl (%)	GFDL_ slice (%)	RCM3_ cgcm3 (%)	WRF_ ccsm (%)	Median (%)
Apalachicola R at outlet	ACF	98	120	105	86	113	64	101
Salt River near Roosevelt	Ariz	58	77	131	87	79	90	83
Kenai R at Soldotna	Cook	ND	267	ND	280	ND	401	280
Suwanee R at outlet	GaFla	105	141	121	95	136	78	113
Illinois R at Marseilles, IL	Illin	88	126	100	94	103	73	97
Maumee R at outlet	LErie	105	184	127	133	129	59	128
Amite R at outlet	LPont	76	108	91	77	92	64	84
Minnesota R at outlet	Minn	115	137	202	82	182	228	159
Elkhorn R at outlet	Neb	119	133	152	48	148	154	141
Merrimack R at outlet	NewEng	112	141	131	119	125	121	123
Tongue R at outlet	PowTon	102	92	145	67	127	235	115
Rio Grande R below Albuquerque	RioGra	81	64	120	62	74	86	77
Sacramento R at outlet	Sac	101	91	95	96	99	93	95
Los Angeles R at outlet	SoCal	98	115	99	100	101	93	99
S. Platte R at outlet	SoPlat	94	88	98	75	103	114	96
Susquehanna R at outlet	Susq	92	121	105	90	108	87	98
Neuse R at outlet	TarNeu	100	175	139	118	129	74	123
Trinity R at outlet	Trin	33	199	87	36	93	102	90
Colorado R near State Line	UppCol	85	94	122	86	92	91	91
Willamette R at outlet	Willa	131	113	108	82	127	102	111

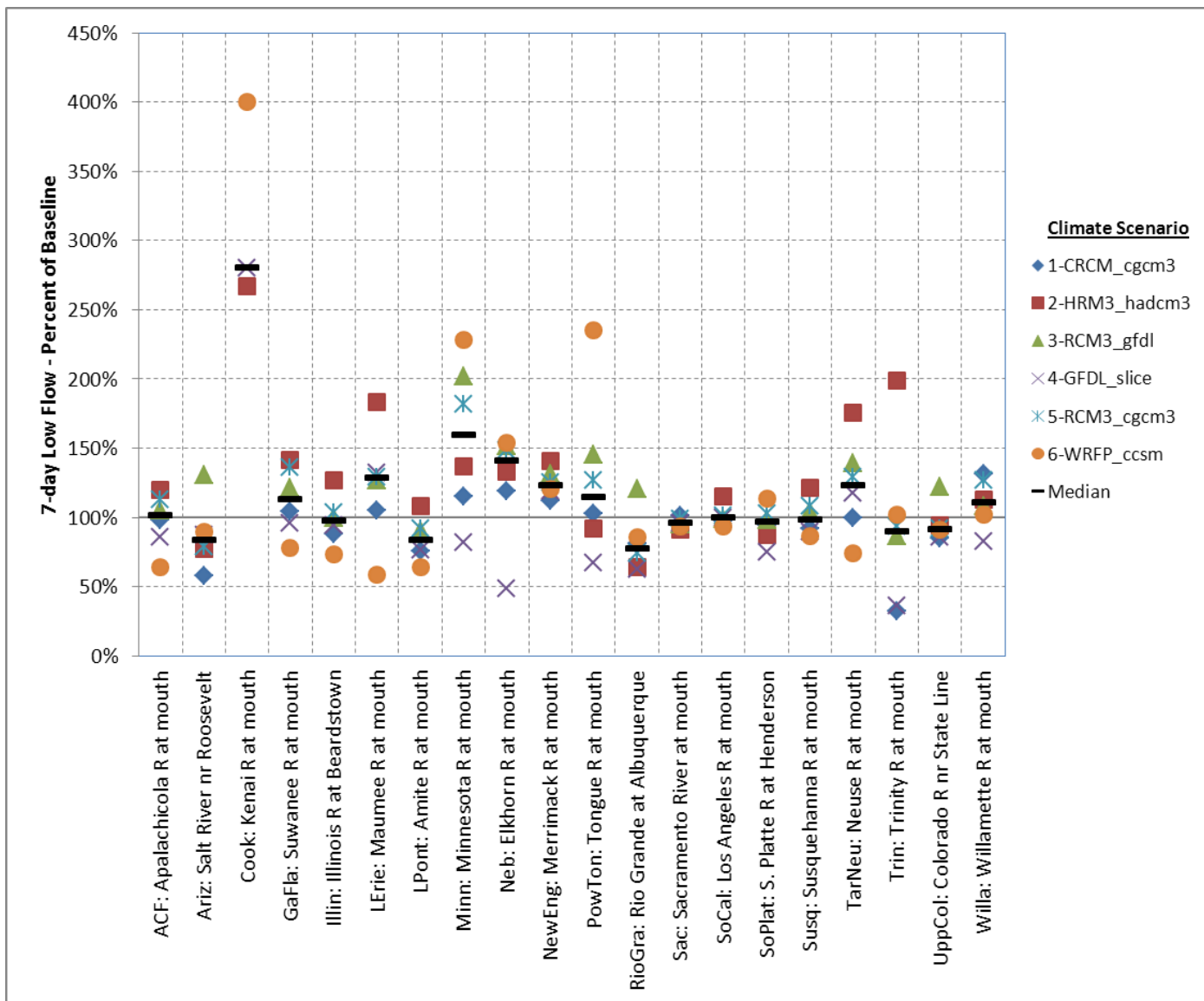


Figure 7-6. Simulated 7-day low flow relative to current conditions (NARCCAP climate scenarios with urban development) for selected downstream stations.

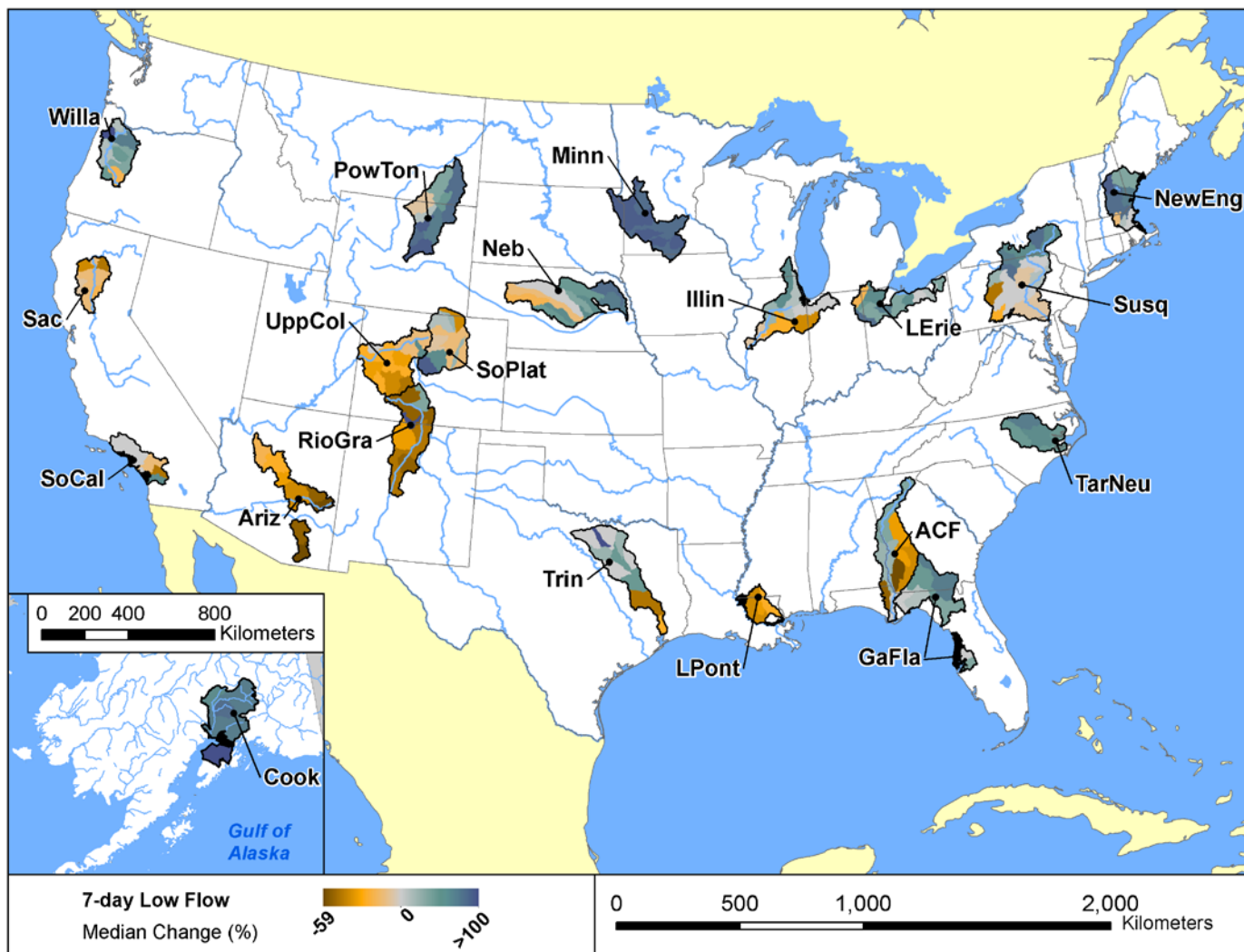


Figure 7-7. Median simulated percent changes in 7-day average low flow volume for six NARCCAP scenarios relative to current conditions by HUC-8 (median of NARCCAP climate scenarios with urban development).

Note: Cook Inlet results do not include land-use change.

Table 7-20. Simulated 100-year peak flow (log-Pearson III; climate and land-use change scenarios; percent relative to current conditions) for selected downstream stations

Station	Study area	CRCM_ cgcm3 (%)	HRM3_ hadcm3 (%)	RCM3_ gfdl (%)	GFDL_ slice (%)	RCM3_ cgcm3 (%)	WRFp_ ccsm (%)	Median (%)
Apalachicola R at outlet	ACF	117	145	110	90	128	94	114
Salt River near Roosevelt	Ariz	119	101	104	68	121	66	102
Kenai R at Soldotna	Cook	ND	132	ND	125	ND	132	132
Suwanee R at outlet	GaFla	131	145	130	95	158	107	130
Illinois R at Marseilles, IL	Illin	121	155	109	103	129	98	115
Maumee R at outlet	LErie	96	107	88	94	94	93	94
Amite R at outlet	LPont	107	152	110	100	107	66	107
Minnesota R at outlet	Minn	84	83	96	87	89	96	88
Elkhorn R at outlet	Neb	128	117	110	93	139	102	114
Merrimack R at outlet	NewEng	116	134	113	141	90	82	115
Tongue R at outlet	PowTon	118	113	133	82	121	146	119
Rio Grande R below Albuquerque	RioGra	90	77	108	66	72	92	83
Sacramento R at outlet	Sac	105	98	122	117	102	131	111
Los Angeles R at outlet	SoCal	100	112	194	124	158	93	118
S. Platte R at outlet	SoPlat	132	126	101	129	163	152	131
Susquehanna R at outlet	Susq	108	130	107	129	173	101	118
Neuse R at outlet	TarNeu	71	294	163	113	227	64	138
Trinity R at outlet	Trin	97	107	108	60	87	107	102
Colorado R near State Line	UppCol	78	83	97	91	93	84	87
Willamette R at outlet	Willa	116	131	114	79	116	95	115

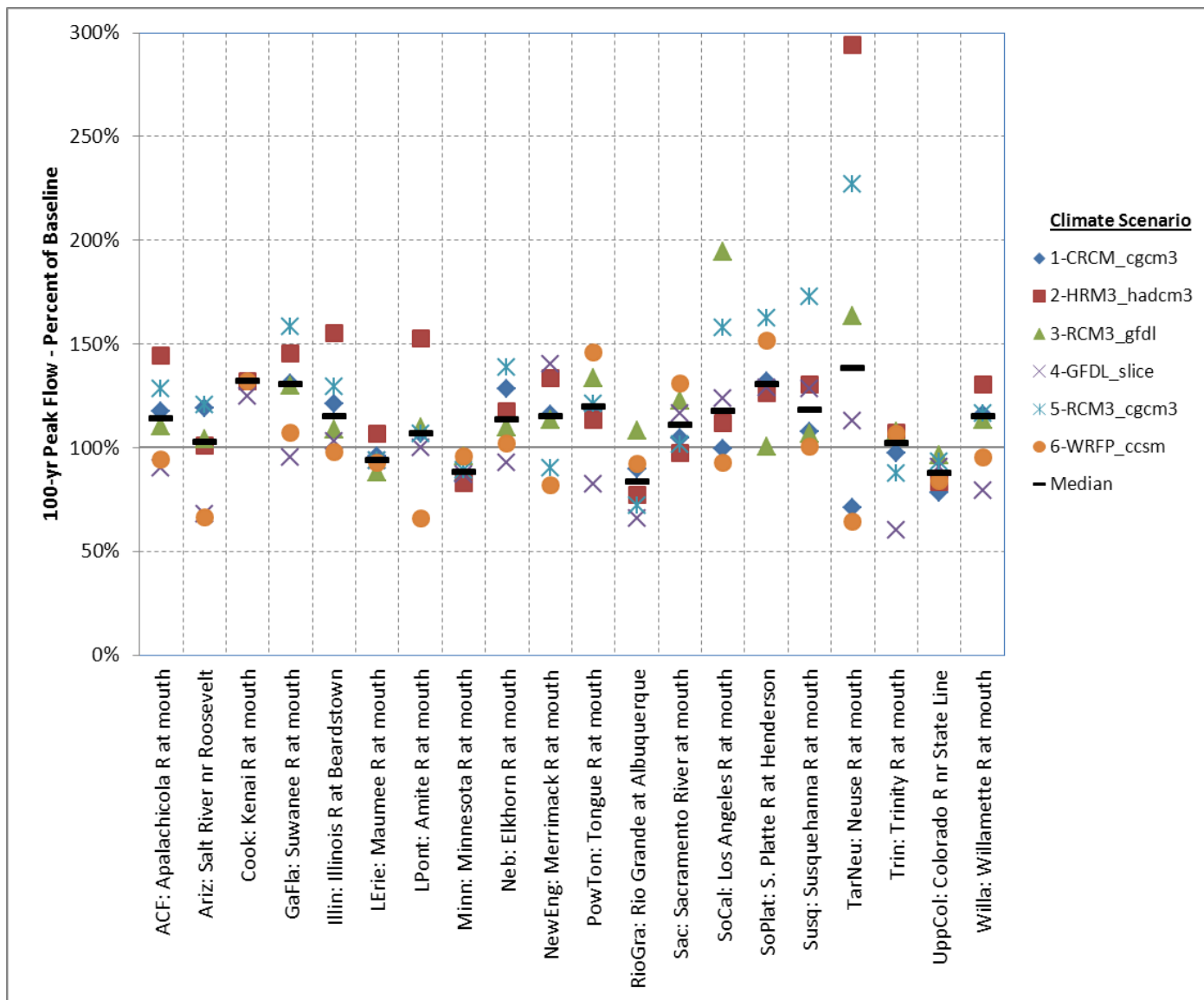


Figure 7-8. Simulated 100-year peak flow relative to current conditions (NARCCAP climate scenarios with urban development) for selected downstream stations.

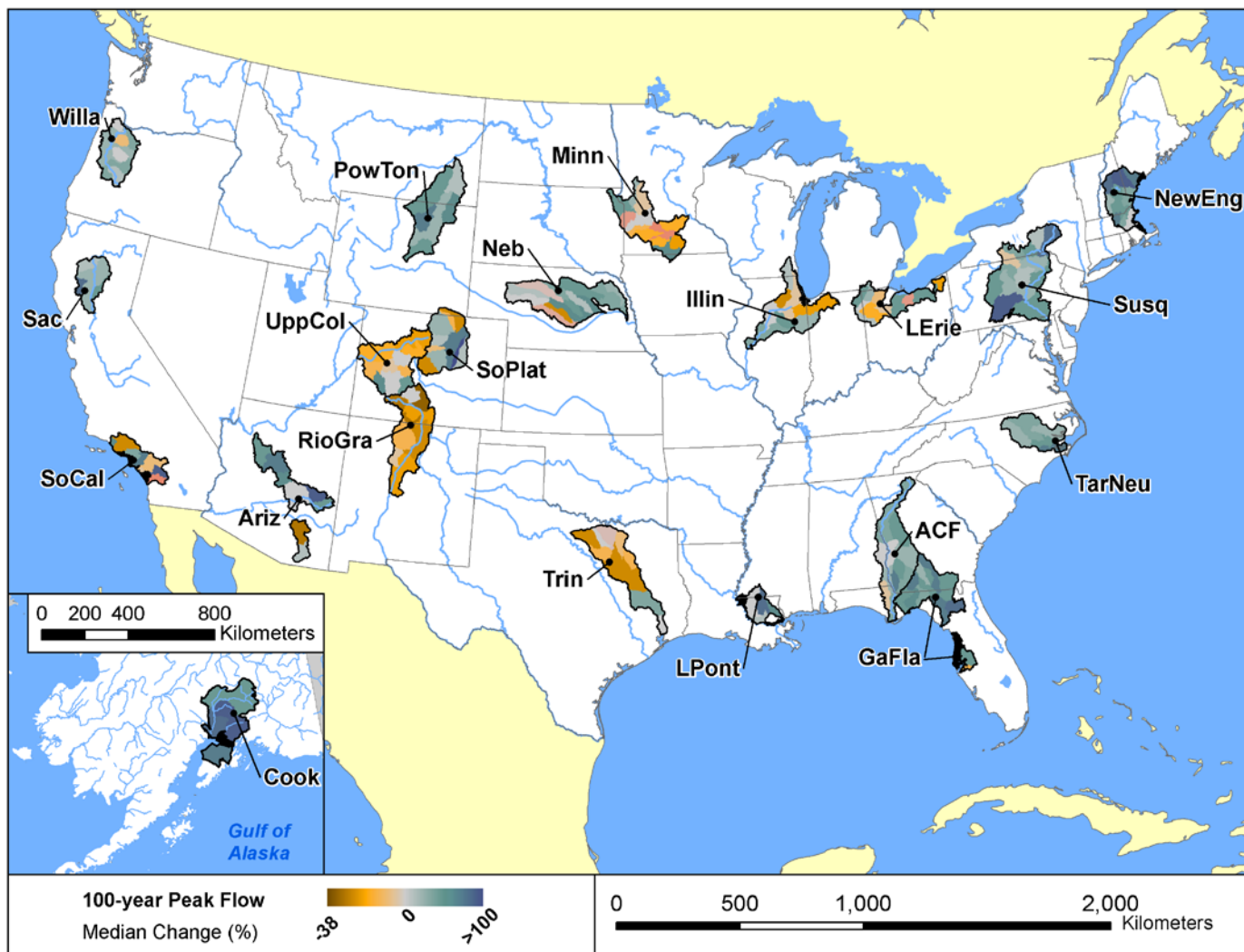


Figure 7-9. Median simulated percent changes in 100-year peak flow for six NARCCAP scenarios relative to current conditions by HUC-8 (median of NARCCAP climate scenarios with urban development).

Note: Cook Inlet results do not include land-use change.

Table 7-21. Simulated change in the number of days to streamflow centroid (climate and land-use change scenarios; relative to current conditions) for selected downstream stations

Station	Study area	CRCM_ cgcm3	HRM3_ hadcm3	RCM3_ gfdl	GFDL_ slice	RCM3_ cgcm3	WRF_ ccsm	Median
Apalachicola R at outlet	ACF	-2	-2	1	8	-6	1	-1
Salt River near Roosevelt	Ariz	-18	41	28	17	-5	54	22
Kenai R at Soldotna	Cook		-3		-5		-1	-3
Suwanee R at outlet	GaFla	-3	17	25	-8	-5	11	4
Illinois R at Marseilles, IL	Illin	-11	6	-2	-12	-1	-14	-6
Maumee R at outlet	LErie	-2	-4	1	0	10	-8	-1
Amite R at outlet	LPont	-14	14	-23	-7	-5	-11	-9
Minnesota R at outlet	Minn	-13	-19	-6	-15	-3	2	-9
Elkhorn R at outlet	Neb	-12	6	1	-15	-6	2	-2
Merrimack R at outlet	NewEng	-17	-14	-19	-13	-9	-18	-16
Tongue R at outlet	PowTon	-6	-3	1	-16	-4	7	-3
Rio Grande R below Albuquerque	RioGra	25	6	3	11	14	17	13
Sacramento R at outlet	Sac	-4	-7	-4	-1	-3	-8	-4
Los Angeles R at outlet	SoCal	6	48	-3	10	-3	0	3
S. Platte R at outlet	SoPlat	-11	-19	-13	-18	-2	-11	-12
Susquehanna R at outlet	Susq	-18	16	-6	-12	-5	0	-6
Neuse R at outlet	TarNeu	-13	23	31	-11	11	-5	3
Trinity R at outlet	Trin	17	23	31	4	7	25	20
Colorado R near State Line	UppCol	-11	-14	-7	-10	-8	-11	-10
Willamette R at outlet	Willa	3	-8	-1	3	1	8	2

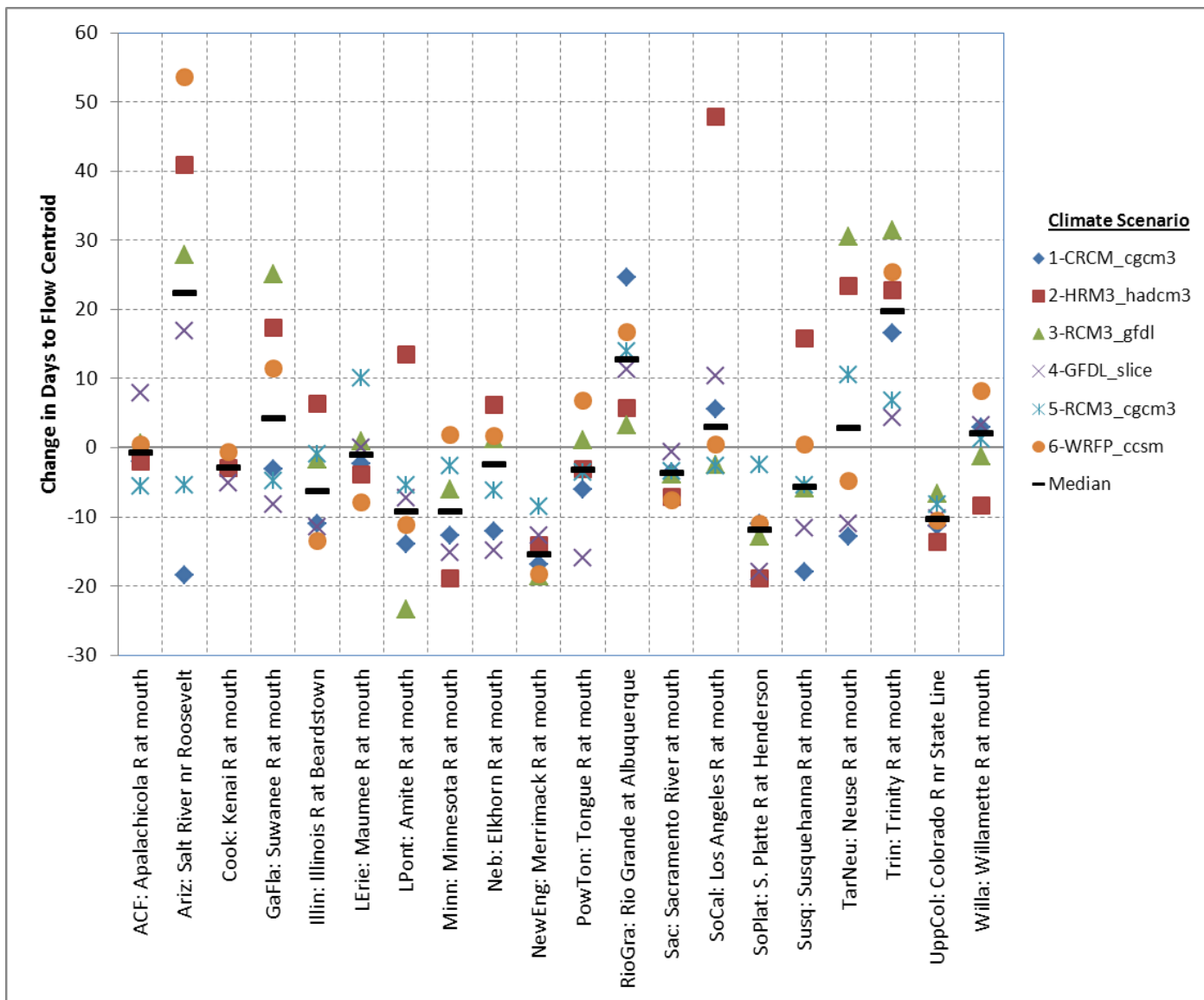


Figure 7-10. Simulated change in days to streamflow centroid relative to current conditions (NARCCAP climate scenarios with urban development) for selected downstream stations.

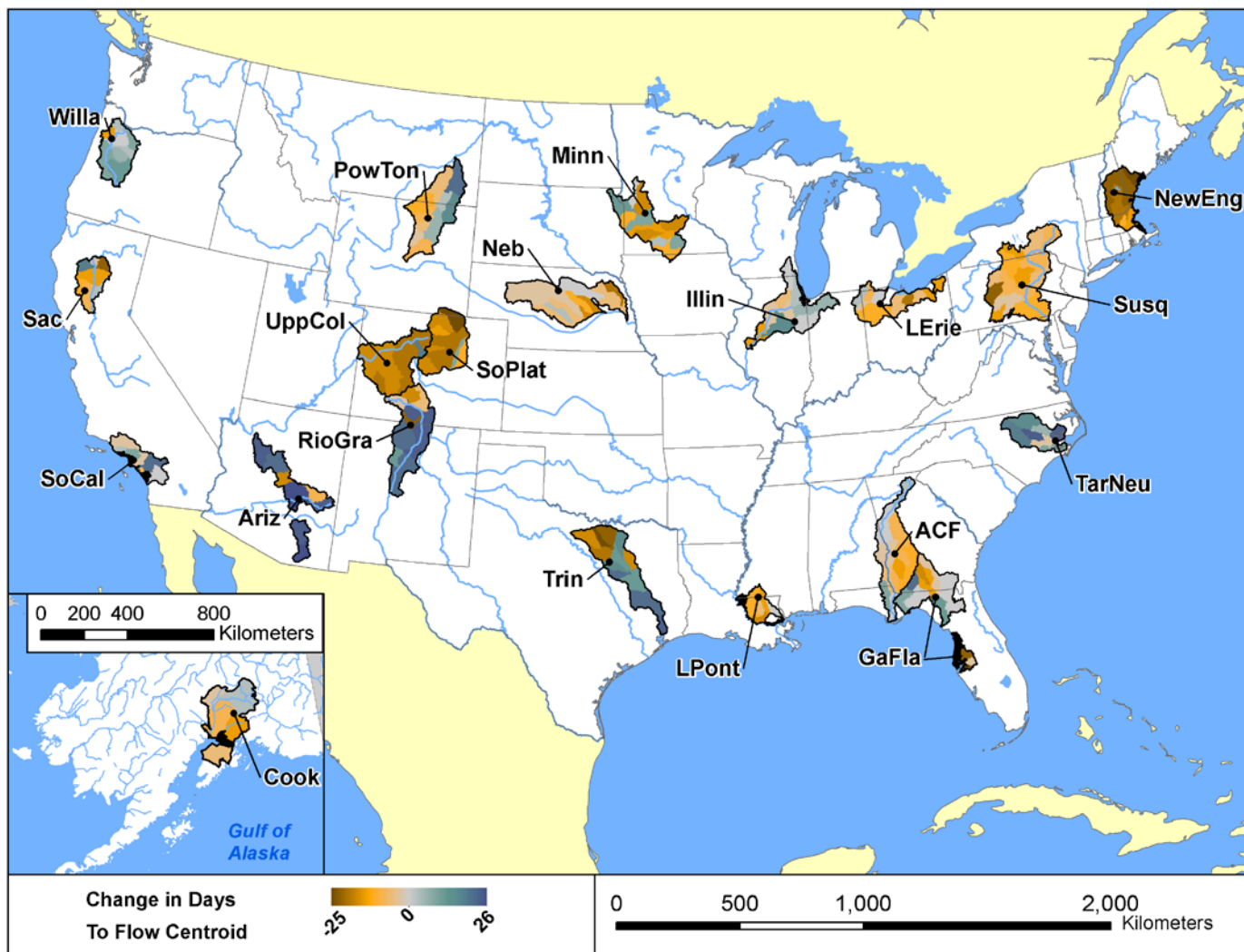


Figure 7-11. Median simulated change in the number of days to streamflow centroid for six NARCCAP scenarios relative to current conditions by HUC-8 (median of NARCCAP climate scenarios with urban development).

Note: Cook Inlet results do not include land-use change.

Table 7-22. Simulated Richards-Baker flashiness index (climate and land-use change scenarios; percent relative to current conditions) for selected downstream stations

Station	Study area	CRCM_ cgcm3 (%)	HRM3_ hadcm3 (%)	RCM3_ gfdl (%)	GFDL_ slice (%)	RCM3_ cgcm3 (%)	WRFPP_ ccsm (%)	Median (%)
Apalachicola R at outlet	ACF	106	125	109	94	126	90	107
Salt River near Roosevelt	Ariz	81	103	121	98	103	119	103
Kenai R at Soldotna	Cook	ND	94	ND	102	ND	96	96
Suwanee R at outlet	GaFla	93	62	76	116	59	185	84
Illinois R at Marseilles, IL	Illin	105	103	102	106	105	103	104
Maumee R at outlet	LErie	100	102	100	101	100	97	100
Amite R at outlet	LPont	105	105	106	104	104	102	104
Minnesota R at outlet	Minn	105	112	108	101	109	108	108
Elkhorn R at outlet	Neb	97	101	97	96	98	97	97
Merrimack R at outlet	NewEng	102	104	100	102	99	94	101
Tongue R at outlet	PowTon	102	108	104	100	103	109	104
Rio Grande R below Albuquerque	RioGra	109	117	95	120	103	106	108
Sacramento R at outlet	Sac	124	103	113	109	117	124	115
Los Angeles R at outlet	SoCal	104	125	103	105	108	104	105
S. Platte R at outlet	SoPlat	103	95	105	91	113	110	104
Susquehanna R at outlet	Susq	107	111	107	110	112	103	109
Neuse R at outlet	TarNeu	95	112	114	97	102	90	100
Trinity R at outlet	Trin	71	69	72	73	70	68	70
Colorado R near State Line	UppCol	101	107	111	105	103	101	104
Willamette R at outlet	Willa	102	105	100	98	101	102	102

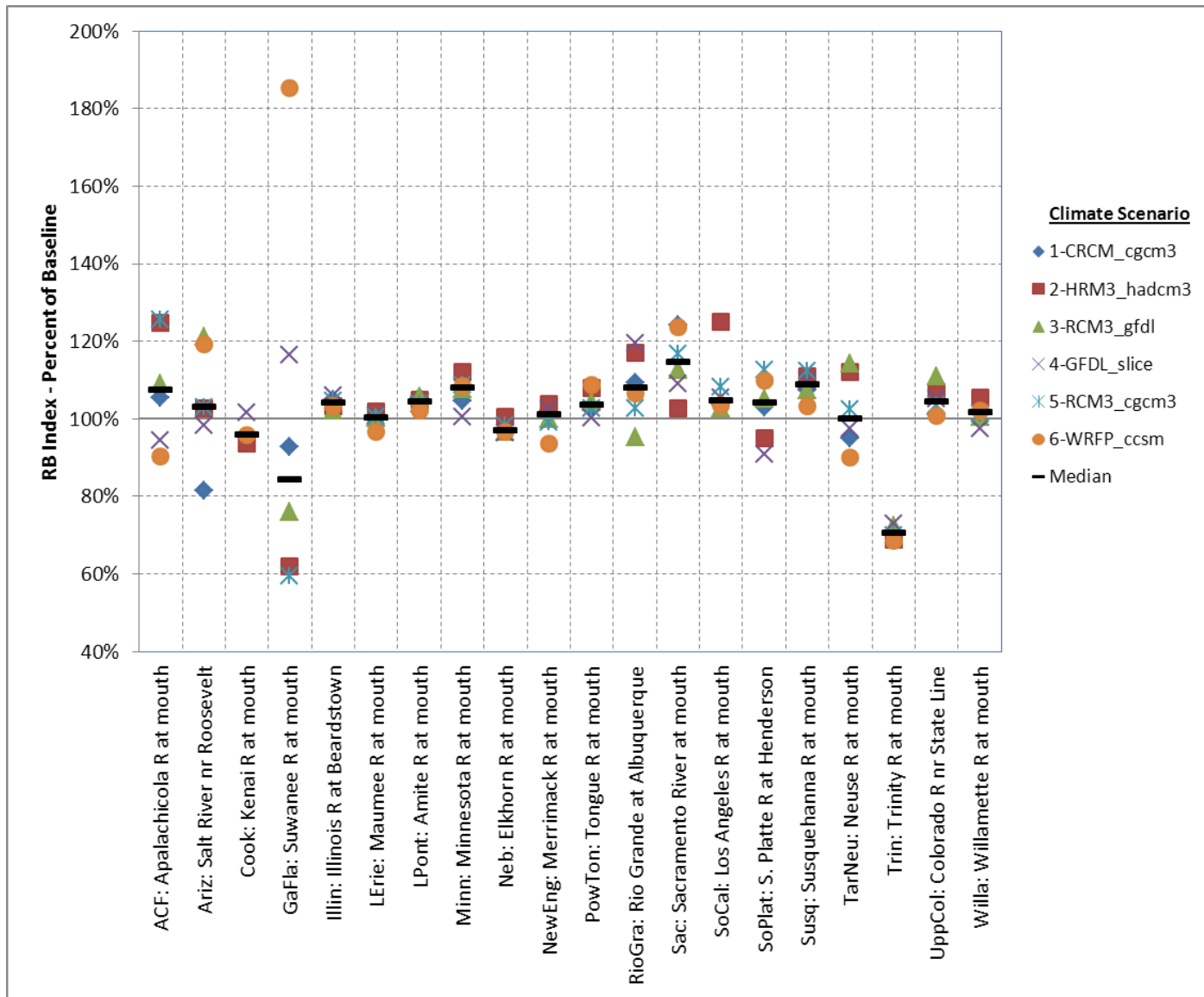


Figure 7-12. Simulated Richards-Baker flashiness index relative to current conditions (NARCCAP climate scenarios with urban development) for selected downstream stations.

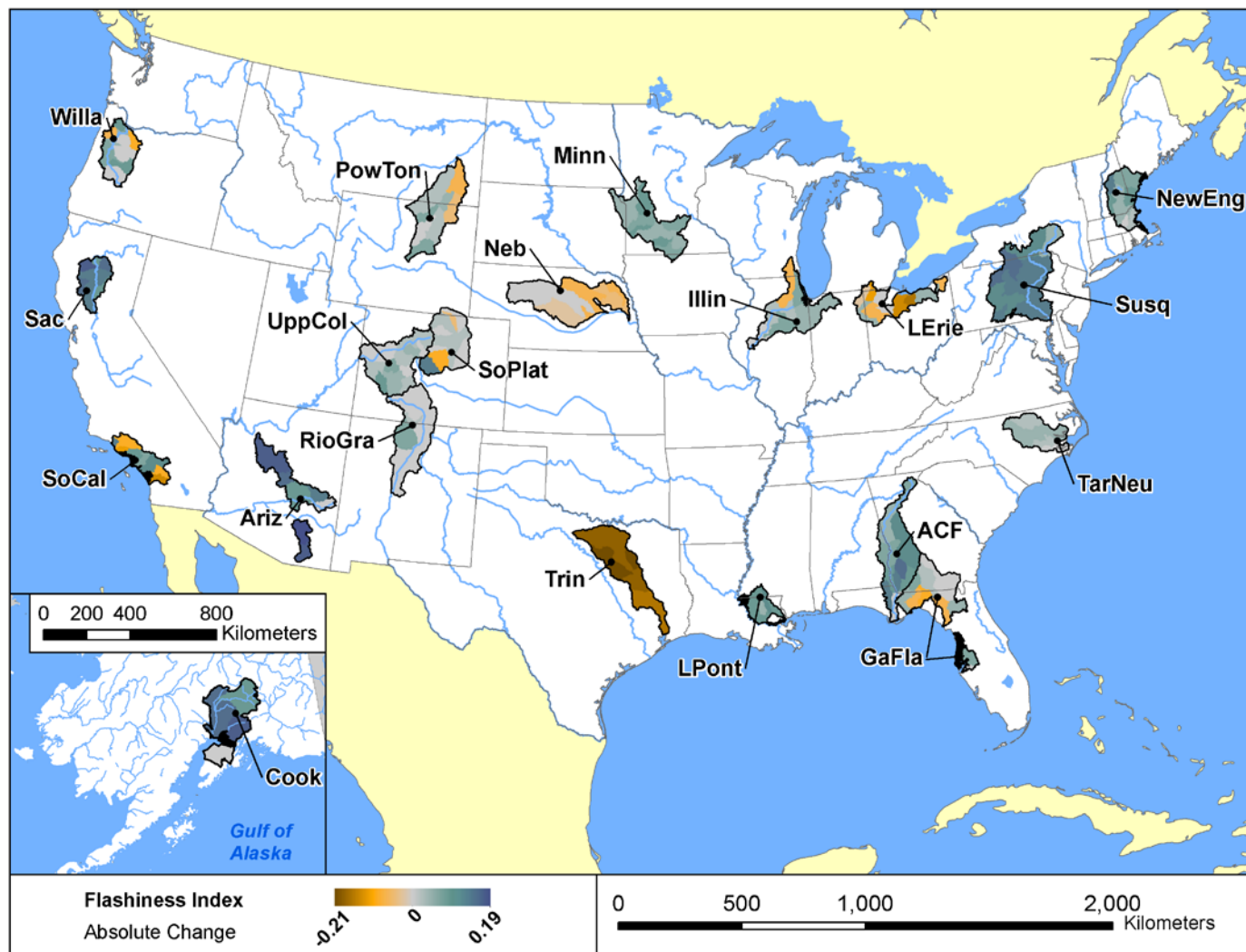


Figure 7-13. Simulated absolute changes in the Richards-Baker flashiness index for six NARCCAP scenarios relative to current conditions by HUC-8 (median of NARCCAP climate scenarios with urban development).

Note: Cook Inlet results do not include land-use change.

Regional differences also occur in the degree of agreement among simulated watershed responses to climate change scenarios. Table 7-23 shows the CV (standard deviation divided by the mean) for SWAT-simulated percentage changes in different streamflow endpoints at the downstream location of each study site for the six NARCCAP scenarios (calculated without land-use change to isolate the impacts of climate). The CV for total streamflow is large at some stations, such as Salt River and Tongue River, indicating poor model agreement on the magnitude of change. Note that CVs on total streamflow are artificially reduced at some stations (e.g., Colorado River, Sacramento River) due to the presence of constant upstream boundary conditions (representing interbasin transfers for the Colorado and releases from an upstream dam on the Sacramento River). The largest divergences among simulated high flows are seen at different stations than the largest divergences among total streamflow volume estimates.

CVs were also calculated reflecting the variability in response across the selected downstream stations for all study areas for each NARCCAP climate change scenario. Table 7-24 shows these values along with the average absolute difference from the median of all scenarios for each NARCCAP scenario. For total streamflow volume, the CCSM downscaled with WRF has both the greatest station-to-station variability (highest CV) and largest average absolute difference from the median of all six simulations.

Simulated changes in pollutant loads are shown in Tables 7-25 through 7-27, and Figures 7-14 through 7-19. Changes in projected pollutant loads are qualitatively similar to those seen for response to climate change only, but further increased in areas with significant new urban development. In general, projected changes in pollutant loads follow a pattern similar to the changes in total streamflow volume. Total suspended solids loads (see Figure 7-15) increase in most basins, except for declines in the Rocky Mountain and Southwest study areas where overall streamflow decreases. The large increases in solids loads for some basins (especially sand bed rivers in the west) are mostly driven by channel scour. These results should be considered highly uncertain given the simplified approach to channel scour included in SWAT version 2005 and the differences among individual models in calibration to channel scour. The regional pattern for total phosphorus loads is similar, as much of the total phosphorus load is driven by erosion (see Figure 7-17), with the notable exception of the Cook Inlet basin in Alaska. The regional pattern for total nitrogen loads is also generally similar, with some additional variability associated with the interactions of plant growth and erosion (see Figure 7-19).

Changes in the timing of nutrient load delivery may be even more significant for ecological impacts (c.f., Tu, 2009; Wilson and Weng, 2011; Tong et al., 2011; Marshall and Randhir, 2008). Potential ecological impacts of changes in timing of pollutant delivery simulated in the rich data set generated by this study remain to be evaluated.

7.6. WATER BALANCE INDICATORS

Several additional endpoints—identified here as water balance indicators—were calculated for each study area. Water balance indicators are defined in Section 4.3. This section presents results describing the SWAT-simulated changes in these indicators in response to the six mid-21st century NARCCAP climate change and urban development scenarios.

Table 7-28 provides a summary of water balance indicators for each study area. Figures 7-20 through 7-24 show the median values for changes in water balance metrics for simulations using

the six NARCCAP climate change scenarios at each study location. As stated previously, median values are presented here only as an indicator of variability within and among study areas and should not alone be considered indicative of broad regional trends. Appendices X and Y provide more detailed results for changes in water balance indicators including analysis at additional locations in each study area.

Table 7-23. Coefficient of variation of SWAT-simulated changes in streamflow by study area in response to the six NARCCAP climate change scenarios for selected downstream stations

Station	Study area	Total flow	100-yr peak	7-day low flow
Apalachicola R at outlet	ACF	0.038	0.037	0.043
Salt River near Roosevelt	Ariz	0.091	0.060	0.067
Kenai R at Soldotna	Cook	0.021	0.001	0.172
Suwanee R at outlet	GaFla	0.089	0.043	0.053
Illinois R at Marseilles, IL	Illin	0.023	0.039	0.033
Maumee R at outlet	LErie	0.035	0.004	0.137
Amite R at outlet	LPont	0.023	0.070	0.029
Minnesota R at outlet	Minn	0.066	0.004	0.198
Elkhorn R at outlet	Neb	0.064	0.024	0.128
Merrimack R at outlet	NewEng	0.005	0.046	0.009
Tongue R at outlet	PowTon	0.293	0.039	0.273
Rio Grande R below Albuquerque	RioGra	0.039	0.028	0.056
Sacramento R at outlet	Sac	0.003	0.016	0.001
Los Angeles R at outlet	SoCal	0.032	0.100	0.005
S. Platte R at outlet	SoPlat	0.044	0.029	0.019
Susquehanna R at outlet	Susq	0.005	0.057	0.017
Neuse R at outlet	TarNeu	0.055	0.534	0.101
Trinity R at outlet	Trin	0.079	0.036	0.378
Colorado R near State Line	UppCol	0.013	0.006	0.020
Willamette R at outlet	Willa	0.008	0.030	0.028

Table 7-24. Coefficient of variation of SWAT-simulated changes in streamflow by NARCCAP climate scenario for selected downstream stations

RCM/GCM	Total flow		100-yr peak flow		7-day low flow	
	CV	Average absolute difference from median (%)	CV	Average absolute difference from median (%)	CV	Average absolute difference from median (%)
CRCM_cgcm3	0.016	14.66	0.032	14.97	0.058	27.95
HRM3_hadcm3	0.068	15.38	0.166	19.76	0.163	23.45
RCM3_gfdl	0.026	19.54	0.035	18.52	0.073	27.32
GFDL_slice	0.049	18.37	0.048	17.56	0.264	20.10
RCM3_cgcm3	0.036	16.06	0.108	25.00	0.068	21.52
WRFp_ccsm	0.167	25.25	0.063	19.83	0.571	31.89

Table 7-25. Simulated total suspended solids load (climate and land-use change scenarios; percent relative to current conditions) for selected downstream stations

Station	Study area	CRCM_ cgcm3 (%)	HRM3_ hadcm3 (%)	RCM3_ gfdl (%)	GFDL_ slice (%)	RCM3_ cgcm3 (%)	WRF_ ccsm (%)	Median (%)
Apalachicola R at outlet	ACF	126	147	128	93	145	53	127
Salt River near Roosevelt	Ariz	89	79	184	66	106	74	84
Kenai R at Soldotna	Cook	ND	234	ND	196	ND	244	234
Suwanee R at outlet	GaFla	121	177	139	90	182	74	130
Illinois R at Marseilles, IL	Illin	117	142	115	128	121	91	119
Maumee R at outlet	LErie	123	170	127	154	130	87	128
Amite R at outlet	LPont	99	113	125	82	110	70	104
Minnesota R at outlet	Minn	104	117	183	76	192	219	150
Elkhorn R at outlet	Neb	122	131	147	60	162	162	139
Merrimack R at outlet	NewEng	119	129	119	123	112	86	119
Tongue R at outlet	PowTon	108	84	169	66	153	351	131
Rio Grande R below Albuquerque	RioGra	61	54	115	50	60	72	60
Sacramento R at outlet	Sac	138	94	121	118	99	108	113
Los Angeles R at outlet	SoCal	75	121	86	85	90	69	86
S. Platte R at outlet	SoPlat	95	91	98	84	104	108	97
Susquehanna R at outlet	Susq	118	108	109	116	118	85	112
Neuse R at outlet	TarNeu	108	201	164	117	145	84	131
Trinity R at outlet	Trin	64	126	64	28	85	115	74
Colorado R near State Line	UppCol	80	90	124	82	89	85	87
Willamette R at outlet	Willa	124	111	108	89	121	97	110

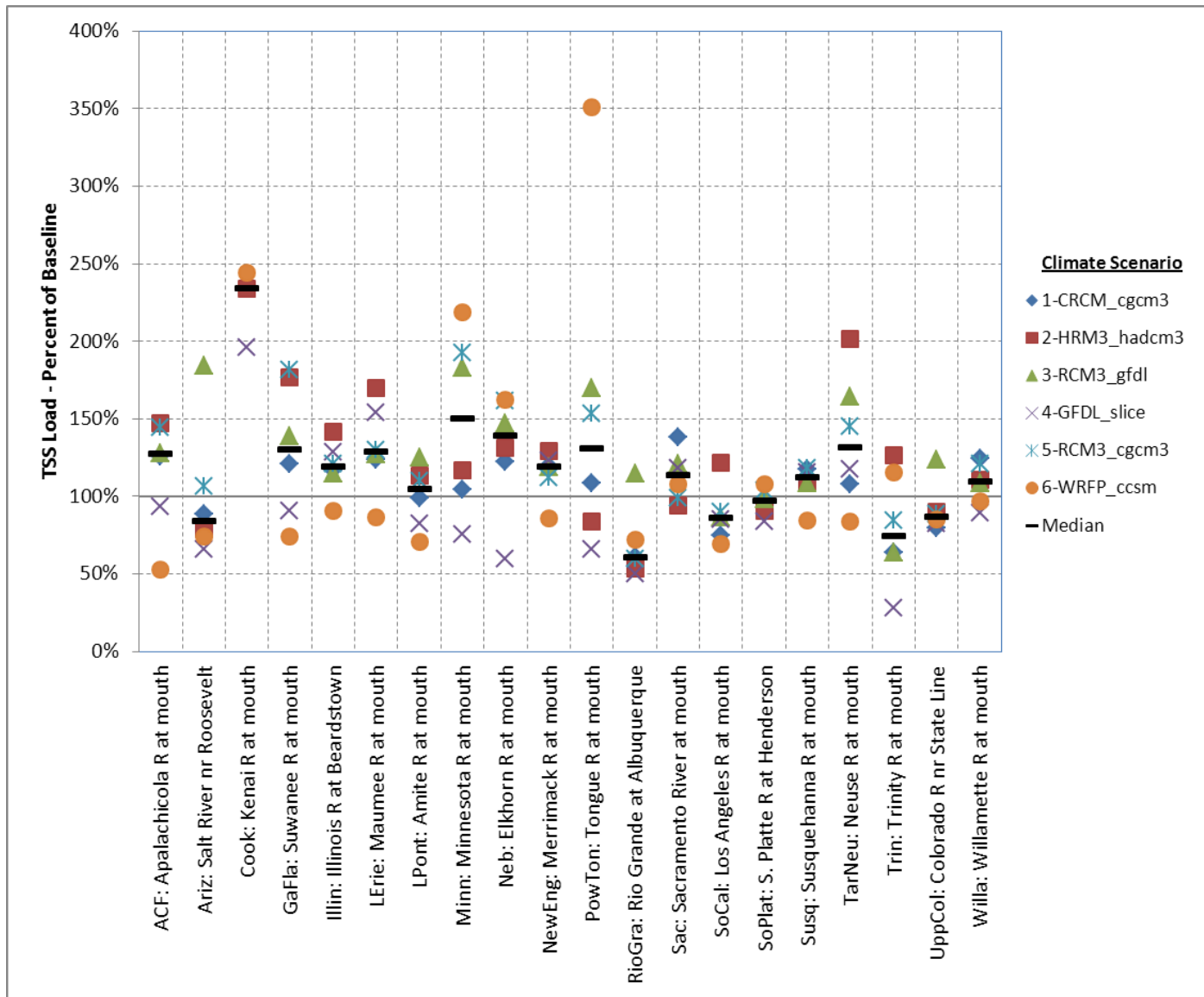


Figure 7-14. Simulated total suspended solids load relative to current conditions (NARCCAP climate scenarios with urban development) for selected downstream stations.

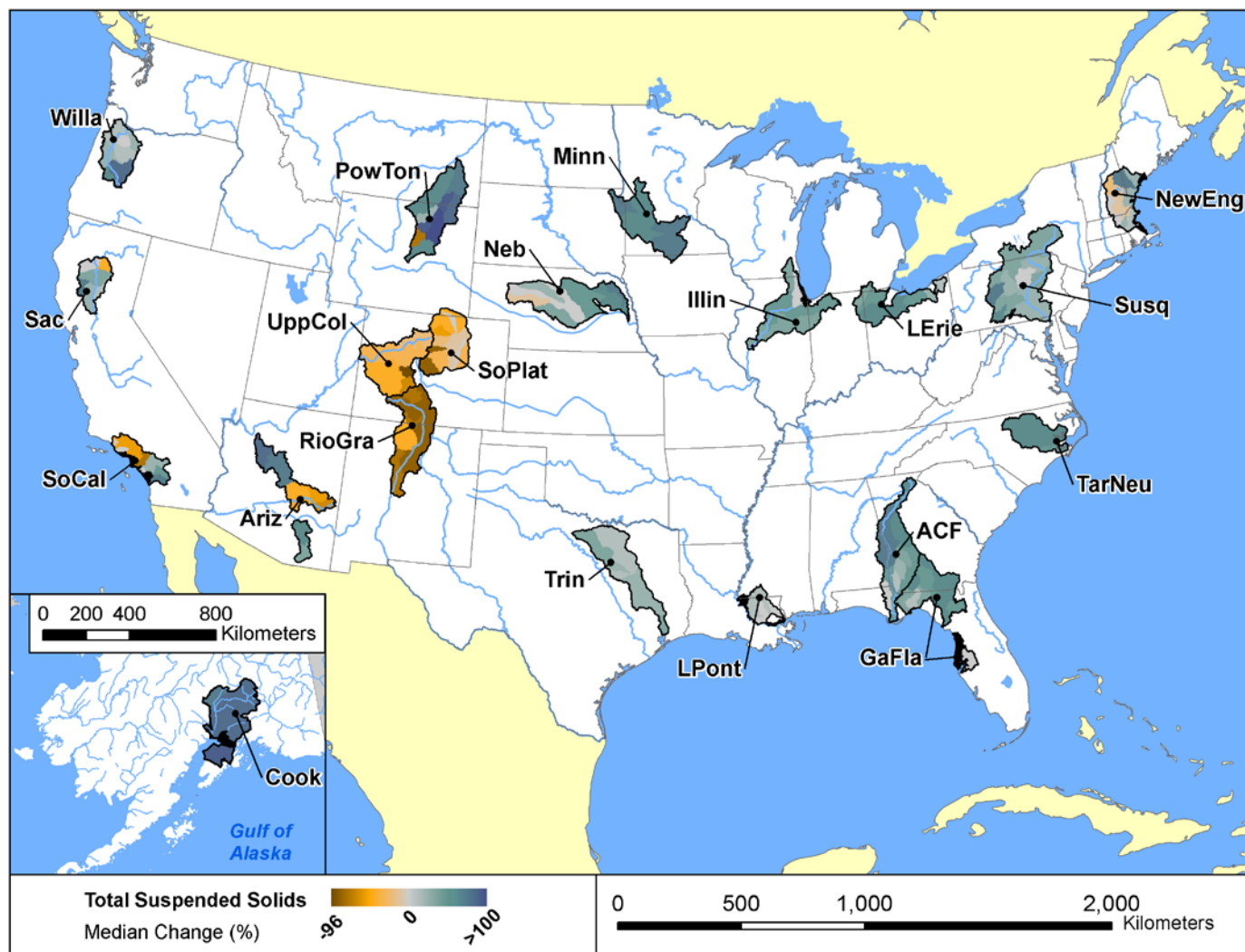


Figure 7-15. Median simulated percent changes in total suspended solids loads for six NARCCAP scenarios relative to current conditions by HUC-8 (median of NARCCAP climate scenarios with urban development) for selected downstream stations.

Note: Cook Inlet results do not include land-use change.

Table 7-26. Simulated total phosphorus load (climate and land-use change scenarios; percent relative to current conditions) for selected downstream stations

Station	Study area	CRCM_ cgcm3 (%)	HRM3_ hadcm3 (%)	RCM3_ gfdl (%)	GFDL_ slice (%)	RCM3_ cgcm3 (%)	WRF_ ccsm (%)	Median (%)
Apalachicola R at outlet	ACF	139	153	136	119	150	107	138
Salt River near Roosevelt	Ariz	82	84	156	70	107	88	86
Kenai R at Soldotna	Cook	ND	89	ND	90	ND	113	90
Suwanee R at outlet	GaFla	125	190	149	96	189	82	137
Illinois R at Marseilles, IL	Illin	107	112	107	113	108	99	107
Maumee R at outlet	LErie	121	155	136	151	120	89	128
Amite R at outlet	LPont	123	144	147	103	125	89	124
Minnesota R at outlet	Minn	97	115	151	97	138	160	126
Elkhorn R at outlet	Neb	118	124	138	65	145	148	131
Merrimack R at outlet	NewEng	116	125	116	120	111	97	116
Tongue R at outlet	PowTon	107	86	163	67	148	324	127
Rio Grande R below Albuquerque	RioGra	51	40	125	49	37	64	50
Sacramento R at outlet	Sac	102	88	106	117	97	110	104
Los Angeles R at outlet	SoCal	78	128	102	83	89	71	86
S. Platte R at outlet	SoPlat	93	81	104	75	113	115	99
Susquehanna R at outlet	Susq	128	106	110	127	114	108	112
Neuse R at outlet	TarNeu	123	259	184	134	183	103	158
Trinity R at outlet	Trin	148	188	153	98	155	187	154
Colorado R near State Line	UppCol	80	88	120	82	84	84	84
Willamette R at outlet	Willa	100	98	97	94	100	96	97

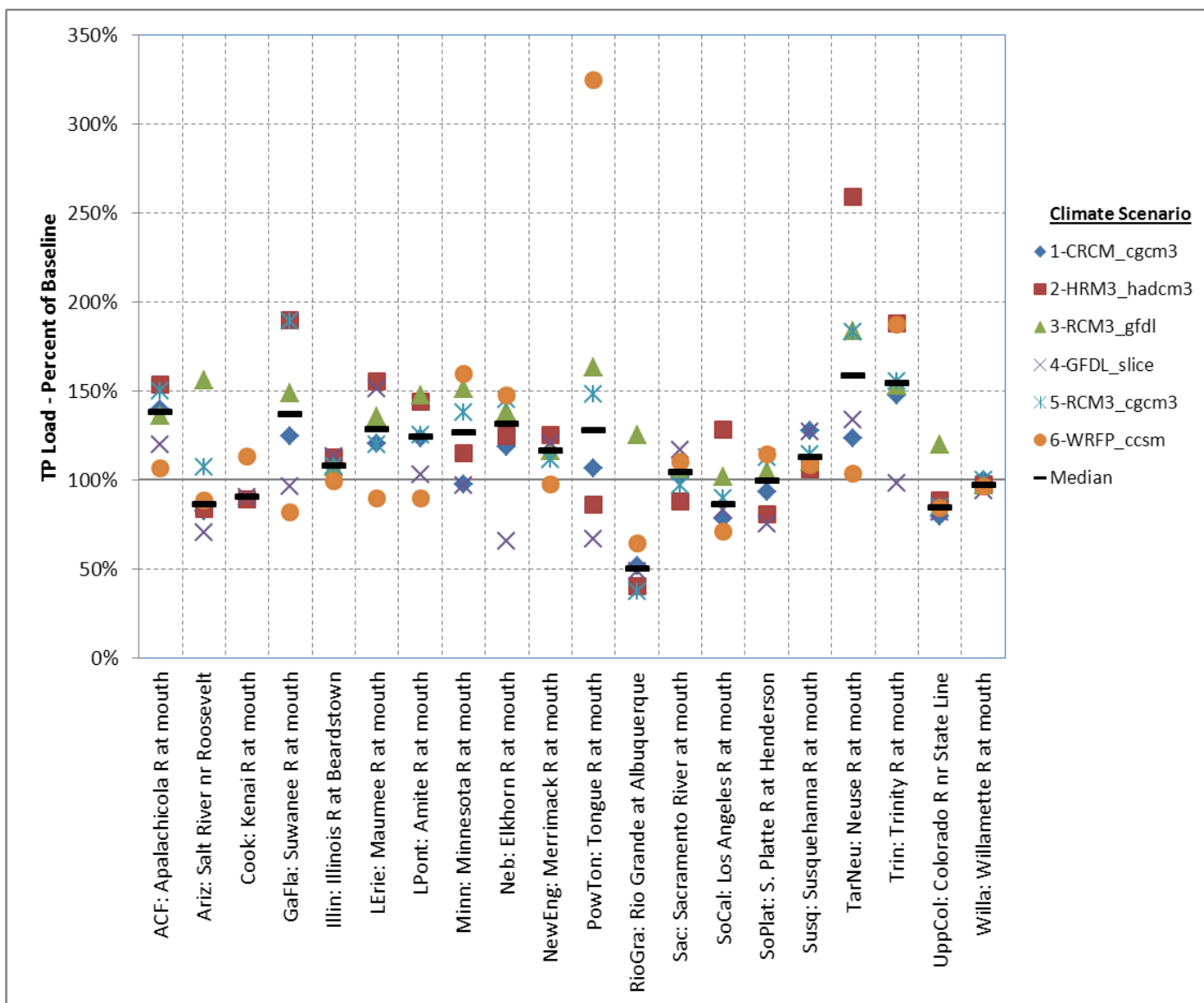


Figure 7-16. Simulated total phosphorus load relative to current conditions (NARCCAP climate scenarios with urban development) for selected downstream stations.

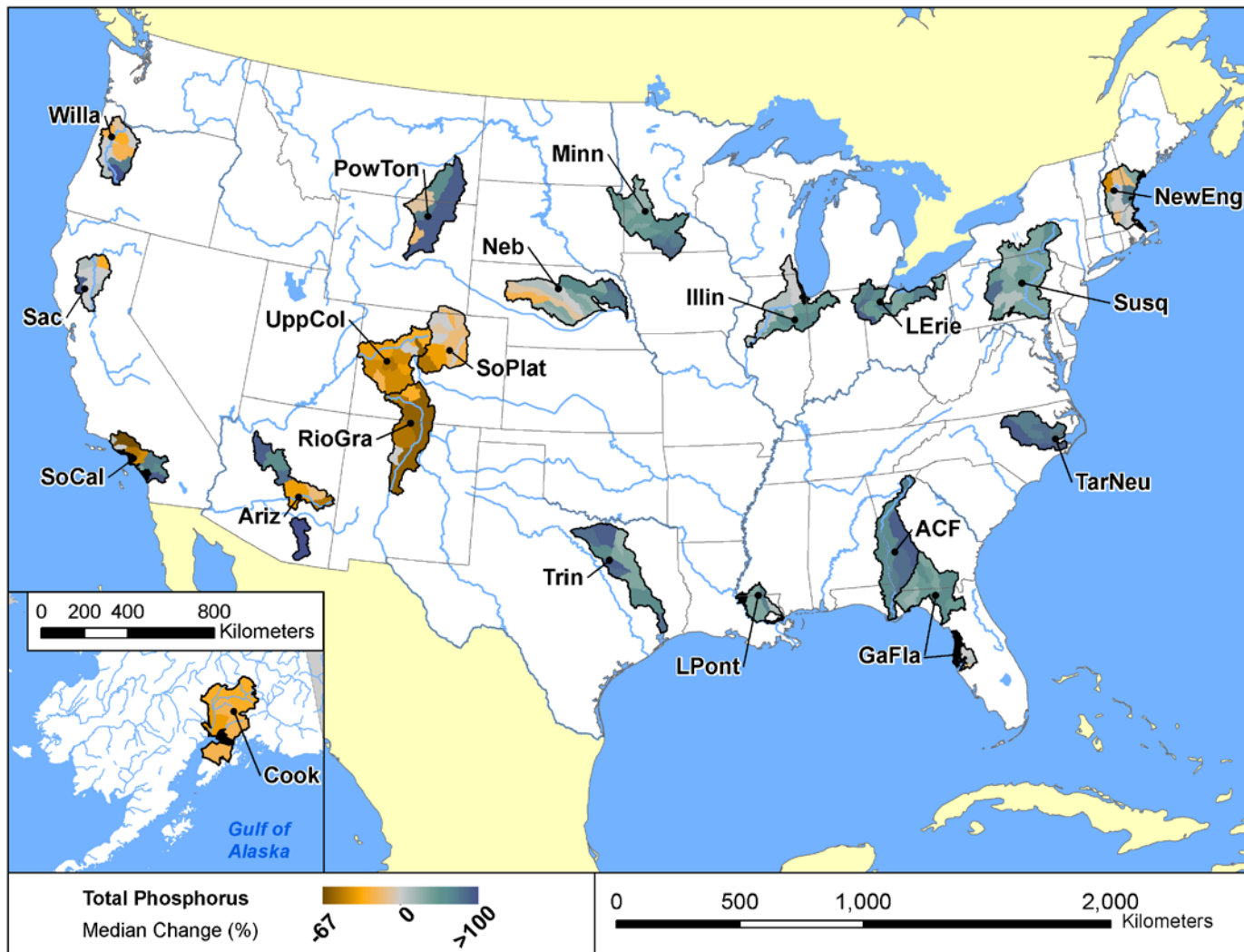


Figure 7-17. Median simulated percent changes in total phosphorus loads for six NARCCAP scenarios relative to current conditions by HUC-8 (median of NARCCAP climate scenarios with urban development).

Note: Cook Inlet results do not include land-use change.

Table 7-27. Simulated total nitrogen load (climate and land-use change scenarios; percent relative to current conditions) for selected downstream stations

Station	Study area	CRCM_egcm3 (%)	HRM3_hadcm3 (%)	RCM3_gfdl (%)	GFDL_slice (%)	RCM3_egcm3 (%)	WRFPP_ccsm (%)	Median (%)
Apalachicola R at outlet	ACF	117	126	116	107	123	96	117
Salt River near Roosevelt	Ariz	90	91	142	87	105	85	91
Kenai R at Soldotna	Cook	ND	200	ND	175	ND	223	200
Suwanee R at outlet	GaFla	129	167	139	113	171	86	134
Illinois R at Marseilles, IL	Illin	103	117	105	109	107	93	106
Maumee R at outlet	LErie	127	158	161	190	125	94	142
Amite R at outlet	LPont	130	152	153	113	127	95	128
Minnesota R at outlet	Minn	126	130	163	104	158	170	144
Elkhorn R at outlet	Neb	93	97	145	88	104	107	100
Merrimack R at outlet	NewEng	123	131	121	124	116	103	122
Tongue R at outlet	PowTon	109	91	165	71	148	320	128
Rio Grande R below Albuquerque	RioGra	50	38	127	48	37	65	49
Sacramento R at outlet	Sac	104	94	105	113	103	111	104
Los Angeles R at outlet	SoCal	125	159	154	102	96	101	113
S. Platte R at outlet	SoPlat	89	72	95	65	112	120	92
Susquehanna R at outlet	Susq	161	146	146	155	149	131	147
Neuse R at outlet	TarNeu	120	207	166	125	155	105	140
Trinity R at outlet	Trin	140	187	142	93	153	186	148
Colorado R near State Line	UppCol	73	82	111	76	80	79	80
Willamette R at outlet	Willa	106	98	97	91	105	95	97

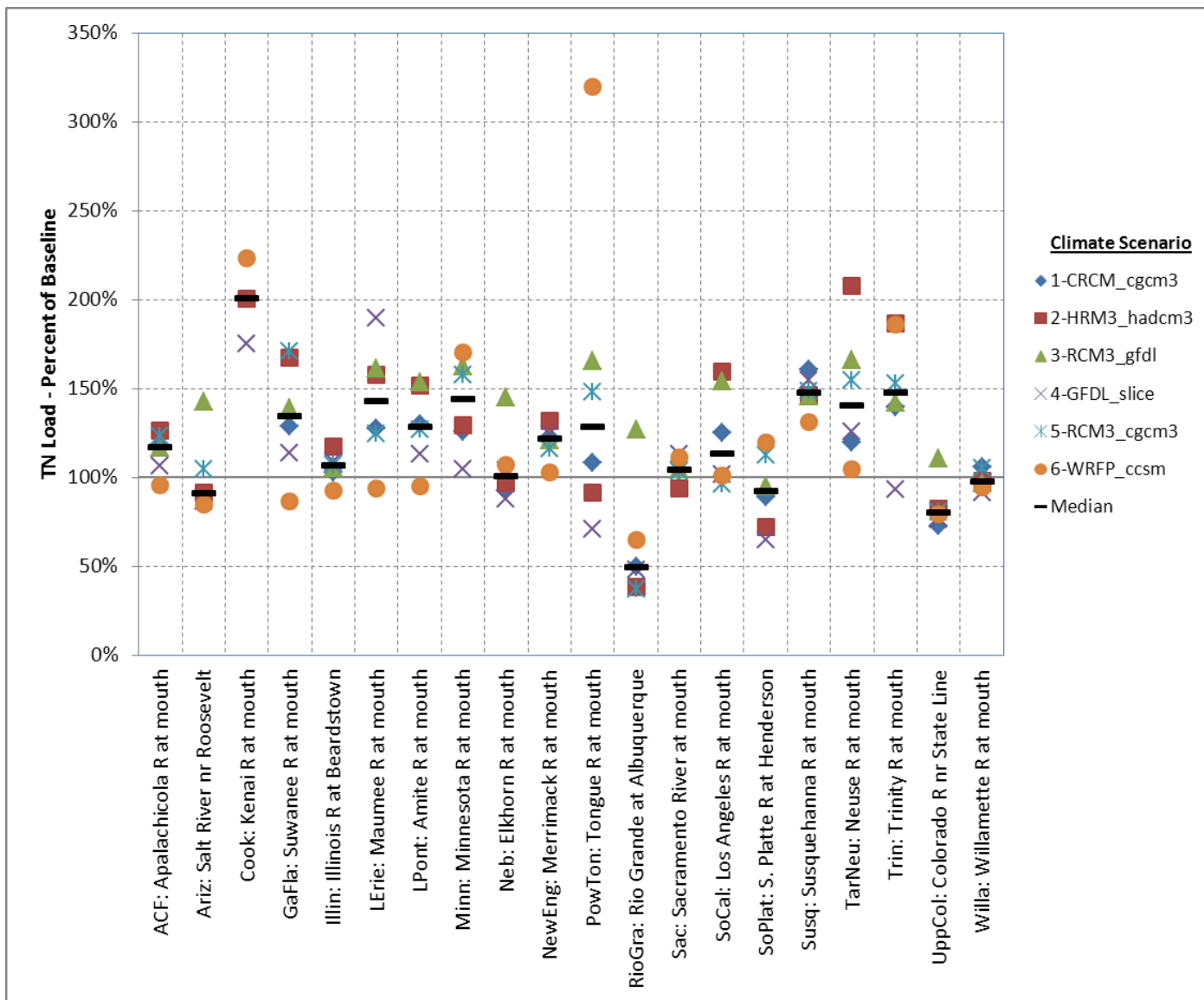


Figure 7-18. Simulated total nitrogen load relative to current conditions (NARCCAP climate scenarios with urban development) for selected downstream stations.

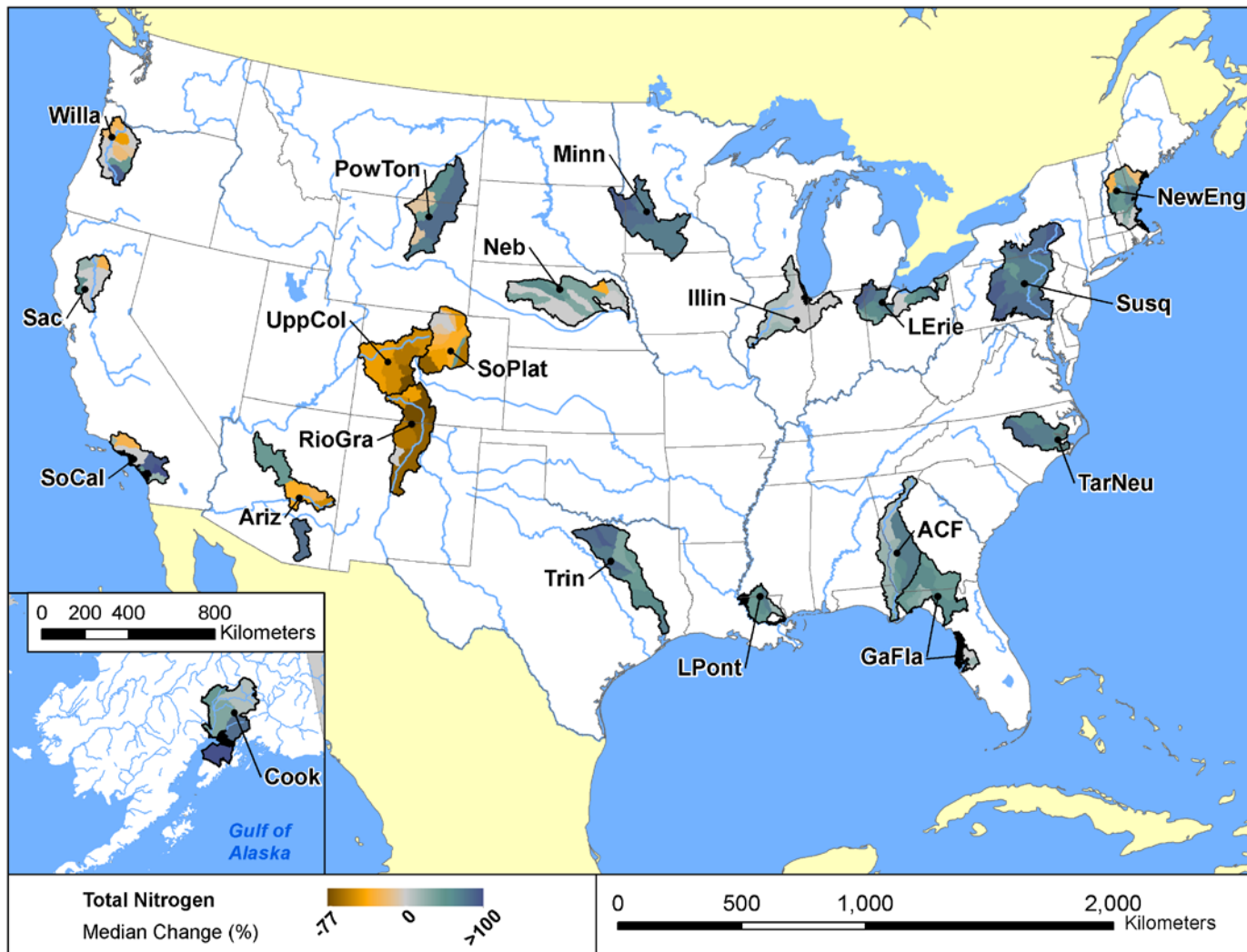


Figure 7-19. Median simulated percent changes in total nitrogen loads for six NARCCAP scenarios relative to current conditions by HUC-8 (median of NARCCAP climate scenarios with urban development).

Note: Cook Inlet results do not include land-use change.

Table 7-28. Simulated percent changes in water balance statistics for study areas (NARCCAP climate with land-use change scenarios; median percent change relative to current conditions)

Study Area	Dryness Ratio (fraction of precipitation lost to ET) (%)	Low Flow Sensitivity (baseflow generation, cfs/mi²) (%)	Surface Runoff Fraction of Flow (%)	Snowmelt Fraction of Flow (%)	Deep Recharge Rate (depth) (%)
ACF	0	-16	22	-57	-14
Ariz-Salt	1	-10	-5	-46	-15
Ariz-San Pedro	-1	-7	23	-52	-12
Ariz-Verde	-2	-3	7	-50	4
Cook	-8	22	4	-12	-43
GaFla-North	-10	47	-8	-32	39
GaFla-Tampa	-6	8	11	-72	7
Illin	-1	-7	15	-39	-6
LErie	-3	22	-4	-32	20
LPont	-10	59	-14	-22	47
Minn	-5	28	49	-24	24
Neb-Elkhorn	0	3	16	-24	1
Neb-Loup	-3	12	-1	-33	13
NewEng	-1	-6	1	-82	-5
PowTon-Powder	-7	18	-1	-18	NA
PowTon-Tongue	-6	5	6	-17	-8
RioGra	2	-28	3	-1	-28
Sac	0	-4	4	-45	-6
SoCal	-2	-5	7	-54	1
SoPlat	-1	-6	1	-17	NA
Susq	0	-6	16	-31	-5
TarNeu	-8	15	5	-49	15
Trin	-4	-1	2	-43	0
UppCol	1	-8	-4	-15	-16
Willa	-11	5	1	-68	6

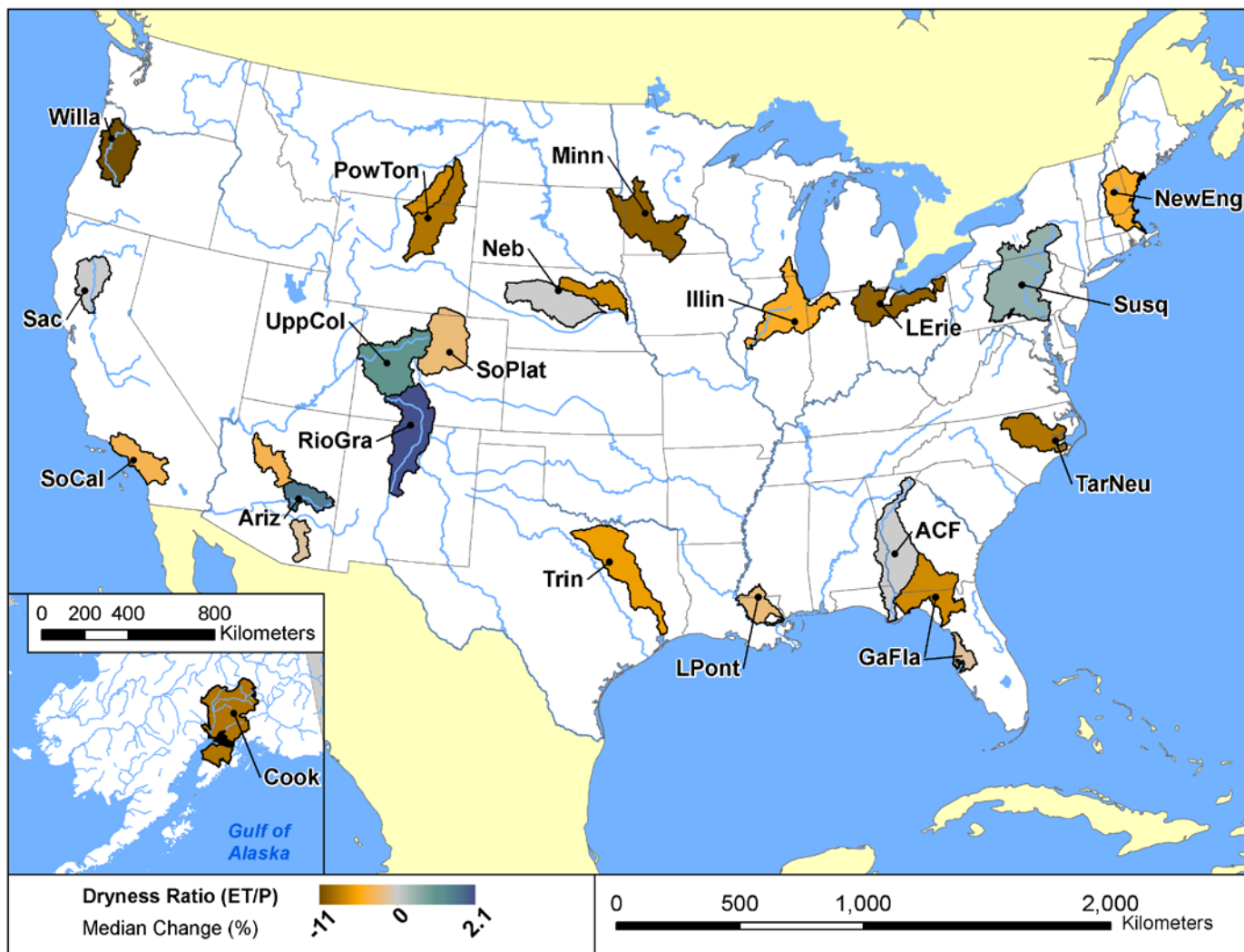


Figure 7-20. Median simulated percent changes in watershed Dryness Ratio for six NARCCAP scenarios relative to current conditions (median of NARCCAP climate scenarios with urban development).

Note: Dryness ratio is the fraction of input precipitation lost to ET. Cook Inlet results do not include land-use change.

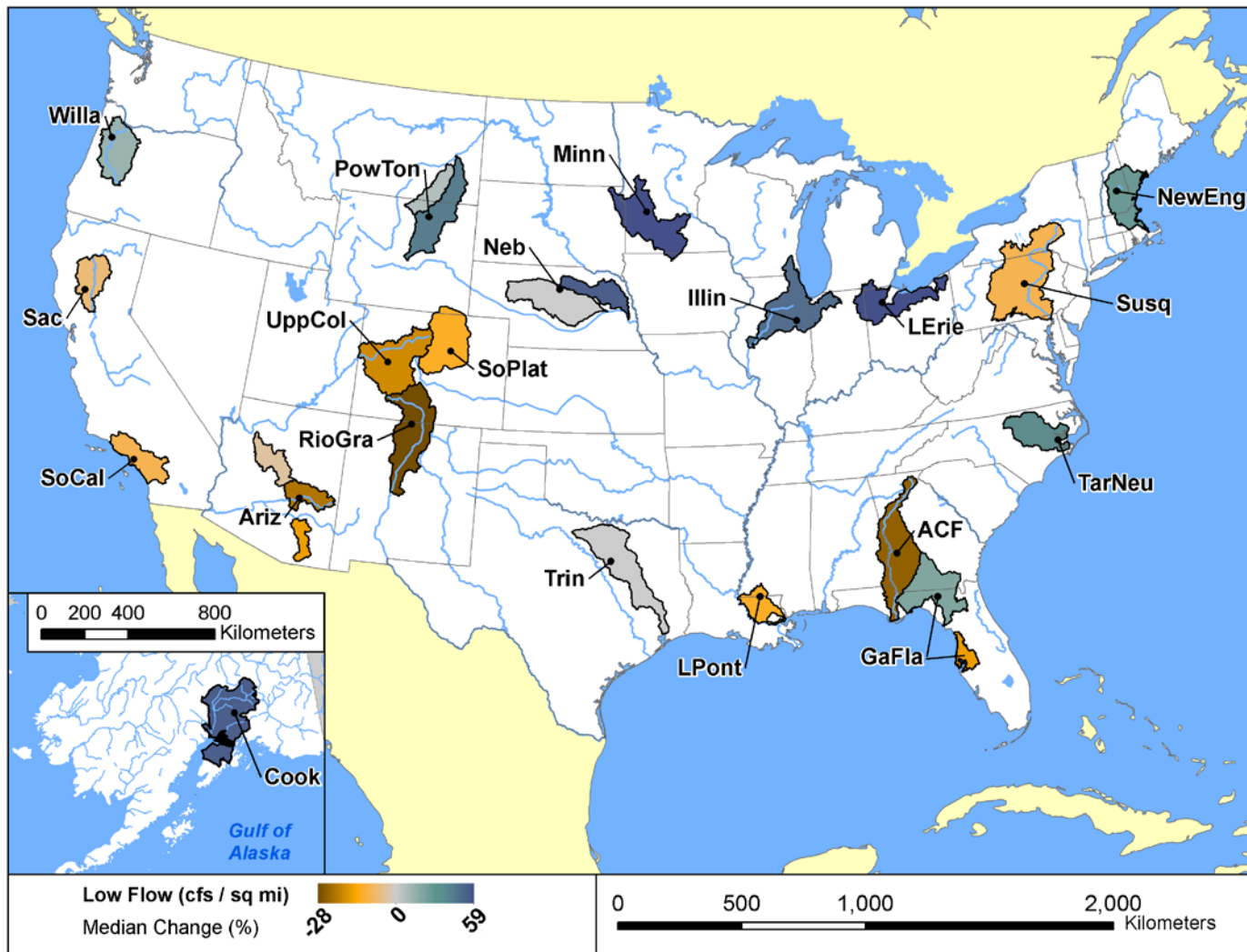


Figure 7-21. Median simulated percent changes in watershed Low Flow Sensitivity for six NARCCAP scenarios relative to current conditions (median of NARCCAP climate scenarios with urban development).

Note: Low Flow Sensitivity is the rate of streamflow generation by baseflow (cfs/mi²). Cook Inlet results do not include land-use change.

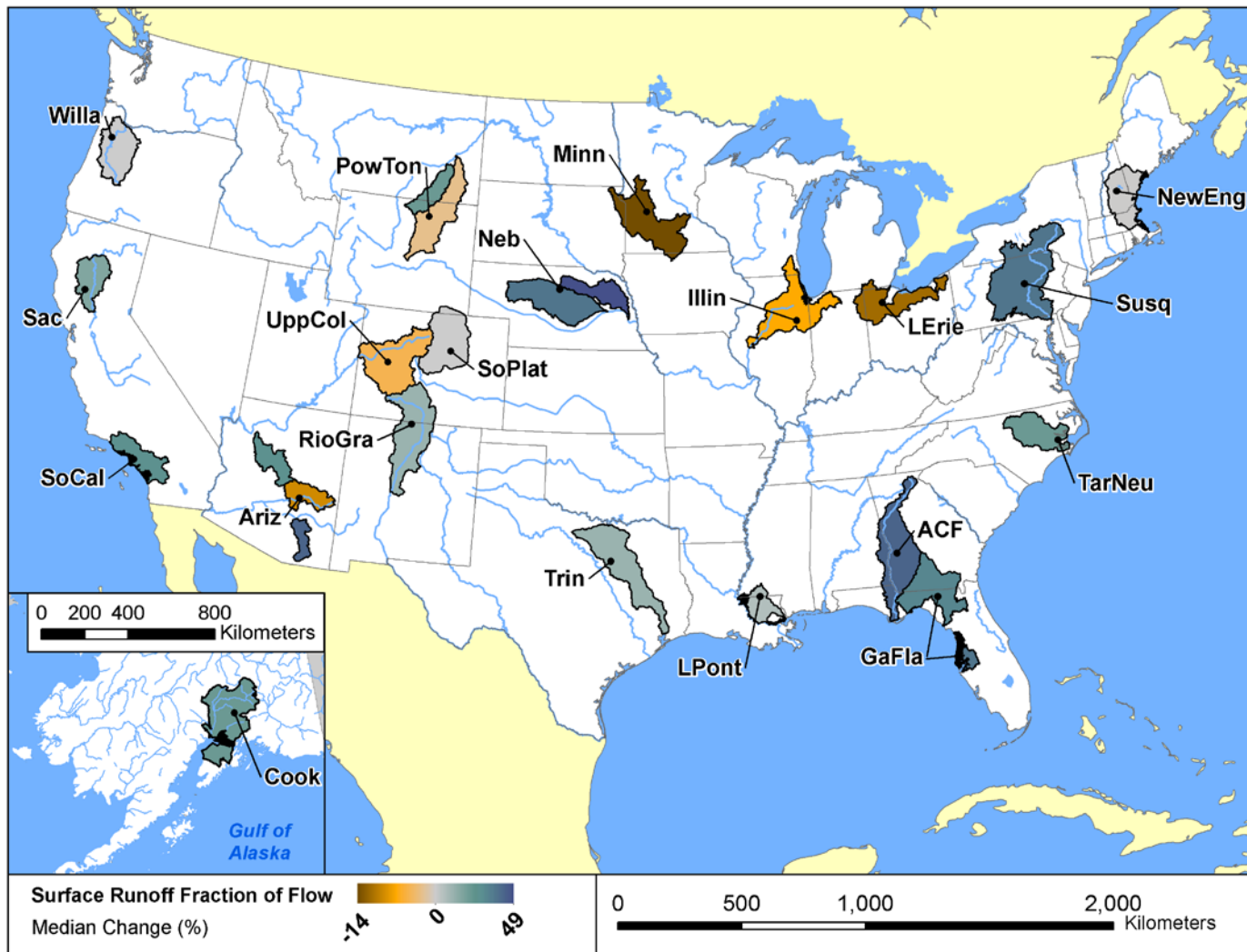


Figure 7-22. Median simulated percent changes in watershed Surface Runoff Fraction for six NARCCAP scenarios relative to current conditions (median of NARCCAP climate scenarios with urban development).

Note: Surface Runoff Fraction is the fraction of streamflow contributed by overland flow pathways. Cook Inlet results do not include land-use change.

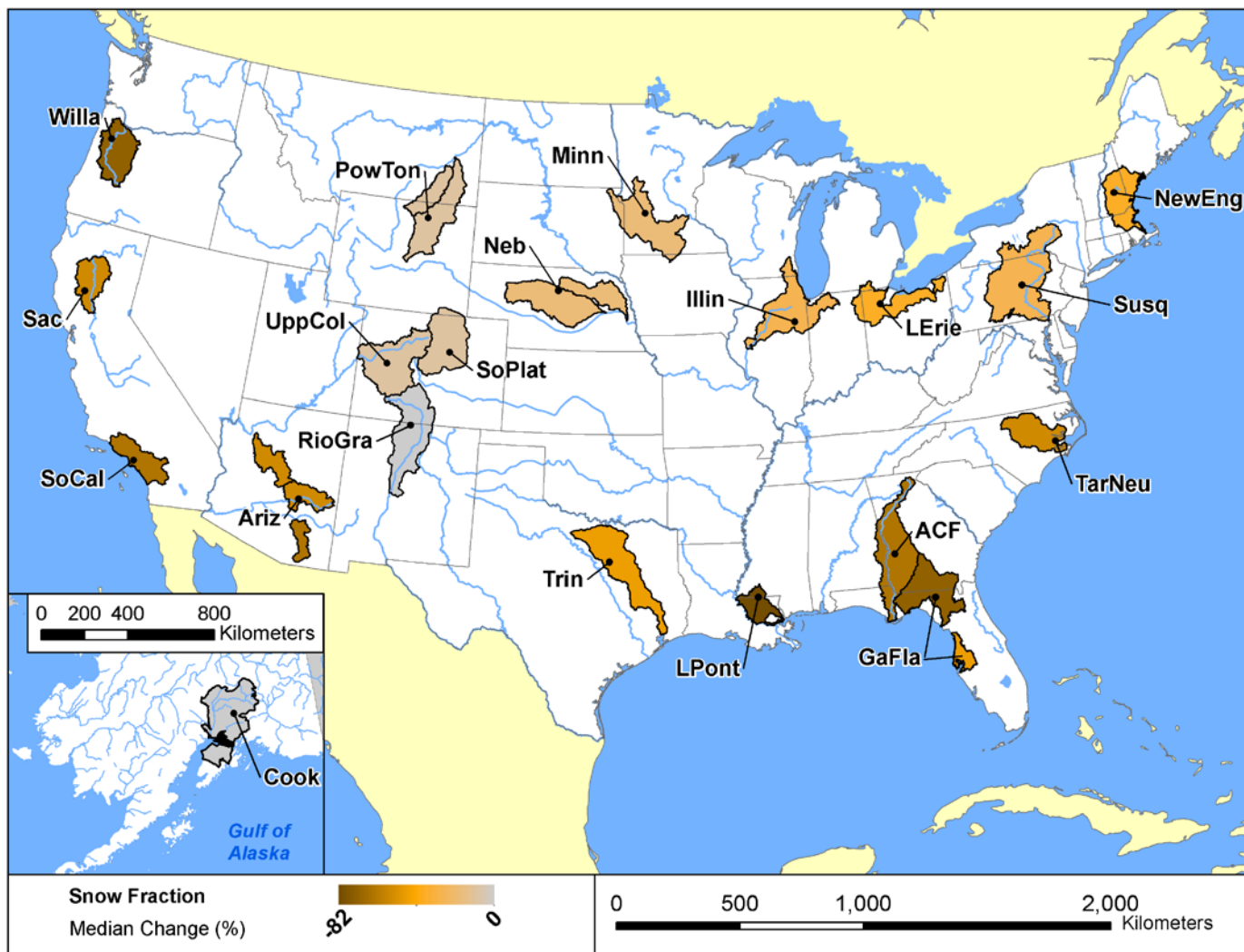


Figure 7-23. Median simulated percent changes in watershed Snowmelt Fraction for six NARCCAP scenarios relative to current conditions (median of NARCCAP climate scenarios with urban development).

Note: Snowmelt Fraction is the fraction of streamflow contributed by snowmelt. Cook Inlet results do not include land-use change.

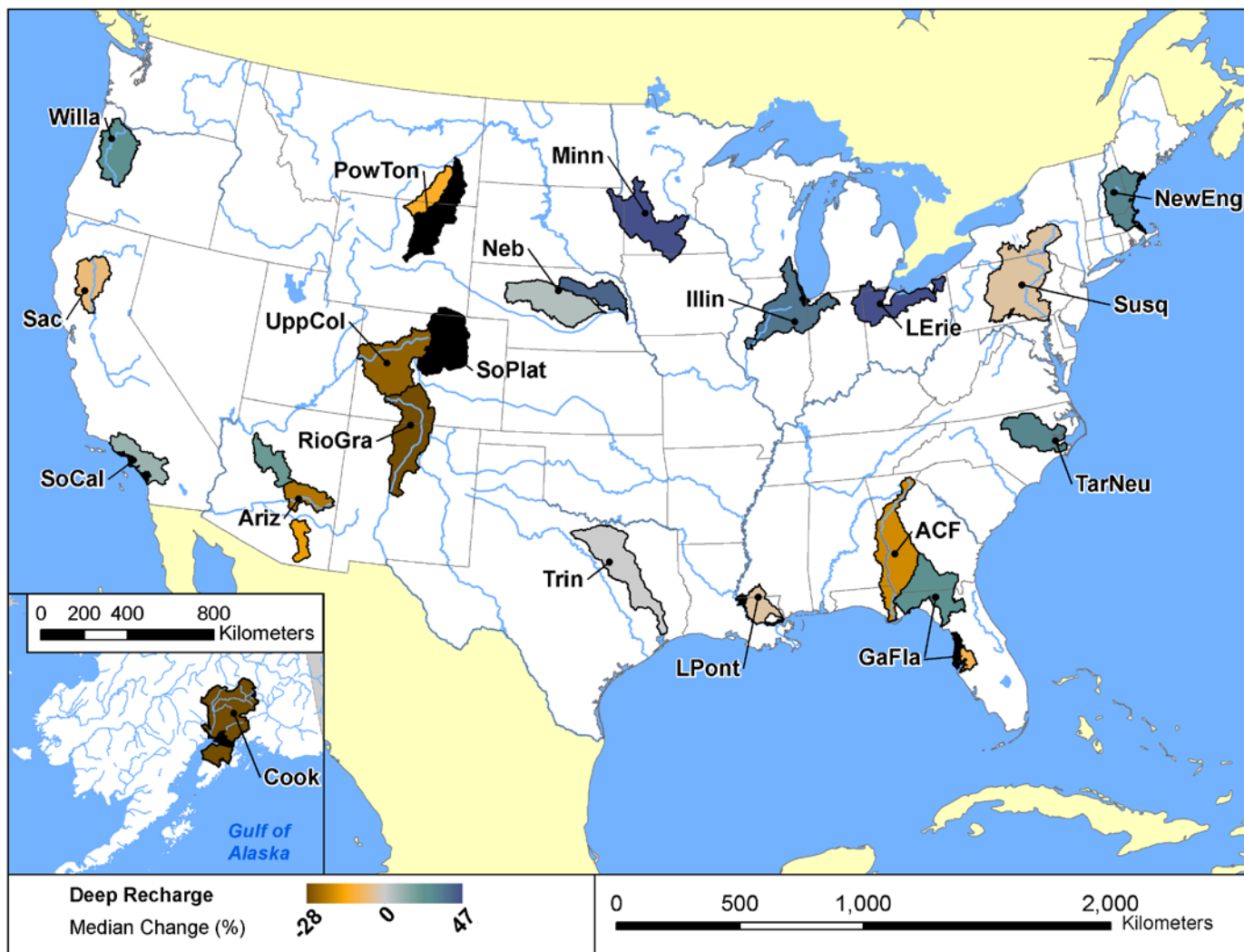


Figure 7-24. Median simulated percent changes in watershed Deep Recharge for six NARCCAP scenarios relative to current conditions (median of NARCCAP climate scenarios with urban development).

Note: Deep Recharge is the depth of water recharging deep aquifers per unit time. Cook Inlet results do not include land-use change. Areas shown in black have no deep recharge simulated.

The water balance summaries are presented as averages over whole watersheds. These are generally consistent with the project study areas, except that several study areas (e.g., Central Nebraska) were simulated using more than one SWAT model and thus show multiple results. Figure 7-20 shows the change in the Dryness Ratio, expressed as the ratio of ET to precipitation. The central tendency of the Dryness Ratio is estimated to increase in the southern Rocky Mountains and adjacent parts of Arizona, consistent with median decreases in simulated mean annual streamflow (see Figure 7-4).

Another aspect of low flows is shown by the Low Flow Sensitivity metric—the average rate of baseflow generation per square mile of watershed area. This metric (see Figure 7-21) decreases in areas for which the Dryness Ratio increases. However, it also decreases in various other watersheds (such as SoCal and ACF) for which there is little change in the Dryness Ratio. Areas where the Low Flow Sensitivity metric decreases may be expected to experience difficulties in maintaining minimum streamflow for aquatic life support or for meeting wasteload dilution expectations.

The Surface Runoff Fraction (the fraction of streamflow contributed by overland flow pathways) increases strongly for various study areas on the east coast and some other areas, mostly due to intensification of rainfall events in climate models (see Figure 7-22). Study areas for which the Surface Runoff Fraction strongly increases, such as ACF and Ariz-San Pedro, are those where the Low Flow Sensitivity decreases despite relatively small changes in the Dryness Ratio.

Snowmelt Fraction, the fraction of runoff that is due to melting snow (see Figure 7-23) declines in all watersheds. The strongest percentage declines (in southern and coastal areas) are somewhat misleading, as these watersheds generally have small amounts of snow. The lesser percentage declines throughout the Rockies are of greater concern to water management in the west.

The combination of a greater fraction of surface runoff in many watersheds coupled with increased dryness and reduced total streamflow in many western watersheds leads to a reduction in projected Deep Recharge (rates of recharge to deep aquifers) in many study areas (see Figure 7-24). The risks are estimated to be particularly acute in the Rockies and the ACF basins. In other areas, increased precipitation in the models counteracts other forces through mid-century, including the critical recharge areas in central Nebraska.

7.7. MODELING ASSUMPTIONS AND LIMITATIONS

Model simulations in the study provide an improved understanding of streamflow and water quality sensitivity in different regions of the United States to a range of plausible mid-21st century climate change and urban development scenarios. The study also illustrates certain challenges associated with the use of watershed models for conducting scenario-based studies of climate change impacts. In the process, this study adds to our knowledge of how to implement such investigations.

A number of sources of uncertainty must be considered in interpreting results from watershed hydrologic and water quality simulations of response to climate change—including uncertainty in the emissions scenario, uncertainty in the GCM simulations of future climate, uncertainty in the downscaling of these GCM outputs to the local scale, and uncertainty in the watershed

models used to translate potential changes in local climate to watershed response. The strong dependence of streamflow and water quality on climate drivers (e.g., temperature, precipitation, etc.) means that accurate weather data is necessary to generate accurate estimates of future flow and water quality conditions. Inherent in the scenario approach to modeling climate futures is uncertainty in knowledge of future climate conditions. It is therefore necessary to choose a range of scenarios that reflect the full, plausible set of future conditions.

Simulation results showed a wide range of watershed responses to differences in climatic forcing. Results suggest the variability resulting from scenarios based on different methods of downscaling with a single GCM can be of the same order of magnitude as the variability among GCMs. In many cases, simulations for scenarios based on different downscaling approaches with a single GCM do not agree even in the direction of projected changes relative to current values. In part, this issue reflects the skill associated with RCM simulations. A recent study by Racherla et al. (2012) investigated the value added by using an RCM (the Weather Research and Forecasting or WRF model) with the GCM GISS-ModelE2 and concluded that the RCM does not achieve holistic improvement in the simulation of seasonally and regionally averaged surface temperature or precipitation for historical data. They further suggested that no strong relationship exists between skill in capturing climatological means and skill in capturing climate change. If RCMs do not add considerable value to the global simulation, the underlying uncertainties can only be reduced by improving the global-scale climate simulations.

As with any study of this type, simulation results are conditional upon the specific methods, models, and scenarios used. The simulated range of response in this study is limited by the particular set of climate model projections available in the NARCCAP archives (the subset of BCSD projections was selected to match those in the NARCCAP set). For example, all climate change scenarios evaluated in this study are based on the IPCC A2 greenhouse gas emissions storyline. While simulations in this study represent a credible set of plausible future climatic conditions, the scenarios evaluated should not be considered comprehensive of all possible futures. A recent summary by Mote et al. (2011) concludes that ensemble scenarios with a limited number of projections taken from the full set of available climate models yields results that differ little from those achieved from larger sets given the current state of science; furthermore, attempting to preselect the “best” models based on measures of model skill does little to refine the estimate of central tendency of projected change. Mote et al. recommend a sample size of approximately ten climate scenarios, which is greater than the six used in this study. Inclusion of additional sources and types of scenarios could alter the ranges of change simulated in this study. Similarly, alternative urban and residential development scenarios would also expand the ensemble range of future responses.

Watershed model simulations developed here also do not consider feedback effects of human and ecological adaptation to change. In essence, the climate-land use-watershed system is considered independent of management and adaptation in this study. At the most direct level, various aspects of human water management such as operation of dams, water use, transboundary water inputs, and point source discharges are considered fixed at present levels. In fact, we know these will change. For instance, a warmer climate is likely to result in increased irrigation withdrawals for crops, while more intense precipitation is likely to result in changes in operating rules for dams. In some cases, the models are driven by fixed upstream boundary conditions (e.g., the Sacramento River model). There was, however, insufficient

knowledge of these changes to incorporate them into the scenarios. The analyses thus provide an increased understanding of the marginal changes in watershed responses due to potential changes in climate and urban and residential development, but do not account for the net changes from all factors, including human use and management of water.

At a more sophisticated level, both natural and human communities are likely to adapt to climate changes, influencing the watershed response. The SWAT plant growth model takes into account the effects of changed climate on plant growth as a function of CO₂, temperature, water stress, and nutrient availability. However, it does not take into account changes in the type of land cover that may occur as a result of such stresses—either slowly, as through a gradual shifting of ecological niches, or catastrophically, as might occur through drought-induced forest fires. Human adaptations that affect watershed processes will also occur. For example, crop types (or total area in crops) are likely to change as producers respond to changes in growing season length and water availability (e.g., Polsky and Easterling, 2001). Simulation models are not yet available to provide a credible analysis of such feedback loops at the scale necessary for evaluating watershed responses.

In addition, many of the modeled study areas are highly managed systems influenced by dams, water transfers and withdrawals, and point and nonpoint pollution sources. Given the difficulty inherent in modeling watershed response at the large spatial scale used in this study, detailed representation of all management and operational activities was not possible. Results therefore represent the potential response of watersheds to different change scenarios, but should not be considered quantitative forecasts of future conditions.

7.7.1. Model Calibration

Reliably reproducing the baseline period is important for any study of watershed response to climate change because any biases present in the model calibration are likely to also affect the future simulations of streamflow (Prudhomme and Davies, 2009), possibly with nonlinear amplification. The experiences of this project emphasize the importance (and challenges) of calibration and validation for watershed models. Water quality calibration is particularly challenging due to limited amounts of readily available monitoring data. Additional efforts similar to the one presented here should either focus on watersheds for which well-calibrated models already exist (and the effort of assembling water quality input and monitoring data from multiple sources has already been completed) or allocate sufficient time and budget to conduct detailed, site-specific calibration.

The calibration process can introduce modeler bias, which could be mitigated through use of an automated model calibration scheme. We avoided this option based on past experience with the SWAT and HSPF models in which automated calibration often converges to physically unrealistic model parameter sets. It may, however, be advisable to pursue stepwise, guided model calibration with carefully specified parameter constraints to avoid the effects of user bias, as was done, for example, in recent USGS simulations of watershed-scale streamflow response to climate change using the PRMS model (Hay et al., 2011). PRMS, however, only addresses streamflow and has a much more parsimonious data set than does SWAT or HSPF. Nonetheless, the advantages of controlling for modeler bias may make use of a semiautomated calibration procedure desirable.

The significance of calibration bias is mitigated by focusing on projected changes relative to baseline conditions as compared to actual future values. If biases are consistent and linear between the baseline and future condition, the effect of such biases will tend to cancel out when relative change is calculated. There is, however, no guarantee that biases will be linear. Further testing to evaluate the effects of alternative model calibrations on the simulated response of different study areas would be desirable.

7.7.2. Watershed Model Selection

Simulation results are sensitive to the watershed model applied. In the pilot studies, both HSPF and SWAT appeared capable of providing similar quality of fit to observed streamflow at the large basin scale and to pollutant loads at the monthly scale, while HSPF, using a shorter time step, was better able to resolve streamflow at smaller spatial scales and better able to match observed concentrations when fully calibrated. An important result of model comparisons conducted in this study is the significant effect that increased atmospheric CO₂ concentrations (effects of reduced stomatal conductance that decrease ET) appeared to have on the water balance. SWAT's integrated plant growth model takes this effect into account, whereas HSPF does not.

It is unclear, however, how well SWAT is able to represent the complex processes affecting plant growth, nutrient dynamics, and water budgets under changing climate. For example, as CO₂ levels increase, leaf level reductions in stomatal conductance and evapotranspiration may be offset by increased plant growth and leaf area. The effects of CO₂ on plant growth may also be altered over time due to nutrient limitation (Reich et al., 2006). Further study is required to better understand how climate change will affect these processes. It should also be noted that SWAT (as implemented here, using version SWAT2005) has limitations in its representation of a number of important watershed processes, including simplified simulation of direct runoff using a curve number approach, erosion prediction with MUSLE that does not fully incorporate changes in energy that may occur with altered precipitation regimes, and a simplistic representation of channel erosion processes that appears unlikely to provide a firm foundation for simulating channel stability responses to climate change. More recent versions of SWAT considerably expand the options for simulating channel erosion, but do not appear to be fully validated at this time and are limited by the model's use of a daily time step for hydrology.

These considerations suggest that a more sophisticated watershed model formulation, combining a plant growth model (as in SWAT) with a more detailed hydrologic simulation would be preferable for evaluating watershed responses to climate change. However, even if such a model was available, fully validated, and ready for use, it would likely require a significantly higher level of effort for model implementation and calibration.

Comparison of change scenarios using HSPF and SWAT suggests one must proceed with caution when attempting to estimate even relative aggregate impacts at a national scale through use of watershed models with different underlying formulations. For example, a national synthesis that drew conclusions from a mix of models, some of which did and others of which did not include explicit simulation of effects of increased CO₂ on evapotranspiration, could reach erroneous conclusions regarding the relative intensity of impacts in different geographical areas.

8. SUMMARY AND CONCLUSIONS

This report describes watershed modeling in 20 large, U.S. drainage basins (6,000–27,000 mi² or 15,000–60,000 km²) to characterize the sensitivity of streamflow, nutrient (nitrogen and phosphorus) loading, and sediment loading to a range of potential mid-21st century climate futures, to assess the potential interaction of climate change and urbanization in these basins, and to improve our understanding of methodological challenges associated with integrating existing tools (e.g., climate models, downscaling approaches, and watershed models) and data sets to address these scientific questions. Study areas were selected to represent a range of geographic, hydroclimatic, physiographic, land use, and other watershed attributes. Other important criteria used in site selection included the availability of necessary data for calibration and validation of watershed models, and opportunities for leveraging the availability of preexisting watershed models.

Models were configured by subdividing study areas into modeling units, followed by continuous simulation of streamflow and water quality for these units using meteorological, land use, soil, and stream data. A unique feature of this study is the use of a consistent watershed modeling methodology and a common set of climate and land-use change scenarios in multiple locations across the nation. Models in each study area are developed for current (1971–2000) observed conditions, and then used to simulate results under a range of potential mid-21st century (2041–2070) climate change and urban development scenarios. Watershed modeling was conducted at each study location using the SWAT model and six climate change scenarios based on dynamically downscaled (50 × 50 km²) output from four of the GCMs used in the IPCC 4th Assessment Report for the period 2041–2070 archived by the NARCCAP. Scenarios were created by adjusting historical weather series to represent projected changes in climate using a change factor approach. To explore the potential interaction of climate change and urbanization, simulations also include urban and residential development scenarios for each of the 20 study watersheds. Urban and residential development scenarios were acquired from EPA’s national-scale ICLUS project.

In a subset of five study areas (the Minnesota River, the Susquehanna River, the Apalachicola-Chattahoochee-Flint, the Salt/Verde/San Pedro, and the Willamette River Basins), additional simulations were conducted to assess the variability in simulated watershed response resulting from use of different watershed models and different approaches for downscaling GCM climate change scenarios. In these study areas, watershed simulations were also run with eight additional scenarios derived from the same four GCMs used in NARCCAP: four scenarios interpolated to station locations directly from the GCM output, and four scenarios based on BCSD statistically downscaled climate projections described by Maurer et al. (2007). In addition, in these five study areas, all scenario simulations were run independently with a second watershed simulation model, the HSPF.

Given the large size of study areas, calibration and validation of all models was completed by first focusing on a single HUC-8 within the larger study area (preferably one with a good record of streamflow gaging and water quality monitoring data), and then extending the calibration to adjacent areas with modifications as needed to achieve a reasonable fit at multiple spatial scales.

Large-scale GCM projections are generally consistent in showing a continued warming trend over the next century (although with sometimes significant regional-scale disagreements in the magnitude of this warming), but offer a much wider range of plausible outcomes in other aspects of local climate—particularly the timing and intensity of precipitation and the energy inputs (in addition to air temperature) that determine potential evapotranspiration—that interact to create watershed responses.

The simulated watershed responses to these changes provide an improved understanding of system sensitivity to potential climate change and urban development scenarios in different regions of the country and provide a range of plausible future hydrologic and water quality change scenarios that can be applied in various planning and scoping frameworks. The results illustrate a high degree of regional variability in the response of different streamflow and water quality endpoints to a range of potential mid-21st century climatic conditions in different regions of the nation. Watershed hydrologic response is determined by the interaction of precipitation and evapotranspiration, while water quality response is largely dependent on hydrology. Comparison of simulations in all 20 study areas for the 2041–2070 time horizon suggest potential streamflow volume decrease in the Rockies and interior southwest, and increases in the east and southeast coasts. Wetter winters and earlier snowmelt are likely in many of the northern and higher elevation watersheds. Higher peak flows will also increase erosion and sediment transport; nitrogen and phosphorus loads are also likely to increase in many watersheds.

Both the selection of an underlying GCM and the choice of downscaling method have a significant influence on the streamflow and water quality simulations. In many cases, the range of simulated responses across the different climate models and downscaling methodologies do not agree in direction. The ultimate significance of any given simulation of future change will depend on local context, including the historical range of variability, thresholds and management targets, management options, and interaction with other stressors. The simulation results in this study do, however, clearly illustrate that the potential streamflow and water quality response in many areas could be large.

Watershed simulations were run in all study areas with and without projected mid-21st century changes in urban and residential development. These results suggest that at the HUC-8 spatial scale evaluated in this study, watershed sensitivity to projected urban and residential development will be small relative to the changes resulting from climate change. It is important, however, to qualify this result. The finest spatial scale reported in this study is that of an 8-digit HUC, and most urbanized areas are located on larger rivers downstream of multiple 8-digit HUCs. Over the whole of individual study areas, urban and residential growth scenarios represented changes in the amount of developed land on the order of <1 to about 12% of total watershed area and increases in impervious surfaces on the order of 0 to 5% of total watershed area. The effects of urban development on adjacent water bodies at higher levels of development are well documented. It is thus likely that at smaller spatial scales within study areas where the relative fraction of developed land is greater, the effects of urbanization will be greater. Identifying the scale at which urbanization effects become comparable to the effects of a changing climate is an important topic for future research.

The simulation results also illustrate a number of methodological issues related to impacts assessment modeling. These include the sensitivities and uncertainties associated with use of

different watershed models, different approaches for downscaling climate change simulations from global models, and the interaction between climate change and other forcing factors, such as urbanization and the effects of changes in atmospheric CO₂ concentrations on evapotranspiration. Uncertainty associated with differences in emission scenarios and climate model sensitivities is well known and widely discussed in previous assessments of climate change impacts on water (e.g., IPCC, 2007; Karl et al., 2009). This study illustrates a potentially significant additional sensitivity of watershed simulations to the method selected for downscaling GCM model output. Results of the intercomparison of climate change data sets suggest that the variability between downscaling of a single GCM with different RCMs can be of the same order of magnitude as the ensemble variability between GCMs.

This study also suggests potentially important sensitivity of results to the use of different hydrologic models (HSPF and SWAT in this study), associated with differences in process representation, such as accounting for the influence of increased atmospheric CO₂ on evapotranspiration. One notable insight from these results is that, in many watersheds, climate change (when precipitation amount and/or intensity is altered), increasing urbanization, and increasing atmospheric CO₂ can have similar or additive effects on streamflow and pollutant loading (e.g., a more flashy runoff response with higher high flows and lower low flows). The results, while useful as guidance for designing and conducting similar impacts assessment studies, are only a first step in understanding what are likely highly complex and context-dependent relationships. Further study and evaluation of the implications of these and other questions is necessary for improving the plausibility and relevance of coupled climate-hydrology simulations, and ultimately for informing resource managers and climate change adaptation strategies.

The model simulations in this study contribute to a growing understanding of the complex and context-dependent relationships between climate change, land development, and water in different regions of the nation. As a first order conclusion, results indicate that in many locations future conditions are likely to be different from past experience. In the context of decision making, being aware and planning for this uncertainty is preferable to accepting a position that later turns out to be incorrect. Results also provide a plausible envelope on the range of streamflow and water quality responses to mid-21st century climate change and urban development in different regions of the nation. In addition, in many study areas the simulations suggest a likely direction of change of streamflow and water quality endpoints. This information can be useful in planning for anticipated but uncertain future conditions. The sensitivity studies evaluating different methodological choices help to improve the scientific foundation for conducting climate change impacts assessments, thus building the capacity of the water management community to understand and respond to climate change.

Understanding and responding to climate change is complex, and this study is only an incremental step towards fully addressing these questions. It must be stressed that results are conditional upon the methods, models, and scenarios used in this study. Scenarios represent a plausible range but are not comprehensive of all possible futures. Several of the study areas are also complex, highly managed systems; all infrastructure and operational aspects of water management are not represented in full detail. Finally, changes in agricultural practices, water demand, other human responses, and natural ecosystem changes such as the prevalence of forest fire (e.g., Westerling et al., 2006) or plant disease that will influence streamflow and water

quality are not considered in this study. Further study is required to continue to build the scientific foundation for assessing these and other questions relevant to the scientific and watershed management communities.

Successful climate change adaptation strategies will need to encompass practices and decisions to reduce vulnerabilities across a wide range of plausible future climatic conditions. Where system thresholds are known, knowledge of the range of potential changes can help to identify the need to consider future climate change in water planning. Many of these strategies might also help reduce the impacts of other existing stressors. It is the ultimate goal of this study to build awareness of the potential range of future watershed response so that where simulations suggest large and potentially disruptive changes, the management community will respond to build climate resiliency.

REFERENCES

- Ainsworth, EA; Rogers, A. (2007) The response of photosynthesis and stomatal conductance to rising [CO₂]: mechanisms and environmental interactions. *Plant Cell Environ* 30:258–270.
- Alexander, LV; Zhang, X; Peterson, TC; et al. (2006) Global observed changes in daily climate extremes of temperature and precipitation. *J Geophys Res* 111(D05109). doi: 10.1029/2005JD006290.
- Alexander, RB; Smith, RA; Schwarz, GE; et al. (2008) Differences in phosphorus and nitrogen delivery to the Gulf of Mexico from the Mississippi River Basin. *Environ Sci Technol* 42(3):822–830.
- Allan, RP; Soden, BJ. (2008) Atmospheric warming and the amplification of precipitation extremes. *Science* 321(5895):1481–1484.
- Allan, RJ. (1986) The role of particulate matter in the fate of contaminants in aquatic ecosystems. Scientific Series 142. Inland Waters Directorate, Environment Canada, Ottawa.
- Allen, RG; Pereira, LS; Raes, D; et al. (1998) Crop evapotranspiration: guidelines for computing crop water requirements. Irrigation and Drainage Paper 56. Food and Agriculture Organization of the United Nations, Rome. Available online at http://www.engr.scu.edu/~emaurer/classes/ceng140_watres/handouts/FAO_56_Evapotranspiration.pdf
- Allen, RG; Walter, IA; Elliott, RL; et al. (2005) The ASCE standardized reference evapotranspiration equation. Reston, VA: American Society of Civil Engineers.
- Anandhi, A; Frei, A; Pierson DC; et al. (2011) Examination of change factor methodologies for climate change impact assessment. *Water Resour Res* 47(W03501):doi:10.1029/2010WR009104.
- Baker, DB; Richards, P; Loftus, TT; et al. (2004) A new flashiness index: characteristics and applications to Midwestern rivers and streams. *J Am Water Resour Assoc* 40(2):503–522.
- Berg, EE; Henry, JD; Fastie, CL; et al. (2006) Spruce beetle outbreaks on the Kenai Peninsula, Alaska, and Kluane National Park and Reserve, Yukon Territory: relationship to summer temperatures and regional differences in disturbance regimes. *For Ecol Manage* 227:219–232.
- Bernacchi, CJ; Kimball, BA; Quarles, DR; et al. (2007) Decreases in stomatal conductance of soybean under open-air elevation of [CO₂] are closely coupled with decreases in ecosystem evapotranspiration. *Plant Physiol* 143:134–144.

-
- Bicknell, BR; Imhoff, JC; Kittle JL, Jr; et al. (2001) Hydrological simulation program—Fortran (HSPF). User's manual for release 12. U.S. Environmental Protection Agency, National Exposure Research Laboratory, Athens, GA, in cooperation with U.S. Geological Survey, Water Resources Division, Reston, VA.
- Bicknell, BR; Imhoff, JC; Kittle JL, Jr; et al. (2005) HSPF version 12.2 user's manual. U.S. Environmental Protection Agency, National Exposure Research Laboratory, Office of Research and Development, Athens, GA.
- Bosch, NS; Allan, JD; Dolan, DM; et al. (2011) Application of the Soil and Water Assessment Tool for six watersheds of Lake Erie: model parameterization and calibration. *J Great Lakes Res* 37:263–271.
- Bouraoui, F; Galbiati, L; Bidoglio, G. (2002) Climate change impacts on nutrient loads in the Yorkshire Ouse catchment (UK). *Hydrol Earth Syst Sci* 6:197–209.
- Burwell, RE; Timmons, DR; Holt, RF. (1975) Nutrient transport in surface runoff as influenced by soil cover and seasonal periods. *Soil Sci Soc Am J* 39(3):523–528.
- Cao, L; Bala, G; Caldeira, K; Nemani, R; Ban-Weiss, G. (2010) Importance of carbon dioxide physiological forcing to future climate change. *PNAS* 107(21):9513–9518.
- CECWG (Commission for Environmental Cooperation Working Group). (1997) Ecological regions of North America—toward a common perspective. Commission for Environmental Cooperation, Montreal. Available online at <http://www.calepa.ca.gov/education/eei/Curriculum/Grade11/1186/1186EnvGuide.pdf>
- Chang, H; Evans, BM; Easterling, DR. (2001) The effects of climate change on streamflow and nutrient loading. *J Am Water Resour Assoc* 37(4):973–985.
- Cox, P; Stephenson, D. (2007) A changing climate for prediction. *Science* 317(5835):207–208.
- Crawford, NH; Linsley, RK. (1966) Digital simulation in hydrology: Stanford watershed model IV. Technical Report 39. Department of Civil Engineering, Stanford University, CA. Available online at <http://www.hydrocomp.com/publications/StanfordModelIV.PDF>
- Dai, A. (2006) Precipitation characteristics in eighteen coupled climate models. *J Clim* 19:4605–4630.
- Donigian, AS, Jr. (2000) HSPF training workshop handbook and CD. Lecture #19: calibration and verification issues. U.S. Environmental Protection Agency Headquarters, Washington Information Center, 10–14 January, 2000. Prepared for U.S. Environmental Protection Agency, Office of Water, Office of Science and Technology, Washington, DC.
- Duda, P; Kittle, J, Jr; Gray, M; et al. (2001) WinHSPF Version 2.0: an interactive Windows interface to HSPF (WinHSPF) user's manual. AQUA TERRA Consultants, Decatur, GA. Available online at http://www.epa.gov/athens/research/ftable/toc_intr.pdf

-
- Easterling, WE; Rosenberg, NJ; McKenney, MS; et al. (1992) Preparing the erosion productivity impact calculator (EPIC) model to simulate crop response to climate change and the direct effects of CO₂. *Agric For Meteorol* 59(1-2):17-34.
- Emori, S; Brown, SJ. (2005) Dynamic and thermodynamic changes in mean and extreme precipitation under changed climate. *Geophys Res Lett* 32(L17706)
doi:10.1029/2005GL023272
- Ficklin, DL; Luo, Y; Luedeling, E; et al. (2009) Climate change sensitivity assessment of a highly agricultural watershed using SWAT. *J Hydrol* 374(1/2):16-29.
- Follett, RF. (1995) Fate and transport of nutrients: nitrogen. Working Paper No. 7. U.S. Department of Agriculture, Agricultural Research Service, Soil-Plant-Nutrient Research Unit, Fort Collins, CO. Available online at http://www.nrcs.usda.gov/wps/portal/nrcs/detail/national/technical/?cid=nrcs143_014202
- Garen, DC; Moore, DS. (2005) Curve number hydrology in water quality modeling: uses, abuses, and future directions. *J Am Water Resour Assoc* 41(2):377-388.
- Garrick, M; Cunnane, C; Nash, JE. (1978) A criterion of efficiency for rainfall-runoff models. *J Hydrol* 36(3-4):375-381.
- Gassman, PW; Reyes, MR; Green, CH; et al. (2007) The Soil and Water Assessment Tool: historical development, applications, and future research directions. *Trans Am Soc Agri Biol Eng* 50(4):1211-1250.
- Gesch, D; Oimoen, M; Greenlee, S; Nelson, C; Steuck, M; Tyler, D. (2002) The national elevation dataset. *Photogramm Eng Remote Sens* 68(1):5-11.
- Gleckler, PJ; Taylor, KE; Doutriaux, C. (2008) Performance metrics for climate models. *J Geophys Res* 113(D06104): doi:10.1029/2007JD008972.
- Groisman, PY; Knight, RW; Karl, TR. (2012) Changes in intense precipitation over the central United States. *J Hydrometeorol* 13:47-66.
- Gutowski, WJ; Hegerl, GC; Holland, GJ; et al. (2008) Causes of observed changes in extremes and projections of future changes. In: Karl, TR; Meehl, GA; Miller, CD; et al; eds. *Weather and climate extremes in a changing climate. Regions of focus: North America, Hawaii, Caribbean, and U.S. Pacific Islands. Report by the U.S. Climate Change Science Program. Global Change Research, Washington, DC; p. 81-116. Available online at http://www.agci.org/dB/PDFs/Publications/07S1_USCCSP.pdf*
- Hawkins, E; Sutton, R. (2009) The potential to narrow uncertainty in regional climate predictions. *Bull Am Meteor Soc* 90:1095-1107.
- Hay, LE; Markstrom, SL; Ward-Garrison, C. (2011) Watershed-scale response to climate change through the twenty-first century for selected basins across the United States. *Earth Interact* 15:1-37.

-
- Homer, C; Huang, C; Yang, L; et al. (2004) Development of a 2001 national landcover database for the United States. *Photogramm Eng Remote Sens* 70(7):829–840.
- Homer, C; Dewitz, J; Fry, J; et al. (2007) Completion of the 2001 national land cover database for the conterminous United States. *Photogramm Eng Remote Sens* 73(4):337–341. Available online at <http://www.epa.gov/mrlc/pdf/april-07-highlight.pdf>
- Hurd, B; Leary, N; Jones, R; et al. (1999) Relative regional vulnerability of water resources to climate change. *J Am Water Resour Assoc* 35(6):1399–1409.
- IPCC (Intergovernmental Panel on Climate Change). (2001) Climate change 2001: the scientific basis. In: Houghton, JT; Ding, Y; Griggs, DJ; et al.; eds. *Intergovernmental panel on climate change: working group I*. Cambridge, UK: Cambridge University Press.
- IPCC (Intergovernmental Panel on Climate Change). (2007) Climate change 2007: synthesis report—summary for policymakers. Available online at: http://www.ipcc.ch/pdf/assessment-report/ar4/syr/ar4_syr_spm.pdf.
- Jensen, ME; Burman, RD; Allen, RG. (1990) Evapotranspiration and irrigation water requirements. *ASCE Manuals and Reports on Engineering Practice No. 70*. ASCE, NY.
- Johnson, T; Weaver, C. (2009) A framework for assessing climate change impacts on water and watershed systems. *Environ Manage* 43:118–134.
- Karl, TR; Knight, RW. (1998) Secular trends of precipitation amount, frequency, and intensity in the United States. *Bull Am Meteorol Soc* 79(2):231–241.
- Karl, TR; Melillo, JM; Peterson, TC; eds. (2009) *Global climate change impacts in the United States*. Cambridge, UK: Cambridge University Press.
- Kharin, VV; Zwiers, FW; Zhang, X; et al. (2013) Changes in temperature and precipitation extremes in the CMIP5 ensemble. *Clim Change* 119(2):345–357. DOI 10.1007/s10584-013-0705-8
- Kundzewicz, ZW; Mata, LJ; Arnell, NW; et al. (2007) Freshwater resources and their management. In: Parry, ML; Canziani, OF; Palutikof, JP; et al; eds. *Climate change 2007: impacts, adaptation and vulnerability. Contribution of Working Group II to the Fourth Assessment Report of the Intergovernmental Panel on Climate Change*. Cambridge, UK: Cambridge University Press; pp. 173–210.
- Leakey, ADB; Ainsworth, EA; Bernacchi, CJ; et al. (2009) Elevated CO₂ effects on plant carbon, nitrogen, and water relations: six important lessons from FACE. *J Exp Bot* 60(10):2859–2876.
- Legates, DR; McCabe, GJ, Jr. (1999) Evaluating the use of “goodness-of-fit” measures in hydrologic and hydroclimatic model validation. *Water Resour Res* 35(1):233–241.

-
- Lempert, RJ; Groves, DG; Popper, SW; et al. (2006) A general, analytic method for generating robust strategies and narrative scenarios. *Manage Sci* 52(4):514–528.
- Lumb, AM; McCammon, RB; Kittle, JL, Jr. (1994) User's manual for an expert system (HSPEXP) for calibration of the hydrological simulation program-FORTRAN. U.S. Geological Survey Water Resources Investigation Report 94-4168. U.S. Geological Survey, Reston, VA.
- Luo, Y; Ficklin, DL; Liu, X; et al. (2013) Assessment of climate change impacts on hydrology and water quality with a watershed modeling approach. *Sci Total Environ* 450–451:72–82.
- Marshall, E; Randhir, T. (2008) Effect of climate change on watershed system: a regional analysis. *Clim Change* 89(3/4):263–280.
- Maurer, EP; Brekke, L; Pruitt, T; et al. (2007) Fine-resolution climate projections enhance regional climate change impact studies. *Eos Trans Am Geophys Union* 88(47):504.
- Mearns, L. (2009) The North American regional climate change assessment program (NARCCAP): overview of phase II results. *Earth Environ Sci Trans* 6(022007): doi:10.1088/1755-1307/6/2/022007.
- Mesinger, F; DiMego, G; Kalnay, E; et al. (2006) North American regional reanalysis. *Bull Am Meteorol Soc* 87(3):343–360.
- Milly, PCD; Dunne, K; Vecchia, A. (2005) Global pattern of trends in streamflow and water availability in a changing climate. *Nature* 438:347–350.
- Milly, PCD; Betancourt, J; Falkenmark, M; et al. (2008) Stationarity is dead: Whither water management? *Science* 319:573–574.
- Monteith, DT; Evans, CD; Reynolds, B. (2000) Are temporal variations in the nitrate content of UK upland freshwaters linked to the North Atlantic Oscillation? *Hydrol Processes* 14(10):1745–1749.
- Monteith, JL. (1965) Evaporation and the environment. In: *The state and movement of water in living organisms. XIXth Symposium, Swansea. Soc Exp Biology, Vol 19. Cambridge, UK. Cambridge University Press; pp. 205–234.*
- Moriasi, DN; Arnold, JG; Van Liew, MW; et al. (2007) Model evaluation guidelines for systematic quantification of accuracy in watershed simulations. *Trans Am Soc Agri Biol Eng* 50(3):885–900.
- Mote, P; Brekke, L; Duffy, PB; et al. (2011) Guidelines for constructing climate scenarios. *Eos Trans Am Geophys Union* 92(31):257–258.
- Murdoch, PS; Baron, JS; Miller, TL. (2000) Potential effects of climate change on surface-water quality in North America. *J Am Water Resour Assoc* 36(2):347–366.

-
- Nash, JE; Sutcliffe, JV. (1970) River flow forecasting through conceptual models part I—a discussion of principles. *J Hydrol* 10(3):282–290.
- Neitsch, SL; Arnold, JG; Kiniry, JR; et al. (2005) Soil and water assessment tool, theoretical documentation. Grassland, Soil and Water Research Laboratory, U.S. Department of Agriculture, Agricultural Research Service, Temple, TX. Available online at <http://swat.tamu.edu/media/1292/swat2005theory.pdf>
- Paul, MJ; Meyer, JL. (2001) Streams in the urban landscape. *Annu Rev Ecol Syst* 32:333–365.
- Poff, NL; Tokar, S; Johnson, P. (1996) Stream hydrological and ecological responses to climate change assessed with an artificial neural network. *Limnol Oceanogr* 41(5):857–863.
- Polsky, C; Easterling, WE. (2001) Adaptation to climate variability and change in the U.S. Great Plains: a multi-scale analysis of Ricardian climate sensitivities. *Agric Ecosyst Environ* 85(1–3):133–144.
- Preston, SD; Bierman, VJ, Jr; Silliman, SE. (1989) An evaluation of methods for the estimation of tributary mass loads. *Water Resour Res* 25(6):1379–1389.
- Prudhomme, C; Davies, H. (2009) Assessing uncertainties in climate change impact analyses on the river flow regimes in the UK. Part 1: baseline climate. *Clim Change* 93(1–2):177–195.
- Pyke, C; Warren, M; Johnson, T; et al. (2011) Assessment of low impact development for managing stormwater with changing precipitation due to climate change. *Landsc Urban Plan* 103(2):166–173.
- Racherla, PN; Shindell, DT; Faluvegi, GS. (2012) The added value to global model projections of climate change by dynamical downscaling: a case study over the continental U.S. using the GISS-ModelE2 and WRF models. *J Geophys Res-Atmos* 117(D20118): doi:10.1029/2012JD018091.
- Raisanen, J. (2007) How reliable are climate models? *Tellus A* 59:2–29.
- Reich, PB; Hungate, BA; Luo, Y. (2006) Carbon-nitrogen interactions in terrestrial ecosystems in response to rising atmospheric carbon dioxide. *Annu Rev Ecol Evol Syst* 37:611–636.
- Sarewitz, D; Pielke, RA, Jr; Byerly, R, Jr. (2000) Introduction: death, taxes, and environmental policy. In: Sarewitz, D; Pielke, RA, Jr; Byerly, R, Jr; eds. *Prediction: science, decision making, and the future of nature*. Washington, DC: Island Press.
- SCS (Soil Conservation Service). (1972) Hydrology guide for use in watershed planning. National engineering handbook, section 4: hydrology, supplement A. U.S. Department of Agriculture, Natural Resources Conservation Service, Washington, DC.
- Seaber, PR; Kapinos, FP; Knapp, GL. (1987) Hydrologic unit maps. Water-Supply Paper 2294. U.S. Geological Survey, Denver, CO.

-
- Sharpley, AN; Williams, JR; eds. (1990) EPIC—erosion productivity impact calculator, 1. Model documentation. U.S. Department of Agriculture, Agricultural Research Service. Tech Bull 1768.
- Stainforth, DA; Allen, MR; Tredger, ER; et al. (2007) Confidence, uncertainty, and decision-support relevance in climate predictions. *Phil Trans R Soc A* 365:2145–2161.
- Stockle, CO; Williams, JR; Rosenberg, NJ; et al. (1992) A method for estimating the direct and climatic effects of rising atmospheric carbon dioxide on growth and yield of crops: part 1—modification of the EPIC model for climate change analysis. *Agric Syst* 38:225–238.
- Suddick, EC; Davidson, EA; eds. (2012) The role of nitrogen in climate change and the impacts of nitrogen-climate interactions on terrestrial and aquatic ecosystems, agriculture, and human health in the United States. Technical report submitted to the U.S. National Climate Assessment. North American Nitrogen Center of the International Nitrogen Initiative (NANC-INI), Woods Hole Research Center, Falmouth, MA. Available online at <http://www.whrc.org/resources/publications/pdf/SuddicketalWHRC.12.pdf>
- Sun, Y; Solomon, S; Dai, A; et al. (2006) How often does it rain? *J Clim* 19:916–934.
- SWCS (Soil and Water Conservation Society). (2003) Conservation implications of climate change: soil erosion and runoff from cropland. Ankeny, IA: Soil and Water Conservation Society.
- TAMU (Texas A&M University). (2010) SWAT—soil and water assessment tool. Available online at <http://swatmodel.tamu.edu/software/arcswat>.
- Taner, MU; Carleton, JN; Wellman, M. (2011) Integrated model projections of climate change impacts on a North American lake. *Ecol Model* 222(18):3380–3393.
- Tetra Tech. (2008a) Quality assurance project plan for watershed modeling to evaluate potential impacts of climate and land-use change on the hydrology and water quality of major U.S. drainage basins. Prepared for the Office of Research and Development Global Change Research Program, U.S. Environmental Protection Agency, Washington, DC.
- Tetra Tech. (2008b) Minnesota River basin turbidity TMDL and Lake Pepin excessive nutrient TMDL, model calibration and validation report. Prepared for Minnesota Pollution Control Agency, St. Paul, MN.
- Tong, STY; Sun, Y; Ranatunga, T; et al. (2011) Predicting plausible impacts of sets of climate and land-use change scenarios on water resources. *Appl Geogr* 32(2):477–489.
- Trenberth, KE; Dai, A; Rasmussen, RM; et al. (2003) The changing character of precipitation. *Am Meteorol Soc* 84:1205–1217.
- Trenberth, KE; Jones, PD; Ambenje, P; et al. (2007) Observations: surface and atmospheric climate change. In: Solomon, S; Qin, D; Manning, M; et al; eds. *Climate change 2007: the physical science basis*. Contribution of working group I to the fourth assessment

-
- report of the intergovernmental panel on climate change. Cambridge, UK and New York: Cambridge University Press.
- Tu, J. (2009) Combined impact of climate and land-use changes on streamflow and water quality in eastern Massachusetts, USA. *J Hydrol* 379(3–4):268–283.
- USDA (United States Department of Agriculture). (1991) State soil geographic (STATSG0) data base; data use information. Miscellaneous Publication 1492. National Soil Survey Center, Natural Resources Conservation Service, Fort Worth, TX.
- U.S. EPA (Environmental Protection Agency). (1984) Report to congress: nonpoint source pollution in the U.S. Office of Water Program Operations, Water Planning Division, Washington, DC.
- U.S. EPA (Environmental Protection Agency). (2000) Estimating hydrology and hydraulic parameters for HSPF. BASINS Technical Note 6. Office of Water, Washington, DC; EPA-823-R00-012. Available online at http://water.epa.gov/scitech/datait/models/basins/upload/2000_08_14_BASINS_tecnote6.pdf
- U.S. EPA (Environmental Protection Agency). (2001) BASINS version 3.0 user's manual. Office of Water, Washington, DC; EPA-823-B-01-001. Available online at http://water.epa.gov/scitech/datait/models/basins/upload/2009_04_03_BASINS_b3docs_usermanual.pdf
- U.S. EPA (Environmental Protection Agency). (2002) Nitrogen: multiple and regional impacts. Clean Air Markets Division, Washington, DC; EPA-430-R-01-006. Available online at <http://www.epa.gov/airmarkets/resource/docs/nitrogen.pdf>
- U.S. EPA (Environmental Protection Agency). (2008) Using the BASINS meteorological database—version 2006. BASINS Technical Note 10. Office of Water, Washington, DC. Available online at http://water.epa.gov/scitech/datait/models/basins/upload/2009_04_13_BASINSs_tecnote10.pdf
- U.S. EPA (Environmental Protection Agency). (2009a) BASINS 4.0—fact sheet. Office of Water, Washington, DC. Available online at <http://www.epa.gov/waterscience/BASINS/fs-basins4.html> (accessed January 27, 2010).
- U.S. EPA (Environmental Protection Agency). (2009b) BASINS 4.0 climate assessment tool (CAT): supporting documentation and user's manual. Global Change Research Program, National Center for Environmental Assessment, Office of Research and Development, Washington, DC; EPA-600-R-08-088F. Available online at <http://cfpub.epa.gov/ncea/cfm/recordisplay.cfm?deid=203460>
- U.S. EPA (Environmental Protection Agency). (2009c) ICLUS V1.2 user's manual: ArcGIS tools and datasets for modeling US housing density growth. Global Change Research Program, National Center for Environmental Assessment, Office of Research and Development, Washington, DC; EPA-600-R-09-143A.

-
- U.S. EPA (Environmental Protection Agency). (2010) NHDPlus user guide. Office of Water, Washington, DC. Available online at ftp://ftp.horizon-systems.com/NHDPlus/NHDPlusV1/documentation/NHDPLUSV1_UserGuide.pdf.
- USGS (United States Geological Survey). (1982) Guidelines for determining flood flow frequency. Bulletin #17B of the Hydrology Subcommittee, Interagency Advisory Committee on Water Data, Reston, VA. Available online at http://water.usgs.gov/osw/bulletin17b/dl_flow.pdf
- Volkery, A; Ribeiro, T. (2009) Scenario planning in public policy: understanding use, impacts and the role of institutional context factors. *Technol Forecast Soc Change* 76(9):1198–1207.
- Walsh, CJ; Roy, A; Feminella, J; et al. (2005) The urban stream syndrome: current knowledge and the search for a cure. *J N Am Benthol Soc* 24(3):706–723
- Wang, S-Y; Gillies, RR; Takle, ES; et al. (2009) Evaluation of precipitation in the Intermountain Region as simulated by the NARCCAP regional climate models. *Geophys Res Lett* 36(L11704) doi:10.1029/2009GL037930.
- Westerling, AL; Hidalgo, HG; Cayan, DR; et al. (2006) Warming and earlier spring increases western U.S. forest wildfire activity. *Science* 313(5789):940–943.
- Whitehead, PG; Wilby, RL; Battarbee, RW; et al. (2009) A review of the potential impacts of climate change on surface water quality. *Hydrol Sci* 54:101–123.
- Wilcox, BP; Rawls, WJ; Brakensiek, DL; et al. (1990) Predicting runoff from rangeland catchments: a comparison of two models. *Water Resour Res* 26(10):2401–2410.
- Williams, J.R. (1975) Sediment-yield prediction with universal equation using runoff energy factor. In: Present and prospective technology for predicting sediment yield and sources: proceedings of the sediment-yield workshop, November 28–30, 1972. U.S. Department of Agriculture Sedimentation Lab, Oxford, MS. ARSS-40; pp. 244–252. .
- Williams, MW; Losleben, M; Caine, N; et al. (1996) Changes in climate and hydrochemical responses in a high-elevation catchment in the Rocky Mountains, USA. *Limnol Oceanogr* 41(5):939–946.
- Wilson, CO; Weng, Q. (2011) Simulating the impacts of future land use and climate changes on surface water quality in the Des Plaines River watershed, Chicago Metropolitan Statistical Area, Illinois. *Sci Total Environ* 409(20):4387–4405.
- Winchell, M; Srinivasan, R; DiLuzio, M; et al. (2008) ArcSWAT 2.1 interface for SWAT 2005, user's guide. U.S. Department of Agriculture, Agricultural Research Service, Temple, TX. Available online at http://www.geology.wmich.edu/sultan/5350/Labs/ArcSWAT_Documentation.pdf



Printed with vegetable-based ink on paper that contains a minimum of 50% post-consumer fiber content and processed chlorine free.

ISSUE



National Center for Environmental Assessment (8601)
Office of Research and Development
Washington, DC 20460